



# **Valorisation of by-products from brewing and canned fish industry: characterization of hydrolysates with antihypertensive and antioxidant activities**

Thesis submitted to Universidade do Porto, in partial fulfillment of requirements for  
the degree of Ph.D. in Sustainable Chemistry

**Elsa Marisa Ferreira Vieira**

Under the supervision of:

Prof. Dra. Isabel Maria Pinto Leite Viegas Oliveira Ferreira

co-supervision of:

Prof. Dra. Helena Maria Ferreira da Costa Ferreira Carmo

co-supervision of:

Cathedral Professor Olívia Maria de Castro Pinho

Porto

May, 2016

© AUTHORISED THE PARTIAL REPRODUCTION OF THIS THESIS (SUBJECT TO THE APPROVAL OF THE PUBLISHERS OF JOURNALS IN WHICH THE ARTICLES WERE PUBLISHED) ONLY FOR RESEARCH PURPOSES THROUGH A WRITTEN DECLARATION OF THE PERSON CONCERNED THAT SUCH PLEDGES.

*Elsa Mariana Ferreira Vieira*



This work has been supported by Fundação para a Ciência e a Tecnologia (FCT) through grant no. PEst-C/EQB/LA0006/2011 and to the PhD grant (SFRH/BD/81845/2011) financed by Programa Operacional Potencial Humano - Quadro de Referência Estratégico Nacional - Tipologia 4.1 - Formação Avançada (POPH-QREN) subsidised by Fundo Social Europeu (FSE) and national funds from Ministério da Ciência, Tecnologia e Ensino Superior (MCTES).



The experimental work presented in this thesis was undertaken under the Ph.D. Programme in Sustainable Chemistry (REQUIMTE), hosted by Universidade do Porto and Universidade Nova de Lisboa. The experimental work was mainly performed in the Laboratory of Bromatology and Hydrology, Department of Chemical Sciences, Faculty of Pharmacy, University of Porto (Portugal).

## **ACKNOWLEDGEMENTS**

I wish to express my deepest gratitude:

To my supervisor Professor Doctor Isabel Ferreira, co-supervisor Professor Doctor Helena Carmo and co-supervisor Cathedratric Professor Olívia Pinho for the opportunity to develop this project, as well, for the guidance provided during the course of my Ph.D.

To Fundação para a Ciência e Tecnologia (FCT) by the PhD grant (SFRH/BD/81845/2011) financed by Programa Operacional Potencial Humano - Quadro de Referência Estratégico Nacional - Tipologia 4.1 - Formação Avançada (POPH-QREN) subsidised by Fundo Social Europeu (FSE) and national funds from Ministério da Ciência, Tecnologia e Ensino Superior (MCTES), which made possible the accomplishment of the present work.

To Doctor José das Neves and Doctor Diana Dias da Silva for their collaboration in the cell culture work. Thanks for their availability, guidance and concern demonstrated during all the experimental work.

To Professor Doctor Rui Vitorino for his collaboration with the Mass Spectrometry analysis in the Department of Chemistry, University of Aveiro. Thanks for the warm welcoming and concern during the experimental work.

To Professor Doctor John Van Camp for accepting me in the Research Group Food Chemistry and Human Nutrition (nutriFOODchem). Thanks for his invaluable scientific input and fruitful discussions.

To Doctor Charlotte Grootaert for sharing her scientific knowledge with me and for the direct laboratory supervision, precise guidelines, scientific accuracy and friendship during my internship at nutriFOODchem laboratory, and not least, for her expert proof-reading of manuscript.

To the collaborators from the Laboratory of Bromatology and Hydrology: Sara Cunha, Armindo Melo e Edgar Pinto for their valuable scientific knowledge and assistance in the development of parts of the experimental work.

To Unicer - Bebidas de Portugal, S.A. (Leça do Balio, Portugal), in the name of its production director, for providing the yeast surplus samples used in this study.

To Conservas Ramirez & Cia (Filhos), S.A. (Matosinhos, Portugal), in the name of its production director, for providing the sardine by-product samples used in this study.

To all my great researcher colleagues at the Department of Food Safety and Food Quality in University of Gent (Belgium), for their warm welcome, full integration and assistance during my internship at nutriFOODchem laboratory.

To all my special friends at the Laboratory of Bromatology and Hydrology: Francisca, Sónia, Olga, Joana, Anabela C., Anabela B., Filipa and Antónia, for the support, encouragement, exchange of knowledge and continuous presence during this journey. Thanks for creating such a relaxing, pleasant and inspiring working environment.

To my parents, my sister and José for the constant support and encouraging words during the intense laboratory work in the course of my Ph.D. and during the last period of writing process.

*“Take these broken wings and learn to fly”*

Paul McCartney

## ABSTRACT

A large amount of agro-industrial by-products is annually generated by canned fish industry and brewing process - mostly brewer's spent grain (BSG) and brewer's spent yeast (BSY). Since the main uses of these wastes are animal feed or incineration, sustainable practices demand for economic and environmental valorization. One possible approach is the recovery of protein fraction from these by-products for production of autolysates/ hydrolysates with potential biological properties and, thus, with greater commercial interest.

This PhD research work aimed to produce BSY autolysates, sardine protein hydrolysates (SPH) and BSG protein hydrolysates with antioxidant and angiotensin-I converting enzyme inhibitory (ACE-I) activities, with potential use as new bioactive food ingredients. To achieve this purpose, a BSY extract was obtained by mechanic disruption procedure to recover valuable compounds (enzymes, proteins, vitamins, antioxidant compounds) and produce BSY autolysates, SPH and BSG protein hydrolysates by the action of BSY proteases. The processing conditions for autolysis/ hydrolysis were optimized by response surface methodology and monitorization was performed by chromatographic, electrophoretic, hydrolysis degree (DH) and/ or protein recovery analyses. Autolysate/ hydrolysates were characterized in relation to proximate composition, molecular weight distribution and hydrophobicity; the antioxidant activities were screened by chemical and/or cell-based assays and the ACE-I was measured by a fluorimetric assay. Ultrafiltration (UF) membranes were used to concentrate the bioactive fraction. In order to predict the *in vivo* bioavailability of the bioactive compounds, the impact of gastrointestinal (GI) digestion and the permeability through Caco-2 and Caco-2/HT29-MTX cell models were also evaluated. Mass spectrometry was performed to confirm the molecular mass range of compounds permeated in the transport assays.

Data showed that the BSY autolysate, produced at 36°C for 6 h, at pH of 6, presented TPC, FRAP and ACE-I activity ( $IC_{50}$ ) of 385  $\mu$ M GAE/mL, 374  $\mu$ M TE/mL and 379  $\mu$ g protein/mL, respectively. After simulated GI digestion, BSY autolysate exhibited a protective effect against oxidative stress induced by hydrogen peroxide in Caco-2 cells and good permeability through Caco-2 and Caco-2/HT29-MTX cell models. Regarding to SPH production, data showed that sarcoplasmic proteins from sardine by-products were effectively hydrolysed by BSY proteases. Under the optimum hydrolysis conditions, E/S ratio 0.27:1 U/mg (0.725 U/mL), 50°C for 7 h, at pH of 6, sarcoplasmic SPH presented a FRAP value of 290  $\mu$ M TE/mL and an ACE-

I activity ( $IC_{50}$ ) of 164  $\mu$ g protein/mL. These activities were enhanced by UF (10 kDa-membrane). The ACE-I of SPH remained unchanged upon GI digestion (117  $\mu$ g protein/mL), but no ACE-I activity was detected after cell transport, suggesting the degradation of ACE-I peptides by brush-border peptidases. Antioxidant activity increased after GI digestion (344  $\mu$ M TE/mL) and sarcoplasmic SPH bioactive compounds permeated across Caco-2 and Caco-2/HT29-MTX co-culture cell monolayers, providing further evidence of intestinal absorption. Additionally, Mass spectrometry revealed that peptides with m/z between 1000 and 5000 were transported across Caco-2/HT29-MTX co-culture cell monolayer, presumably via transcytosis mechanisms. The sarcoplasmic SPH also exhibited anti-inflammatory activity in TNF- $\alpha$  simulated endothelial cells through the inhibition of NO, ROS and pro-inflammatory cytokines production, MCP-1, VEGF, IL-8 and ICAM-1. In addition, BSY proteases hydrolysed muscle and viscera proteins from sardine by-products, but in a lesser extent compared with Alcalase® and Neutrase®. However, viscera SPH prepared by BSY proteases presented significantly higher emulsion, foaming and oil binding properties compared with other viscera SPH. Besides sardine proteins (animal origin), BSY proteases efficiently hydrolysed the BSG proteins (vegetal origin). Under the hydrolysis conditions optimized, E/S ratio of 0.29:1 U/mg (0.725 U/mL), 50°C, 6 h, at pH of 6.0, BSG protein hydrolysate presented DH of 17.1%, TPC of 1.65 mg GAE/mL and FRAP value of 1.88 mg TE/mL. The main BSY proteases responsible for the BSG protein hydrolysis were indicated as belonging to the class of serine peptidases and metallopeptidases. Compared with treatments by commercial enzymes, BSY proteases were less efficient to hydrolyse the BSG proteins; Alcalase® prompted the highest TPC (0.083 mg GAE/mg dw) and ACE-I activity (385  $\mu$ g protein/mL). Moreover, <10 kDa UF fractions inhibited the intracellular ROS generation and exerted a protective ability against hydrogen peroxide induced oxidative damage in Caco-2 and HepG2 cell lines, indicating its potential use in food systems as natural antioxidants. Overall, this research suggested that BSY autolysates, SPH and BSG protein hydrolysates can be considered a high added-value ingredient with promising nutraceutical applications.

**Keywords:** Brewer's spent yeast, brewer's spent grain, sardine protein hydrolysate, antioxidant activity, angiotensin- I converting enzyme.



## RESUMO

Anualmente são produzidas grandes quantidades de sub-produtos agro-alimentares por parte das indústrias conserveira e cervejeira (levedura e *dreche*). Dado que as principais aplicações destes sub-produtos são a alimentação animal e incineração, recomendam-se práticas sustentáveis que promovam a sua valorização económica e ambiental. Uma possível aplicação é a recuperação da fração proteica destes sub-produtos para produção de autolisados/ hidrolisados com potenciais propriedades biológicas, e, por isso, com maior interesse sob o ponto de vista comercial.

O trabalho desenvolvido nesta tese de doutoramento teve como objetivo a produção de autolisados de levedura de cerveja, hidrolisados proteicos de sardinha e hidrolisados proteicos da *dreche*, com atividades antioxidante e de inibição da enzima conversora da angiotensina I (ECA), para potencial uso como ingredientes bioativos na indústria alimentar. De forma a atingir estes objetivos, extratos de levedura de cerveja foram obtidos por disrupção mecânica para recuperar os compostos biológicos (enzimas, proteínas, vitaminas, compostos antioxidantes) e utilizar as proteases na produção dos referidos autolisados/ hidrolisados. As condições de autólise/ hidrólise foram otimizadas por metodologia de superfície de resposta e a monitorização dos processos foi avaliada por métodos de cromatografia, eletroforese, grau de hidrólise (GH) e recuperação da proteína. Os autolisados/ hidrolisados foram caracterizados relativamente à sua composição nutricional, distribuição dos pesos moleculares e hidrofobicidade; as atividades antioxidantes foram avaliadas por ensaios químicos e por modelos celulares e a atividade inibitória da ECA foi avaliada por um método fluorimétrico. A ultrafiltração (UF) foi empregue para concentrar a fração bioativa. A biodisponibilidade dos compostos bioativos foi avaliada através dos ensaios de simulação da digestão gastrointestinal (GI) e de transporte intestinal através de dois modelos celulares: Caco-2 e co-cultura Caco-2/HT29-MTX.

Os resultados mostraram que o autolisado de levedura de cerveja, produzido a 36°C por 6 h, a pH 6, apresentou um teor de fenólicos totais (FT), FRAP e inibição da ECA (IC<sub>50</sub>) de 385 µM GAE/mL, 374 µM TE/mL e 379 µg proteína/mL, respetivamente. Após simulação da digestão GI, o autolisado de levedura de cerveja exibiu um efeito protetor contra o *stress* oxidativo induzido por peróxido de hidrogénio nas células Caco-2 e uma boa permeabilidade através das monocamadas celulares Caco-2 e Caco-2/HT29-MTX. Relativamente à produção de hidrolisados proteicos de sardinha, os resultados evidenciaram que as proteínas sarcoplasmáticas extraídas dos sub-produtos de sardinha foram eficazmente hidrolisadas pelas proteases da levedura de cerveja. Aplicando as condições de hidrólise otimizadas, relação enzima substrato de 0.27:1 U/mg (0.725 U/mL), 50°C por 7 h, a pH 6, os hidrolisados de proteínas sarcoplasmáticas apresentaram um valor de FRAP de 290 µM TE/mL e uma atividade de inibição da ECA de 164 µg proteína/mL. Ambas as atividades foram melhoras por UF (membrana de 10 kDa). Apesar da atividade inibitória da ECA do

hidrolisado de proteínas sarcoplasmáticas de sardinha não ter sido alterada após a simulação da digestão GI (117 µg proteína/mL), esta propriedade não foi detetada após o transporte celular; este resultado sugere que os compostos bioativos que atravessaram as monocamadas Caco-2 e Caco-2/HT29-MTX foram degradados pelas peptidases da bordadura em escova. A atividade antioxidante também aumentou após o ensaio de simulação da digestão GI e os compostos bioativos atravessaram as monocamadas Caco-2 e Caco-2/HT29-MTX, evidenciando potencial absorção intestinal *in vivo*. Adicionalmente, os resultados de espectrometria de massa mostraram que péptidos com m/z entre 1000-5000 atravessaram a monocamada Caco-2/HT29-MTX, provavelmente por mecanismos de transcitose. O hidrolisado de proteínas sarcoplasmáticas de sardinha também apresentou propriedades anti-inflamatórias em células endoteliais estimuladas pelo fator de necrose tumoral (TNF-α), visível pelos resultados de inibição da produção de óxido nítrico, espécies reativas de oxigénio e das citocinas pro-inflamatórias MCP-1, VEGF, IL-8 and ICAM-1. As proteases do extrato de levedura também conseguiram hidrolisar as proteínas musculares e viscerais dos sub-produtos de sardinha, embora de forma menos eficaz quando esta hidrólise foi comparada com a promovida pelas enzimas comerciais Alcalase® e Neutrase®. Contudo, comparativamente aos outros hidrolisados de proteínas viscerais, o tratamento com proteases da levedura de cerveja produziu hidrolisados com melhores propriedades de emulsão, formação de espuma e capacidade de retenção de gordura. Adicionalmente estas proteases também conseguiram hidrolisar as proteínas da *dreche* (origem vegetal). Aplicando as condições de hidrólise otimizadas, relação enzima substrato de 0.29:1 U/mg (0.725 U/mL), 50°C por 6 h, a pH 6, os hidrolisados proteicos da *dreche* apresentaram um GH de 17.1%, TF de 1.65 mg GAE/mL e um valor de FRAP de 1.88 mg TE/mL. Os resultados apontam que as principais proteases responsáveis por esta hidrólise pertencem à classe das peptidases de serina e metaloproteases. No estudo comparativo da hidrólise das proteínas da *dreche* com proteases comerciais, as proteases da levedura de cerveja revelaram menor eficácia; contrariamente o tratamento com Alcalase® produziu hidrolisados com maior teor em FT (0.083 mg GAE/mg peso seco) e atividade inibitória da ECA (385 µg proteína/mL). Além disso, a fração menor de 10 kDa inibiu a produção de espécies reativas de oxigénio e exerceu um efeito protetor contra o *stress* oxidativo induzido por peróxido de hidrogénio nas linhas celulares Caco-2 e HepG2.

Em conclusão, este estudo sugere que os autolisados de levedura de cerveja, hidrolisados proteicos de sardinha e hidrolisados proteicos da *dreche* podem ser considerados ingredientes bioativos, apresentando promissoras aplicações na área dos nutracêuticos.

**Palavras-chave:** autolisados de levedura de cerveja, hidrolisados proteicos de sardinha e hidrolisados proteicos da *dreche*, atividade antioxidante, atividade inibitória da enzima conversora da angiotensina.

## LIST OF PUBLICATIONS

The information present in this dissertation was submitted to international peer reviewing, toward publication in international scientific journals and some of them were presented as oral / poster communications in scientific meetings, as detailed next:

### *Publications in international peer-review journals*

1. Elsa F. Vieira, Joana Carvalho, Edgar Pinto, Sara C. Cunha, Agostinho A. Almeida, Isabel M.P.L.V.O. Ferreira. (2016). Nutritive value, antioxidant activity and phenolic compounds profile of Brewer's spent yeast extract. (*submitted*).
2. Elsa F. Vieira, Sara C. Cunha, Isabel M.P.L.V.O. Ferreira. (2016). A bioactive ingredient obtained from the inner cellular content of Brewer's spent yeast. (*submitted*).
3. Elsa F. Vieira, Armindo Melo, Isabel M.P.L.V.O. Ferreira. (2016). Autolysis of intracellular content of brewer's spent yeast to maximize ACE-inhibitory and antioxidant activities. (*submitted*).
4. Elsa F. Vieira, José das Neves, Rui Vitorino, Diana Dias da Silva, Helena Carmo, Isabel M.P.L.V.O. Ferreira. (2016). Impact of *in vitro* gastrointestinal digestion and transepithelial transport on antioxidant and ACE-inhibitory activities of brewer's spent yeast autolysate. (*submitted*).
5. Elsa F. Vieira, Isabel M.P.L.V.O. Ferreira (2016). Antioxidant and antihypertensive hydrolysates obtained from by-products of cannery sardine and brewing industries. International Journal of Food Properties. DOI:10.1080/10942912.2016.1176036.
6. Elsa F. Vieira, José das Neves, Rui Vitorino, Isabel M.P.L.V.O. Ferreira. (2016). Simulated gastrointestinal digestion and *in vitro* intestinal permeability of bioactive protein hydrolysates obtained from canned sardine and brewing by-products. (*submitted*).
7. Elsa F. Vieira, John Van Camp, Isabel M.P.L.V.O. Ferreira, Charlotte Grootaert. (2016). Anti-inflammatory activity of a hydrolysate from canned sardine and brewing by-products through inhibition of TNF- $\alpha$ -induced endothelial dysfunction in a co-culture model of Caco-2 and endothelial cells. (*submitted*).
8. Elsa F. Vieira, Olívia Pinho, Isabel M.P.L.V.O. Ferreira (2016). Characterization of hydrolysates obtained from muscle and viscera proteins of canned sardine by-products. (*submitted*).

9. Elsa F. Vieira, M. Angélica M. Rocha, Elisabete Coelho, Olívia Pinho, Jorge A. Saraiva, Isabel M.P.L.V.O. Ferreira, Manuel A. Coimbra. (2014). Valuation of brewer's spent grain using a fully recyclable integrated process for extraction of proteins and arabinoxylans. *Industrial Crops and Products*, 52, 136-143.
10. Elsa F. Vieira, Juliana Teixeira, Isabel M.P.L.V.O. Ferreira. (2016). Valorisation of brewers' spent grain and spent yeast through protein hydrolysates with antioxidant properties. *European Food Research and Technology*. DOI: 10.1007/s00217-016-2696-y.
11. Elsa F. Vieira, Diana Dias da Silva, Helena Carmo, Isabel M.P.L.V.O. Ferreira. (2016). Antioxidant and ACE inhibitory activities of hydrolysates of brewers' spent grain proteins by proteases from spent yeast or by commercial enzymes: protective capacity in Caco-2 and HepG2 cells. (*submitted*).

#### *Oral Communications in Scientific Meetings*

1. Tiago Almeida, Cristina Moura, Elsa F. Vieira, Olívia Pinho, Isabel M.P.L.V.O. Ferreira. (2012). "Proteolytic activity of surplus yeast extracts". 5<sup>th</sup> Meeting of Young Researchers of University of Porto (IJUP2012), Porto, Portugal.
2. Joana Carvalho, Elsa F. Vieira, Sónia Meireles, Tiago Brandão, Isabel M.P.L.V.O. Ferreira. (2014). "Effect of serial repitching on proteolytic and bioactive properties of brewer's spent yeast extracts: storage stability evaluation". 7<sup>th</sup> Meeting of Young Researchers of University of Porto (IJUP2014). Porto, Portugal.
3. Elsa F. Vieira, Isabel M.P.L.V.O. Ferreira. (2015). "Intestinal transport of sardine (*Sardine pichardus*) protein hydrolysate prepared from action of *Saccharomyces* brewing yeast surplus proteases - assessment of antioxidant and ACE-inhibitory activities". 15<sup>th</sup> International Nutritional & Diagnostics Conference, Prague, Czech Republic.
4. Elsa F. Vieira, Sandra J. Vieira, Isabel M.P.L.V.O. Ferreira. (2015). "Optimization of brewer's spent grain protein hydrolysis by proteases from *Saccharomyces* brewing surplus using Response Surface Methodology". Euro Food Chem XVIII Conference, Madrid, Spain.

*Poster Communications in Scientific Meetings*

1. Elsa F. Vieira, Isabel M.P.L.V.O. Ferreira. (2014). "Optimization by RSM of enzymatic proteolysis of sardine sarcoplasmic protein hydrolysates (*Sardina pilchardus*) produced by proteases from *Saccharomyces* brewing by-product and evaluation of potential antioxidant and ACE inhibitory activities". The 2014 Belgian Peptide Group Meeting, Ghent, Belgium.
2. Elsa F. Vieira, José das Neves, Isabel M.P.L.V.O Ferreira. (2014). "Simulated gastrointestinal digestion and *in vitro* intestinal absorption of potential antioxidant and ACE inhibitory peptides from *Saccharomyces* brewing by-product extract". Total Food Conference 2014 science and technology for the economic and sustainable exploitation of agri-food chain wastes and co-products, Norwich, United Kingdom.
3. Elsa F. Vieira, Isabel M.P.L.V.O Ferreira. (2015). "Comparison of functional, antioxidant and ACE-inhibitory activities of sardine (*Sardinella pilchardus*) viscera protein hydrolysates using proteases from brewers' yeast surplus (*Saccharomyces pastorianus*) and commercial proteases". 15<sup>th</sup> International Nutritional & Diagnostics Conference, Prague, Czech Republic.
4. Elsa F. Vieira, Teixeira J., Isabel M.P.L.V.O. Ferreira. (2015). "Valuation of spent brewer's yeast as natural source of proteases and bioactive compounds: Influence of serial repitching". Euro Food Chem XVIII Conference, Madrid, Spain.



## TABLE OF CONTENTS

ACKNOWLEDGEMENTS.....	v
ABSTRACT .....	vii
RESUMO .....	ix
LIST OF PUBLICATIONS.....	xi
TABLE OF CONTENTS .....	xv
LIST OF FIGURES.....	xxiv
LIST OF ABBREVIATIONS .....	xxix
 Motivation and research aims.....	 1
Thesis outline .....	5

## PART I

### “Brewer’s spent yeast extracts”

<b>CHAPTER 1 .....</b>	<b>11</b>
Literature review	
Brewer’s spent yeast: potential source of biological compounds and proteases for application in the production of food hydrolysates	
 1.1. Brewer’s spent yeast.....	 13
1.1.1. By-product .....	13
1.1.2. Nutritional composition.....	13
1.1.3. Antioxidant system.....	15
1.1.4. Enzymatic system .....	17
1.1.5. Potential applications .....	18
1.2. Production of BSY extract .....	20
1.3. Biological activities of BSY extract.....	23
1.4. Screening methods to search for autolysates/ hydrolysates bioactivity .....	25
1.4.1. <i>In vitro</i> antioxidant chemical activity .....	26
1.4.2. Antihypertensive activity.....	28
1.5. Bioavailability methods .....	31
1.5.1. Simulated GI digestion .....	31
1.5.2. Cell culture systems .....	31
1.5.3. <i>In vivo</i> assays .....	34

<b>CHAPTER 2</b> .....	35
Nutritive value, antioxidant activity and phenolic compounds profile of Brewer's spent yeast extract	

ABSTRACT .....	37
2.1. INTRODUCTION .....	37
2.2. MATERIAL AND METHODS .....	38
2.2.1. Reagents and standards .....	38
2.2.2. Samples .....	39
2.2.3. BSY extract preparation .....	39
2.2.4. Proximate composition .....	39
2.2.5. Amino acid composition and chemical score .....	39
2.2.6. Analyses of minerals .....	40
2.2.6.1. Sample preparation .....	40
2.2.6.2. Inductively coupled plasma mass spectrometry analysis .....	40
2.2.6.3. Atomic absorption spectrometry analysis .....	40
2.2.7. Analysis of B-complex vitamins .....	40
2.2.7.1. Extraction of B-complex vitamins .....	40
2.2.7.2. Preparation of B-complex vitamins standard solution .....	41
2.2.7.3. Chromatographic conditions for separation of B-complex vitamins .....	41
2.2.8. Antioxidant activity of BSY extracts .....	41
2.2.8.1. Ferric reducing antioxidant potential (FRAP) assay .....	41
2.2.8.2. DPPH radical scavenging capacity assay .....	42
2.2.8.3. Ferricyanide reducing power (RP) assay .....	42
2.2.9. Extraction of phenolic compounds .....	42
2.2.9.1. HPLC analysis of phenolic compounds .....	42
2.3. RESULTS AND DISCUSSION .....	43
2.3.1. Nutritional composition of BSY extracts .....	43
2.3.1.1. Amino acid composition .....	43
2.3.1.2. Minerals content .....	45
2.3.1.3. B-complex vitamins content .....	45
2.3.2. Antioxidant activity .....	46
2.3.3. Phenolic compounds .....	46
2.4. CONCLUSIONS .....	48

<b>CHAPTER 3</b> .....	49
A bioactive ingredient obtained from the inner cellular content of Brewer's spent yeast	

ABSTRACT .....	51
3.1. INTRODUCTION .....	51
3.2. MATERIAL AND METHODS .....	53
3.2.1. Chemicals, reagents and equipments .....	53
3.2.2. Samples .....	53
3.2.3. Preparation of BSY extracts .....	53
3.2.4. Proximate composition .....	54



3.2.5. Sodium dodecyl sulfate polyacrylamide gel electrophoresis .....	54
3.2.6. Amino acid composition and chemical score of BSY extract proteins.....	55
3.2.7. Determination of biological properties of BSY extracts .....	55
3.2.7.1. Enzyme activity assay .....	55
3.2.7.2. Total phenolic content (TPC) and total flavonoid content (TFC) .....	55
3.2.7.3. Antioxidant activity of BSY extracts .....	56
3.2.7.4. ACE-I activity .....	56
3.2.8. Effect of storage conditions on the stability of BSY biological properties	57
3.2.9. Statistical analysis.....	57
3.3. RESULTS AND DISCUSSION .....	57
3.3.1. Proximate composition of freeze-dry BSY extracts.....	57
3.3.2. Amino acid composition of BSY protein fraction .....	58
3.3.3. Molecular weight distribution of BSY extract protein fraction .....	59
3.3.4. Proteolytic activity of BSY extracts .....	61
3.3.5. TPC, TFC and antioxidant activity of BSY extracts.....	62
3.3.6. ACE-I activity of BSY extracts.....	64
3.3.7. Stability of biological activity of frozen BSY extracts.....	64
3.4. CONCLUSIONS .....	66

## **CHAPTER 4 .....**

Autolysis of intracellular content of brewer's spent yeast to maximize ACE-inhibitory and antioxidant activities

ABSTRACT .....	69
4.1. INTRODUCTION.....	69
4.2. MATERIAL AND METHODS .....	70
4.2.1. Reagents .....	70
4.2.2. Brewer's spent yeast (BSY) extract.....	70
4.2.3. Autolysis of BSY extract.....	71
4.2.4. Analytical Methods .....	71
4.2.4.1. Determination of Total Phenolic content .....	71
4.2.4.2. Determination of Ferric Ion Reducing Antioxidant Power .....	71
4.2.4.3. Determination of ACE-I activity .....	71
4.2.5. Experimental design, modelling and optimization of autolysis conditions	72
4.2.6. Statistical analysis.....	72
4.3. RESULTS AND DISCUSSION .....	72
4.3.1. Experimental design .....	72
4.3.2. Analysis of response surfaces.....	76
4.3.3. Validation of the RSM model.....	78
4.4. CONCLUSIONS .....	79

<b>CHAPTER 5</b> .....	81
Impact of <i>in vitro</i> gastrointestinal digestion and transepithelial transport on antioxidant and ACE-inhibitory activities of brewer's spent yeast autolysate	
ABSTRACT .....	83
5.1. INTRODUCTION .....	83
5.2. MATERIAL AND METHODS .....	84
5.2.1. Reagents and cells .....	84
5.2.2. Equipments .....	85
5.2.3. Preparation of BSY autolysates and <i>in vitro</i> GI digestion.....	85
5.2.4. <i>In vitro</i> biological activity.....	86
5.2.5. Cell-based assays .....	86
5.2.5.1. Cell culture maintenance and generation of cell monolayers.....	86
5.2.5.2. Cell viability determination .....	86
5.2.5.3. Mitochondrial integrity determination .....	87
5.2.5.4. ROS levels production .....	87
5.2.5.5. Permeability experiments .....	88
5.2.6. Peptide analyses by RP-HPLC and by MALDI-TOF .....	89
5.2.7. Statistical analysis .....	89
5.3. RESULTS AND DISCUSSION.....	89
5.3.1. Impact of <i>in vitro</i> GI digestion of BSY autolysate biological activity.....	89
5.3.2. Intestinal permeability of peptides from BSY autolysate .....	92
5.3.3. Biological activity of BSY permeates .....	98
5.4. CONCLUSIONS .....	99

## PART II

### “Sardine protein hydrolysates”

<b>CHAPTER 6</b> .....	103
Literature review	
Development of sardine protein hydrolysates and their health promoting ability	
6.1. Canned sardine industry .....	105
6.2. Nutritional composition of sardine by-product .....	105
6.3. Potential applications of SPH.....	106
6.4. Preparation of SPH.....	107
6.4.1. Preparation of Sardine Protein concentrate (SPC) .....	107
6.4.2. Protein hydrolysis .....	109
6.4.3. SPH concentration and purification .....	110
6.4.4. Identification of bioactive peptides from SPH.....	111
6.5. Nutritional composition of SPH .....	111
6.6. Bioactivities of SPH and derived peptides.....	113
6.7. Functional properties of SPH .....	113

6.7.1. Solubility .....	113
6.7.2. Emulsifying properties.....	114
6.7.3. Foaming.....	114
6.7.4. Water binding capacity.....	115
6.7.5. Oil binding capacity .....	115

## **CHAPTER 7 ..... 121**

Antioxidant and antihypertensive hydrolysates obtained from by-products of cannery sardine and brewing industries

ABSTRACT .....	123
7.1. INTRODUCTION.....	123
7.2. MATERIAL AND METHODS .....	124
7.2.1. Standards and reagents.....	124
7.2.2. Equipment.....	125
7.2.3. By-products.....	125
7.2.4. Preparation of the Sardine sarcoplasmic protein extracts (SPE) .....	125
7.2.5. Extraction of Brewer's spent yeast (BSY) proteases.....	126
7.2.6. Enzymatic hydrolysis .....	126
7.2.7. Hydrolysis rate (HR %).....	126
7.2.8. Protein recovery (PR %) and % of peptides formed .....	127
7.2.9. Degree of hydrolysis (DH %).....	127
7.2.10. Ferric reducing ability (FRAP) .....	127
7.2.11. Reducing power method (RP) .....	128
7.2.12. ACE-I activity .....	128
7.2.13. SDS-Polyacrylamide gel electrophoresis (SDS-PAGE) .....	128
7.2.14. SPH amino acid composition .....	128
7.2.15. Experimental design, modelling and optimization.....	129
7.2.16. Statistical analysis.....	129
7.3. RESULTS AND DISCUSSION .....	129
7.3.1. Optimization of hydrolysis conditions .....	131
7.3.2. Analysis of response surfaces.....	133
7.3.3. Validation of RSM model.....	133
7.3.4. Characterization of SPH obtained under optimum conditions.....	134
7.4. CONCLUSIONS .....	136

## **CHAPTER 8 ..... 137**

Simulated gastrointestinal digestion and *in vitro* intestinal permeability of bioactive protein hydrolysates obtained from canned sardine and brewing by-products

ABSTRACT .....	139
8.1. INTRODUCTION.....	139
8.2. MATERIAL AND METHODS .....	140
8.2.1. Materials and cells .....	140

8.2.2. By-products .....	141
8.2.3. Preparation and fractionation of SPH .....	141
8.2.4. <i>In vitro</i> Simulated GI Digestion .....	141
8.2.5. Ferric reducing antioxidant potential (FRAP) assay .....	142
8.2.6. ACE-I activity assay .....	142
8.2.7. Cell viability study .....	143
8.2.8. Permeability experiments .....	143
8.2.9. Reversed-phase high performance liquid chromatography .....	144
8.2.10. Mass spectrometry .....	145
8.2.11. Statistical analysis .....	145
8.3. RESULTS AND DISCUSSION.....	145
8.3.1. Effect of Ultrafiltration on biological activities of SPH.....	145
8.3.2. Effect of simulated GI digestion on bioactivities of SPH<10 kDa .....	146
8.3.3. Cellular viability of SPH.GI<10 kDa .....	147
8.3.4. Intestinal permeability of SPH.GI<10 kDa .....	148
8.3.5. Effect of intestinal transport on the bioactivity of SPH.GI<10 kDa.....	154
8.4. CONCLUSIONS .....	154

## CHAPTER 9 .....155

Anti-inflammatory activity of a hydrolysate from canned sardine and brewing by-products through inhibition of TNF- $\alpha$ -induced endothelial dysfunction in a co-culture model of Caco-2 and endothelial cells

ABSTRACT .....	157
9.1. INTRODUCTION .....	157
9.2. MATERIAL AND METHODS .....	159
9.2.1. Reagents and standards and cells .....	159
9.2.2. By-products.....	159
9.2.3. Preparation of SPH .....	159
9.2.4. Desalting of SPH.....	160
9.2.5. Protein content.....	160
9.2.6. Cell culture routine .....	160
9.2.7. Cell viability experiments.....	160
9.2.8. <i>In vitro</i> cell culture models.....	161
9.2.9. Exposure to TNF- $\alpha$ to induce endothelial inflammation.....	162
9.2.9.1. Cell viability study .....	162
9.2.9.2. Determination of intracellular reactive oxygen species (ROS) .....	162
9.2.9.3. Inhibition of NO production .....	162
9.2.9.4. Inhibition of pro-inflammatory cytokines production.....	163
9.2.10. Statistical analysis .....	163
9.3. RESULTS .....	163
9.3.2. Establishment of the co-culture model.....	164
9.3.3. Effects on viability of endothelial cells .....	164
9.3.4. Effects on NO production in endothelial cells.....	166
9.3.5. Effects on ROS levels in endothelial cells.....	167
9.3.6. Effects on inflammation markers expression .....	167

9.4. DISCUSSION .....	172
9.5. CONCLUSIONS .....	173

<b>CHAPTER 10 .....</b>	<b>175</b>
Characterization of hydrolysates obtained from muscle and viscera proteins of canned sardine by-products	

ABSTRACT .....	177
10.1. INTRODUCTION .....	177
10.2. MATERIAL AND METHODS .....	178
10.2.1. Reagents and standards .....	178
10.2.2. Equipments .....	179
10.2.3. Sardine by-products and proteolytic enzymes .....	179
10.2.4. Hydrolyses of muscle and viscera proteins .....	179
10.2.5. Determination of DH% and molecular weight profile of hydrolysates ..	180
10.2.6. Proximate composition .....	180
10.2.7. Determination of antioxidant and ACE-I activities .....	180
10.2.8. Determination of techno-functional properties .....	181
10.2.9. Colour measurement .....	181
10.2.10. Statistical analysis .....	181
10.3. RESULTS AND DISCUSSION .....	182
10.3.1. DH and molecular weight distribution profile of SPH .....	182
10.3.2. Protein and lipid content of SPH .....	182
10.3.3. Determination of antioxidant and ACE-I activities .....	184
10.3.4. Techno-functional properties of SPH .....	185
10.3.4.1. Solubility .....	185
10.3.4.2. Emulsifying properties .....	186
10.3.4.3. Foaming properties .....	187
10.3.4.4. Water Binding Capacity (WBC) .....	188
10.3.4.5. Oil Binding Capacity (OBC) .....	188
10.3.5. Colour of SPH .....	190
10.4. CONCLUSIONS .....	190

## PART III

### “Brewer’s spent grain protein hydrolysates”

<b>CHAPTER 11</b>	193
Literature review	
Development of brewer’s spent grain protein hydrolysates and their health promoting ability	
11.1. Brewer’s spent grain by-product: characteristics and potential applications	195
11.2. Preparation of Brewer’s spent grain protein hydrolysates	199
11.2.1. Extraction of BSG proteins	199
11.2.2. Hydrolysis of BSG proteins	199
11.3. Biological properties of BSG protein hydrolysate	200
 <b>CHAPTER 12</b>	 205
Valorisation of Brewers’ spent grain and spent yeast through protein hydrolysates with antioxidant properties	
ABSTRACT	207
12.1. INTRODUCTION	207
12.2. MATERIAL AND METHODS	208
12.2.1. By-products	208
12.2.2. Reagents	209
12.2.3. Apparatus	209
12.2.4. Preparation of BSY proteases	209
12.2.5. Preparation of BSG protein fraction	210
12.2.6. Enzymatic Hydrolysis	210
12.2.6.1. Experimental Design	210
12.2.6.2. Determination of DH% and HR%	211
12.2.6.3. Determination of total phenolic content (TPC)	211
12.2.6.4. Ferric Ion Reducing Antioxidant Power (FRAP) assay	211
12.2.7. Effect of potential inhibitors of BSY proteases	212
12.2.8. Statistical analysis	213
12.3. RESULTS AND DISCUSSION	213
12.3.1. Influence of pH on solubility and hydrolysis of BSG protein fraction	213
12.3.2. Central composite design and response surface method	214
12.3.3. The effect of temperature, time and E/S ratio on the response value	215
12.3.4. Validation of the RSM model	219
12.3.5. Hydrolysis monitoring by RP-HPLC	219
12.3.6. Effect of potential natural inhibitors of BSY proteases	220
12.3.7. Effect of potential inhibitors of BSY proteases	221
12.4. CONCLUSIONS	222

<b>CHAPTER 13 .....</b>	<b>223</b>
Antioxidant and ACE inhibitory activities of hydrolysates of brewers' spent grain proteins by proteases from spent yeast or by commercial enzymes: protective capacity in Caco-2 and HepG2 cells	
<b>ABSTRACT .....</b>	<b>225</b>
<b>13.1. INTRODUCTION .....</b>	<b>225</b>
<b>13.2. MATERIAL AND METHODS .....</b>	<b>226</b>
13.2.1. Reagents and cells .....	226
13.2.2. Equipments .....	227
13.2.3. BSG protein extraction .....	227
13.2.4. BSY proteases and commercial enzymes .....	227
13.2.5. Preparation of Brewers' spent grain protein hydrolysates .....	228
13.2.6. Determination of DH% and PR % .....	228
13.2.7. Characterization of BSG protein hydrolysates .....	230
13.2.7.1. Proximate composition analysis .....	230
13.2.7.2. Molecular weight distribution profile .....	230
13.2.7.3. Proteins and peptides profile .....	230
13.2.8. Ultrafiltration of BSG protein hydrolysates .....	230
13.2.9. ACE-I activity .....	231
13.2.10. Chemical antioxidant activities .....	231
13.2.11. Cell-based antioxidant activities .....	231
13.2.11.1. Cell culture routine .....	231
13.2.11.2. Samples preparation to cell culture studies .....	232
13.2.11.3. Cell viability determination .....	232
13.2.11.4. Mitochondrial integrity determination .....	232
13.2.11.5. ROS production .....	233
13.2.12. Statistical analysis .....	233
<b>13.3. RESULTS AND DISCUSSION .....</b>	<b>234</b>
13.3.1. Measuring the extent of hydrolysis .....	234
13.3.2. Proximate composition of BSG protein hydrolysates .....	234
13.3.3. Molecular weight distribution and peptides/proteins profile .....	235
13.3.4. Effect of UF on ACE-I activity of BSG protein hydrolysates .....	237
13.3.5. Effect of UF on antioxidant activity of BSG protein hydrolysates .....	238
13.3.6. Cellular antioxidant activities .....	239
<b>13.4. CONCLUSIONS .....</b>	<b>242</b>
 <b>GENERAL CONCLUSIONS .....</b>	 <b>245</b>
<b>FUTURE PROSPECTS .....</b>	<b>251</b>
<b>BIBLIOGRAFIC REFERENCES .....</b>	<b>257</b>

## LIST OF FIGURES

Figure i.1. Recovery of added value compounds from brewing and canned sardine agro-industrial by-products for production of SPH and BSG protein hydrolysates...	3
Figure i.2. Schematic overview of the organization of this thesis, with indication of the different chapters included in each part (I, II and III). ....	7
Figure 1.1. Microscopic structure of yeast cell and proximate composition (% dw) of BSY..	14
Figure 1.2. Classes of natural antioxidants of yeast cells.....	16
Figure 1.3. Classification of disruption techniques .....	20
Figure 1.4. Yeast wall mechanical disruption, using glass beads, applied at laboratorial scale. ....	22
Figure 1.5. Physiological effects of food derived bioactive peptides on major body systems. ....	25
Figure 1.6. Polarized epithelial cells with different types of intercellular contacts and different absorption and transport mechanisms of compounds through intestinal epithelium membrane .....	32
Figure 1.7. Two-chamber transwell transport model .....	33
Figure 3.1. SDS-PAGE profiles of BSY extracts .....	61
Figure 3.2. Biological activities stability of MIST BSY extract, stored at -25°C for 6 months. ....	65
Figure 4.1. Response surface and contour plots for interaction effects of temperature (°C) and time (h) autolysis on Total phenolics (A), FRAP (B) and ACE-I activity (C). ....	77
Figure 4.2. Response surface and contour plots for interaction effects of temperature (°C) and time (h) autolysis on the desirability index for combined responses of BSY autolysate. ....	79
Figure 5.1. Cell viability (%) (A) and TMRE mitochondrial inclusion (%) (B) after 24 h of exposure (37°C, 5% CO <sub>2</sub> ) to digested BSY autolysate at different protein concentrations .....	91
Figure 5.2. Protective effect of the digested BSY autolysate on ROS levels after 24 h of exposure (37°C, 5% CO <sub>2</sub> ) at different protein concentrations (mg/mL) under no stress treatment (A) and after oxidative stress induced by hydrogen peroxide (6 h exposure) (B).....	92
Figure 5.3. RP-HPLC chromatographic profile of digested BSY autolysate before (0 min) and after permeability (180 min) through Caco-2 cell monolayers (A) and Caco-2/HT29 co-culture cell monolayers (B) .....	93
Figure 5.4. MALDI-TOF mass spectra of digested BSY autolysate added to the apical compartment at the beginning of transport experiment (A) and five	



concentrated permeate taken from the basolateral compartment after 180 min of a permeability experiment across Caco-2/HT29-MTX co-culture cell monolayer (B).....	94
Figure 5.5. Comparative <i>in vitro</i> cumulative permeability of BSY peptides across Caco-2 cell monolayers (A) and Caco-2/HT29-MTX co-culture cell monolayers (B).....	96
Figure 6.1. Flow diagram for the preparation of fish protein hydrolysates and bioactive peptides, at laboratorial and industrial scales. ....	108
Figure 6.2. Different fractions obtained in the SPC preparation. ....	107
Figure 7.1. The RP-HPLC profiles of (i) SPE plus BSY proteases [S+E] without hydrolysis; (ii) SPH presenting HR=9.3% (25°C, 1.50 h); and (iii) SPH presenting HR=83% (50°C, 7.00 h).....	130
Figure 7.2. Counter plots for interaction effects of temperature (°C) and time (h) on Hydrolysis Rate (%) (A); Antioxidant activity determined by FRAP assay (B) and ACE-I activity (C) of SPH.....	134
Figure 7.3. SDS-PAGE profiles of sarcoplasmic proteins plus BSY proteases [S+E] without hydrolysis and SPH.....	135
Figure 8.1. Effect of SPH.GI<10 kDa at different peptide concentrations on Caco-2 cell viability, after 24 h of incubation at 37°C, 5% CO <sub>2</sub> (MTT assay). ....	148
Figure 8.2. RP-HPLC chromatographic profiles of SPH.GI<10 kDa added to the apical side at the beginning of permeability experiment (A) and collected from the basolateral side after 180 min of transport across Caco-2/HT29-MTX co-culture cell monolayer (B), and after 180 min of transport across Caco-2 cell monolayer (C).....	149
Figure 8.3. Comparative permeability (P% as mean values ± standard deviation bars) for sum of peptides fractions 1-11 from SPH.GI<10 kDa in Caco-2 cell after 180 min (37°C) of transport across Caco-2 cell monolayer and Caco-2/HT29 co-culture cell monolayer .....	152
Figure 8.4. MALDI-TOF mass spectra of SPH.GI<10 kDa taken from the basolateral side after 180 min of a permeability experiment across Caco-2/HT29-MTX co-culture cell monolayer. ....	153
Figure 9.1. Effect of Ultrafiltration and Desalting processes of SPH, at the same protein concentration of 1.0 mg/mL on differentiated Caco-2 (A) and EAhy926 (B) cells viability (%) (MTT assay) after 24 h of incubation (37°C, 10% CO <sub>2</sub> ) .....	165
Figure 9.2. Effect of desalted SPH<10 kDa at different protein concentrations (0.1, 0.5, 1.0, 2.0 and 5.0 mg protein/mL) on differentiated Caco-2 and EAhy926 cells viability (%) (MTT assay) after 24 h of incubation (37°C, 10% CO <sub>2</sub> ) .....	166
Figure 9.3. Effect of SPH<10 kDa (and metabolites) at the protein concentrations of 0.5 and 2.0 mg/mL on EAhy926 cells viability (%), after 4 h of incubation (37°C, 10% CO <sub>2</sub> ) in the co-culture and standard models, under TNF-α-induced inflammatory (1 h of TNF-α 10 ng/mL stimulation) and non-inflammatory conditions .....	168

Figure 9.4. Effect of SPH<10 kDa (and metabolites) at the protein concentrations of 0.5 and 2.0 mg/mL on NO production of EAhy926 cells after 4 h of incubation (37°C, 10% CO<sub>2</sub>) in the co-culture and standard models, under TNF- $\alpha$ -induced inflammatory (1 h of TNF- $\alpha$  10 ng/mL stimulation) and non-inflammatory conditions.

169

Figure 9.5. Effect of SPH<10 kDa (and metabolites) at the protein concentrations of 0.5 and 2.0 mg/mL on intracellular ROS levels of EAhy926 cells, after 4 h of incubation (37°C, 10% CO<sub>2</sub>) in the co-culture and standard models, under TNF- $\alpha$ -induced inflammatory (1 h of TNF- $\alpha$  10 ng/mL stimulation) and non-inflammatory conditions

170

Figure 9.6. Effect of SPH<10 kDa (and metabolites) at protein concentrations of 0.5 and 2.0 mg/mL on the secretion of MCP-1 (A); VEGF (B); IL-8 (C) and ICAM-1 (D) in EAhy926 cells, after 4 h of incubation (37°C, 10% CO<sub>2</sub>) in the co-culture and standard models, under TNF- $\alpha$ -induced inflammatory (1 h of TNF- $\alpha$  10 ng/mL stimulation) and non-inflammatory conditions.

171

Figure 10.1. SE-HPLC profiles of muscle (MUSC) and viscera (VISC) SPH produced by Brewer's spent yeast proteases (Bsy), Alcalase® (Alc) and Neutrase® (Ntr) action. Hydrolyses were performed at 50°C for 7 h, using an E/S ratio of 0.20:1 U/mg (1 U/mL)

183

Figure 10.2. Solubility profiles of muscle (MUSC) and visceral (VISC) SPH as a function of pH (4-10 range) obtained by treatment with Brewer's spent yeast proteases (Bsy), Alcalase® (Alc) and Neutrase® (Ntr) action

186

Figure 11.1. Schematic structure of a barley grain (A) and the BSG (B).

195

Figure 12.1. Effect of pH on solubility of BSG protein fraction, at 25°C, (A). Effect of pH on hydrolysis of BSG protein fraction by BSY proteases, at 37°C, (B).

214

Figure 12.2. Response surface plots for the effects of variable incubation temperature (°C), incubation time (h) and E/S ratio (U/mg) on the responses: (A) Degree of Hydrolysis (DH %); (B) Total Phenolic contents (TPC) and (C) FRAP activity.

218

Figure 12.3. Chromatograms obtained by RP-HPLC analysis of BSG proteins hydrolysates

220

Figure 13.1. SE-HPLC (A) and RP-HPLC (B) profiles of BSG protein hydrolysates with different DH (%), obtained after enzymatic hydrolysis with BSY extract (BSYH), Neutrase® (NTH) and Alcalase® (ALH).

236

Figure 13.2. Comparison of ACE-I activity (A), Total Phenolic Content (B) and FRAP (C) of BSG protein starting material (NT, no treatment), full BSG protein hydrolysates (BSYH, NTH, ALH) and respective <10 kDa and <3 kDa fractions.

238

Figure 13.3. Effect of BSG protein hydrolysates (<10 kDa fractions) on cell viability (%) and TMRE mitochondrial inclusion (%) in Caco-2 cell line (A) and HepG2 cell line (B), after 24 h of incubation at 37°C, 5% CO<sub>2</sub>.

241

Figure 13.4. Protective effect of BSG protein hydrolysates (<10 kDa fractions at concentrations of 0.1 and 1.0 mg/mL) for 24 h against oxidative stress induced by H<sub>2</sub>O<sub>2</sub> (6 h of exposure) in Caco-2 cell line (A) and HepG2 cell line (B).

242

## LIST OF TABLES

Table 1.1. Potential applications of BSY as functional food ingredients for animal and human nutrition.....	19
Table 1.2. Biological activities assessed in BSY autolysates and hydrolysates ....	24
Table 1.3. Classification of <i>in vitro</i> analytical methods for evaluation of the antioxidant activity of food protein hydrolysates and bioactive compounds.....	27
Table 1.4. <i>In vitro</i> analytical methods used for evaluation of the ACE-I activity of food hydrolysates and bioactive peptides.....	30
Table 2.1. Nutritional composition of BSY extract.....	44
Table 2.2. Mean content (mg/100 g dw) of phenolic compounds of BSY extracts in the free and bound fractions.....	47
Table 3.1. Proximate composition (% dw) of freeze-dried BSY extracts .....	58
Table 3.2. Amino acid composition of BSY extracts (g/100 g protein) and comparison with FAO/WHO reference protein .....	60
Table 3.3. Biological activity of BSY extracts, namely proteolytic activity, ACE-I activity, Total Phenolic Content (TPC), Total Flavonoid Content (TFC) and antioxidant activity .....	63
Table 4.1. Experimental design for evaluation the effects of autolysis conditions on biological properties of BSY autolysate .....	74
Table 4.2. Analysis of variance (ANOVA) for Total phenolic content, Antioxidant activity and ACE-I activity of BSY autolysate.....	75
Table 4.3. Performance of RSM model in predicting the optimum autolysis conditions to enhance the biological activities of BSY autolysate .....	78
Table 5.1. Apparent permeability coefficient ( $P_{app}$ ) of BSY peptides (P1-P6) after 180 min of transport across Caco-2 cell and Caco-2/HT29-MTX co-culture cell models .....	98
Table 5.2. FRAP and ACE-I activity of Caco-2 and Caco-2/HT29-MTX co-culture cell model permeates at different times of transport, five-fold concentration of permeates .....	99
Table 6.1. Degree of hydrolysis (DH %) and proximate composition (% dw) obtained for various SPH.....	112
Table 6.2. Summary of ACE-I activity reported for various SPH and derived bioactive peptides .....	116
Table 6.3. Summary of antioxidant activity reported for various SPH and derived bioactive peptides .....	117
Table 6.4. Summary of techno-functional properties reported for various SPH...	119
Table 7.1. Results from experimental design by CCD for evaluation the effects of hydrolysis temperature and time conditions on HR, FRAP and ACE-I activity ....	132

Table 8.1. Antioxidant and ACE-I activities of SPH, its fractions <10 kDa and <3 kDa and the <i>in vitro</i> GI digest of SPH<10 kDa .....	146
Table 8.2. Cumulative percentage permeability (P%) of SPH.GI<10 kDa peptides through the Caco-2/HT29-MTX co-culture cell monolayer and through Caco-2 cell monolayer for 180 min (37°C, 5% CO <sub>2</sub> ) .....	150
Table 10.1. Antioxidant and ACE-I activities of muscle (MUSC) and visceral (VISC) SPH produced by Brewer's spent yeast proteases (Bsy), Alcalase® (Alc) and Neutrase® (Ntr) action.....	185
Table 10.2. Techno-functional properties and colour and of muscle (MUSC) and visceral (VISC) SPH obtained by treatment with Brewer's spent yeast proteases (Bsy), Alcalase® (Alc) and Neutrase® (Ntr) .....	189
Table 11.1. Proximate composition (% dw) and potential applications of BSG....	197
Table 11.2. Treatments applied to extract the BSG proteins, to produce the BSG protein hydrolysates and its biological activities when it was evaluated .....	201
Table 12.2. Procedure for studying the effect of inhibitors of BSY proteases on BSG proteins .....	213
Table 12.1. Experimental design for evaluation of the effects of hydrolysis conditions at pH 6.0 on Hydrolysis Degree (DH %), total phenolic content (TPC) and FRAP Assay of BSG protein fraction by BSY proteases.....	215
Table 12.3. Model summary and analysis of variance (ANOVA) for Degree of Hydrolysis (Y1), TPC (Y2) and FRAP (Y3).....	217
Table 12.4. Effect of inhibitors on BSG protein hydrolysis by BSY proteases .....	222
Table 13.1. Conditions used for preparation of BSG protein hydrolysates .....	229
Table 13.2. Hydrolysis yield (%) and proximate composition (% dw) of BSG protein hydrolysates .....	235

## LIST OF ABBREVIATIONS

AAS	Atomic absorption spectrometry
Abz	<i>o</i> -aminobenzoylglycyl- <i>p</i> -nitrophenylalanylproline
ACE	Angiotensin-converting enzyme
ACE-I	Angiotensin-converting enzyme inhibitory
API	Aminopeptidase I
BHT	Butylated hydroxytoluene
BSA	Bovine serum albumin
BSG	Brewer's spent grain
BSY	Brewer's spent yeast
Caco-2	Human adenocarcinoma colon cancer cell monolayer
CCD	Central composite design
CHP	Cyclo-His-Pro
CE	Catechin equivalents
CPY	Carboxypeptidase Y
CPS	Carboxypeptidase S
DAD	Diode array detector
DH	Degree of hydrolysis
DMEM	Dulbecco's modified eagle medium
DMSO	Dimethyl sulfoxide
DPPH	2,2-diphenyl-1-picrylhydrazyl
DPP-IV	Dipeptidyl-peptidase IV
DRIs	Dietary Reference Intakes
dw	Dry weight
EAA	Essential amino acid
EAI	Emulsifying activity index
EFSA	European Food Safety Authority
ESI	Emulsifying stability index
E/S	Enzyme substrate ratio
ET	Electron transfer
FAA	Flavour amino acid
FAO	Food and agriculture organization of the United Nations
FAPGG	N-[3-(2-furyl)acryloyl]-L-phenylalanyl-glycyl-glycine
FE	Foam expansion
FS	Foam stability

FRAP	Ferric reducing antioxidant power
FPLC	Fast performance liquid chromatography
GAE	Gallic acid equivalents
GC/MS	Gas chromatography mass spectrometry
GFC	Gel filtration chromatography
GI	Gastrointestinal
GRAS	Generally recognized as safe
GSH	Glutathione
GSSG	Oxidized glutathione
HAT	Hydrogen atom transfer
HBBS	Hank's balanced salt solution
HepG2	Human hepatocarcinoma monolayer
HHL	N- $\alpha$ -hippuryl-L-histidyl-L-leucine
H29-MTX	Mucous-secreting HT29-MTX
H <sub>2</sub> O <sub>2</sub>	Hydrogen peroxide
HPLC	High performance liquid chromatography
HR	Hydrolysis rate
IC <sub>50</sub>	Peptide concentration required to inhibit ACE activity by 50%
ICAM-1	Intercellular adhesion molecule-1
ICP-MS	Inductively coupled plasma mass spectrometry
IL-8	Interleukin-8
LC	Liquid chromatography
LC-MS	Liquid chromatography mass spectrometry
LOD	Limit of detection
LOQ	Limit of quantification
MALDI-TOF	Matrix-assisted laser desorption/ionization time of flight
MCP-1	Monocyte chemoattractant protein 1
MTT	3-(4,5-Dimethylthiazol-2-yl)-2,5-diphenyltetrazolium bromide
MWCO	Molecular weight cut-off
NADPH	Reduced nicotinamide adenine dinucleotide phosphate
NO	Nitric oxide
NSI	Nitrogen solubility index
<i>nd</i>	Not detected
<i>np</i>	Not performed
<i>nq</i>	Not quantified
<i>nr</i>	Not reported

OBC	Oil binding capacity
P <sub>app</sub>	Apparent permeability coefficient
PBS	Phosphate buffered saline
PDA	Photodiode array detection
PER	Protein efficiency ratio
PR	Protein recovery
PrA	Protease A
PrB	Protease B
RAS	Renin-angiotensin system
RNA	Ribonucleic acid
RNS	Reactive nitrogen species
ROS	Reactive oxygen species
RP	Reducing power
RP-HPLC	Reverse-phase high performance liquid chromatography
RSM	Response surface methodology
SDS-PAGE	Sodium dodecyl sulfate polyacrylamide gel electrophoresis
SE-HPLC	Size exclusion high performance liquid chromatography
SHR	Spontaneously hypertensive rats
SPE	Sarcoplasmic protein extract
SPH	Sardine protein hydrolysate
TAA	Total amino acids
TE	Trolox equivalents
TEER	Transepithelial electrical resistance
TMRE	Tetramethylrhodamine ethyl ester perchlorate
TNBS	Trinitrobenzenesulfonic acid
TNF- $\alpha$	Tumor necrosis factor $\alpha$
TPC	Total phenolic content
TPTZ	2,4,6-tris(1-pyridyl)-5-triazine
UF	Ultrafiltration
VEGF	Vascular endothelial growth factor
WBC	Water binding capacity





## MOTIVATION AND RESEARCH AIMS

Brewing and canned fish industry generate annually significant amounts of by-products. Due to the global intense pressure towards green environmental technology, finding alternatives to reduce the pollution arising from these two agro-industrial activities is a major cause of concern. Efforts have been done to reduce the amount of waste by finding alternative uses for by-products apart from the current general use for animal feed or incineration. The main challenge is to convert the underutilized by-products into more profitable and marketable products. An alternative is to extract the protein fraction of these by-products and hydrolyze to obtain biological active peptides. The search for Angiotensin I-converting enzyme (ACE) inhibitors and antioxidants, with little or no side effects compared to the available synthetic ACE inhibitors (such as, captopril) and antioxidants forms (such as,  $\alpha$ -tocopherol and butylated hydroxyanisole) have received great attention (1).

In Portugal, two important industries facing this challenge are the Unicer- Bebidas de Portugal, S.A. brewing (Leça do Balio, Portugal) and the canned sardine industry Conservas Ramirez & Cia (Filhos), SA (Matosinhos, Portugal). The main by-products generated by the brewing are brewer's spent grain (BSG), brewer's spent yeast (BSY) and brewer's spent hops (2). In 2013, Unicer brewing generated 42.261 tonnes of by-products, corresponding more than 96% to BSG (36.958 tonnes) and yeast surplus (6.257 tonnes) (3). These by-products contain more than 20% of protein and are generally sold for local producers as protein supplements for cattle feed (2). Other possibility is incineration, however it comprises an environmental problem due the gas emission effects (4). Several attempts have been described to reuse BSG and BSY through the recovery of valuable nutrients or production of protein hydrolysates (5), (6). BSG protein hydrolysates have been recognized to possess antioxidant, anti-inflammatory,  $\alpha$ -glucosidase inhibitory and dipeptidyl-peptidase IV (DPP-IV) inhibitory activities (6). Technological-functional properties of BSG protein isolates/hydrolysates have also been studied (7), (8). Concerning to BSY, applications in aquaculture, food industry, cosmetic and pharmacology are described (5), (9), (10). Moreover, several laboratory preparations of yeast enzymes have been characterized and purified, from which protease B (PrB) and Carboxypeptidase Y (CPY) have been the most extensively studied (11).

Canned sardine industry generated annually several solid wastes including heads, tails and viscera, which constitute more than 40% of the original raw material (12), (13). In 2009, Conservas Ramirez & Cia (Filhos), SA generated 5.060 tonnes of by-products (14). This material is an important source of proteins, being traditionally transformed into powdered fish flour for animal feed (12). However, to increase the commercial value of sardine proteins by-product, an interesting alternative is to digest these proteins into biologically active peptides (15-17). Certainly, the current conditions of handling and preservation of sardine by-products must be improved if they are intended as raw material for the production of Sardine Protein Hydrolysates (SPH). Additionally, as sardine is a pelagic-oil fish, the oil recovery should be an important step because its presence in the obtained SPH represents a problem due to its oxidation (13). SPH have industrial applications well evidenced by the commercial products available in the market, such as, Valtryon® and Lapis Suport® (18), (19). Industrial application of SPH include food and feed industry, agriculture, biotechnology, cosmetics and biomedical sectors due to their nutritional value, biological activities and good functional properties, particularly high water solubility. The main biological properties of SPH reported included: antioxidant, antihypertensive, antithrombotic, immunomodulatory, antimicrobial, among others (12), (13), (20).

The major goal of this thesis was to find new application for the by-products generated from the brewing and canned fish industry, as a source of bioactive hydrolysates and its potential use for production of new bioactive ingredients. For this purpose, a BSY extract was obtained by mechanic disruption procedure to recover valuable compounds (enzymes, proteins, vitamins, antioxidant compounds) and chemically and nutritionally characterized. SPH and BSG protein hydrolysates were produced by the action of proteases present in the BSY extract. The antioxidant and ACE-I activities of BSY extract, SPH and BSG protein hydrolysates were screened by chemical and cell-based assays. In order to predict the *in vivo* bioavailability of the bioactive compounds generated, the impact of gastrointestinal (GI) digestion and the permeability through Human adenocarcinoma colon cancer cell monolayer (Caco-2) and Caco-2/HT29-MTX cell models were also evaluated, aiming to find valorization of these agro-industrial by-products, which is advisable from both economic and environmental standpoints. Figure i.1 presents a schematic overview of the major aims of this thesis.

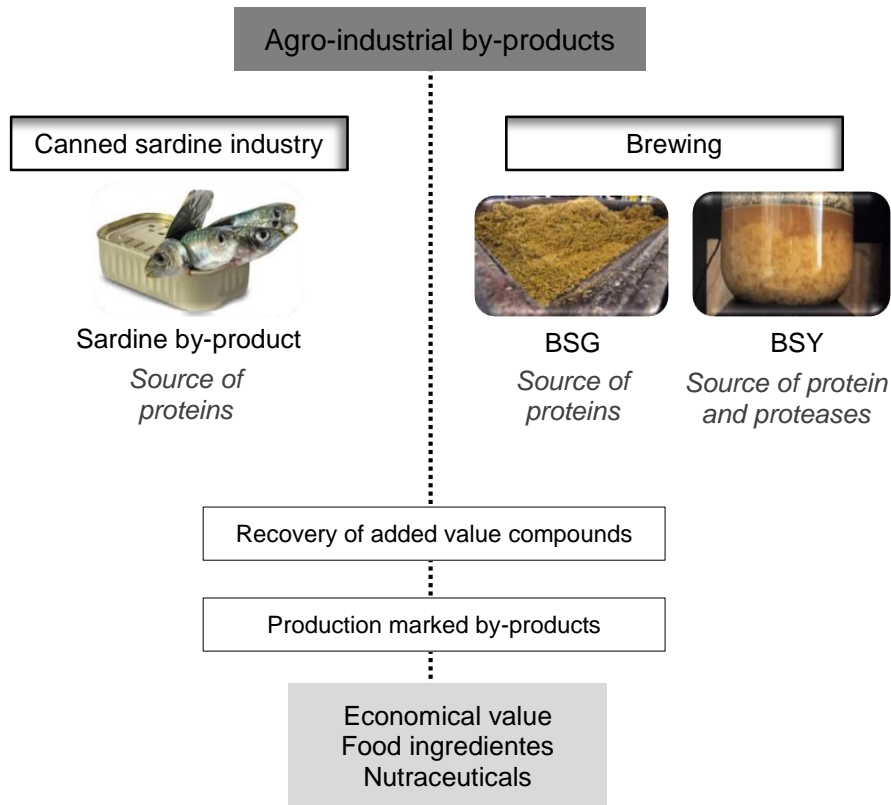


Figure i.1. Recovery of added value compounds from brewing and canned sardine agro-industrial by-products for production of SPH and BSG protein hydrolysates.

To accomplish the main goal of this thesis, different specific objectives were established:

1. Assess the biological activities of BSY extract prepared by mechanical disruption and its stability during storage at -25°C for 6 months;
2. Study the influence of number of reuses of yeast in beer fermentation step on the biological activities of the BSY extract;
3. Optimize the autolysis conditions to enhance the antioxidant and ACE-I activities of the BSY extract;
4. Assess the stability of the antioxidant and ACE-I activities of the BSY autolysate to GI proteases and to transport across Caco-2 and Caco-2/HT29-MTX co-culture models;

5. Optimize the hydrolysis of sardine sarcoplasmic proteins by BSY proteases to produce a SPH with enhanced antioxidant and ACE-I activities;
6. Evaluate of the effect of Ultrafiltration membranes in the antioxidant and ACE-I activities of the SPH, prepared by action of BSY proteases;
7. Assess the stability of the antioxidant and ACE-I activities of the SPH, prepared by action of BSY proteases to GI proteases and to transport across Caco-2 and Caco-2/HT29-MTX co-culture models;
8. Screen for the anti-inflammatory activity of the SPH, prepared by action of BSY proteases;
9. Compare the functional properties of muscle and viscera SPH prepared by BSY proteases and by the commercial enzymes Alcalase® and Neutrase®;
10. Optimize the hydrolysis conditions of BSG proteins by the BSY proteases to produce a BSG protein hydrolysate with enhanced antioxidant and ACE-I activities;
11. Compare the antioxidant and ACE-I activities of the BSG protein hydrolysate prepared by BSY proteases and by the commercial enzymes Alcalase® and Neutrase®.

## THESIS OUTLINE

This thesis is divided in three parts (**Part I**, **Part II** and **Part III**), which closely mimic the development of the research program. Each part is organized in two sections: a “Literature review” and the “Experimental work”. Chapters regarding to “Experimental work” are related with each other, and the approach chosen in each one was dependent on the conclusions attained in previous one(s). Each chapter contain their own introduction, material and methods, experimental results and discussion, and a brief conclusion. The text of this thesis is overall organized in thirteen chapters followed by the “General conclusions and Future prospects” obtained with this thesis. Figure i.2 presents a schematic overview of the organization of this thesis.

**Part I** entitled “Brewer’s spent yeast extract” includes Chapter 1 to 5. **Chapter 1** is a literature overview of BSY nutritional characteristics and applications, the common cell disruption processes used to produce BSY extracts; as well as, the main biological activities reported for BSY autolysates and hydrolysates.

- **Chapter 2** describes the potential use of a BSY extract prepared by mechanical disruption as a source of proteolytic enzymes and antioxidant and ACE-I activities;
- **Chapter 3** explores the influence of the yeast reuse during beer fermentation step on the proteolytic activity and antioxidant and ACE-I activities of the BSY extract prepared by mechanical disruption;
- **Chapter 4** reports the autolysis optimization of the BSY extract to enhance its antioxidant and ACE-I activities;
- **Chapter 5** describes the simulated GI digestion and the *in vitro* intestinal cell permeability of the BSY autolysate with enhanced antioxidant and ACE-I activities.

**Part II** entitled “Sardine protein hydrolysates” includes Chapter 6 to 10. **Chapter 6** is a literature overview of the canned sardine by-product, it describes the characterization of sardine sarcoplasmic proteins, the typical process adopted for the manufacturing of SPH and the main biological activities reported.

- **Chapter 7** reports the hydrolysis optimization of the sardine sarcoplasmic proteins by BSY proteases to produce a SPH with antioxidant and ACE-I activities;
- **Chapter 8** describes the simulated GI digestion and the *in vitro* intestinal cell permeability of the SPH with antioxidant and ACE-I activities;

- **Chapter 9** explores the potential anti-inflammatory properties of the SPH prepared by action of the BSY proteases;
- **Chapter 10** compares the biological activities and techno-functional properties of different muscle and viscera SPH prepared by action of BSY proteases and the commercial enzymes: Alcalase® and Neutrase®.

**Part III** entitled “Brewer’s spent grain protein hydrolysates includes Chapters 11 to 13. **Chapter 11** is a literature overview of the BSG nutritional characteristics and applications, it also describes the typical enzymatic process adopted for the manufacturing of BSG protein hydrolysates and the main biological activities reported.

- **Chapter 12** reports the hydrolysis optimization of BSG proteins by BSY proteases with antioxidant and ACE-I activities;
- **Chapter 13** compares the biological activities of different BSG protein hydrolysates prepared by action of BSY proteases and the commercial enzymes: Alcalase® and Neutrase®.

The experimental work was mainly developed in the following research laboratories:

- LAQV/REQUIMTE, Laboratory of Bromatology and Hydrology, Department of Chemical Sciences, Faculty of Pharmacy, University of Porto (Portugal);
- UCIBIO/REQUIMTE, Laboratory of Toxicology, Department of Chemical Sciences, Faculty of Pharmacy, University of Porto (Portugal);
- CICS, Department of Pharmaceutical Sciences, Instituto Superior de Ciências da Saúde-Norte (Portugal);
- QOPNA, Mass Spectrometry Center, Department of Chemistry, University of Aveiro (Portugal);
- Research Group Food Chemistry and Human Nutrition, Department of Food Safety and Food Quality, Faculty of Bioscience Engineering, University of Gent (Belgium).

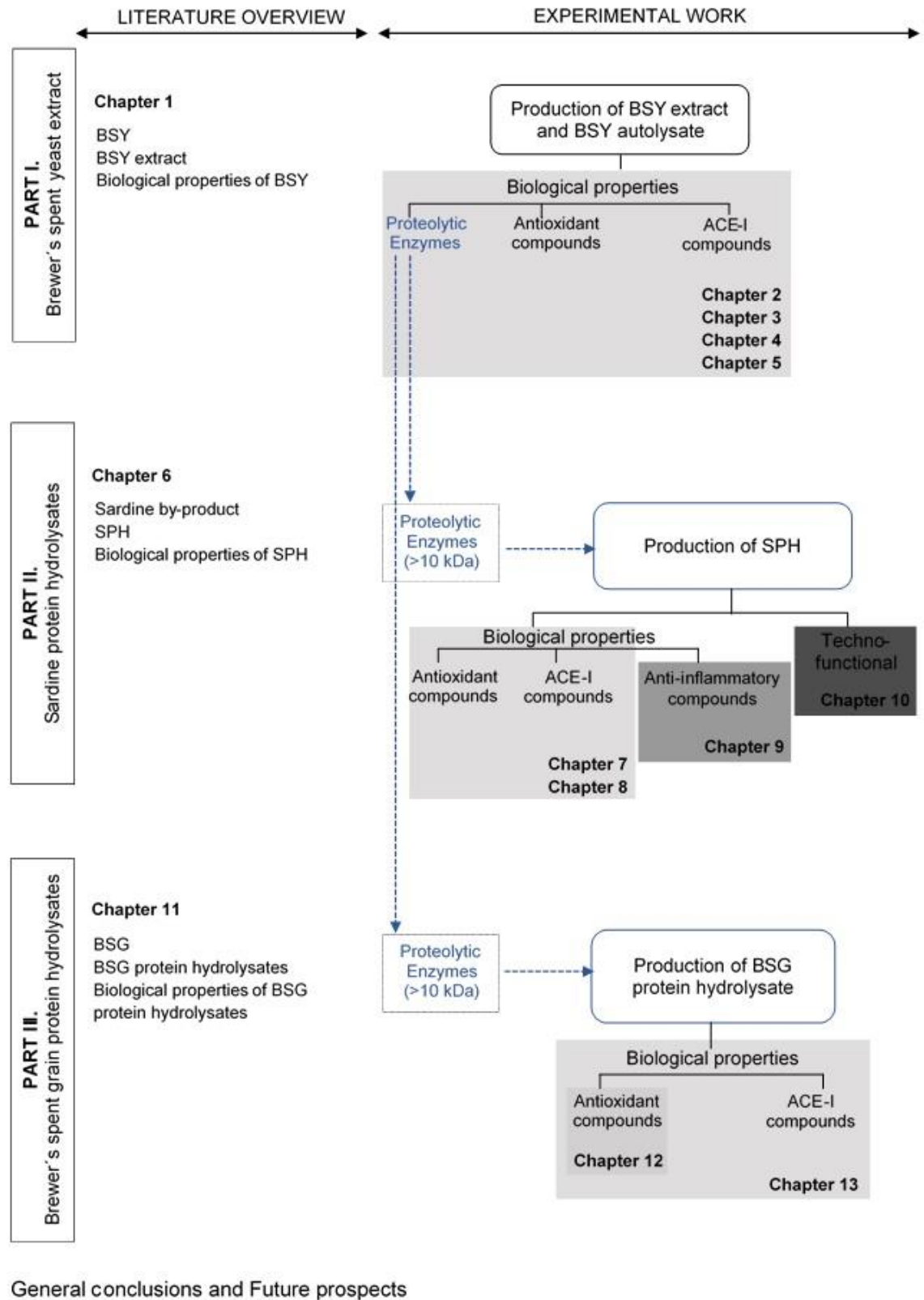


Figure i.2. Schematic overview of the organization of the Ph.D. thesis, with indication of the different chapters included in each part (I, II and III).





# **PART I**

## **“Brewer’s spent yeast extracts”**

---

### **Chapter 1**

#### **Literature review**

*Brewer’s spent yeast: potential source of biological compounds and proteases for application in the production of food hydrolysates*

### **Chapter 2**

*Nutritive value, antioxidant activity and phenolic compounds profile of Brewer’s spent yeast extract*

### **Chapter 3**

*A bioactive ingredient obtained from the inner cellular content of Brewer’s spent yeast*

### **Chapter 4**

*Autolysis of intracellular content of brewer’s spent yeast to maximize ACE-inhibitory and antioxidant activities*

### **Chapter 5**

*Impact of in vitro gastrointestinal digestion and transepithelial transport on antioxidant and ACE-inhibitory activities of brewer’s spent yeast autolysate*



# CHAPTER 1

## Literature review

*Brewer`s spent yeast: potential source of biological compounds and proteases for application in the production of food hydrolysates*

---

This chapter presents a literature overview of BSY nutritional characteristics and applications, the common cell disruption processes used to produce BSY extracts; as well as, the main biological activities reported for BSY autolysates and hydrolysates.



## 1.1. Brewer's spent yeast

### 1.1.1. By-product

Brewer's yeast is an important ingredient in the beer production. Besides the ethanol and carbon dioxide production, yeast cells are responsible for the formation of compounds essential for the sensorial profile of beer, namely organic acids, esters, aldehydes, ketones and sulfur compounds (5). Brewer's yeast are conventionally classified into the categories of Ale and Lager yeasts. Lager ("bottom-fermenting") yeast are *Saccharomyces pastorianus* strains that run the fermentation at cool temperatures (8-15 °C) and forms a cloudy mass (floculates) on the bottom of the vessel, while Ale yeast ("top-fermenting") are *Saccharomyces cerevisiae* strains that run the fermentation in the temperature range of 16-25 °C and rise to the surface of the vessel, facilitating their collection by skimming (5), (21).

During beer fermentation stage, and depending on the fermentation conditions of each brewery, yeast tends to multiply between three to six fold in the reactor, especially during the early hours when oxygen is supplied to the wort (5), (22). It is a common practice in brewing the reuse of the cell mass generated by inoculation in a new fermentation tank. The number of reuses depend on species, type of beer produced, and amount of the wort extract and the microbiological viability of yeasts. Typically, yeast mass can be reused between 3 to 10 times without compromising the sensory quality of beer. Yeast cells that are removed from the process generates a solid by-product called Brewer's spent yeast (BSY) (22).

BSY is the second major by-product from brewing process (after BSG) (5). In lager fermentation, the typical total amount of BSY produced ranges between 1.7 kg/m<sup>3</sup> and 2.3 kg/m<sup>3</sup> of final product (23). It is composed by 10-14% total solids, including yeast solids, beer solids and trub solids (5).

### 1.1.2. Nutritional composition

On a dry weight (dw) basis, cell wall constitutes 15-20% of the yeast weight, comprising 80-90% polysaccharides, particularly glucans and mannans, and a small amount of proteins and lipids (3). The mannans from cell wall are linked to proteins and are commonly described as mannoproteins, these are important structural components of the cell wall. Figure 1.1 illustrates the microscopic structure of yeast cell and the proximate composition (% dw) of BSY.

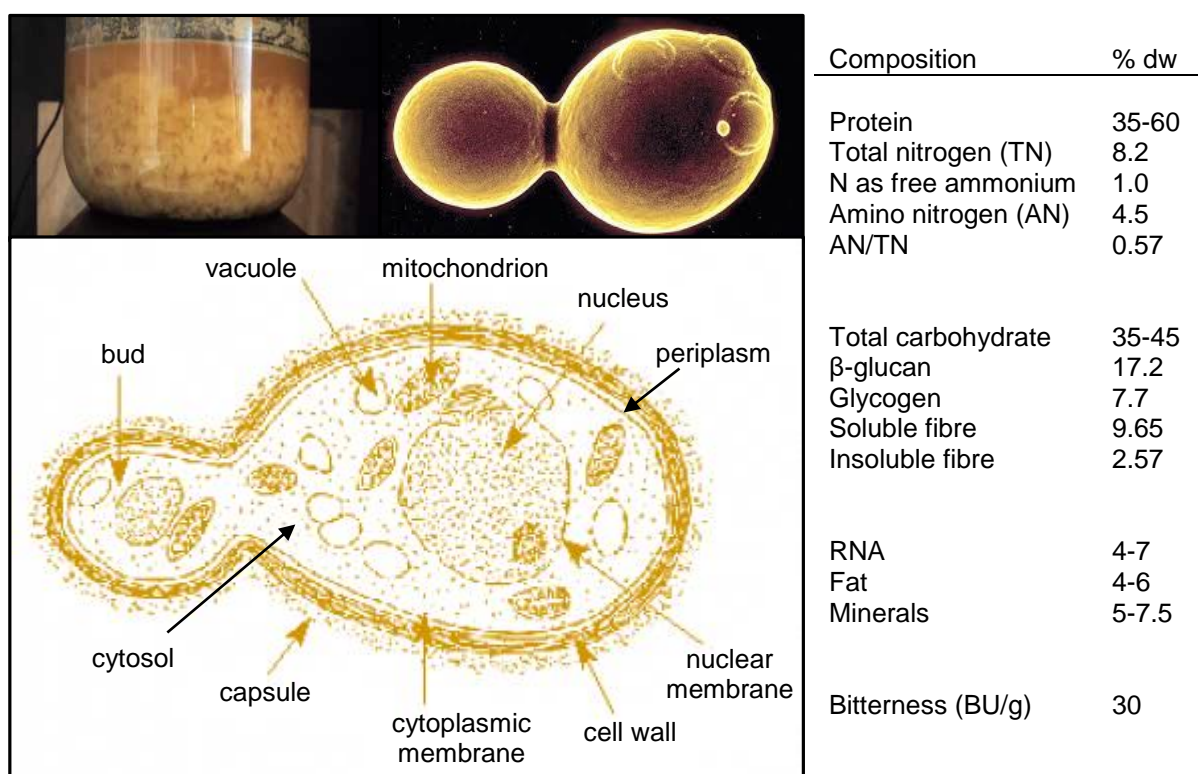


Figure 1.1. Microscopic structure of yeast cell and proximate composition (% dw) of BSY. The figure yeast diagram was taken from Northern Arizona University (2008) (24). Proximate composition is based on chemical analysis reported by (22), (25-27).

The nutritional composition of BSY has been reported by several authors (22), (24-27). BSY is predominantly composed by proteins, ranging between 35 and 60% (dw), which have high biological value, representing between 70-85% of casein value (25), (28). The most abundant amino acids of BSG are lysine, leucine, valine, tryptophan, threonine and phenylalanine, and it is slightly deficient in sulfur amino acids, such as, cysteine and methionine (29), (30). The amino acids score of BSY is 98.1%, presenting a well-balanced amino acid profile for human consumption (25). Other components of BSY are carbohydrates (35-45%); lipids (4-6%); and minerals (5-7.5%), namely calcium, phosphorus, potassium, selenium, chromium, magnesium and iron (6), (22), (30-32). BSY is a good source of a biologically active form of chromium trivalent, known as glucose tolerance factor, which has been extensively studied for its medicinal properties (5). The yeast intracellular compartment is mostly composed of soluble proteins, B-complex vitamins, nucleic acids, minerals and enzymes (5).

### **1.1.3. Antioxidant system**

Reactive oxygen species (ROS) and reactive nitrogen species (RNS) can damage different cell macromolecules, being related to the development of several diseases (33). Yeast cells contain enzymatic and non-enzymatic defense systems to protect their cellular constituents and maintain the cellular redox state. Figure 1.2. presents the main classes of antioxidant defense in yeast cells. The antioxidant mechanisms of yeast have been reviewed by several authors (33-37). Several enzymes, including catalase, superoxide dismutase, glutathione reductase, thioredoxin reductase and methionine reductase, are capable of removing ROS and RNS and their products and/or repairing the damage caused by oxidative stress (35). Catalase catalyses the breakdown of hydrogen peroxide to oxygen and water, while superoxide dismutases catalyses the breakdown of superoxide anion to hydrogen peroxide and oxygen. The enzymes glutathione reductase and thioredoxin reductase require nicotinamide adenine dinucleotide phosphate (NADPH) to reduce oxidized glutathione (GSSG) and thioredoxin, respectively. The enzyme glutathione reductase is primarily responsible for the reduction of GSSG and maintenance of the glutathione (GSH)/GSSG ratio in cell, whereas the enzyme glutathione peroxidase catalyses the reduction of hydroperoxides, using GSH as a reductant. Thioredoxin peroxidase reduces both hydrogen peroxide and alkyl hydroperoxides, in combination with thioredoxin reductase, thioredoxin and NADPH.

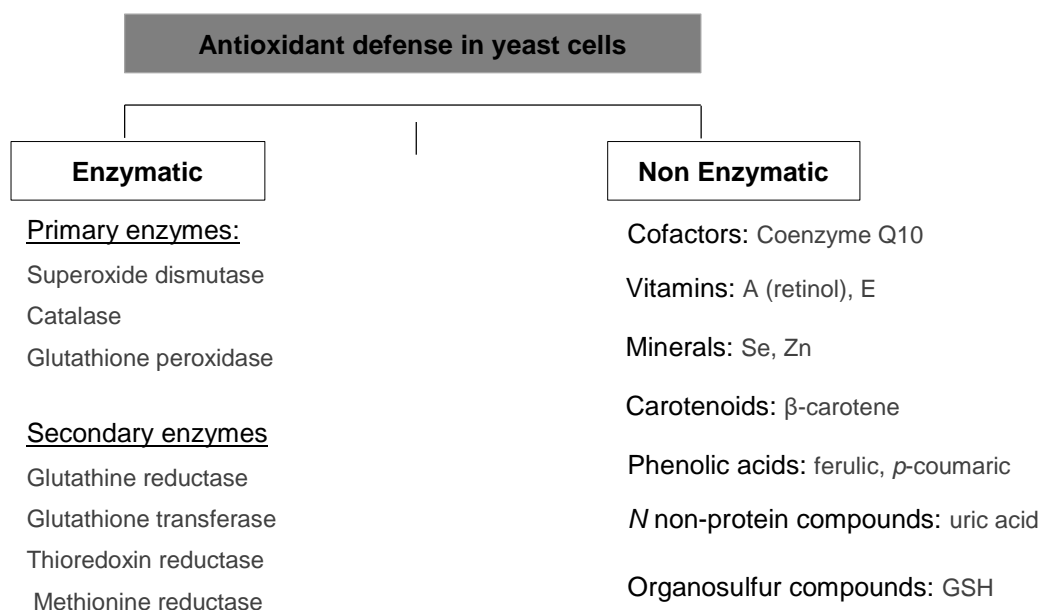


Figure 1.2. Classes of natural antioxidants of yeast cells. Adapted from (38).

Besides the enzymatic protection against ROS and RNS, there are small molecules, soluble in aqueous or (in some cases) lipid environments, that act as radical scavengers. Some examples include Coenzyme Q10, GSH, polyamines, glutaredoxin, ascorbic acid, phenolic compounds, vitamin E and vitamin A (35). Recently it has been proposed that methionine residues exposed on the surface of proteins can also act as antioxidants to protect the active sites of proteins (35). GSH, a tripeptide  $\gamma$ -L-glutamyl-L-cystinylglycine, acts as a radical scavenger, reacting with oxidants to produce GSSG. In addition to GSH, amino acid-derived polyamines have also been implicated in protecting yeast against oxidative stress. Other example are glutaredoxins, a class of small proteins with an active site containing two redox sensitive cysteines, which act as a source of electrons for ribonucleotide reductase.

Although yeasts are non-photosynthetic microorganisms, some yeasts can biosynthesize carotenoids and phenolic compounds. Due to their free radical scavenging and/or provitamin A (carotene) potential, carotenoids and phenolic compounds prevent various types of cancer and other diseases (39). According to Moreira [PhD dissertation] (40), ferulic acid and *p*-coumaric acid are the main contributors for the phenolic composition of BSY. Although yeasts synthesize erythroascorbate instead of ascorbate, there are few reports describing the presence of ascorbic acid in *Saccharomyces cerevisiae* (35), (41). Vitamin E acts as a lipid-based radical chain breaking molecule with scavenging capacity



for free radicals, such as, lipid peroxy, alkoxy and hydroxyl radicals. Trolox, a water-soluble analog of vitamin E, decreased the levels of hydrogen peroxide and superoxide, as well as, increased the activity of enzymatic antioxidants in yeast. Vitamin E has also been described to have regulatory actions in inducing antioxidant enzymes synthesis. Other micronutrients, such as, manganese, copper, zinc and selenium, are components of antioxidant enzymes and have been reported in yeast (33).

#### **1.1.4. Enzymatic system**

Yeast vacuole has a slightly acidic environment (pH ~6.2) compared with the cytosol (pH ~7.2) and contains several proteases, including protease A (PrA), PrB, CPY, carboxypeptidase S (CPS), aminopeptidase I (API), aminopeptidase Co and dipeptidyl aminopeptidase B (11), (42), (43). These vacuolar exopeptidases and endopeptidases are released from autolyzed cells and may promote protein degradation to generate smaller peptide fragments (44). These enzymes are classified as metalloproteases, serine proteases and aspartyl proteases (11). In brief, serine proteases comprise a large family whose enzymatic activity is mediated by a characteristic catalytic triad consisting of asparagine, histidine and serine. In contrast, metalloproteases depend on metal ions, especially  $Zn^{2+}$  for their catalytic function, and the aspartyl proteases are characterized by two catalytic asparagine residues, mediating an acid-base hydrolysis reaction (11).

PrA is a monomeric 42 kDa aspartyl endoprotease with a key role for the vacuolar protease activation cascade. PrB, CPY and AP depend on PrA for proteolytic activation. PrB is a 76 kDa serine endoproteases; CPY is a serine carboxypeptidase and initially synthesized as a ~60 kDa precursor; CPS is a zinc-dependent metallo-carboxypeptidase and initially synthesized as a ~64 kDa precursor and AP1 is a zinc-dependent metallo-aminopeptidase and initially synthesized as a ~61 kDa precursor (11).

#### **1.1.5. Potential applications**

BSY is currently underutilized, sold primarily as inexpensive animal feed after inactivation by heat (45). Alternatives are incineration of this organic solid waste, or put into landfill, both procedures causes losses of its proteins and amino acids, and other useful substances (46) and causes environmental concerns (47).

Due to the fact that BSY holds the GRAS status (Generally Recognized as Safe), it can be used in food and pharmaceutical industries (10), (48). BSY should not be confused with “brewer’s type yeasts” or “nutritional yeasts”, which are pure yeasts usually grown under controlled production conditions for specifically use as a nutritional supplement (5), (31), (49). As referred, BSY possess high quality proteins, which contains essential amino acids, particularly, lysine, isoleucine and threonine. Therefore supplements of brewer’s yeast are useful for low-calorie diets that are deficient in proteins (5). However, a limiting factor in utilization of BSY as a protein source for human consumption is its high content of ribonucleic acid (RNA) content. Some reagents and techniques are used for isolation of yeast protein with low RNA content (5), (50).

BSY can be used in food industry to produce yeast protein concentrates, usually commercialized in the form of powders, flakes or tablets or in liquid form (5). BSY can also be used to produce BSY extracts, presenting several biological properties, to be applied in aquaculture, food, cosmetic and pharmaceutical industries (9), (10), (36), (51-53). Moreover, yeast cells contain numerous enzymes, being the industrial extraction of these enzymes an interesting field to explore. Potential applications of BSY were reviewed by our research group (5). The potential applications of BSY as functional food ingredients for animal and human nutrition are described on Table 1.1.

Table 1.1. Potential applications of BSY as functional food ingredients for animal and human nutrition

Yeast-derived products	Potential applications	Reference
Vitamins (riboflavin, folic acid and biotin)	- used as colorants of foods - used as vitamin supplements	(36), (54)
Minerals (selenium, chromium, zinc, iron, copper, manganese)	- used as mineral supplements - extraction of glucose tolerance factor	(36)
Lipids (lecithin, choline, glycerol, inositol, glycolipids)	- contribute to flavour of foodstuffs - used as emulsifiers and surfactants - used to fortify foods and food supplements	(36)
RNA (ribonucleotides: 5'-IMP, 5'-GMP)	- enhance mouthfeel of soups, sauces, marinades, soft drinks, cheese spreads, and seasonings – contribute to the “meaty” flavour	(50)
Dietary fiber (glucans, mannans, chitin)	- potent immunostimulant used as additive in diet of several animals - lower serum cholesterol level and reduce the risk of heart diseases	(27), (55-59)
Proteins (mannoproteins)	- used as protein supplement - used as gelling and emulsifying agents - lower serum cholesterol level and reduce the risk of heart diseases	(25), (30), (56), (60), (61)
Amino acids (monosodium glutamate, MSG)	- contribute to flavour of foodstuffs	(36), (62)
Peptides (CHP), Cyclo-His-Pro (GSH), $\gamma$ -L-glutamyl-L-cysteinyl-glycine) (AdoMet), S-Adenosyl-L-methionine)	- used in glucose tolerance/ antidiabetic agent - used as antioxidant - used in pharmaceutical industry	(45), (63)
Enzymes (PrA, PrB, oxidoreductase)	- used to block Maillard reaction of dicarbonyl intermediates, thereby preventing their decomposition to off-flavour final products	(36), (54), (64), (65)
Phenolics and Flavonoids (sterols, gallic acid, catechin)	- antioxidant activity	(36), (40)
Carotenoids (astaxanthin, lutein, torulene, $\beta$ -carotene, $\gamma$ -carotene, lycopene, torulahordin, zeaxanthin)	- used as food colorants	(36)

## 1.2. Production of BSY extract

The cytoplasm of yeast cell is a valuable source of proteins, peptides, enzymes, RNA, minerals, vitamins, among other compounds. The recovery of these intracellular compounds implies an efficient breakage of the cell walls; the final product is called yeast extract (48), (66). The identification of a suitable cell disruption method is very important to promote an efficient and cost effective recovery of the intracellular products with reduced contaminants and minimal micronization of cell debris (67), (68).

Disruption technique can be classified into mechanical (employing shear force) and non-mechanical (physical, chemical or enzymatic lysis) methods, as summarized in Figure 1.3.

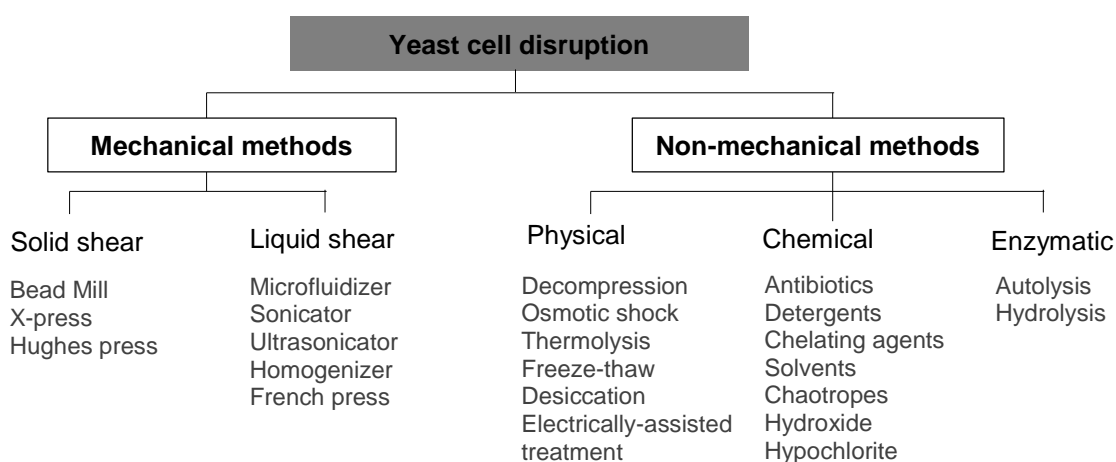


Figure 1.3. Classification of disruption techniques. Adapted from (69).

The non-mechanical methods, particularly the autolysis process, are commonly used at the laboratorial scale (50). In opposite, the mechanical methods are most appropriate for large-scale disruption and allow high recovery yields. In the mechanical methods, cell wall is broken due to stress produced by high pressure, cavitation, sonication, ultrasound or abrasion during rapid agitation with glass beads (69). Its application is restrict due to the temperature elevation, requiring multiple steps of cooling, and the large quantity of cell debris in the final products (66), (67). At laboratorial scale, cell disruption using glass beads is routinely used, as well as, some high-pressure methods as the Hughes press or the French press. Bead mill, high pressure homogenizer and high-intensity ultrasound are mechanical methods scalable for industrial use (69).

In the Ultrasonication method, an intense shear action induced by high frequency sonic waves is used for cell wall disintegration. This method creates high shear force by high-frequency ultrasound (above 16 kHz) (66). Although ultrasonic is rather effective for lysis of yeast cells, it is usually accompanied by temperature increase, high content of cell debris and undesirable formation of chemical compounds (67). In the Bead Mill method, compounds are released from cells due to the action of circulating beads dispersed in the fluid (66), (70), it can be operated either in batch or in a continuous recycling mode (70). The major disadvantages of using Bead Mill and homogenizer are the poor selectivity in product release (i.e. the co-release of contaminants) and micronization of the cell debris, either of which can substantially increase the costs of subsequent downstream operation (46). The efficiency of mechanical cell disruption is usually monitored by measuring the amounts of proteins released; the activity of recovered enzymes or the number of surviving cells (69).

The limitations associated with mechanical methods have inspired search of alternative methods for recovery of intracellular compounds from BSY. Currently, application of electrotechnologies, such as, the Pulsed electric field and High-voltage electrical discharges, are promising for intracellular extraction from bio-suspensions (68). Additionally, Electroporation has many advantages when compared with other disruption techniques, since it exerts a minimal undesirable impact on liquid components inside and outside the cell and can be done without significant temperature increase and formation of cell debris (67). Also, Lamoolphak *et al.* (47) used Hydrothermal decomposition of yeast cells for production of proteins and amino acids (using subcritical or supercritical water).

Recovery of enzymes fraction by Ultrasonication and Bead Mill methods are the most effective for the destruction of cell wall while maintaining enzymes activity (70). In order to optimize the yield of cell disruption, beads with 0.25-0.75 mm of diameter and 40-50% cells (wet weight) is recommended (69). The pH of the disruption media also plays an important role because the enzymes/ proteins released after cell disruption must maintain their activity/ native structure (71). Figure 1.4. displays an example of yeast wall mechanical disruption (using glass beads) procedure, applied at laboratorial scale.

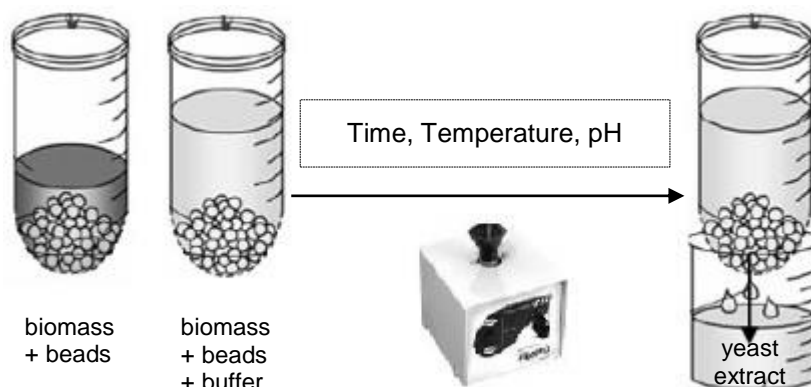


Figure 1.4. Yeast wall mechanical disruption, using glass beads, applied at laboratorial scale.

Non-mechanical processes of yeast cell wall disruption are alternatives to mechanical disruption techniques and include physical, chemical and enzymatic methods (70). Physical methods result in large cell debris, which is a limitation for separation of soluble proteins, enzymes or other bio-products (69). An example is Decompression, based on introducing a pressurized subcritical or supercritical gas into the cells causing the cell disruption. Other possibilities are the Osmotic shock, where a cell suspension is diluted after equilibration in high osmotic pressure, and the Thermolysis. Chemical permeabilization can be promoted by antibiotics (penicillin, polymyxin), chelating agents (EDTA), chaotropes (urea, guanidine, ethanol), detergents (Triton-X, sodium dodecyl sulphate, sodium lauryl sarcosinate), solvents (toluene, chloroform, acetone) or by hydroxides and hypochlorites. However, chemical permeabilization with solvents or detergents does not result in the release of intracellular enzymes (69).

The term autolysis means 'self-destruction', it represents self-degradation of the cellular constituents of a cell by its own enzymes (5), (72). The first step is disorganization of membranous systems, including cytoplasmic membrane and other organelles. This allows that the enzymes come in contact with cellular constituents, which are degraded and solubilized. The proteases attack the proteins and break them down into smaller constituent units, such as, peptides and amino acids. Likewise, enzyme nuclease degrades RNA and DNA yielding compounds, namely, nucleosides, mononucleotides and polynucleotides. Glucanases and proteases degrade the cell wall constituents such as, glucans and mannoproteins, which make the cell wall to become porous. Consequently, the autolysate (the mixture of degraded cellular components) leaks through the cell wall into the surrounding medium (73). Yeast autolysis is strongly influenced by temperature and pH (72).

By contrast, hydrolysis is accomplished by proteolytic enzymes and cell wall lysis enzymes. This process aims the production of a yeast extract with a low salt content (48). Several kinds of enzymes from bacterial, vegetable, yeast or animal origin have been used to produce BSY extracts, including Glucanases (74); Proteases (74), (75); Nucleases (29), (74); Deaminases (29), (74); Pepsin (75); Trypsin (75); Pancreatin (76); (77); Flavourzyme (29), (45), (48), (76), (78); Protamex (10), (45), (48), (78); Alcalase (45) and Neutrase (45).

### 1.3. Biological activities of BSY extract

BSY autolysates and hydrolysates are a source of nutrients and bioactive compounds, acting as nutraceuticals in animal and human nutrition (5). The recent patent by Esteves *et al.* (79) describes a method for obtaining peptide and polysaccharide extracts from BSY by hydrolysis with an enzymatic extract of *Cynara scolymus* flowers (55°C, 3 h), followed by Ultrafiltration (UF) techniques. These BSY hydrolysates are claimed to present anti-hypertensive, anti-inflammatory, anti-ulcerative, antioxidant, antidiabetic, prebiotic, anticancer, antimicrobial and anti-obesity properties, with potential applications in the human and animal diet, as well, in pharmaceuticals. A summary of biological activities of BSY autolysates/ hydrolysates, as well as, the process preparation employed is presented in Table 1.2.

BSY extracts have also been used as source of enzymes to produce protein hydrolysates from different food matrices. For instance, bovine skimmed milk digested with purified PrB from the cell-free extract of the BSY was found to inhibit proliferation activity of HL-60 cells (44). The same authors also reported an ACE-I activity ( $IC_{50}$ ) of 0.42 mg of protein/mL when skimmed milk was digested with the same purified PrB (64). Additionally, application of crude BSY protease extract to pineapple (80); papaya juice (81); beetroot and carrot juices (82); starch (83) and dairy products (84), (85) appears quite promising.

Table 1.2. Biological activities assessed in BSY autolysates and hydrolysates

BSY extract preparation		BSY protein hydrolysis		Fraction / Purification	Assay	Bioactivity assessed	Reference
Method	Process	Enzyme	Hydrolysis				
ACE-I activity							
Cultivation	30°C, 24 h	Pepsin	E/S ratio: 1% (w/v), 37°C, 12 h, pH 2	(1) 5 kDa MWCO UF, (2) SE-HPLC, (3) RP-HPLC	HHL <sup>a</sup> as substrate	0.070 mg peptide /mL	(75)
<i>np</i>	<i>np</i>	Alcalase	E/S ratio: <i>nr</i> 50°C, 12 h, pH 7.5-8.5	(1) peptide adsorption trough an resin column, (2) SE-HPLC, (3) RP-HPLC, (4) Gel filtration HPLC	HHL <sup>a</sup> as substrate	3.0-3.4 µmol peptide/L	(86)
Antioxidant activity							
8% BSY suspension	<i>np</i>	Flavourzyme	E/S ratio: <i>nr</i> 50°C, 48 h, pH 7.0	Acid treatment, activated carbon and 5 kDa MWCO UF	ABTS DPPH	IC <sub>50</sub> = 0.9 mg peptide/mL IC <sub>50</sub> = 1.9 mg peptide/mL	(45)
<i>np</i>	<i>np</i>	Pancreatine	E/S ratio: <i>nr</i> 50°C, 5 h, pH 7.5-8.9	<i>np</i>	ABTS	IC <sub>50</sub> = 1.3 mg peptide/mL	(77)
Antidiabetic activity							
8% BSY suspension	<i>np</i>	Flavourzyme	E/S ratio: <i>nr</i> 50°C, 48 h, pH 7.0	Acid treatment, activated carbon and 5 kDa MWCO UF	CHP <sup>b</sup>	CHP = 674.0 µg/g	(45)

<sup>a</sup> HHL, Hippuryl-L-histidyl-L-leucine.

<sup>b</sup> CHP, Cyclo-His-Pro (is an endogenous cyclic dipeptide structurally related to hypothalamic tyrotropin-releasing hormone, suggested to relate glycemic control in diabetes). DPPH, 2,2-diphenyl-1-picrylhydrazyl; ABTS, 2,2'-azino-bis(3-ethylbenzthiazoline-6-sulphonic acid), MWCO, molecular weight cut-off.  
*np*, not performed, *nr*, not reported.



#### 1.4. Screening methods to search for autolysates/ hydrolysates bioactivity

Autolysates/ hydrolysates may contain bioactive peptides that have a positive impact on body function and positive influence on health beyond their basic role as nutrient sources (87). Bioactive peptides have low molecular weight (i.e. 3-20 amino acid residues) and their activity is based on size, amino acid composition and sequence. Furthermore, their biological responses depend on the ability to cross the intestinal epithelium and enter the blood circulation, or to bind directly to specific epithelial cell surface receptor sites to exert physiological functions of the organism (88), (89).

Several biological activities have been reported for food protein hydrolysates and for specific peptide sequences derived from these hydrolysates, namely, antioxidant, antihypertensive, anti-inflammatory, immunomodulatory, neuroactive, antimicrobial, mineral and hormonal regulating properties (Figure 1.5). Several *in vitro* methods have been developed for screening these properties and were reviewed by several authors (38), (87-99). The following section will focus on the *in vitro* antioxidant and ACE-I activities assays.

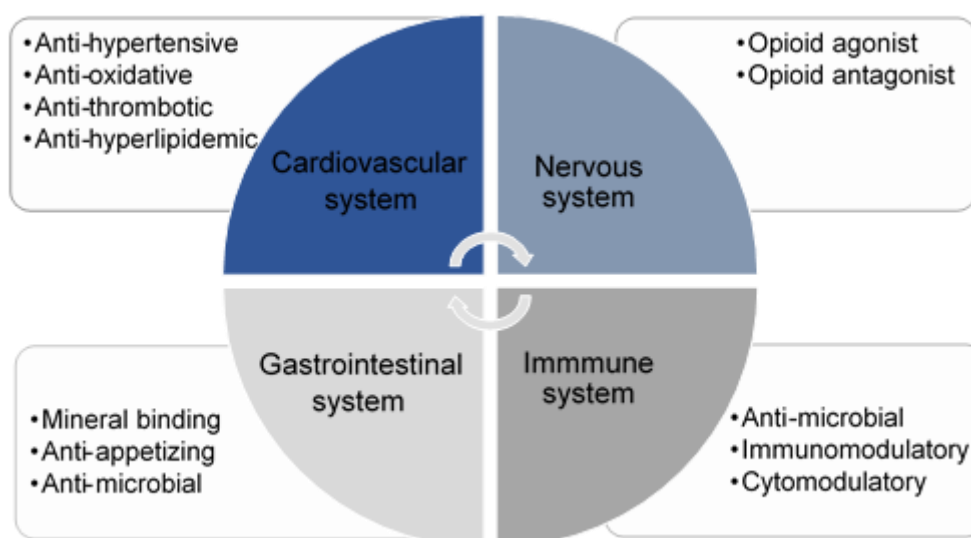


Figure 1.5. Physiological effects of food derived bioactive peptides on major body systems. Adapted from (100).

#### **1.4.1. *In vitro* Antioxidant chemical activity**

When the balance between the production and neutralization of ROS, RNS and free radicals by the antioxidant defense system is compromised, cells suffer the consequences of oxidative stress (38), (97), (101). The main targets of ROS, RNS and free radicals are proteins, DNA, RNA, sugars and lipids. Oxidative stress is linked to the development of several diseases, such as, neurodegenerative disorders, hypertension, inflammation, cancer, diabetes, Alzheimer disease, Parkinson's disease and ageing problems (38). Due to the potential health risks of synthetic antioxidants, as butylated hydroxyanisole (BHA), butylated hydroxytoluene (BHT) tert-butylhydroquinone (TBHQ) and propyl gallate (PG), the search for safe natural antioxidants is important (97), (102).

Due to the complexity of different oxidative processes and the possibility that an antioxidant acts by different mechanisms, it is very difficult to select a suitable antioxidant assay that measures the overall antioxidant potential of the compound (94). Moreover, the conditions of the assay and the antioxidants solubility in the reaction media may affect the antioxidant activity assessed (88). For this reason, various methods are suggested to measure the antioxidant activity (103). Specific assays have not yet been developed or standardized to measure the antioxidant activity of food hydrolysates (103).

The methods used for determining the antioxidant activity of a compound are classified in two main groups according to the chemical reactions involved: assays based on the hydrogen atom transfer reaction (HAT) and assays based on the electron transfer (ET) (97). HAT-based methods measure the ability of an antioxidant to quench free radicals by hydrogen donation; reactions are solvent and pH independent and are quite rapid. The main limitation of HAT assays is the presence of reducing agents (including metals), which can lead to incorrect high apparent reactivity (97). ET-based methods detect the ability of an antioxidant to quench free radicals, metals and/or carbonyls by electron transference (90). Other chemical assays that measure the scavenging capacity of individual ROS, such as, superoxide anion, singlet oxygen, hydrogen peroxide, hydroxyl radical and peroxynitrite, have been currently used and reviewed by several authors (90), (96), (98). Table 1.3 summarizes the most widely used assays for determination of the antioxidant activity of food protein hydrolysates and bioactive compounds.

Table 1.3. Classification of *in vitro* analytical methods for evaluation of the antioxidant activity of food protein hydrolysates and bioactive compounds. Adapted from (90), (94) and (96).

Classification	Assay		Principle of the method	Determination
HAT	ORAC	Oxygen radical absorbance capacity	Peroxyl radical reacts with a fluorescent probe to form a non-fluorescent product	Spectrofluorometry
	TRAP	Total radical trapping antioxidant parameter	Reaction between ROO· generated by AAPH and a target probe	Spectrofluorometry
	LPIC	Lipid peroxidation inhibition capacity	Uses a Fenton-like system (Co(II) + H <sub>2</sub> O <sub>2</sub> ) to induce lipid (e.g. fatty acid) peroxidation	Spectrophotometry
	ABTS	2,2'- azinobis (3-ethylbenzothiozoline-6-sulfonic acid)	ABTS radical reduction by oxidants	Spectrophotometry
ET	TEAC	Trolox equivalent antioxidant capacity	ABTS radical reduction by oxidants in comparison with trolox, a water soluble analogue of vitamin E	Spectrophotometry
	FRAP	Ferric ion reducing antioxidant parameter	Fe(III) complex reduction to Fe (II) by oxidants	Spectrophotometry
	DPPH	2,2-diphenyl-1- picrylhydrazyl	DPPH radical reduction by oxidants	Spectrophotometry
	CUPRAC	Cupric ion reducing antioxidant capacity	Cu (II) reduction to Cu (I) by antioxidants	Spectrophotometry
	TPC	Total phenolic assay by Folin-Ciocalteau reagent	Oxidation of phenolics in basic medium resulting in the molybdenum oxide (MoO <sub>4</sub> <sup>+</sup> ) formation	Spectrophotometry
	DMPD	N,N-dimethyl- <i>p</i> -Phenylenediamine assay	DMPD radical reduction by oxidants	Spectrophotometry
	RP	Reducing Power	Fe(III) complex reduction to Fe (II) by oxidants	Spectrophotometry

#### 1.4.2. Antihypertensive activity

Hypertension is strongly associated with cardiovascular diseases, leading to premature morbidity and mortality (104), (105). Emerging evidence indicates that bioactive peptides can promote antihypertensive effects via different mechanisms. The main group of antihypertensive peptides corresponds to the inhibitors of ACE. However, bioactive peptides can also interact with the renin-angiotensin system (RAS), Angiotensin II receptor, arginine-nitric oxide pathway, endothelin system and  $\text{Ca}^{2+}$  channels (105).

Physiologically, hypertension occurs when renin produces Angiotensin I from angiotensinogen (103). ACE (EC 3.4.15.1) is a zinc metallocarboxypeptidase, commonly found in vascular endothelial cells and neuroepithelial cells. This enzyme plays a significant physiological role in regulating blood pressure in the RAS; ACE can convert the inactive Angiotensin I into a potent vasoconstrictor, the Angiotensin II. At the same time, ACE also inactivates Bradykinin, a potent vasodilatory peptide. Hence, as ACE raises blood pressure, specific inhibitors of ACE are used as pharmaceuticals to treat hypertension (89), (103), (106), (107). Currently, several synthetic ACE-I, such as, captopril, lisinopril, enalapril and fosinopril, are been used to treat hypertension, however, they are known to have strong side effects, including coughing, taste disturbance and skin rash (15), (107). Therefore, the search for natural ACE-inhibitory peptides derived from food proteins with no side effects is of great importance (89).

Several methods are described in literature to evaluate the ACE-Inhibitory (ACE-I) activity of a compound, which include spectrophotometric, fluorometric, radiochemical, capillary electrophoresis, and HPLC methods (107). Synthetic substrates, such as, *N*-α-hippuryl-L-histidyl-L-leucine (HHL), *N*-[3-(2-furyl)acryloyl]-L-phenylalanyl-glycyl-glycine (FAPGG) and *o*-aminobenzoylglycyl-*p*-nitrophenylalanylproline (Abz-Gly-Phe-(NO<sub>2</sub>)-Pro (Abz) are used for measuring the *in vitro* ACE-I activity. HPLC, spectrophotometer, or spectrofluorometer are needed when HHL, FAPGG or Abz are used, respectively. Natural substrates as Angiotensin-I and Bradykinin are also used in these assays, but in a lesser extent (108). Table 1.4 summarizes the methods currently used to assess the ACE-I activity of food hydrolysates and bioactive peptides. ACE-I values are commonly expressed as IC<sub>50</sub> values, i.e., the concentration of peptide needed to inhibit 50% of the ACE activity.

It should be highlighted that different methods and/or experimental conditions influence the ACE-I values, even with identical amino acid sequence (107). The IC<sub>50</sub> value

strongly depends on various reaction parameters, such as, nature and concentration of substrate, volume, enzyme quantity and detection methods of reaction products (108). Thus, comparison between  $IC_{50}$  values of hydrolysate or peptides could lead to biased conclusions if all parameters are not considered. For example, the  $IC_{50}$  value of the same bioactive peptide Ile-Val-Tyr (IVY) was reported to be 0.479 mM by Iroyukifujita *et al.* (109), 2.399 mM by Wu *et al.* (110) and 14.74 mM by Miyakoshi *et al.* (111). Other example is the peptide VY, which exhibited an  $IC_{50}$  of 10  $\mu$ M by Matsufuji *et al.* (112) when FAPGG was used as substrate and an  $IC_{50}$  value of 16  $\mu$ M by Terashima *et al.* (113), using HHL as substrate.

Table 1.4. *In vitro* analytical methods used for evaluation of the ACE-I activity of food hydrolysates and bioactive peptides

Substrate			Detection	Principle	Reference
Synthetic	HHL	<i>N</i> - $\alpha$ -hippuryl-L-histidyl-L-leucine	HPLC	HHL as substrate of ACE is hydrolyzed to hippuric acid (HA) and His-Leu (HL)	(114)
			MEKC <sup>a</sup>		(115)
					(116)
	FAPGG	<i>N</i> -[3-(2-furyl)acryloyl]-L-phenylalanyl-glycyl-glycine	Spectrophotometry	FAPGG as a substrate of ACE is hydrolyzed to FAG and Gly-Gly	(117)
					(118)
					(119)
Natural	Abz	Abz-Gly-Phe-(NO <sub>2</sub> )-Pro	Spectrofluorometry	Abz as substrate of ACE is hydrolyzed to Abz-Gly ( <i>o</i> -aminobenzoylglycine (fluorescent product))	(120)
					(121)
					(122)
	Angiotensin-I		HPLC	Angiotensin I as substrate of ACE is hydrolyzed to Angiotensin-II or bradykinin fragment 1-5, respectively	(104)
					(108)
	Bradykinin		HPLC		

<sup>a</sup> Micellar Electrokinetic Chromatography

## 1.5. Bioavailability methods

Studies related with bioactivity of food hydrolysates and bioactive peptides are mostly restricted to *in vitro* experiments. In fact, only limited numbers of clinical trials were conducted to test their efficacy as functional ingredients in humans (102), (123). However, before exploitation of food hydrolysates and bioactive peptides as functional ingredients for human nutrition, its stability in the GI tract, absorption and bioavailability in the human organism must be investigated. Bioaccessibility is usually defined as the quantity or fraction that is released from the food matrix in the GI tract and becomes available for absorption. It is usually evaluated by *in vitro* digestion procedures, generally simulating gastric and small intestinal digestion, followed by Caco-2 cells uptake (123). Bioavailability is defined as the fraction of ingested nutrient or compound that reaches the systemic circulation and is used by the body; besides GI digestion and absorption, also includes metabolism, tissue distribution and bioactivity.

### 1.5.1. Simulated GI digestion

Proteolysis by GI enzymes is a critical factor that determines the biological activity of food hydrolysates. During this process, Pepsin and Pancreatin can hydrolyze the food hydrolysate, leading to (i) modifications of the biological peptide sequences already present in the food hydrolysate; (ii) increasing formation of existing active peptides, and/or (iii) the creation of new active peptides from sequences not previously exhibiting biological activity in the food hydrolysate.

### 1.5.2. Cell culture systems

Compared with expensive and time-consuming animal studies and human clinical trials, *in vitro* cultured cell model systems allow for rapid and inexpensive screening of active compounds (88). Caco-2 cell monolayers, due to their similarity to the intestinal endothelium cells, have been the most commonly reported model system in the literature for studying intestinal permeability of bioactive compounds (124). This model can also be used to evaluate the cytotoxicity of the compounds at the concentrations intended to be used to obtain the desired bioactivity, as well as, to study the potential to inhibit intracellular oxidation and to reduce inflammatory responses (88).

Upon culturing as a monolayer, Caco-2 cells differentiate to form tight junctions between cells that will serve as a model of paracellular movement of compounds across the

monolayer. Caco-2 cells monolayers express transporter proteins, efflux proteins, and Phase II conjugation enzymes to model a variety of transcellular pathways and metabolize the test compounds (125). The ability of individual peptides to cross the membrane depends on their molecular size, hydrophobicity and resistance to brush-border peptidases (88), (124).

As depicted in Figure 1.6., the intestinal epithelium membrane presents four possible transport mechanisms: (a) larger water-soluble peptides can cross the intestinal barrier by paracellular transport via the tight junction between cells; (b) highly lipid-soluble peptides may diffuse via the transcellular route; (c) peptides may also enter the enterocytes via transcytosis; (d) while small di- and tri-peptides may be absorbed intact across the brush border membrane using  $H^+$  coupled PepT1 transporter system. The intestinal basolateral membrane also possesses a peptide transporter, which facilitates the exit of hydrolysis-resistant small peptides from the enterocyte into the portal circulation (126-128).

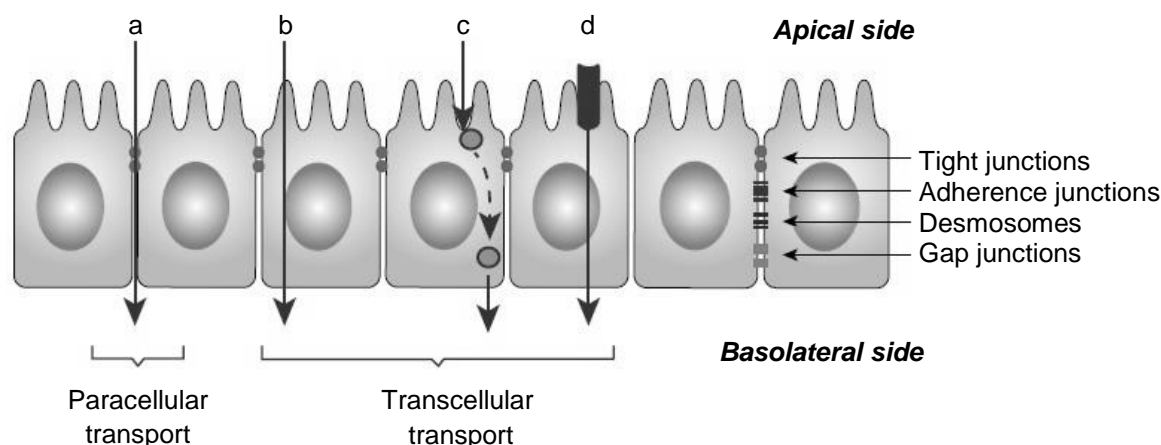


Figure 1.6. Polarized epithelial cells with different types of intercellular contacts and different absorption and transport mechanisms of compounds through intestinal epithelium membrane. Legend: (a) paracellular transport; (b) passive diffusion of molecules from the apical to the basolateral side; (c) vesicle-mediated transcytosis and (d) carrier-mediated uptake and diffusion through the epithelial cell layer. Adapted from (128).

However, Caco-2 cell model do not closely simulate the composition of the human epithelial layer, which contains several types of cells (128), (129). To overcome some of these limitations, combinations of Caco-2 cells with mucus-producing goblet cell, such as, HT29-MTX cells, have been proposed as co-culture models for permeation studies (130),



(131). Co-culture of Caco-2/HT29-MTX cells leads to the establishment of monolayers with intermediate properties regarding transepithelial electrical resistance (TEER), peptide hydrolysis and absorption. The proportion of 90:10, expressed as initial cell seeding for Caco-2/HT29-MTX cells, is the most prevalent in the literature and accepted to better mimic the natural epithelial barrier (129), (132), (133). Compared to Caco-2 monolayer, the expression of goblet cells in HT29-MTX cell line increases absorption of lipophilic compounds (131), (133).

Semipermeable plastic supports that can be fitted into the wells of multi-well culture plates are usually used in cell culture models (Figure 1.7.). Cells are exposed to the bioactive compounds either from the apical (upper compartment) or the basolateral side (lower compartment) of the transwell system to evaluate, respectively, the cellular uptake and cellular efflux of the test compounds. After incubation for various time periods, aliquots from the opposite chambers are removed for the determination of the concentration of test compounds and its percentage of permeability.

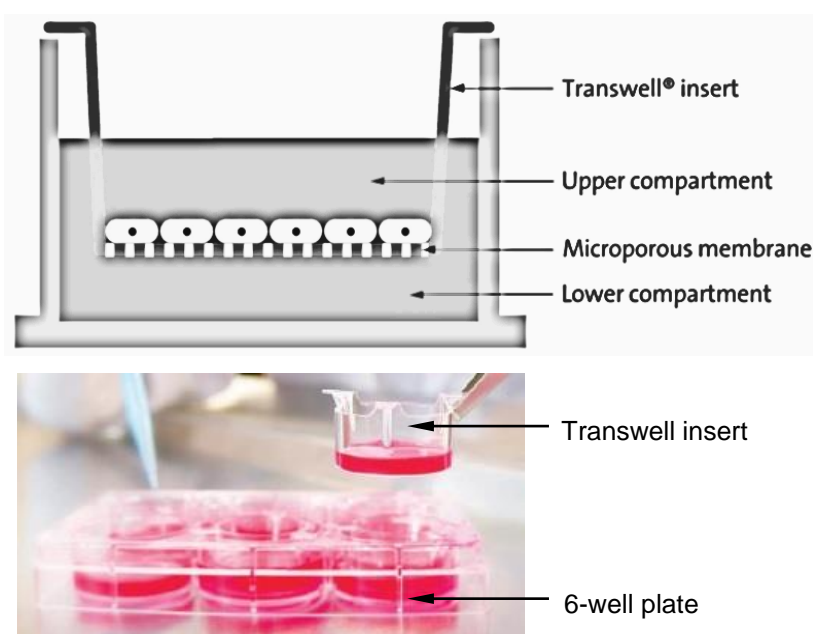


Figure 1.7. Two-chamber transwell transport model. Adapted from [www.corning.com](http://www.corning.com).

### **1.5.3. *In vivo* assays**

Once the potential biological activity of the food hydrolysates and bioactive peptides is established through *in vitro* assay methods, animal studies and human clinical trials should be conducted to confirm the desired biological function (102). To date, only a small number of studies evaluated the efficacy of food hydrolysates bioactivity in humans (134) and in animal models, such as, spontaneously hypertensive rats (SHR) (101), (135). Results from the *in vivo* assays are crucial for a bioactive compound be approved by the European Food Safety Authority (EFSA, Panel on Dietetic Products, Nutrition and Allergies) as a new functional food or nutraceutical formulation (18).

## CHAPTER 2

### *Nutritive value, antioxidant activity and phenolic compounds profile of Brewer's spent yeast extract*

---

This chapter describes the potential use of a BSY extract prepared by mechanical disruption as a source of proteolytic enzymes and biological activities, as antioxidant and ACE-I activities.



## ABSTRACT

Brewer's spent yeast (BSY) is the second major by-product from the brewing process. Mechanical disruption of yeast cell wall can be used to obtain  $\beta$ -glucan rich ingredients with applications in food industry and separation of inner yeast content with potential applications as food and nutraceutical ingredients. In this work, the nutritional composition, including minerals and B-complex vitamins, together with the antioxidant activity and phenolic compounds profile of BSY extract, prepared by mechanic disruption of BSY and removal of yeast cell wall, was investigated. Composition analysis showed that lyophilised BSY extract presented 64.1% of proteins and 4.0% of RNA. The amino acid profile showed a high proportion of essential amino acids. The BSY extract also contains macrominerals (Na, K, Ca, Mg) and increased content of trace elements, such as, Zn (11.90 mg/100 g dw), Fe (1.76 mg/100 g dw), and Mn (0.56 mg/100 g dw), and vitamins B3 (77.2 mg/100 mg dw), B6 (55.1 mg/100 g dw) and B9 (3.0 mg/100 g dw) when compared with other BSY extracts described in the literature. It also presents antioxidant activity, confirmed by three different assays. HPLC-DAD analysis showed that two phenolic compounds were detected as free forms, gallic acid (21.3 mg/100 g dw) and ( $\pm$ ) catechin (34.2 mg/100 g dw), and alkaline hydrolysis released other bounded phenolic compounds: protocatechuic acid and *p*-coumaric acid. The nutritive value, antioxidant properties and phenolic composition of the lyophilised BSY extract indicates that it can be an interesting ingredient for food and nutraceutical industries.

## 2.1. INTRODUCTION

Brewer's spent yeast (BSY) is the second major by-product from the brewing process. It is low in calories, fat and carbohydrates, however, it can be a valuable source of inexpensive fibre, mainly  $\beta$ -glucans (136-139), nucleotides (50), vitamins and minerals (5).

In the brewing process, serial repitching of *Saccharomyces* biomass is usual; thus, yeast is reused four to six times before its disposal (140). Yeast presents adaptive response to oxidative stress similar to that of human cells, consequently vitamins, namely B6 and B12, and minerals (enzyme co-factors), such as, zinc, copper and manganese can accumulate in yeast (51). Moreover, *Saccharomyces* adsorb phenolic compounds from exterior medium, increasing its antioxidant activity and phenolic compounds content (141). Although these compounds exhibit biological activities, such as, prevention of age-related diseases, inhibition of cancer cell proliferation and enhancement of immune response (9), (45), (76), (142), until now efforts to recover bioactive compounds from BSY are limited.

Moreover, the separation of yeast compounds for use in food applications requires efficient means of disrupting cell walls and separating the products of interest. Mechanical processes can be used to separate yeast cell-wall  $\beta$ -glucans, which are known for lowering cholesterol and triacylglycerols in blood, enhancing the immune system and the anti-inflammatory activity, stimulating the skin cell response to combat free radicals and delaying aging process. EFSA has already approved the use of *Saccharomyces*  $\beta$ -glucans - referred to as “yeast beta-glucans” - as a new food ingredient and suggests a use ranging between 50 and 200 mg per serving (143). However, new applications for the inner cell content are needed to make the process of  $\beta$ -glucans’ separation profitable.

Attempts to reuse the BSY in biotechnological processes include production of flavour enhancers (48), (50). In a previous work, mechanical rupture of cell wall, using glass beads, to separate cell wall constituents and produce a yeast extract rich in nucleotides that can be used as flavour enhancers was described (50). However, the full characterization of this extract is of major relevance to find new applications for BSY. Thus, the goal of this work was to study the nutritional composition, the minerals and B-complex vitamins content, the antioxidant activity and the phenolic profile of the BSY extract obtained by mechanical disruption, removal of cell wall and lyophilisation, to assess its potential interest as an ingredient in food and nutraceutical industries.

## 2.2. MATERIAL AND METHODS

### 2.2.1. Reagents and Standards

HPLC grade solvents were from Merck (Darmstadt, Germany). Iron (III) chloride hexahydrate; 2,4,6-tripyridyl-s-triazine (TPTZ); 2,2-diphenyl-1-picrylhydrazyl (DPPH); 6-hydroxy-2,5,7,8-tetramethylchroman-2-carboxylic acid (Trolox); potassium ferricyanide and trichloroacetic acid (TCA) were purchased from Sigma Chemical Co. (St. Louis, MO, USA). Ultrapure water was obtained from a Seralpur Pro 90 CN water purification. For mineral analysis, all solutions were prepared using polypropylene laboratory ware: pipette tips (VWR, Radnor, PA), volumetric flasks (Kartell, Milan, Italy) and centrifuge tubes (TRP, Trasadingen, Switzerland). High purity  $\text{HNO}_3$  ( $\geq 69\%$  w/w, TraceSELECT® Ultra, from Fluka, L’Isle d’Abeau Chesnes, France) and  $\text{H}_2\text{O}_2$  (30% v/v, TraceSELECT® from Fluka, Seelze, Germany) were used as received. Mineral standard solutions were prepared from AccuTrace™ (AccuStandard®, New Haven, CT, USA) 10  $\mu\text{g/mL}$  multi-element ICP-MS standards. Single-element standard solutions of Na, K, Ca, Mg and Fe, water-soluble vitamins and polyphenol standards were obtained from Sigma Chemical Co. (St. Louis, MO, USA).

### 2.2.2. Samples

Six different batches of BSY biomasses, collected between January and March of 2014 and with 3, 4, 5 and 6 repitchings in the brewing fermentation step, were kindly supplied as slurry by Unicer brewing (Leça do Balio, Portugal). Biomasses were transported to the laboratory under refrigerated conditions, protected from light and stored at 4°C until extract preparation (1 day maximum).

### 2.2.3. BSY extract preparation

The debittering process and the mechanical disruption procedure of the yeast cells were performed as described by Vieira *et al.* (50). All steps were carried out under refrigerated conditions to minimize autolysis. Yeast cell wall was removed by centrifugation and the resulting clear supernatants (extracts of the inner yeast content) obtained from the six BSY biomasses were freeze-dried and stored at -20°C until further analyses.

### 2.2.4. Proximate composition

The composition of BSY extracts were analysed in triplicate and mean results were expressed as % dw. Moisture content was determined at 105°C until constant weight. Total nitrogen was analysed by the Kjeldahl method (144) and protein content was estimated using factor conversion of 6.25; free  $\alpha$ -amino nitrogen was measured by the ninhydrin method using glycine as standard (145). Total lipid and ash contents were determined according to AOAC methods (144) and total carbohydrate was determined by difference. RNA was extracted according to Liwarska-Bizukojc and Ledakowicz (146) method; the concentration of RNA was determined based on Hebert *et al.* (147) method.

### 2.2.5. Amino acid composition and chemical score

BSY extracts were submitted to protein hydrolysis with 6 M HCl at 110°C for 24 h and further derivatization was conducted according to the method validated by Pérez-Palacios *et al.* (148). All amino acids except tryptophan were separated by Gas chromatography-mass spectrometry (GC/MS) and the relative amino acid composition was expressed as g/100 g of protein. The parameters used for estimating the nutritive value of the BSY extract protein fraction were: 1) essential amino acid (EAA) index, calculated considering essential amino acids in the standard protein as described by FAO/WHO (149); chemical score; and protein efficiency ratio (PER) calculated from the equation developed by Lee *et al.* (150). The chemical score and PER were calculated using the following equations (1 and 2):

$$\text{Chemical score} = \text{EAA in BSY extract} / \text{EAA in standard protein} \quad (1)$$

$$\text{PER (Eq. 3)} = -1.816 + 0.435[\text{Met}] + 0.780[\text{Leu}] + 0.211[\text{His}] - 0.944[\text{Tyr}] \quad (2)$$

## **2.2.6. Analyses of minerals**

### **2.2.6.1. Sample preparation**

Microwave-assisted acid digestion was performed in PTFE vessels using 300 mg of sample, 4 mL of 69% (w/w) HNO<sub>3</sub> and 1 mL of 30% (v/v) H<sub>2</sub>O<sub>2</sub> and the following microwave heating program: 250 W for 1 min, 0 W for 2 min, 250 W for 5 min, 400 W for 5 min, and 600 W for 5 min. After digestion, vessels content was transferred to 25 mL volumetric flasks and the volume was made-up with ultrapure water. Solutions were then analysed by Inductively coupled plasma mass spectrometry (ICP-MS) and Atomic absorption spectrometry (AAS).

### **2.2.6.2. Inductively coupled plasma mass spectrometry analysis**

ICP-MS analyses were carried out under the following instrumental conditions: argon flow rate 14 L/min; auxiliary argon flow rate 0.8 L/min; nebulizer flow rate 0.95 L/min; RF power 1550 W. The elemental isotopes (m/z ratios) <sup>52</sup>Cr, <sup>55</sup>Mn, <sup>57</sup>Fe, <sup>59</sup>Co, <sup>65</sup>Cu, <sup>66</sup>Zn, <sup>82</sup>Se and <sup>95</sup>Mo were monitored for analytical determinations; <sup>45</sup>Sc, <sup>89</sup>Y, <sup>115</sup>In and <sup>159</sup>Tb were used as internal standards. The instrument was tuned daily for maximum signal sensitivity and stability, as well as, for low oxides and double charged species formation using the Tune B iCAP Q solution (Thermo Fisher Scientific; 1 µg/L of Ba, Bi, Ce, Co, In, Li and U in 2% HNO<sub>3</sub> + 0.5% HCl). The internal standard solution was prepared by appropriate dilution of the corresponding AccuStandard® (New Haven, CT, USA) solution (ICP-MS-200.8-IS-1: 100 µg/mL of Sc, Y, In, Tb and Bi). Calibration standards were prepared from a SCP Science (Baie-d'Urfé, Quebec, Canada) 100 µg/mL multi-element ICP-MS standard solution (*PlasmaCAL* SCP-33-MS). The detection limits were calculated as the concentration corresponding to 3 standard deviations of 10 replicate integrations of the blank (HNO<sub>3</sub> 2% v/v).

### **2.2.6.3. Atomic absorption spectrometry analysis**

Determination of Na, K, Ca and Mg was performed using a Perkin Elmer (Überlingen, Germany) 3100 flame (air-acetylene) atomic absorption spectrometer instrument.

## **2.2.7. Analysis of B-complex vitamins**

### **2.2.7.1. Extraction of B-complex vitamins**

Extraction of vitamins from BSY extracts was performed according to Parlog *et al.* (151). The lyophilized extract (1 g) was homogenized with 10 mL of mobile phase A (50 mM ammonium acetate/methanol, 99:1), sonicated for 30 min at 27±3°C in ultrasonic water bath (FungiLab SA, Barcelona, Spain), centrifuged and then filtered through a 0.22 µm membrane, prior to HPLC injection.



#### 2.2.7.2. Preparation of B-complex vitamins standard solution

The aqueous stock solutions of each vitamin were prepared every week and stored in the refrigerator in amber-glass bottles to protect vitamins from light-induced oxidation. Individual standard stock solutions of vitamin B2 (riboflavin), B3 (nicotinic acid), B6 (pyridoxine), and B12 (cyanocobalamin) were prepared by dissolving 10 mg of each compound in 10 mL of ultrapure water containing 0.01% of trifluoroacetic acid, as described by Grotzkyj *et al.* (152). Standard stock solution of folic acid (B9) was prepared by dissolving 10 mg of the compound in 100 mL of pure water containing 4 mL of 1 M NaOH, as described by Ciulu *et al.* (153). Working standard solutions were prepared fresh daily and kept protected from light. The calibrations curves were made by running 6 different standard solutions (6 concentration levels) of each vitamin in the HPLC system.

#### 2.2.7.3. Chromatographic conditions for separation of B-complex vitamins

High Performance Liquid Chromatography (HPLC) analysis was carried out according to the procedure described by Parlog *et al.* (151). The injection volume was 30  $\mu$ L and all samples were run in triplicate. Photodiode array detection (PDA) was used to perform spectral scans over the range 230-360 nm and quantification was conducted at 260 nm for B2, B3 and B6, and at 280 nm for B9 and B12. Peak identification and purity were investigated by comparing the UV spectra of each individual compound when analysed in mixtures or in single compound standard solutions. Analysis was carried out using an analytical HPLC system (Jasco, Tokyo, Japan), equipped with a quaternary low pressure gradient HPLC pump (Jasco PU-1580), a degasification unit (Jasco DG-1580-53 3-line degasser), an autosampler (Jasco AS-2057-PLUS), a MD-910 multiwavelength detector (Jasco) and a 7125 Rheodyne injection valve (California, USA). The column was a Chrompack P 300 RP (polystyrenedivinylbenzene copolymer, 8  $\mu$ m, 300 $\text{\AA}$ , 150 x 4.6 mm i.d.) (Chrompack, Middleburg, The Netherlands). Data acquisition was accomplished using Borwin Controller software, version 1.50 (JMBS Developments, Le Fontanil, France).

#### 2.2.8. Antioxidant activity of BSY extracts

##### 2.2.8.1. Ferric reducing antioxidant potential (FRAP) assay

The measurement of the Ferric reducing antioxidant potential assay (FRAP) was done according to Jansen and Ruskovska (154). Trolox was used as standard at 0.0025-0.125 mg/mL to generate a calibration curve and results (mean values  $\pm$  standard deviation) were expressed as milligrams of Trolox Equivalent per gram of dry weight BSY extract (mg TE/100 g dw).

#### **2.2.8.2. DPPH radical scavenging capacity assay**

The 2,2-Diphenyl-1-picrylhydrazyl radical-scavenging capacity (DPPH) assay was performed as described by Herald *et al.* (155). Trolox was used as standard at 0.0025-0.125 mg/mL to generate a calibration curve and data was reported as means  $\pm$  standard deviation for three replications. Results (mean  $\pm$  standard deviation) were expressed as milligrams of Trolox Equivalent per gram of dry weight BSY extract (mg TE/100 g dw).

#### **2.2.8.3. Ferricyanide reducing power (RP) assay**

The ferricyanide reducing power (RP) was determined as described by Almeida *et al.* (156). Trolox was used as standard at 0.0025-0.125 mg/mL to generate a calibration curve and results (mean  $\pm$  standard deviation) were expressed as milligrams of Trolox Equivalent per gram of dry weight BSY extract (mg TE/100 g dw).

#### **2.2.9. Extraction of phenolic compounds**

The extraction of phenolic compounds was conducted as described by Khamam *et al.* (157): 50 mg of lyophilized BSY extract were homogenized with 1 mL of mobile phase A for extraction of free phenolic compounds, whereas bounded phenolic compounds were extracted after alkaline hydrolysis: 50 mg of lyophilized BSY extract was treated with 1 mL of 2 M NaOH for 2 h at room temperature and constant agitation (250 rpm). After centrifugation at 5,000 rpm for 5 min, the resultant extract was acidified to pH 2 using 6 M HCl and extracted three times with diethyl ether. The ether extracts were mixed, evaporated to the dryness under vacuum at 35°C and finally dissolved in 1 mL of mobile phase A.

##### **2.2.9.1. HPLC analysis of phenolic compounds**

HPLC analysis was carried out according to the procedure described by Khanam *et al.* (157) with some adjustments. The binary mobile phase consisted of 6% (v/v) glacial acetic acid in water (solvent A) and acetonitrile (solvent B) and was pumped at a flow rate of 0.7 mL/min, for a total run time of 75 min, at temperature of 35°C. A gradient program was used as follows: 0-3.5% B for 11 min, 3.5-5% B for 9 min, 5-10% B for 3 min, 10-13% B for 7 min, 13-15% B for 15 min, 15-30% B for 15 min, 30-50% B for 5 min, 50-100% B for 5 min and returning to the starting conditions for 5 min (0% B) before the next sample injection. The injection volume was 20  $\mu$ L. PDA was used to perform spectral scans over the range 190-400 nm and quantification was conducted at 236 nm for ( $\pm$ )-catechin, (-)-epicatechin and rutin; at 260 nm for protocatechuic and vanillic acids; at 280 nm for gallic, syringic and cinnamic acids; at 320 nm for the derivatives of cinnamic acid (caffeic, *p*-coumaric, chlorogenic and ferulic acids) and at 350 nm for isoquercetin. Phenolic compounds identification was performed by comparison with retention times and spectra of standards,

as well as, co-elution after fortification with the standards. Quantification was based on external standards calibration and samples were analysed in triplicate. The HPLC system was from Gilson (Villiers le Bel, France), consisting of two pumps (305 and 306), an 805 manometric module, a 811C dynamic mixer, an injection port with a 20  $\mu$ L loop (Rheodyne, Rohnert Park, California, USA) and a PDA (Varian, Santa Clara, California, USA) controlled by a data processor software (Varian Santa Clara, California, USA). Chromatographic separation was achieved with a 150 x 4.6 mm, Spherisorb® ODS-2 80Å (3  $\mu$ m particle size) column from Waters (Milford, Massachusetts, USA).

## 2.3. RESULTS AND DISCUSSION

### 2.3.1. Nutritional composition of BSY extracts

The proximate composition of freeze-dried BSY extracts obtained using a mechanic disruption process is shown in Table 2.1. BSY extracts contained low moisture (7.7%), low fat content (1.3% dw) and high protein content (64.1% dw), which contributes to its stability during storage. Protein content was in agreement with the value reported by Caballero-Córdoba and Sgarbieri (25), in which a mechanic disruption using glass beads was also the process used for BSY extract production, although an alkaline treatment was previously performed for debittering of brewer's yeast. The ash content (14.0%) and the total amino nitrogen (3.8%) were in agreement with the values reported by Saksinchai *et al.* (26), in which a autolysis process (50°C, 20 h) was adopted to produce the BSY extract. Also, the RNA content (4.0%) was in agreement with Vieira *et al.* (50), confirming the potential use of this extract for flavour enhancers production.

#### 2.3.1.1. Amino acid composition

The amino acid composition of BSY extracts and chemical scores are also presented in Table 2.1. Results indicated an amino acid profile rich in essential amino acids compared to the reference amino acid pattern recommended by FAO/WHO (1990) (149) for adult humans. These results also agree with the amino acid profile obtained by Caballero-Córdoba and Sgarbieri (25). Generally, S-amino acids (methionine and cysteine) are the limiting factor to the nutritive value of yeast protein. However, as reported in Table 2.1, S-amino acids were above the FAO/WHO reference (149). Essential amino acids account for about 40% of total amino acids, being in agreement with the reference value recommended by FAO/WHO (149). The protein efficiency ratio (PER) was 2.4 and BSY extracts presented a high content of the flavour enhancer amino acids (glutamic acid, aspartic acid, glycine and alanine), accounting to 34.0% of total amino acids. The amino acid composition

indicates that protein fraction of BSY extracts presents a good potential for applications in food and dietary supplement industries as a protein rich ingredient.

Table 2.1. Nutritional composition of BSY extract

Proximate composition	(g/100 g dw)	AA	(g/100 g protein)	Reference Protein <sup>b</sup>	Chemical Score
Moisture	7.7 ± 0.12	Alanine <sup>d</sup>	9.3±0.2	-	
Ash	14.0 ± 0.20	Arginine <sup>c</sup>	6.0±0.4	-	
Protein	64.1 ± 0.21	Aspartic acid <sup>d</sup>	5.9±0.2	-	
α-amino nitrogen	3.8 ± 0.23	Cysteine	2.2±0.0	-	
Fat	1.3 ± 0.04	Glutamic acid <sup>d</sup>	15.0±0.5	-	
Carbohydrates <sup>a</sup>	12.9 ± 0.11	Asparagine <sup>e</sup>	2.0±0.0	-	
RNA	4.0 ± 0.16	Glutamine	3.1±0.3	-	
		Glycine <sup>d</sup>	3.7±0.5	-	
<b>Macrominerals</b>	<b>(mg/100 g dw)</b>	Histidine <sup>c</sup>	11.9±0.9	1.6	7.5±0.8
Sodium (Na)	1228.6 ± 22.0	Isoleucine <sup>c</sup>	3.2±0.0	1.3	2.5±0.1
Potassium (K)	91.5 ± 69.0	Leucine <sup>c</sup>	3.5±0.1	1.9	1.9±0.1
Calcium (Ca)	27.1 ± 0.40	Lysine <sup>c</sup>	3.2±0.3	1.6	2.0±0.4
Magnesium (Mg)	273.6 ± 2.31	Methionine <sup>c</sup>	2.3±0.1	1.7	1.3±0.0
		Phenylalanine <sup>c</sup>	3.0±0.0	-	
<b>Trace elements</b>	<b>(mg/100 g dw)</b>	Proline	2.7±0.0	-	
Chromium (Cr)	0.019 ± 0.000	Serine	4.6±0.3	-	
Iron (Fe)	1.760 ± 0.030	Threonine <sup>c</sup>	2.6±0.0	0.9	2.9±0.1
Manganese (Mn)	0.564 ± 0.013	Tyrosine	2.2±0.0	-	
Cobalt (Co)	0.030 ± 0.001	Valine <sup>c</sup>	4.5±0.1	1.3	3.5±0.0
Molybdenum (Mo)	0.003 ± 0.000	Tryptophan	<i>nd</i>	1.6	
Zinc (Zn)	11.90 ± 0.291	TAA	90.9±5.4		
Copper (Cu)	0.364 ± 0.001	EAA <sup>c</sup>	40.2±2.6		
Selenium (Se)	0.030 ± 0.000	FAA <sup>d</sup>	33.9±3.1		
<b>Vitamins</b>	<b>(mg/100 g dw)</b>	PER	2.4±0.1		
Nicotinic acid (B3)	77.2 ± 1.10				
Pyridoxine (B6)	55.1 ± 2.51				
Folic acid (B9)	3.0 ± 0.01				
Riboflavin (B2)	<i>nq</i> (0.329)				
Cyanocobalamin (B12)	<i>nq</i> (0.256)				

Data are expressed as mean values ± standard deviation.

<sup>a</sup> Calculated by subtraction of crude protein, total fat, moisture and ash contents from the total weight.

<sup>b</sup> Suggested profile of essential amino acid (EAA) requirements for adults, FAO/WHO (1990).

*nq*: not quantified, concentrations <LOQ (values represented in brackets in mg/100 g); *nd*: not determined; Total amino acids (TAA); Essential amino acid (EAA)<sup>c</sup>; Flavour amino acids (FAA)<sup>d</sup>; Protein efficiency ratio (PER).

### 2.3.1.2. Minerals content

The macrominerals (Na, K, Ca, Mg) and trace elements (Cr, Fe, Mn, Cu, Co, Mo, Se, Zn) composition of BSY extracts is also presented in Table 2.1. Due to the lack of information regarding the mineral composition of BSY extracts prepared by mechanic disruption using glass beads, as performed in this work, results were compared with the mineral profile of BSY extracts reported by Alvim *et al.* (28), in which a dehydrated yeast extract was prepared by spray dryer. The sodium content, 1228.6 mg/100 g dw, was lower than data reported by Alvim *et al.* (28), 1475 mg/100 g dw. By the contrary, the potassium content (91.5 mg/100 g dw) was similar to the content reported by Alvim *et al.* (28), 99 mg/100 g dw. Both minerals play an important role in the regulation of cell acid-base balance and water retention, and are essential for ribosomal protein synthesis. The calcium and magnesium contents were 27.1 mg/100 g dw and 273.6 mg/100 g dw, respectively. These elements helps in bone formation, muscle function, neurotransmission, cell division and blood coagulation, and magnesium is important in the appropriate utilization of vitamins B and E and in maintaining fluid and electrolyte balance. According to the National Academy of Science (158), the Dietary Reference Intakes (DRIs) of Na, K, Ca and Mg for a young adult are 1500, 4700, 1000 and 420 mg, respectively.

Concerning to trace elements, mean contents of 0.019 mg/100 g dw and 0.030 mg/100 g dw were found for Cr and Mo, respectively, whereas the content of Zn was 11.90 mg/100 g dw, Fe content was 1.755 mg/100 g dw and Mn content was 0.564 mg/100 g dw. According to the National Academy of Science (158), the DRIs of these elements for a young adult are 0.025-0.035 mg for Cr, 0.045 mg for Mo, 8-11 mg for Zn, 8-18 mg for Fe, and 1.8-2.3 mg for Mn. The BSY extract can be used as supplement to fulfil these requirements.

### 2.3.1.3. B-complex vitamins content

Vitamins B3, B6 and B9 were quantified in the BSY extracts (Table 2.1). The mean content of vitamin B3 (77.2 mg/100 g dw) was significantly higher than the content reported by Pinto *et al.* (32) (0.79 mg/100 g dw) for lyophilized brewer's yeast surplus obtained after alkaline treatment without removal of cell wall. Brewer's yeast is considered one of the best dietary sources of vitamin B3; this vitamin participates in several metabolic functions and also assists in antioxidant and detoxification functions. The mean content of vitamin B6 was 55.1 mg/100 g dw, which was significantly higher than the content reported by Pinto *et al.* (32) for lyophilized brewer's yeast surplus, which was 9.99 mg/100 g dw. This vitamin plays a vital role in the function of several enzymes that catalyse essential chemical reactions in the human body, especially those involved in protein and amino acid metabolism. Regarding to vitamin B9, the mean content found (3.0 mg/100 g dw) was also higher than

the values reported by Pinto *et al.* (32) (0.25 mg/100 g dw). This vitamin plays a central role in one-carbon metabolism; derivatives of folate act as co-factors, carrying one-carbon units for various reactions in the cell, such as, synthesis of certain amino acids and nucleotides (159). Vitamins B2 and B12 were not detected in BSY extracts. Pinto *et al.* (32) quantified both vitamins (at 1.38 and 75.8 mg/100 g dw mean levels, respectively), but only in the lyophilised BSY without any treatment. These results indicate that the processes used to obtain the BSY extracts significantly influence their vitamin composition, but the removal of yeast wall concentrated the content of vitamins B3, B6 and B9.

### 2.3.2. Antioxidant activity

The mean values of antioxidant activity of BSY extracts evaluated by FRAP, DPPH and RP were, respectively,  $261 \pm 14$ ;  $59.7 \pm 2.5$  and  $127.6 \pm 1.0$  mg TE/100g dw. Significant positive correlations were observed between results from FRAP *versus* DPPH ( $R^2 = 0.9721$ ) and *versus* RP ( $R^2 = 0.8750$ ), and also between DPPH *versus* RP ( $R^2 = 0.9632$ ).

### 2.3.3. Phenolic compounds

The free and bound phenolic compounds were analysed by HPLC. As shown in Table 2.2, only gallic acid and ( $\pm$ )-catechin were quantified in the free fraction, being the ( $\pm$ )-catechin the most representative compound (62%). In the bound fraction, six phenolic compounds were quantified in the following order of abundance: cinnamic acid (1.2 mg/100 g dw), gallic acid (2.1 mg/100 g dw), ferrulic acid (9.2 mg/100 g dw), *p*-coumaric acid (10.3 mg/100 g dw), protocatechuic acid (13.1 mg/100 g dw) and (+)-catechin (24.6 mg/100 g dw). The total phenolic compounds content in the free and bound fractions were, respectively, 55.5 mg/100 g dw and 60.6 mg/100 g dw. No information was found in literature concerning phenolic compounds content in BSY.

Table 2.2. Mean content (mg/100 g dw) of phenolic compounds of BSY extracts in the free and bound fractions

Compound	Free (mg/100 g dw)	Bound (mg/100 g dw)	$\Sigma$ TFC (mg/100 g dw) <sup>a</sup>	Free / $\Sigma$ TPC (%) <sup>b</sup>	Bound / $\Sigma$ TFC (%) <sup>b</sup>
Gallic acid	21.3 $\pm$ 3.5	2.1 $\pm$ 0.5	23.4	38	3
Protocatechuic acid	<i>nq</i> (0.125)	13.1 $\pm$ 1.3	13.1	-	22
( $\pm$ )-Catechin	34.2 $\pm$ 5.8	24.6 $\pm$ 4.1	58.8	62	41
<i>p</i> -Coumaric acid	<i>nq</i> (0.274)	10.3 $\pm$ 1.0	10.3	-	17
Caffeic acid	<i>nq</i> (0.068)	<i>nq</i> (0.068)	-	-	-
Ferulic acid	<i>nq</i> (0.200)	9.2 $\pm$ 0.5	9.2	-	15
Cinnamic acid	<i>nq</i> (0.142)	1.2 $\pm$ 0.0	1.2	-	2
$\Sigma$ TPC	55.5 $\pm$ 9.3	60.6 $\pm$ 7.4	116.1	-	-

Data are expressed as mean values  $\pm$  standard deviation.

<sup>a</sup> Total phenolic content calculated as sum of individual phenolic compounds from free and bound fractions.

<sup>b</sup> Calculated considering the  $\Sigma$  TPC of the free/bound phenolic fraction.

*nq*: not quantified, concentrations <LOQ (values represented in brackets in mg/100 g).

(-): not calculate.

## 2.4. CONCLUSIONS

This study provides a detailed analysis of the nutritional composition, antioxidant activity and phenolic compounds profile of BSY extracts produced by mechanic disruption of brewer's spent yeast (*Saccharomyces pastorianus*) and removal of the cell walls (for separation of  $\beta$ -glucans). Results showed that the extracts from the inner content of BSY cells are a rich source of proteins containing essential amino acids, RNA, vitamins (B3, B6 and B9) and minerals. Higher contents were observed in comparison with other BSY extracts described in the literature. Chromatographic analysis also showed that BSY extracts contains phenolic compounds in both the free and bounded forms: gallic acid, protocatechuic acid, ( $\pm$ )catechin, *p*-coumaric, ferulic and cinnamic acids were quantified. Additionally, BSY extracts present antioxidant activity, which makes this yeast extract a potential ingredient to be used in the formulation of functional foods and nutraceuticals. Moreover, since BSY extracts production complements the use of yeast cell wall for  $\beta$ -glucans and fibre obtaining, it makes the whole process much cost-effective.



## CHAPTER 3

*A bioactive ingredient obtained from the inner cellular  
content of Brewer's spent yeast*

---

This chapter explores the influence of the yeast reuse during beer fermentation step on the proteolytic activity and biological activities of the BSY extract prepared by mechanical disruption.



## ABSTRACT

During brewing, *Saccharomyces* yeast is used in the fermentation process several times until its disposal. Yeast surplus is the second major brewing by-product, mostly used for animal feed. Despite its underutilization, it can be of value as a source of bioactive compounds. In this work, a new ingredient was obtained from the inner cell content of Brewer's spent yeast (BSY) by mechanical disruption of the cell wall of yeast surplus with different number of reuses in the brewing process. Proximate composition, amino acid profile, molecular weight distribution and biological activities (proteolytic, antioxidant and angiotensin converting enzyme-inhibitory (ACE-I) activity) of freeze-dried BSY extracts were assessed. Additionally, the stability of the biological properties of BSY extract during 6 months of storage at -25°C was evaluated.

Proteins were the major components of BSY extracts, its amino acid profile was well-balanced for human consumption. The antioxidant activities of the BSY extracts were not influenced by the serial reuse of yeast biomass in the brewing process, neither by the storage period. However, BSY extracts prepared from yeast with lower number of reuses in brewing process presented the highest proteolytic activity and maximum ACE-I activity. BSY extracts are promising as a protein rich bioactive ingredient for food, nutraceutical or cosmetic industries.

## 3.1. INTRODUCTION

Currently, there is an increased interest in exploitation of yeasts as a natural resource of bioactive compounds for use as ingredients in food. Brewing process produces annually considerable amounts of brewer's spent yeast (BSY), which constitutes a serious environmental problem. This biomass is underutilized, being normally used as low-economical valuable animal feed products (5). However, BSY are GRAS microorganisms, containing several beneficial nutrients, such as, vitamins B complex (folic, biotin), minerals (zinc, chromium, iron, magnesium), nucleic acids, amino acids and glutathione (2). Therefore, nutritional and economical valorization of this relatively inexpensive waste to recover natural compounds has become an important contribution to the sustainable development of the brewing process (27), (36), (63). *Saccharomyces* yeast cells also contain numerous vacuolar proteases, including serine, aspartyl and metalloproteases, which can be used in fermentation processes to obtain hydrolysates with several biological activities (44), (160). Potential applications of BSY has been reviewed by several authors (2), (161). Other alternative is the extraction of the inner yeast cell components, namely,

amino acids, peptides, proteins, carbohydrates, minerals and nucleotides. They can be commercially produced on a large scale by hydrolysis, autolysis or plasmolysis of BSY for use in the food industry, for example as flavour enhancers to replace glutamates and nucleotides in many processed foods (2), (10) or used as healthy food ingredients (61).

Until now, few studies have focused in the bioactive properties of yeasts. Some studies have demonstrated that they may exhibit antioxidant properties, such as, prevention of macular degeneration, inhibition of cancer cell proliferation, enhancement of immune response and increase glucose tolerance (2), (45), (76). These beneficial effects have been attributed to the presence of various functional components, including polysaccharides, flavonoids, phenolic acids and carotenoids (35), (36). Also, enzymatic hydrolysis of yeast substances have generated peptides with high levels of radical scavenging activities, oral glucose tolerance activity and ACE-I effect (76), (86).

Serial repitching of *Saccharomyces* biomass is usual in the brewing process; yeast is reused four to six times before its disposal (5). This practice can induce cellular stress. Several antioxidants can be produced in yeasts grown under stressful conditions or in response to fermentation medium ingredients, such as, phenolics or additives that are known to be toxic to cells grown aerobically (36). Therefore, it can be of interest to understand the influence of yeast repitching in the bioactivity of BSY extracts.

In this work, BSY extracts were prepared from the inner cell content using yeast surplus with different reuses in the fermentation process. Mechanical cell disruption was achieved by vortexing using glass beads, under refrigerated conditions. The proteolytic activity, the antioxidant activity and the ACE-I activity of freeze-dried extracts were evaluated. Furthermore, since BSY extract utilization as a functional ingredient depends largely on the stability upon storage; the effect of frozen storage on the stability of the biological activity was also evaluated. To the best of our knowledge, this is the first description of the influence of serial repitching in the bioactivity of BSY extracts. The use of these BSY extracts with biological properties for food and nutraceutical applications could be an ideal approach to reuse the *Saccharomyces pastorianus* surplus from the brewing process and simultaneously to overcome environmental industrial problems.

## 3.2. MATERIAL AND METHODS

### 3.2.1. Chemicals, reagents and equipments

Folin-Ciocalteu phenol reagent; 2,2-Diphenyl-1-picrylhydrazyl (DPPH); sodium dodecyl sulfate (SDS); 2,4,6-tripyridyl-s-triazine (TPTZ); iron (III) chloride hexahydrate; ascorbic acid; bovine serum albumin (BSA); 6-hydroxy-2,5,7,8-tetramethylchroman-2-carboxylic acid (Trolox); catechin; gallic acid; molecular weight standard (205-6.6 kDa); rabbit lung acetone powder for Angiotensin-I-converting enzyme (ACE) extraction were all purchased from Sigma-Aldrich (St. Louis, MO, USA). Methanol, sodium acetate, sodium carbonate decahydrate, sodium nitrite, aluminum chloride and sodium hydroxide were purchased from Merck (Darmstadt, Germany). *o*-aminobenzoylglycyl-*p*-nitro-phenylalanylproline (*o*-ABz-Gly-Phe(NO<sub>2</sub>)-Pro) was purchased from Bachem Feinchemikalien (Bubendorf, Switzerland). Ultra-pure water was obtained from a Seral-Seralpur Pro 90 CN water purifying system. All reagents used were of analytical grade.

Spectrophotometric analyses were carried out using a BMG LABTECH's SPECTROstar Nano-microplate, cuvette UV/Vis absorbance reader (Offenburg, Germany). Fluorimetric analyses were carried out using a fluorescence microplate reader (FLUOstar Optima, BMG Labtech GmbH). GC-MS analyses were carried out in an Agilent 6890 gas chromatograph (Agilent, Avondale, PA, USA) coupled to a MS detector (Agilent 5973).

### 3.2.2. Samples

Twelve samples of 0.5 kg of BSY (*Saccharomyces pastorianus*) used to produce lager beer were collected: 3 samples of yeast biomass used twice in the brewing process (coded as R2), 3 samples of yeast biomass with three serial reuses in the brewing process (coded as R3), 3 samples of yeast biomass with four serial reuses in the brewing process (coded as R4) and 3 samples of BSY containing a mixture of biomasses with different number of reuses in fermentation process (coded as MIST). All samples were provided as slurry by the Unicer brewing (Leça do Balio, Portugal); transported in a 1 liter glass bottle to laboratory under refrigerated conditions and stored at 4°C until preparation procedure (1 day maximum).

### 3.2.3. Preparation of BSY extracts

All steps were performed under refrigerated temperatures to minimize autolysis. Firstly, BSY was centrifuged at 5,000 x *g* for 15 min at 4°C to remove beer liquor. The biomass was washed three times with phosphate buffer, pH 6.0 (volume ratio 1:3). After centrifugation at 5,000 x *g* during 15 min at 4°C, the yeast cell pellet was weighed and stored under refrigerated conditions. A mechanical disruption method by Vieira *et al.* (50) with some

modifications was adopted to promote the breakdown of yeast cell wall and release the inner content into the extracellular environment. Biomass was destroyed with glass beads with a diameter of 0.60 mm at a ratio 1:1:1 (biomass: phosphate buffer pH 6.0: glass beads); (m/v/m), by vortexing 10 times (1 min each) with 1 min cooling intervals on ice-water bath to keep the temperature below 4°C during the entire process. After removing the glass beads by allowing the suspension to stand, the homogenate was centrifuged at 12,000 x g for 40 min at 4°C (twice) to remove the cell debris. The resulting clear supernatant was carefully collected and freeze-dried. The supernatant was then resuspended in phosphate buffer pH 6.0 and divided into aliquots. These BSY resuspended extracts were used for time zero analysis and subsequently frozen at -25 °C for further analyses (1, 2, 4 and 6 months).

#### **3.2.4. Proximate Composition**

Freeze-dried BSY extracts were assayed for protein content (total nitrogen determined by Kjeldahl method x 6.25), fat content (Soxhlet extraction with n-hexane for 12 h), ash content (incineration in a muffle furnace at 550°C until the ash had a white appearance) and moisture (oven at 105°C until constant weight) according to AOAC official methods (144). All assays were performed in triplicate and the contents were expressed on a dry weight basis (% dw).

#### **3.2.5. Sodium dodecyl sulfate polyacrylamide gel electrophoresis (SDS-PAGE)**

Relative molecular weight profiles of BSY extracts were determined by sodium dodecyl sulfate gel (SDS)-polyacrylamide electrophoresis (PAGE) analysis. Separation gels consisted of a 4% polyacrylamide stacking gel and a 15% polyacrylamide resolving gel and were performed according to Laemmli (162) method. For all BSY extracts, the weight of protein loaded (determined by Lowry method (163)) was 25 µg. Gels were stained in Coomassie brilliant blue R-250 (0.125% in 50% methanol and 10% acetic acid) for 1 h and destained using an acetic acid-methanol mixture (10% acetic acid and 50% methanol) during 1 h, followed by 5% methanol (v/v) and 7% (v/v) acetic acid, repeatedly until the protein bands were clearly visible. The standard proteins were simultaneously run for protein identification: myosin (205 kDa), β-galactosidase (116 kDa), phosphorilase β (97 kDa), transferrin (80 kDa), bovine serum albumin (66 kDa), glutamate dehydrogenase (55 kDa), ovalbumin (45 kDa), carbonic anhydrase (31 kDa), trypsin inhibitor (21 kDa), lysozyme (14 kDa) and aprotinin (6.6 kDa).

### 3.2.6. Amino acid composition and chemical score of BSY extract proteins

BSY extracts were submitted to autolysis with 6 M HCl at 110°C for 24 h and further derivatization was conducted according the validated method of Pérez-Palacios *et al.* (148). Amino acids were separated by Gas chromatography mass spectrometry (GC/MS). The MS system was routinely set in selective ion monitoring (SIM) mode and each compound was quantified based on peak area using one target and one or two qualifier ions. The amount of amino acids were calculated, based on the peak area in comparison with that of the standards. The results were used to determine the relative amino acid composition (expressed as g/100 g of protein). Essential amino acid index was calculated considering the essential amino acids (EAA) in the standard protein, as described by FAO/WHO (149) and the protein efficiency ratio (PER) was calculated considering the equation developed by Lee *et al.* (150). The chemical score and PER were calculated using the following equations (1 and 2):

$$\text{Chemical score} = \text{EAA in test protein} / \text{EAA in standard protein} \quad (1)$$

$$\text{PER (Eq. 3)} = -1.816 + 0.435[\text{Met}] + 0.780[\text{Leu}] + 0.211[\text{His}] - 0.944[\text{Tyr}] \quad (2)$$

### 3.2.7. Determination of biological properties of BSY extracts

Biological properties of BSY were analyzed concerning total phenolic content (TPC), total flavonoid content (TFC), antioxidant activities (DPPH, FRAP and RP), proteolytic activity and ACE-I activity.

#### 3.2.7.1. Enzyme activity assay

Protease activity of BSY extracts was assayed by Sigma's non-specific protease method described by Cupp-Enyard (164). Assays were performed in triplicate. Protease activity was expressed as the number of protease units per mL of enzyme (U/mL). One unit of protease activity (U) was defined as the amount of the enzyme needed to catalyze the formation of 1 µg of tyrosine per 1 min, at 37°C. A commercial protease solution (Alcalase® 2.4L) diluted at 0.2 U/mL was used as positive control, for comparison.

#### 3.2.7.2. Total phenolic content (TPC) and total flavonoid content (TFC)

The method used for TPC determination was similar to that of Herald *et al.* (155). Gallic acid was used as a standard at 12.5-200 µM to produce a calibration curve (average  $R^2 = 0.9975$ ). Total phenolic concentration was expressed as µM GAE (Gallic Acid Equivalent)/mL of sample. The method used for TFC determination was similar to that of Herald *et al.* (155). Catechin was used as a standard at 5-250 µM to generate a calibration curve (average  $R^2 = 0.9983$ ). Total flavonoid concentration was expressed as µM CE (Catechin Equivalent)/mL of sample.

### 3.2.7.3. Antioxidant activity of BSY extracts

The DPPH radical-scavenging capacity assay was performed as described by Herald *et al.* (155). Trolox was used as a standard at 50-500  $\mu\text{M}$  to generate a calibration curve (average  $R^2 = 0.9940$ ). The analyses of BSY extracts were carried out in triplicate and the results were expressed as  $\mu\text{M}$  TE (Trolox Equivalent)/mL of sample. The measurement of the Ferric Reducing Antioxidant Power (FRAP) assay was done by the assay based on the method of Jansen and Ruskovska (154). Trolox was used as a standard at 50-500  $\mu\text{M}$  to generate a calibration curve (average  $R^2 = 0.9956$ ) and results were expressed as mean values  $\pm$  standard deviations as  $\mu\text{M}$  TE (Trolox Equivalent)/mL of sample. The measurement of the Reducing power (RP) was done by the assay based on the method of Almeida *et al.* (156). Trolox was used as a standard at 50-500  $\mu\text{M}$  to generate a calibration curve (average  $R^2 = 0.9942$ ) and results were expressed as  $\mu\text{M}$  TE (Trolox Equivalent)/mL of sample. The intra-assay variation of the DPPH, FRAP and RP assays were, respectively, 2.9%, 3.1% and 4.3%, as determined with three quality control samples. A standard solution of vitamin C (500  $\mu\text{M}$ ) was used as positive control in antioxidant activity assays.

### 3.2.7.4. ACE-I activity

The ACE-I activity was measured using the fluorimetric assay of Sentandreu and Toldrá (121), with the modifications reported by Quirós *et al.* (122). ACE was extracted from rabbit lung acetone powder with 100 mM sodium borate buffer (pH 8.3) containing 300 mM NaCl, according to the procedure described by Minervini *et al.* (165). Prior to assay, the supernatant was diluted 10-fold with 50 mM potassium phosphate buffer, pH 8.3, so that it would have the same ACE activity as the commercial preparation ( $\sim 3$  U/mg of protein). ACE inhibitory percentage (I %) was calculated using the equation 3:

$$I \% = \{(B - A) / (B - C)\} \times 100 \quad (3)$$

where B is the fluorescence of the ACE solution without the inhibitor, BSY extract; A is the fluorescence of the tested sample, BSY extract; and C is the fluorescence of experimental blank, *o*-ABz-Gly-Phe(NO<sub>2</sub>)-Pro dissolved in 150 mM Tris-base buffer (pH 8.3), containing 1.125 M NaCl. The percent inhibition curves (using a minimum of five determinations for each sample peptide concentration) were plotted *versus* protein concentration to estimate the mean IC<sub>50</sub> value, which is defined as the concentration required to decrease the ACE activity by 50% (122).



### 3.2.8. Effect of storage conditions on the stability of BSY extract biological properties

The stability of BSY extracts biological properties during storage at -25°C was investigated. For stability studies, the biological properties of freeze-dried and resuspended BSY extracts, stored at -25°C for 1, 2, 4 and 6 months, were evaluated and compared with the properties presented at initial time (0 months).

### 3.2.9. Statistical analysis

Data were reported as mean  $\pm$  standard deviation of at least triplicate experiments. All statistical analyses were performed using the software SPSS for Windows, version 22.0 (SPSS Inc., Chicago, IL, USA). One-way analysis of variance with Duncan's post hoc test was carried out to ascertain significant differences between BSY extracts with different number of reuses in brewing process. In all cases, 5% significance level ( $p < 0.05$ ) was accepted as denoting significance.

## 3.3. RESULTS AND DISCUSSION

### 3.3.1. Proximate composition of freeze-dry BSY extracts

The moisture content of freeze-dried BSY extracts obtained from yeast surplus with two, three, and four serial reuses in the brewing process and from the mixture of spent yeast with different number of reuses was very similar and ranged between 5.0% and 6.4%. Its proximate composition (% dw) is shown in Table 3.1. The protein fraction was the major component of BSY extracts and its content ranged from 69.8% (R2) to 76.5% (R4). The ash content was around 1%, whereas the lipid content was lower than 1%. Comparison of the proximate compositions of BSY extracts with literature is a difficult task because different processes for cell debittering and lysis were performed and also because they are reported for different *Saccharomyces* species. However, the proximate composition is in agreement with the results obtained by Caballero-Córdoba and Sgarbieri (25), when mechanical cell rupturing process using glass beads was also employed. Statistical treatment of results indicates significant differences concerning the composition of BSY extracts with different reuses in the brewing process; however, the most relevant is the increase of protein content with the increase of yeast repitching.

Table 3.1. Proximate composition (% dw) of freeze-dried BSY extracts

	R2	R3	R4	MIST	Mean
Protein	69.8±2.8 <sup>c</sup>	73.3±4.1 <sup>b</sup>	76.5±2.8 <sup>a</sup>	71.4±0.3 <sup>bc</sup>	72.8±3.7
Lipid	0.5±0.1 <sup>b</sup>	0.6±0.1 <sup>a</sup>	0.6±0.1 <sup>a</sup>	0.5±0.0 <sup>b</sup>	0.6±0.1
Ash	1.2±0.1 <sup>b</sup>	1.3±0.2 <sup>a</sup>	1.4±0.3 <sup>a</sup>	0.6±0.1 <sup>c</sup>	1.1±0.4
<i>nd</i> <sup>A</sup>	28.6±2.6 <sup>a</sup>	24.8±4.3 <sup>b</sup>	21.5±2.9 <sup>c</sup>	27.5±0.3 <sup>ab</sup>	25.6±3.9

R2: 3 samples of yeast biomass used twice in the brewing process; R3: 3 samples of yeast biomass with three serial reuses in the brewing process; R4: 3 samples of yeast biomass with four serial reuses in the brewing process; MIST: 3 samples of yeast surplus containing a mixture of biomass with different number of reuses in the fermentation process. Results are expressed as a mean ± standard deviation (n=9). Values in the same row followed by different superscripted letters indicate significant differences at  $p < 0.05$ , Duncan's post hoc test.

<sup>A</sup> *nd*. not determined; fraction corresponding to sum of carbohydrates, RNA, non-nitrogen fraction and others components.

### 3.3.2. Amino acid composition of BSY protein fraction

The amino acid composition of the BSY protein fraction is presented in Table 3.2. In general, BSY extracts prepared from spent yeast with different reuses in brewing process had a similar amino acid profile ( $p < 0.05$ ). Furthermore, the essential amino acid profile of BSY extracts was considerably higher ( $p < 0.05$ ) than the suggested amino acid pattern recommended by FAO/WHO for adult humans (149). Similar results were observed by Caballero-Córdoba and Sgarbieri (25). BSY extracts were rich in glutamic acid (12.6%-15.8%), histidine (10.5%-11.6%) and alanine (8.0%-8.8%), as quantified by Caballero-Córdoba and Sgarbieri (28). However, these contents were relatively higher, when compared with BSY extracts obtained from other processes, namely autolysis and hydrolysis, as observed by other authors (25), (45), (166). According to Jung *et al.* (45), the amino acids histidine and proline are the components of CHP (Cyclo-His-Pro), an endogenous cyclic dipeptide involved in antioxidant activity of BSY hydrolysates. Generally, S-amino acids (methionine and cysteine) are the limiting factor to the nutritive value of yeast protein (25). However, as reported in Table 3.2, the S-amino acids were above the FAO/WHO reference (149); the contents observed were in accordance with those reported by Caballero-Córdoba and Sgarbieri (25). The essential amino acids ranged between 37.2% and 38.9%, being close to the reference value of 40%, recommended by FAO/WHO

(149). BSY extracts presented a high content of the flavour enhancers, glutamic acid, aspartic acid, glycine and alanine, the sum of which represents 30.1-32.9% of total amino acids. The results of chemical score based on lysine (limiting amino acid) of BSY extracts ranged between 1.3 and 1.7 and the protein efficiency ratio (PER) ranged between 1.6 and 2.4. In general, based on our results, extracts obtained from mechanical disruption of BSY were shown to be high quality nutritional ingredients.

### 3.3.3. Molecular weight distribution of BSY extract protein fraction

The molecular weight of BSY extract proteins were determined by SDS-PAGE. The typical SDS-PAGE profile observed for protein fraction from yeast surplus with two, three, and four serial reuses in the brewing process and from the mixture of spent yeast with different number of reuses was very similar. As shown in Figure 3.1, the electrophoretic patterns of BSY proteins presented seven major bands with 61, 58, 47, 42, 33, 29 and 27 kDa. Also, minor bands were observed with molecular weight lower than 21 kDa and higher than 61 kDa. According to Slaughter and Nomura (167), vacuolar proteases have been identified in a brewing strain of *Saccharomyces cerevisiae*; PrB has a molecular weight of 33 kDa, PrA has 42 kDa and CPY has 61 kDa. The BSY extracts presented 3 bands with these molecular weights, presumably corresponding to the 3 proteases described by Slaughter and Nomura (167). Although, only a purification process of BSY enzymes can confirm protein identification, the proteolytic activity of extracts can be easily evaluated.

Table 3.2. Amino acid composition of BSY extracts (g/100 g protein) and comparison with FAO/WHO reference protein

Amino acids	Ions	Amino acid composition (g/100 g Protein) <sup>a</sup>					FAO/WHO <sup>b</sup>
		R2	R3	R4	MIST		
Alanine <sup>d</sup>	232	8.0±0.3	8.1±0.3	8.8±0.2	8.3±0.1		-
Arginine <sup>c</sup>	286	5.4±0.8	5.5±0.6	6.8±0.8	5.6±0.8		-
Aspartic acid <sup>d</sup>	316	5.9±0.2	5.1±0.2	5.3±0.2	5.1±0.2		-
Cysteine	406	1.4±0.0	1.9±0.0	2.1±0.0	1.1±0.0		-
Glutamic acid <sup>d</sup>	432	12.6±0.4	13.4±0.5	15.8±0.4	14.5±0.4		-
Asparagine	417	2.1±0.0	2.6±0.1	2.2±0.1	2.2±0.0		-
Glutamine	329	2.6±0.2	3.1±0.2	3.3±0.2	2.8±0.2		-
Glycine <sup>d</sup>	218	3.6±0.6	3.7±0.8	2.9±0.3	3.4±0.4		-
Histidine <sup>c</sup>	196	10.6±0.8	10.5±0.8	10.7±0.9	11.6±1.0		1.6
Isoleucine <sup>c</sup>	200	3.5±0.0	3.4±0.1	3.5±0.0	3.0±0.1		1.3
Leucine <sup>c</sup>	200	3.6±0.2	3.5±0.2	3.3±0.0	3.2±0.3		1.9
Lysine <sup>c</sup>	300	2.6±0.2	2.6±0.2	2.7±0.3	2.2±0.2		1.6
Methionine <sup>c</sup>	218	3.1±0.2	3.1±0.1	2.4±0.2	2.7±0.1		1.7
Phenylalanine <sup>c</sup>	336	3.2±0.0	3.2±0.0	3.1±0.0	3.6±0.0		-
Proline	184	2.3±0.0	2.61±0.0	1.9±0.0	2.7±0.0		-
Serine	362	4.2±0.2	4.4±0.3	4.2±0.2	4.6±0.1		-
Threonine <sup>c</sup>	404	2.4±0.0	2.5±0.1	2.5±0.0	2.0±0.1		0.9
Tyrosine	466	2.3±0.0	2.3±0.0	2.4±0.0	2.8±0.0		-
Valine <sup>c</sup>	186	3.6±0.1	3.5±0.2	4.0±0.1	4.3±0.1		1.3
Tryptophan	<i>nd</i>	<i>nd</i>	<i>nd</i>	<i>nd</i>	<i>nd</i>		-
Σ Amino acid (TAA)		82.9±8.6	84.3±9.5	87.9±7.7	85.5±8.4		
Σ Essential amino acid (EAA) <sup>c</sup>		38.0±4.6	37.2±4.6	38.9±4.5	38.1±5.4		
Σ Flavour amino acid (FAA) <sup>d</sup>		30.1±3.0	30.3±3.6	32.9±2.1	31.3±2.4		
EAA/AA		0.5±0.0	0.4±0.0	0.4±0.0	0.5±0.0		
Protein efficiency ratio (PER)		2.4±0.8	2.3±0.7	1.8±0.5	1.6±1.0		
Chemical score <sup>e</sup>		1.6±0.3	1.3±0.3	1.7±0.3	1.4±0.3		

<sup>a</sup> Values represent mean ± standard deviation (n=3).

<sup>b</sup> Suggested profile of EAA requirements for adults (FAO/WHO, 1990).

<sup>c</sup> Essential amino acids.

<sup>d</sup> Flavour amino acids.

<sup>e</sup> Chemical score calculated based on lysine (limitant amino acid).

*nd. not determined.*

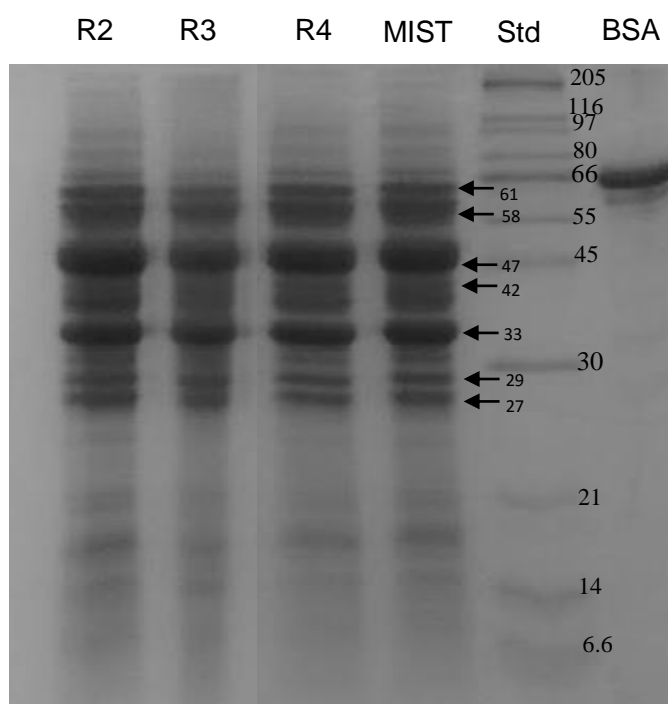


Figure 3.1. SDS-PAGE profiles of BSY extracts. Lane BSA shows bovine serum albumin (66 kDa); lane Std shows molecular weight markers (6.6-205 kDa). A total of 25  $\mu$ g of BSY protein was applied to each well. R2: yeast biomass used twice in the brewing process; R3: yeast biomass with three serial reuses in the brewing process; R4: yeast biomass with four serial reuses in the brewing process; MIST: yeast surplus containing a mixture of biomass with different number of reuses in the fermentation process.

### 3.3.4. Proteolytic activity of BSY extracts

The results of BSY extracts proteolytic activity ranged between 0.14 U/mL (MIST) and 0.22 U/mL (R2), which are in agreement with Slaughter and Nomura (167), who found proteolytic activity of vacuolar proteases ranging between 0.2 and 0.8 U/mL. ANOVA analysis showed differences between the proteolytic activity of different BSY extracts ( $p < 0.05$ ). R2 BSY extract presented the highest proteolytic activity (0.22 U/mL), followed by R3 BSY extract (0.19 U/mL) and R4 BSY extract; (0.18 U/mL), whereas MIST BSY extract present the lowest proteolytic activity, 0.14 U/mL. Literature refers that under stress conditions proteases activity of yeast cells increase and begins to digest its own proteins (168). During this process, natural inhibitors of the major yeast proteases are also digested in a sequential manner, gradually releasing more proteolytic activity (168). However, results from our study showed higher proteolytic activity of BSY extracts obtained from spent yeast with two reuses in the brewing process in comparison with three and four reuses.

### 3.3.5. TPC, TFC and antioxidant activity of BSY extracts

Data reported in Table 3.3 show that TPC of the different BSY extracts varied from 255.7  $\mu\text{M}$  GAE to 304.5  $\mu\text{M}$  GAE, being the highest content obtained for R2 BSY extract and the lowest for the MIST BSY extract. Flavonoid content was measured using the aluminum chloride colorimetric method; the results depicted in Table 3.3 show that TFC varied from 187.2  $\mu\text{M}$  CE/mL (R3 BSY extract) to 308.6  $\mu\text{M}$  CE/mL (R2 BSY extract). The serial repitching of yeast biomass on brewing process does not interfere with TPC and TFC. The potential antioxidant activity observed for BSY extracts can be explained by the presence of antioxidant agents, namely glutathione, *Maillard* reaction products, sulfur-containing amino acids and polysaccharides (35). In this work, the antioxidant potential of the BSY extracts was assessed through different complementary *in vitro* assays and compared to standard antioxidant (ascorbic acid at a concentration of 500  $\mu\text{M}$  TE). Results from DPPH ranged between 245.7  $\mu\text{M}$  TE/mL (R3 BSY extract) and 268.1  $\mu\text{M}$  TE/mL (R4 BSY extract), as presented in Table 3.3. ANOVA analysis showed differences between the DPPH free radical scavenging activity of different BSY extracts ( $p < 0.05$ ). Several compounds, such as, cysteine, glutathione, ascorbic acid, tocopherol, flavonoids, tannins and aromatic amines may reduce DPPH radical by their hydrogen donating ability (9). The RP of BSY extracts ranged between 463.0  $\mu\text{M}$  TE/mL and 565.7  $\mu\text{M}$  TE/mL and the FRAP results ranged from 215.0 to 272.3  $\mu\text{M}$  TE/mL. For both assays, BSY MIST extract showed the lowest antioxidant activities. In general, the analysis of variance (ANOVA) showed differences between the different extracts ( $p < 0.05$ ), indicating different behaviors and consequently bioactivities differences presented by the evaluated BSY extracts. Except for FRAP assay, results were quite comparable with the activity of ascorbic acid at a concentration of 500  $\mu\text{M}$ .

Table 3.3. Biological activity BSY extracts, namely proteolytic activity, ACE-I activity, Total Phenolic Content (TPC), Total Flavonoid Content (TFC) and antioxidant activity

BSY	Prot. Activity (U/mL) <sup>(i)</sup>	IC <sub>50</sub> (µg/mL) <sup>(ii)</sup>	TPC (µM GAE/mL)	TFC (µM CE/mL)	Antioxidant activity		
					FRAP (µM TE/mL)	DPPH (µM TE/mL)	RP (µM TE/mL)
R2	0.22±0.0 <sup>a</sup>	266.3±11.5 <sup>d</sup>	304.5±1.6 <sup>a</sup>	308.6±9.7 <sup>a</sup>	272.3±14.6 <sup>a</sup>	257.5±6.9 <sup>ab</sup>	555.0±4.8 <sup>a</sup>
R3	0.19±0.0 <sup>b</sup>	288.8±6.5 <sup>c</sup>	286.1±54.5 <sup>a</sup>	187.2±82.5 <sup>b</sup>	218.8±43.2 <sup>bc</sup>	245.7±22.5 <sup>b</sup>	513.0±55.9 <sup>ab</sup>
R4	0.18±0.0 <sup>b</sup>	309.8±7.6 <sup>b</sup>	295.5±22.0 <sup>a</sup>	234.4±63.2 <sup>b</sup>	247.4±44.2 <sup>ab</sup>	268.1±6.5 <sup>a</sup>	565.7±48.7 <sup>a</sup>
MIST	0.14±0.0 <sup>c</sup>	468.5±7.5 <sup>a</sup>	255.7±8.1 <sup>b</sup>	239.4±12.1 <sup>b</sup>	215.0±4.2 <sup>c</sup>	267.9±4.1 <sup>a</sup>	463.0±20.0 <sup>b</sup>
Control <sup>(iii)</sup>	0.19±0.0	16±1.0			1077±45.4	282±2.5	627±13.8

R2: 3 samples of yeast biomass used twice in the brewing process; R3: 3 samples of yeast biomass with three serial reuses in the brewing process; R4: 3 samples of yeast biomass with four serial reuses in the brewing process; MIST: 3 samples of yeast surplus containing a mixture of biomass with different number of reuses in the fermentation process. Results are expressed as a mean ± standard deviation (n=9). Values in the same column followed by different subscripted letters indicate significant differences at  $p < 0.05$ , Duncan's post hoc test.

<sup>(i)</sup> 1U = 1 µg of tyrosine equivalent released from casein per min.

<sup>(ii)</sup> IC<sub>50</sub> = concentration (µg protein/mL) of ACE inhibitor required to inhibit 50% of the ACE activity.

<sup>(iii)</sup> Alcalase® diluted at 0.2 U/mL was used as positive control in the enzyme activity assay; Captopril was used as positive control in the ACE-I assay; a standard solution of vitamin C (500 µM) was used as positive control in antioxidant activity assays.

Legend: µM CE (Catechin Equivalent); µM TE (Trolox Equivalent); µM GAE (Gallic Acid Equivalent).

### 3.3.6. ACE-I activity of BSY extracts

In our study, the highest ACE-I activity (lowest  $IC_{50}$  value) was observed for BSY prepared from R2 biomass, 266.3  $\mu\text{g}$  protein/mL, as presented in Table 3.3. In contrast, the BSY extracts prepared from MIST, presented the lowest ACE-I activity, value of 468.5  $\mu\text{g}$  protein/mL. ANOVA analysis shows that the serial repitching of yeast biomass on brewing process influenced significantly this biological property ( $p < 0.05$ ). There is little information in the literature regarding the potential ACE-I of *Saccharomyces* yeast, particularly for BSY. Kim *et al.* (75) reported the ACE-I from *Saccharomyces cerevisiae* extract with an  $IC_{50}$  of 70  $\mu\text{g}/\text{mL}$ , after 24 h of cultivation at 30°C, treatment with pepsin and further purification of the ACE-I peptides by UF, Sephadex G-25 column chromatography and RP-HPLC. According to these authors, the ACE-I activity of the peptide fraction purified was slightly lower than that of the commercial antihypertensive drug captopril. BSY can be considered a good source for antihypertensive compounds due its GRAS status and the absence of adverse effects, such as coughs and allergies, associated with captopril or other synthetic antihypertensive agents.

### 3.3.7. Stability of biological activity of frozen BSY extracts

Freeze-dried BSY extracts maintained its proteolytic activity after 6 months of storage at -25°C, while frozen resuspended BSY extracts presented a significant decrease ( $p < 0.05$ ) of the proteolytic activity after 4 months at -25°C, decreasing to approximately half of the initial value after 6 months. However, no significant differences were observed on the other biological activities of the freeze-dried or frozen resuspended BSY extracts ( $p < 0.05$ ). The results obtained for resuspended BSY extracts of MIST are summarized in Figure 3.2 and highlight that storage time of 6 months (at -25°C) preserve the ACE-I activity, TPC, TFC and antioxidant activity of the BSY extracts.



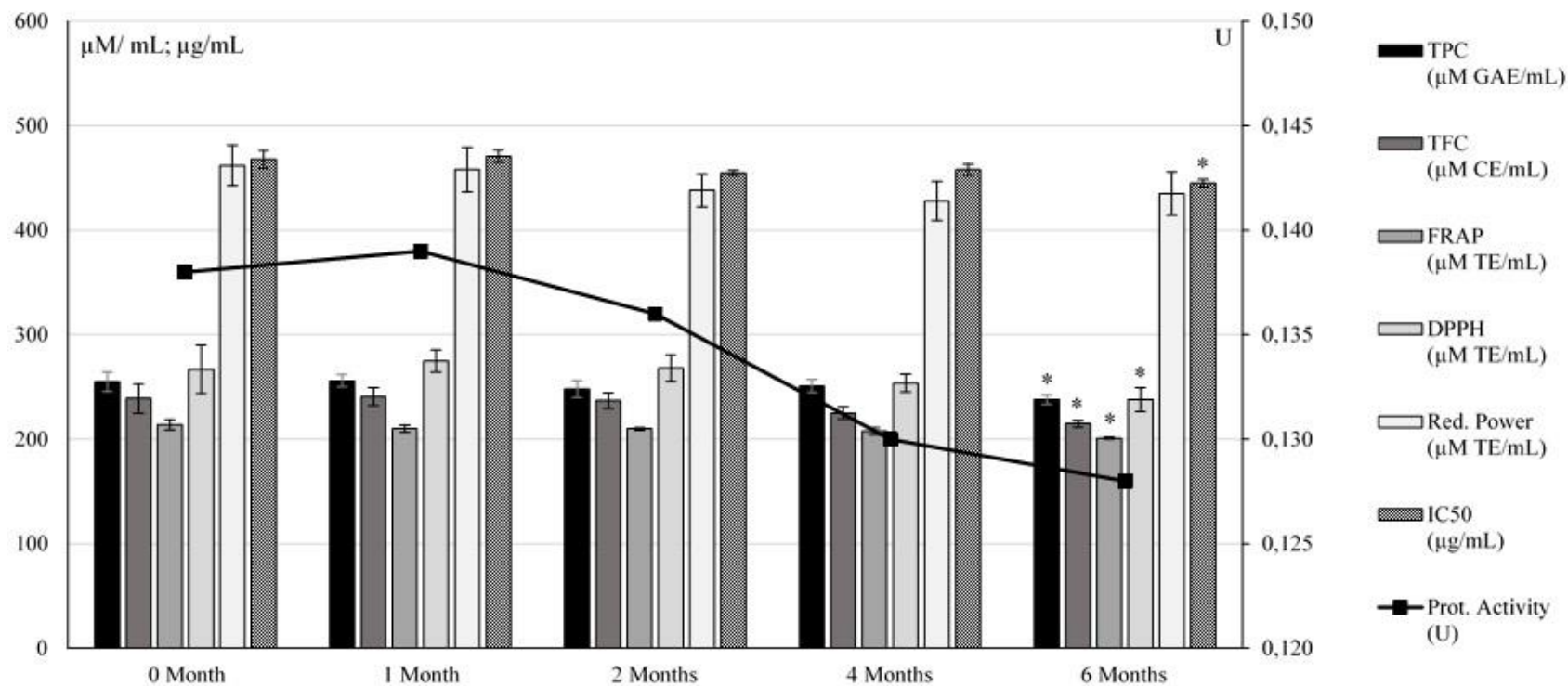


Figure 3.2. Biological activities stability of MIST BSY extract, stored at  $-25^{\circ}\text{C}$  for 6 months. Results are expressed as mean  $\pm$  standard deviation of. Legend:  $\mu\text{M CE}$  (Catechin Equivalent);  $\mu\text{M TE}$  (Trolox Equivalent);  $\mu\text{M GAE}$  (Gallic Acid Equivalent);  $\text{IC}_{50}$  = concentration ( $\mu\text{g/mL}$ ) of ACE inhibitor required to inhibit 50% of the ACE activity;  $1\text{U} = 1\text{ }\mu\text{g}$  of tyrosine equivalent released from casein per min.

\* significantly different from initial value (0 Month),  $p < 0.05$ , Student  $t$  test.

### 3.4. CONCLUSIONS

Proteins are the major components of BSY extracts, its amino acid profile is well-balanced for human consumption. Additionally, those extracts present ACE-I activity and antioxidant activity. The antioxidant activity of BSY extract was comparable to the conventional synthetic antioxidant ascorbic acid, tested at the concentration of 500  $\mu$ M. The number of the yeast reuses in brewing process does not influence significantly the antioxidant activity of yeast extracts, however, proteolytic activity and ACE-I activity reduces with the increase of serial repitching. Good stability of biological activities of BSY extracts was observed during a storage period of 6 months at -25°C, without loss of their TPC, TFC, antioxidant properties, as well, its ACE-I activity. However, its proteolytic activity decrease approximately 50% after 4 months of storage at -25°C when resuspended. Therefore, BSY extracts obtained using mechanical disruption can be explored in functional foods, cosmetic and pharmaceutical products due to their bioactive properties. To the best of our knowledge, this is the first report on the influence of serial repitching of brewing yeast on biological properties of its extracts.

## CHAPTER 4

### *Autolysis of intracellular content of brewer`s spent yeast to maximize ACE-inhibitory and antioxidant activities*

---

This chapter presents the autolysis optimization of the BSY extract to enhance its antioxidant and ACE-inhibitory activities.



## ABSTRACT

Brewer's spent yeast (BSY), the second major by-product from brewing, is recognized as a promising source of potentially bioactive ingredients. Mechanical disruption of BSY cell wall was performed to remove the  $\beta$ -glucans rich fraction and obtain the intracellular content, rich in proteins and enzymes, which were submitted to further autolyses. Response surface methodology (RSM) enabled the prediction of optimum autolysis conditions to achieve the highest Total Phenolic Content (TPC), antioxidant properties (evaluated by FRAP assay) and angiotensin I-converting enzyme inhibitory (ACE-I) activity. Autolysis of BSY inner cell content at 36.0°C, 6.0 h gave a TPC of 385  $\mu$ M GAE/mL, a FRAP value of 374  $\mu$ M TE/mL and an IC<sub>50</sub> value of 379  $\mu$ g/mL. These experimental results were in agreement with the RSM predicted values. The combination of ACE-I and antioxidant activity in one autolysate can be very useful for application as function ingredient for food industry.

## 4.1. INTRODUCTION

Brewer's spent yeast (BSY) (*Saccharomyces* genre) is the second major by-product from brewing (5), which presents a well-balanced amino acid profile, phenolic compounds, peptides, vitamins,  $\beta$ -glucans and nucleotides (36), (50), (86). It is also a source of several proteolytic enzymes, such as, PrA, PrB, CPY, AP1, aminopeptidase C and dipeptidyl aminopeptidase B (11), (44), (64). BSY autolysates and hydrolysates have been reported to possess several biological properties, particularly antioxidant (45), (76), (79), (169) and/or antihypertensive activities (86), (75), (79), (169), (170). Autolysis or self-digestion is often used for intracellular break down of proteins, nucleic acids and other cell constituents. The yeast autolytic process is usually carried out by incubation of yeast cells under moderate agitation and temperatures between 45-60°C for 8-72 h. The major disadvantages are low extraction yield, difficult solid liquid separation due to high content of residue in autolysates, and risk of deterioration due to microbial contamination. Hydrolysis by sonication and digestion by enzymes, such as, trypsin, chymotrypsin flavourzyme, papain, and pancreatin is faster, although more expensive because requires exogenous enzymes (76), (169).

The recovery of yeast cell-wall  $\beta$ -glucans to be used as a food ingredient was approved by the EFSA (143). However, to make the process of  $\beta$ -glucans' separation from BSY profitable, new applications for the inner cell content are required. Cell wall disintegration for  $\beta$ -glucans' separation can be performed by mechanical procedures (46), (50), (66). Ultrasound extraction is highly efficient, but it promotes protein denaturation due

to the increase of temperature (46), (66). Thus, when the main purpose is the recovery of native enzyme fraction for further autolysis of inner cell content, vortexing with glass beads under refrigerated conditions is commonly adopted at laboratorial scale (44), (50). Therefore, the objective of the present study was to produce an autolysate from intracellular BSY content to obtain a functional ingredient. The combination of ACE-I and antioxidant activity in one product could be very useful for the control of cardiovascular diseases. For this purpose, Response Surface Methodology (RSM) was employed to optimize the autolysis process (time and temperature) in order to achieve maximum antioxidant and ACE-I activities.

## 4.2. MATERIAL AND METHODS

### 4.2.1. Reagents

Acetonitrile (HPLC grade) and Folin-Ciocalteu phenol reagent were obtained from Merck (Darmstadt, Germany). Bovine serum albumin (BSA); trifluoroacetic acid (TFA); gallic acid; 2,4,6-tripyridyl-s-triazine (TPTZ); 6-hydroxy-2,5,7,8-tetramethylchroman-2-carboxylic acid (Trolox); commercial angiotensin-I-converting enzyme (ACE) (EC 3.4.15.1, 5.1 U/mg) and the Millipore 5 kDa MWCO UF membranes were purchased from Sigma-Aldrich (St. Louis, MO, USA). ABz-Gly-Phe(NO<sub>2</sub>)-Pro was purchased from Bachem Feinchemikalien (Bubendorf, Switzerland). Ultrapure water was obtained from a Seral-Seralpur Pro 90 CN water purification system from Belgolabo (Overijse, Belgium).

### 4.2.2. Brewer's spent yeast (BSY) extract

The BSY (*Saccharomyces pastorianus*) was supplied as slurry by Unicer brewing (Leça do Balio, Portugal). BSY was collected in 1 liter glass bottle and transported to the laboratory under refrigerated conditions. The BSY extract was prepared according to Vieira *et al.* (50) protocol. Firstly, BSY was washed three times with phosphate buffer, pH 6.0 (volume ratio 1:3). After centrifugation (5,000 x g) during 15 min at 4°C, the yeast cell wall was destroyed with glass beads with a diameter of 0.60 mm at a ratio 1:1:1 (BSY: phosphate buffer pH 6.0: glass beads); (m/v/m), by vortexing 10 times (1 min each) with 1 min cooling intervals on ice-water bath to keep the temperature below 4°C during the entire process. After removing the glass beads by allowing the suspension to stand, the homogenate was centrifuged at 12,000 x g, for 40 min at 4°C, to remove the cell debris. The resulting clear supernatant was collected and kept at -20°C until used.

### 4.2.3. Autolysis of BSY extract

The protein content of BSY extract was determined by the Bradford method (171) and the protease activity was performed according to Cupp-Enyard assay (164). Autolyses were performed using 10 mL of BSY extract, under constant agitation (200 rpm) at different temperatures and times, according to the experimental design described in sub-section 4.2.5. Control samples were BSY extract without any further treatment. Autolyses were terminated by heating the final solutions at 90°C for 15 min, followed by centrifugation at 10,000 x *g* for 10 min.

### 4.2.4. Analytical Methods

#### 4.2.4.1. Determination of Total Phenolic content

The method used for Total Phenolic quantification was similar to that described by Herald *et al.* (155). Gallic acid was used as standard at 10-500 µM to produce a calibration curve (average  $R^2 = 0.9979$ ). Total phenolic content (TPC) was expressed as mean values ± standard deviations, as µM of gallic acid equivalent per mL of BSY autolysate (µM GAE/mL). Spectrophotometric analyses were carried out using a BMG LABTECH's SPECTROstar Nano-microplate, cuvette UV/Vis absorbance reader (Offenburg, Germany).

#### 4.2.4.2. Determination of Ferric ion reducing antioxidant power

Determination of Ferric ion reducing ability (FRAP) was based on the method described by Jansen and Ruskovska (154). Trolox was used as standard at 10-500 µM to produce a calibration curve (average  $R^2 = 0.9943$ ). Results were expressed as mean values ± standard deviations, as µM of Trolox equivalent per mL of BSY autolysate (µM TE/mL).

#### 4.2.4.3. Determination of ACE-I activity

ACE-I activity was measured using the fluorimetric assay of Sentandreu and Toldrá (121), with the modifications reported by Quiros *et al.* (122). ACE-I percentage (I %) was calculated using the equation:

$$I \% = \{(B - A) / (B - C)\} \times 100 \quad (1)$$

where B is the fluorescence of the ACE solution without the inhibitor (BSY autolysate), A is the fluorescence of the tested sample (BSY autolysate) and C is the fluorescence of experimental blank, *o*-ABz-Gly-Phe(NO<sub>2</sub>)-Pro dissolved in 150 mM Tris-base buffer (pH 8.3), containing 1.125 M NaCl. The percent inhibition curves (using a minimum of five determinations for each sample peptide concentration) were plotted *versus* peptide concentration to estimate the mean IC<sub>50</sub> value, which is defined as the concentration required to decrease the ACE activity by 50% (122). Peptide content was determined by

Bradford method (171). Fluorimetric analyses were carried out using a fluorescence microplate reader (FLUOstar Optima, BMG Labtech GmbH).

#### **4.2.5. Experimental design, modelling and optimization of autolysis conditions**

The autolysis conditions that enabled the BSY autolysate with highest antioxidant and ACE-I activities were optimized using a Central composite design (CCD). Two variables, namely, temperature (X1) and time (X2) were included in the model, in which each parameter was examined at five different levels, as shown in Table 4.1. CCD consisted of a complete  $2^2$ -factorial design as cubic points, with four axial points at a distance of  $\alpha = 1.414$  from the design centre and five centre points. The responses used in experimental design were TPC (Y1), antioxidant activity evaluated by FRAP assay (Y2) and ACE-I activity (Y3). The optimal values of response Y were obtained by solving the regression equation and by analysis of 2D contour plots using the predictive equations of RSM. Then, the accuracy of the models was tested by conducting a set of experiments using the critical values optimized; the *t* test was conducted to compare the responses prepared under optimized conditions with those predicted by models.

#### **4.2.6. Statistical analysis**

Analysis of the experimental design, calculation of predicted data and production of surface plots were carried out using the software Design Expert trial version 7 (Stat-Ease Inc., Minneapolis, MN, USA). Statistical analysis of the other analytical results was performed with SPSS 22.0 (SPSS Inc., Chicago, IL, USA). Analysis of variance (ANOVA) of the data was performed, differences were considered significant at  $p < 0.05$ .

### **4.3. RESULTS AND DISCUSSION**

A BSY extract containing 10 mg of proteins/mL was used in the autolyses experiments. The protease activity of the BSY extract was 0.22 U/mL and the pH was 6.0. Before the autolysis process, the BSY extract presented a TPC of 217  $\mu\text{M}$  GAE/mL; a FRAP value of 199  $\mu\text{M}$  TE/mL and an  $\text{IC}_{50}$  value of 481  $\mu\text{g}$  protein/mL.

#### **4.3.1. Validation of the experimental design**

In order to investigate the effect of autolysis conditions on the bioactivity of BSY extract, the experiments were performed in a random manner at different combinations of temperature (X1) and time (X2). The TPC (Y1), FRAP (Y2) and ACE-I activity (Y3) of BSY autolysates were used as response factors for CCD (Table 4.1). Adequacy and significance



of the models were evaluated by analysis of the variance (ANOVA) by means of Fisher's F-test, as detailed in Table 4.2. The independent variable X1 and X2 had a significant effect on all the responses. The interactions between X1.X2 also had significant effect on all responses ( $p < 0.05$ ). Quadratic term for X1 likewise had significant effect on all responses, but quadratic term for X2 only had significant effect on Y1 response. Thus, models presented a quadratic response for the three studied responses.

The quadratic models were validated by two diagnostic residuals, the squared correlation coefficient ( $R^2$ ) and the predictive squared correlation coefficient ( $Q^2$ ). Typical values indicating good models are  $R^2 > 0.75$  and  $Q^2 > 0.60$  (172). The  $R^2$  for checking the fitness of model was very good ( $R^2_{\text{adjust}}$  was relatively close to 1), indicating that model explained 99.9%, 98.2% and 97.0% of the variation on the X1, X2 and X3, respectively. The  $Q^2$  values were respectively 0.8461; 0.9756 and 0.9961 for the three responses, indicating the goodness of the model. The statistical analysis of variance also revealed that the "lack of fit" was not significant ( $p > 0.05$ ) for all the response surface models and the "Adeq Precision" was higher than 4 (as desirable) for all responses, indicating an adequate signal-to-noise ratio. This confirmed the adequacy of model terms to describe the experimental data and for the prediction of the three studied parameters.

Table 4.1. Experimental design for evaluation the effects of autolysis conditions on biological properties of BSY autolysate

run	Independent variables		Dependent variables		
	T (X1) (°C)	t (X2) (h)	Total Phenolics (Y1; TPC $\mu$ M GAE/mL)	Antioxidant activity (Y2; FRAP $\mu$ M TE/mL)	ACE-I activity (Y3; IC <sub>50</sub> $\mu$ g/mL)
1	25.0	1.5	277	235	421
2	50.0	6.0	340	364	506
3	38.0	3.8	347	351	376
4	38.0	3.8	347	360	388
5	20.0	3.8	242	231	431
6	38.0	3.8	346	352	386
7	38.0	1.0	342	321	410
8	55.0	3.8	266	328	538
9	38.0	3.8	348	352	390
10	38.0	3.8	347	351	389
11	38.0	7.0	405	383	380
12	25.0	6.0	330	335	375
13	50.0	1.5	309	337	489

Table 4.2. Analysis of variance (ANOVA) for Total phenolic content, Antioxidant activity and ACE-I activity of BSY autolysate

Source	Sum of Squares			Mean Square			F value			p-value		
	Y1	Y2	Y3	Y1	Y2	Y3	Y1	Y2	Y3	Y1	Y2	Y3
Model	22277.6	25609.0	35587.8	4455.5	5121.8	7117.6	2303.0	130.4	77.3	<0.0001*	<0.0001*	<0.0001*
X1- °C	684.5	9057.0	15329.6	684.5	9057.0	15329.6	353.8	230.5	166.6	<0.0001*	<0.0001*	<0.0001*
X2- h	3800.8	5778.4	755.2	3800.8	5778.4	755.2	1964.6	147.1	8.2	<0.0001*	<0.0001*	0.0242**
X1.X2	120.1	1347.0	990.1	120.1	1347.0	990.1	62.1	34.3	10.8	0.0001*	0.0006*	0.0135**
X1 <sup>2</sup>	15063.7	9271.3	18506.4	15063.7	9271.3	18506.4	7786.3	236.0	201.1	<0.0001*	<0.0001*	<0.0001*
X2 <sup>2</sup>	1199.2	0.1	231.4	1199.2	0.1	231.4	619.9	0.0	2.5	<0.0001*	0.9755	0.1568
Residual	13.5	275.0	644.2	1.9	393	92.0						
Lack of Fit	10.7	212.6	517.5	3.6	70.9	172.5	5.1	4.5	5.4	0.0745	0.0889	0.0676
Pure Error	2.8	62.4	126.7	0.7	15.6	31.7						
Total	22291.1	25884.0	36232.0									
Q <sup>2</sup> (Y1) = 0.8461		R <sup>2</sup> pred (Y1) = 0.9964		R <sup>2</sup> adjust (Y1) = 0.9990		ratio = 172.7						
Q <sup>2</sup> (Y2) = 0.9756		R <sup>2</sup> pred (Y2) = 0.9378		R <sup>2</sup> adjust (Y2) = 0.9818		ratio = 37.2						
Q <sup>2</sup> (Y3) = 0.9961		R <sup>2</sup> pred (Y3) = 0.8930		R <sup>2</sup> adjust (Y3) = 0.9695		ratio = 27.1						

Y1- Total Phenolic Content; Y2- FRAP; Y3- ACE-I activity.

\* Significance at  $p < 0.01$ ; \*\* Significance at  $p < 0.05$ .

#### 4.3.2. Analysis of response surfaces

The relationship between independent and dependent variables was graphically represented by 2D contour plots generated by the RSM model. As shown in Figure 4.1 (surface and contour plots A and B), TPC and FRAP tended to steadily increase at higher temperature (6.0 h) and reached a maximum at the middle of temperature design, while undergo a reduction when autolysis time was extended at higher temperature. Similar behaviour was observed by other authors for other kind of food hydrolysates (173). The minimum values of TPC and FRAP response were observed for lower temperature and time responses. These results suggest that extension of autolysis time enhances the antioxidant and phenolic composition of BSY autolysates. However, for longer autolysis time under high temperature, the negative quadratic effect became significant. This may be attributed to the thermal degradation of phenolic and other antioxidant compounds at higher temperatures.

Concerning to ACE-I activity, as observed in Figure 4.1 (surface and contour plot C), it increased with time over moderate temperature (which means lower  $IC_{50}$  values), however, when the autolysis time was extended at higher temperature, the BSY autolysate presented a reduction in ACE-I activity (higher  $IC_{50}$  values), suggesting degradation of ACE-I peptides. These results are in agreement to those observed for other food hydrolysates (173), (174).

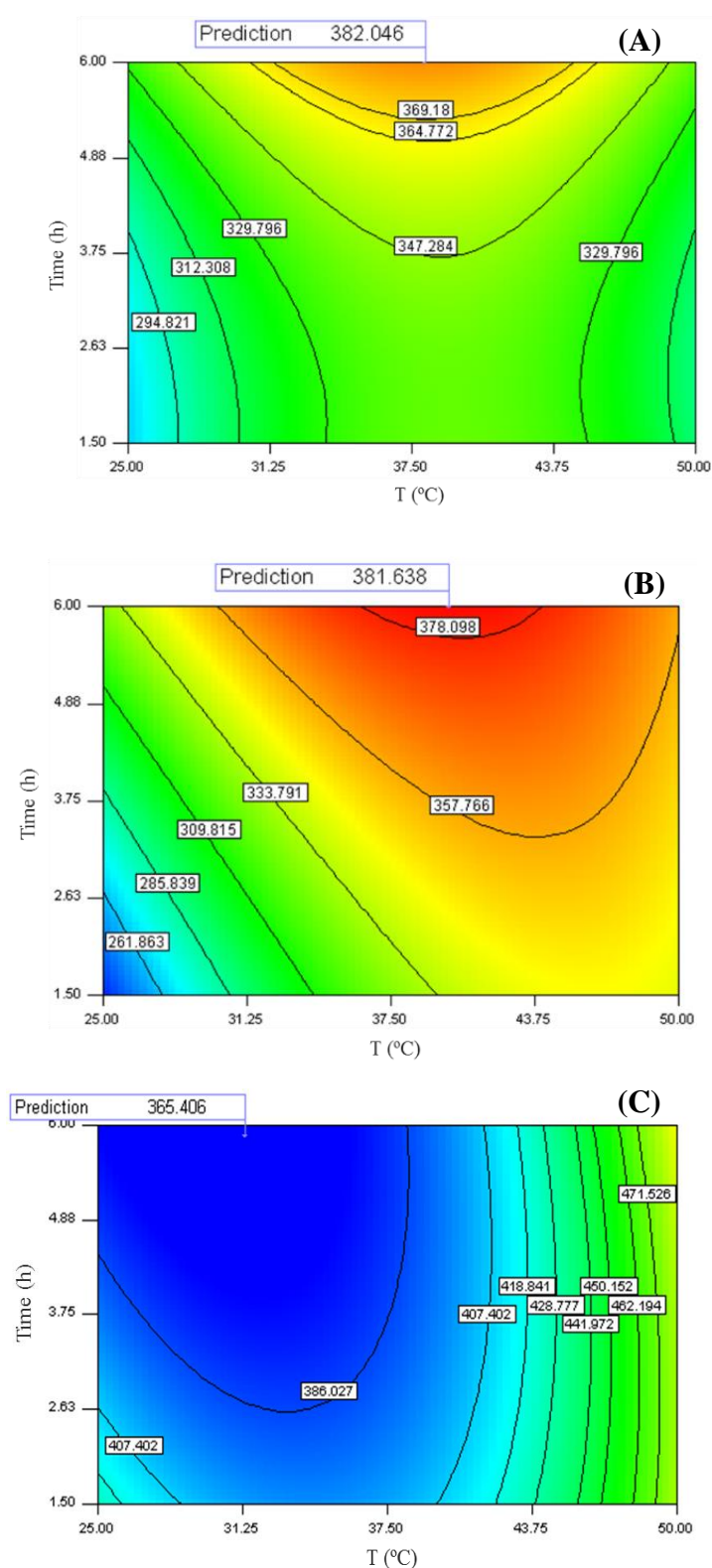


Figure 4.1. Response surface and contour plots for interaction effects of temperature (°C) and time (h) autolysis on Total phenolics **(A)**, FRAP **(B)** and ACE-I activity **(C)**.

#### 4.3.3. Validation of the RSM model

The optimal autolysis conditions to maximize the biological activities of BSY autolysate were predicted by using RSM. For that purpose the response surface was explored and a prediction point was achieved to meet the defined goal, which means maximize the Y1, Y2 responses and minimize the Y3 response. Then, the confirmatory experiments were conducted with the parameters suggested by the experimental models, in three different runs, and the *t* test was applied to confirm the adequacy of the models in predicting the optimum autolysis conditions. Results from numerical optimization are presented in Table 4.3. The maximum TPC for BSY autolysate was predicted for autolysis at 38.0°C, 6.0 h. Under these optimal conditions, the experimental value was 384 µM GAE/mL, which was in agreement ( $p < 0.05$ ) with the predicted value, 382 µM GAE/mL. The maximum FRAP value for BSY autolysate was predicted for autolysis at 40.0°C, 6.0 h. Under these conditions, the experimental value observed was 381 µM TE/mL, being in agreement ( $p < 0.05$ ) with the predicted value, 382 µM TE/mL. The optimal autolysis conditions in order to obtain the higher ACE-I activity (minimum IC<sub>50</sub>) were 31.0°C, 6.0 h; under these conditions, the experimental value obtained was 364 µg/mL, which was in agreement ( $p < 0.05$ ) with the predicted IC<sub>50</sub> value of 365 µg/mL.

Table 4.3. Performance of RSM model in predicting the optimum autolysis conditions to enhance the biological activities of BSY autolysate

Response	Optimum conditions		Predicted value	Experimental value <sup>a</sup>	<i>p</i> value <sup>b</sup>
	Temp (°C)	Time (h)			
TPC (µM GAE/mL)	38.0	6.0	382	384 ± 3	0.345
FRAP (µM TE/mL)	40.0	6.0	382	381 ± 1	0.411
IC <sub>50</sub> (µg/mL)	31.0	6.0	365	364 ± 1	0.401
In combination	36.0	6.0			

<sup>a</sup> Values represent mean ± standard deviation (n=3).

<sup>b</sup> Significance at  $p < 0.05$ .

After single evaluation of response surfaces it was established the same criteria to obtain the optimum experimental conditions for the three responses simultaneously. For that purpose, a statistical toll was employed to explore the response surface of the design and gave a prediction point as a result of defined goals that were introduced. Individual

desirability indices were constructed for each variable of the design. Afterwards, individual desirabilities were combined into a single number and then searched the greatest overall desirability. Desirability indices were built (Figure 4.2) and the optimum conditions obtained were temperature of 36.0°C and autolysis time of 6.0 h, by which the BSY autolysate presented a predicted value for TPC of 381  $\mu\text{M}$  GAE/mL, a FRAP value of 378  $\mu\text{M}$  TE/mL and an  $\text{IC}_{50}$  value of 376  $\mu\text{g}$  protein/mL. Under the optimum conditions, the experimental values were, respectively, 385  $\mu\text{M}$  GAE/mL, 374  $\mu\text{M}$  TE/mL and 379  $\mu\text{g}$  protein/mL. These experimental results were in agreement with the RSM predicted values.

The optimum  $\text{IC}_{50}$  value of BSY obtained in this work is difficult to compare with previous works because the procedure employed to prepare the BSY autolysate is completely different. To best of our knowledge this work is the first attempt to reuse the BSY to produce an autolysate from the inner cell content with enhanced antioxidant and ACE-I activities.

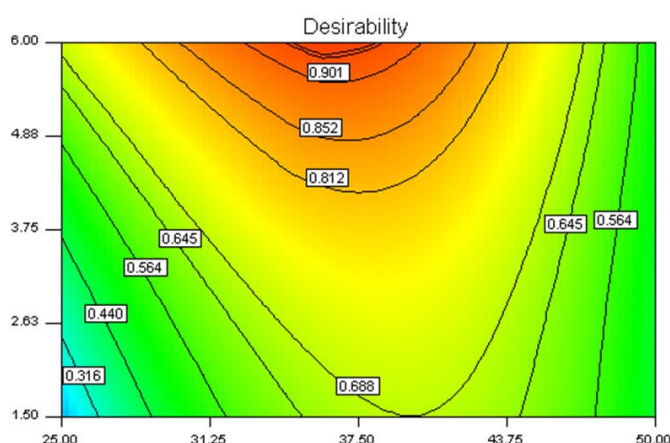


Figure 4.2. Response surface and contour plots for interaction effects of temperature ( $^{\circ}\text{C}$ ) and time (h) autolysis on the desirability index for combined responses of BSY autolysate. Optimum point was identified on the response surface.

#### 4.4. CONCLUSIONS

The BSY extract from inner yeast cell content (rich in proteins and proteases) when submitted to autolysis presented enhanced TPC, FRAP and ACE-I activity (respectively, 385  $\mu\text{M}$  GAE/mL, 374  $\mu\text{M}$  TE/mL and 379  $\mu\text{g}$  protein/mL) compared to the original extract (TPC of 217  $\mu\text{M}$  GAE/mL; a FRAP value of 199  $\mu\text{M}$  TE/mL and an  $\text{IC}_{50}$  value of 481  $\mu\text{g}$  protein/mL). RSM was an efficient statistical methodology to optimize the autolysis conditions; the three biological activities were maximized at 36.0°C, 6.0 h. This autolysate

presents potential for application as ingredient of functional foods due to its antioxidant and ACE-I activities. Further work should be done to assess the bioactivity of peptides from BSY autolysates after GI digestion, their resistance to brush-border peptidases and their susceptibility to intestinal transepithelial transport after GI digestion.



## CHAPTER 5

### *Impact of in vitro gastrointestinal digestion and transepithelial transport on antioxidant and ACE-inhibitory activities of brewer's spent yeast autolysate*

---

This chapter describes the simulated GI digestion and the *in vitro* intestinal cell permeability of the BSY autolysate that presented enhanced antioxidant and ACE-I activities



## ABSTRACT

The impact of *in vitro* gastrointestinal digestion and transepithelial transport on antioxidant and ACE-I activities of brewer's spent yeast (BSY) autolysate obtained from the inner cell content was investigated using Caco-2 cell monolayer and Caco-2/HT29MTX co-culture cell monolayer. Gastrointestinal digestion enhanced both activities (FRAP of 405  $\mu\text{M TE/mL}$  and  $\text{IC}_{50}$  of 345  $\mu\text{g protein/mL}$ ). Within a concentration range of 0.5 to 3.0 mg protein/mL of digested BSY autolysate no cytotoxic effects were observed on Caco-2 cells after 24 h exposition and the response to oxidative stress, induced by hydrogen peroxide, demonstrated the protective role of the BSY autolysate. High apparent permeability coefficient ( $P_{\text{app}}$ ) values for BSY peptides across Caco-2 cell monolayer model ( $12.4\text{--}20.8 \times 10^{-6}$  cm/s) and Caco-2/HT29-MTX cell monolayer ( $14.5\text{--}26.1 \times 10^{-6}$  cm/s) were observed in both models. Antioxidant and ACE-I activities after transepithelial transport suggest that bioactive peptides from digested BSY autolysate and from the action of brush-border peptidases were well absorbed.

## 5.1. INTRODUCTION

Brewer's spent yeast (BSY), the second major by-product from brewing, is currently used as a low-valuable animal feed product (2), (5). However, it owns the GRAS (Generally Recognized as Safe) status and can be valorized through the production of added value functional food ingredients, such as,  $\beta$ -glucans from cell wall (175) and nucleotides (50).

BSY extracts can be obtained by autolysis, plasmolysis and hydrolysis although the most frequent is autolysis (72). The production of BSY autolysates usually involves incubation of cell suspensions of BSY at temperatures ranging from 45 to 60  $^{\circ}\text{C}$  with a reaction time between 8 and 72 h (72), (79), (176). Another possibility not explored in the literature is the autolysis of intracellular content that contains native proteins and proteases, for this purpose a mechanical disruption of BSY cell wall under refrigerated conditions is required (177). After cell wall removing, useful for  $\beta$ -glucans recovery, mild autolysis conditions with lower temperatures and reducing autolysis time can be applied to the inner cell content. BSY autolysates contain bioactive peptides that may have potential applications as food or nutraceutical ingredients due to their antioxidant and ACE-I activities (79). However, the challenge before *in vivo* efficacy studies is to understand the impact of simulated gastrointestinal (GI) digestion; intestinal cell permeability and interaction with intracellular sources of oxidative stress.

The human colorectal adenocarcinoma Caco-2 cell line has been widely used to evaluate the cytotoxicity of bioactive compounds at concentrations used to exert the desired bioactivity in the body, as well as, to study the potential for inhibiting intracellular oxidation (88). Moreover, Caco-2 cell line has been used as *in vitro* model of absorptive enterocytes to evaluate the permeability of drugs and food compounds (131), (178). However, only few studies addressed the intestinal transport of complex mixtures of peptides (127), (178), (179). Furthermore, to the best of our knowledge this is the first study in which the permeability of a BSY autolysate is assessed. The Caco-2 cell monolayers exhibit spontaneous enterocyte-like differentiation under standard culture conditions, showing morphological polarity and expression of brush-border hydrolases, transporters, microvilli and tight junctions, thus mimicking the main characteristics of the human small intestine (133), (178). Nevertheless, this model presents limitations since besides the absorptive enterocytes (80%) the human intestinal epithelial includes other types of cells, including enteroendocrine, goblet and paneth cells. Another disadvantage of the Caco-2 cell line is that the tightness of the monolayer resembles that of the colon and not the small intestine, therefore paracellular transport can be underestimated (180). To overcome these limitations, co-cultures of Caco-2 and mucus-secreting cells (HT29-MTX) have been proposed as a more bio-relevant model of the intestinal epithelium (131), (133), (180).

The major goals of the present study were to investigate: (i) the effect of *in vitro* GI digestion on antioxidant and ACE-I activities of BSY autolysate and the ability of the GI digest to protect Caco-2 cell line regarding viability, mitochondrial integrity and oxidative stress, (ii) the resistance to brush-border peptidases and the susceptibility to intestinal transepithelial transport of BSY peptides, comparing two cell monolayer systems broadly used as models for the small intestine epithelium (Caco-2 and Caco-2/HT29-MTX co-culture cell monolayers), and (iii) the biological activity of BSY permeates.

## 5.2. MATERIAL AND METHODS

### 5.2.1. Reagents and cells

Pepsin; pancreatin; commercial angiotensin-I-converting enzyme (ACE, EC 3.4.15.1, 5.1 U/mg); bovine serum albumin (BSA); trifluoroacetic acid (TFA); 6-hydroxy-2,5,7,8-tetramethylchroman-2-carboxylic acid (Trolox); dimethyl sulfoxide (DMSO); 3-(4,5-dimethylthiazol-2-yl)-2,5-diphenyltetrazolium bromide (MTT) and the Millipore UF membrane 5 kDa were purchased from Sigma-Aldrich (St. Louis, MO, USA). The  $\alpha$ -aminobenzoylglycyl-*p*-nitro-phenylalanylproline ( $\alpha$ -ABz-Gly-Phe(NO<sub>2</sub>)-Pro) was purchased from Bachem Feinchemikalien (Bubendorf, Switzerland). GIBCO Dulbecco's Modified

Eagle Medium (DMEM), heat-inactivated fetal bovine serum (FBS), penicillin/streptomycin, trypsin-EDTA and Hank's balanced salt solution (HBSS, pH 7.0-7.4) were purchased from Invitrogen (Carlsbad, CA). Falcon® translucent polyethylene terephthalate (PET) cell culture inserts (3.0 µm pore size, 24 mm diameter inserts, 4.2 cm<sup>2</sup> effective growth area) were acquired from BD Biosciences (Franklin Lakes, NJ, USA) and 6-well and 96-well microplates were purchased from Corning Costar (Sigma-Aldrich, St. Louis, MO, USA). Human colon carcinoma (Caco-2) cell line was obtained from the American Type Culture Collection (ATCC) and mucus producing HT29-MTX cell line was kindly provided by Dr. T. Lesuffleur (INSERM U178, Villejuif, France).

### 5.2.2. Equipments

The RP-HPLC analyses were carried out using an analytical HPLC system (Jasco, Tokyo, Japan) equipped with a quaternary low pressure gradient HPLC pump (Jasco PU-1580), a degasification unit (Jasco DG-1580-53 3-line degasser), an autosampler (Jasco AS-2057-PLUS), a multiwavelength detector (Jasco MD-910) and a 7125 Rheodyne injector valve (CA, USA). The data acquisition was accomplished using Borwin Controller software, version 1.50 (JMBS Developments, Le Fontanil, France).

Mass Spectrometry (MS) data were acquired using a 4800 MALDI-TOF/TOF (Applied Biosystems, Darmstadt, Germany) mass spectrometer in the *m/z* range of 1000-12000. The MS data was processed using Data Explorer 4.8 Software (Applied Biosystems). Spectrophotometric analyses were carried out using a SPECTROstar Nano-microplate, cuvette UV/Vis absorbance reader (BMG Labtech GmbH, Offenburg, Germany). Fluorimetric analysis were carried out using a fluorescence microplate reader (FLUOstar Optima, BMG Labtech GmbH).

### 5.2.3. Preparation of BSY autolysates and *in vitro* GI digestion

BSY samples (*Saccharomyces pastorianus*) were supplied by Unicer brewing (Leça do Balio, Portugal). Disruption of cell wall to extract the inner yeast content was performed according to Vieira *et al.* (177). BSY autolysates from the inner cell content, presenting 10 mg/mL of proteins determined by the Bradford method (171) and pH 6.0, were submitted to autolysis at 36°C, 6 h and filtered using a 5 kDa MWCO membrane.

To mimic digestion in the stomach and upper intestine, *in vitro* pepsin-pancreatin digestion of BSY autolysate from the inner cell content was performed according to the method described by Samaranayaka *et al.* (181). The digested BSY autolysate was used for screening *in vitro* biological activity (described in sub-section 5.2.4) and for RP-HPLC analysis (described in sub-section 5.2.6). Freeze-drying of digested BSY extract was required for cell assays (described in sub-section 5.2.5).

#### 5.2.4. *In vitro* biological activity

Determination of Ferric ion reducing ability (FRAP) was based on the method of Jansen and Ruskovska (154). Trolox was used as standard at 10-500  $\mu$ M to produce the calibration curve. Results were expressed as mean values  $\pm$  standard deviations of  $\mu$ M of Trolox equivalent per mL ( $\mu$ M TE/mL). Assays were performed in triplicate.

ACE-I activity was measured in triplicate using the fluorimetric assay of Sentandreu and Toldrá (121), with the modifications reported by Quiros *et al.* (122). ACE-I percentage (*I*) was calculated using the equation:

$$I \% = \{(B - A) / (B - C)\} \times 100 \quad (1)$$

where *B* is the fluorescence of the ACE solution without an inhibitor (BSY autolysate); *A* is the fluorescence of the tested sample of BSY autolysate; and *C* is the fluorescence of experimental blank (*o*-ABz-Gly-Phe(NO<sub>2</sub>)-Pro dissolved in 150 mM Tris-base buffer (pH 8.3), containing 1.125 M NaCl). IC<sub>50</sub> values were measured as the concentration required to decrease the ACE activity by 50% (122).

#### 5.2.5. Cell-based assays

##### 5.2.5.1. Cell culture maintenance and generation of cell monolayers

Caco-2 and HT29-MTX cell lines at passage 36 and 47, respectively, were used. The two cell lines were maintained in DMEM supplemented with 10% (v/v) FBS, and 100 U/mL penicillin and 100  $\mu$ g/mL streptomycin, at 37°C under 5% CO<sub>2</sub>, water saturated atmosphere. The medium was changed every other day. For cell permeability studies, 90% confluent Caco-2 and HT29-MTX cells were harvested using trypsin-EDTA and seeded onto permeable membrane supports mounted in 6-well plates. Seeding density was  $2.8 \times 10^5$  cells/mL for Caco-2 cell monolayers and Caco-2/HT29-MTX co-culture model (cell ratio of 90:10), as described by Antunes *et al.* (131). The culture medium was allowed to differentiate for 21 days before permeability experiments. The integrity of the cell monolayers was checked before and after permeability assays by the Transepithelial Electrical Resistance (TEER) using an epithelial voltammeter (EVOM, World Precision Instrument, Sarasota, FL, USA).

##### 5.2.5.2. Cell viability determination

Caco-2 cell viability was determined using the MTT assay described by Laitinen *et al.* (182). Caco-2 cells at densities of  $8 \times 10^4$  cells/well were seeded on 96-well plates in order to obtain a confluent monolayer within 1 day. Then, cells were incubated for 24 h (37°C, 5% CO<sub>2</sub>) with the digested BSY samples at six different concentrations: 0.5; 1.0; 2.0; 3.0; 4.0 and 6.0 mg protein/mL. A negative control (NEGc, cells treated with medium only) and a positive control (POSc, cells treated with medium and 1% Triton X-100) were also included. After

cell treatment with the test samples, the culture medium was aspirated and the attached cells were rinsed with 200  $\mu$ L HBSS, followed by the addition of fresh culture medium containing 0.25 mg/L MTT. After 30 min of incubation (37°C, 5% CO<sub>2</sub>), the formed intracellular crystals of formazan were dissolved using 100  $\mu$ L of DMSO and determined by measuring the absorbance at 570 nm. Data were obtained from three independent experiments, with each plate containing six replicates for each test sample. Cell viability (%) was calculated relative to the maximum viability of NEGc, as follows:

$$\text{Cell viability (\%)} = \left( \frac{\text{Abs sample}}{\text{Abs NEGc}} \right) \times 100 \quad (2)$$

where Absorbance of NEGc was used as a measure of the formazan formed in negative control cells and Absorbance of sample as the measure of the formazan formed after sample test exposure.

#### 5.2.5.3. Mitochondrial integrity determination

Assessment of mitochondrial integrity was performed by measuring the tetramethylrhodamine ethyl ester perchlorate (TMRE) inclusion, according to Dias da Silva *et al.* (183) protocol. Caco-2 cells at the density of 10<sup>5</sup> cells/well were seeded onto 96-well plates. After 24 h, the media was gently aspirated and the cells were incubated with digested BSY autolysate at six different peptide concentrations for 24 h (37°C, 5% CO<sub>2</sub>). Then, cells were rinsed twice with HBSS and incubated at 37°C with 100  $\mu$ L of 2 mM TMRE for 30 min. Then, the media was gently aspirated and replaced by 0.2% BSA in HBSS. Fluorescence was measured at 37°C set to 544 nm excitation and 590 nm emission. TMRE mitochondrial inclusion (%) was calculated relative to the maximum levels of the NEGc. Data were obtained from three independent experiments, with each plate containing six replicates of each test sample.

#### 5.2.5.4. ROS levels production

The intracellular reactive oxygen species (ROS) production was monitored by means of the 2',7'-dichlorodihydrofluorescein diacetate (DCFH-DA) assay, according to Dias da Silva *et al.* (183) protocol. DCFH-DA penetrates into cells and is hydrolyzed to DCFH by intracellular esterases; the presence of ROS can oxidize DCFH to form DCF, a fluorescent product (183). For this determination, Caco-2 cells at the density 10<sup>5</sup> cells/well were seeded onto 96-well plates and allowed to attach for 24 h. On the day of the experiment, the differentiated cells were rinsed with HBSS and incubated with 200  $\mu$ L per well of digested BSY autolysate at six different peptide concentrations for 24 h (37°C, 5% CO<sub>2</sub>). A negative control (NEGc, cells treated with medium only) was also included. After the treatment period, cells were rinsed twice with HBSS and incubated with 10 mM DCFH-DA for 30 min (37°C, 5% CO<sub>2</sub>).

After removal of the DCFH-DA and further washing with HBSS, the formation of 2',7'-dichlorodihydrofluorescein (DCF), due to the oxidation of DCFH-DA in the presence of intracellular ROS, was measured at an excitation wavelength of 485 nm and an emission wavelength of 530 nm. Cell ROS production (%) was calculated relative to the maximum ROS levels of NEGc. Data were obtained from three independent experiments, with each plate containing six replicates of each test sample.

In parallel, the cellular protection of digested BSY autolysate against a cytotoxic agent was induced by addition of 1 mM hydrogen peroxide. For this purpose, cells were also submitted to the 24 h treatment period, but in this case, 1 mM hydrogen peroxide was added 6 h before ROS measurement. Cell ROS production (%) was calculated relative to the maximum ROS levels of positive control (POSc, cells treated with hydrogen peroxide).

#### 5.2.5.5. Permeability experiments

After 21 days of culturing, TEER of the cell monolayers was measured prior to the beginning of transport experiments and only those presenting values higher than 200  $\Omega \cdot \text{cm}^2$  were used. Cell monolayers were pre-equilibrated with fresh HBSS solution, at 37°C, for 30 min. The apical (donor) compartment was filled with 1.5 mL of digested BSY autolysate in HBSS to a final concentration of 3.0 mg protein/mL and basolateral (receptor) compartment was filled with 2.5 mL of HBSS. Cell monolayers were allowed to incubate at 37°C under 5% CO<sub>2</sub> and 95% relative humidity. Samples (1.0 mL) were collected from the basolateral side at 15, 30, 60, 120 and 180 min to analyze the peptides transported across cell monolayers. Fresh HBSS was added in order to complete the initial volume at the basolateral compartment. A control sample, containing only HBSS and no sample solutions was included in the experimental setup. After the permeability experiments, the action of cell proteases on collected permeates was immediately stopped by cold at -90°C and freeze-dried. In order to perform the antioxidant and *in vitro* ACE-I assays (described in sub-section 5.2.4), freeze-dried permeates were dissolved in HBSS (20% the original volume added to apical side). For chromatographic analysis (described in sub-section 5.2.6), freeze-dried permeates were dissolved to the original volume (added to apical side) in solvent A (0.1% TFA in water). The efficiency of peptide transport, expressed as percentage of permeability for each peak (P %), was calculated according to Cinq-Mars *et al.* (127) as follows:

$$P \% = \frac{Ab}{Aa \cdot V} \times 100 \quad (3)$$

where Ab and Aa correspond, respectively, to the RP-HPLC peak areas of the peptide fraction detected in the basolateral and in the apical side and V (mL) is the volume of sample loaded in the apical side. In addition to P (%), the apparent permeation coefficient ( $P_{app}$ ),



expressed in cm/s, was calculated according to Ferraro *et al.* (184) from the following equation:

$$P_{app} = \frac{Q}{A.C.t} \quad (4)$$

where Q is the total amount of permeated peptides during the 180 min of the transport experiment (mg), A is the diffusion area (4.2 cm<sup>2</sup>), C is the apical compartment concentration at time zero (mg/mL), and t is the time of the experiment(s).

#### 5.2.6. Peptide analyses by Reverse-phase HPLC and by MALDI-TOF/TOF

Peptide profiles from digested BSY autolysate (0 min) and permeates (at 15, 30, 60, 120 and 180 min) from Caco-2 and Caco-2/HT29-MTX co-culture cell permeability assays were analysed by RP-HPLC, according to the method described by Ferreira *et al.* (185). Additionally, analyses by matrix-assisted laser desorption/ionisation time of-flight/time-of-flight (MALDI-TOF/TOF) mass spectrometry were also performed to determine the molecular mass of the peptide mixture. For this purpose, the digested BSY autolysate and five-fold concentrated permeates from Caco-2/HT29-MTX cell model were cleaned with ZipTip C18 (Millipore) using the manufacturer's instructions. Then, the eluted samples were premixed with matrix (3 mg/mL alpha-cyano-4-hydroxycinnamic acid (CHCA) in 50% (v/v) aqueous acetonitrile, 0.1% TFA), spotted onto a target plate, and dried at room temperature. The 4800 MALDI-TOF/TOF was calibrated using horse myoglobin [m/z 16952.56 (+1); m/z 8476.78 (+2); m/z 5651.85 (+3)] and cytochrome c [m/z 12349.72 (+1); m/z 6177.94 (+2)].

#### 5.2.7. Statistical analysis

The student *t*-test was performed to compare the permeability profile between the two cell models; one-way analysis of variance (ANOVA) was carried out for comparing multiple samples, followed by Duncan's post-hoc test. Differences with *p* < 0.05 were considered significant. All statistical calculations were performed using SPSS 22.0 (SPSS software, Chicago, USA).

### 5.3. RESULTS AND DISCUSSION

#### 5.3.1. Impact of *in vitro* GI digestion of BSY autolysate on the biological activity

The autolysate obtained from the inner cell content of BSY presented both antioxidant and ACE-I activities, the FRAP value was 374±12 µM TE/mL and IC<sub>50</sub> was 379±10 µg protein/mL. The *in vitro* pepsin-pancreatin digestion significantly (*p* < 0.05) enhanced both activities, since FRAP value increased to 405±9 µM TE/mL and IC<sub>50</sub> decreased to 345±10

µg protein/mL, probably due to the stability of the existing antioxidant and ACE-I compounds to digestion and the generation of small peptides presenting these activities.

The viability of Caco-2 cells after treatment with the digested BSY autolysate, assessed by the MTT assay, indicates no toxic effects concerning mitochondrial enzyme activity after exposition (24 h at 37°C, 5% CO<sub>2</sub>) to the digested BSY autolysate at concentrations between 0.5 and 4.0 mg protein/mL (Figure 5.1.A). Moreover, concentrations up to 3.0 mg protein/mL significantly increased the MTT reduction by Caco-2 cells, reflecting higher metabolic competence. It is not uncommon for some chemicals/compounds to induce an increase in cellular metabolic activity, which would result in increased mitochondrial succinate dehydrogenase activity (186). As the protocol performed in the present study uses cells at confluence, the attained data is not compatible with cell proliferation. However, at the highest concentration, 6.0 mg protein/mL, the viability of Caco-2 cells significantly ( $p < 0.05$ ) decreased to around 70%.

TMRE assay indicates that exposition of Caco-2 cells to the digested BSY autolysate at concentrations lower or equal to 4.0 mg protein/mL did not cause significant mitochondrial disruption (Figure 5.1.B). Conversely, it was observed an increase of the inner mitochondrial membrane potential, which is consistent with the effects obtained in the MTT assay. The mitochondrial membrane potential is a central parameter controlling calcium homeostasis and ATP synthesis (both involved in several vital cellular processes). Accordingly, mitochondrial hyperpolarization has been directly correlated with cell survival (187).

Concerning the overall oxidative stress in Caco-2 cells under normal conditions (no oxidative stress), high inhibition of ROS production was observed for concentrations lower than 3.0 mg protein/mL ( $p < 0.05$ ) after exposure for 24 h to digested BSY autolysate (Figure 5.2.A), suggesting a protective antioxidant effect of Caco-2 cells. A significant increase in ROS production occurred in the presence of hydrogen peroxide when compared with unstressed conditions (Figure 5.2.B). However, digested BSY autolysate presented a protective effect on Caco-2 cells, as evidenced by the lower ROS generation ( $p < 0.05$ ). The concentration of 3.0 mg protein/mL was selected for permeability experiments taking in consideration the results from cell viability, mitochondrial membrane potential and oxidative stress response.

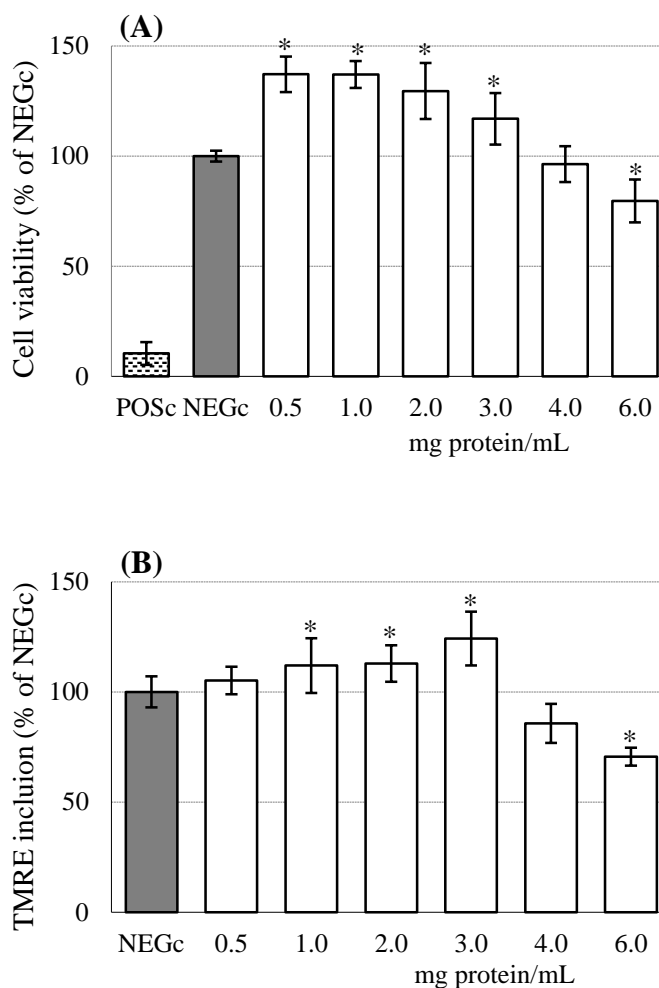


Figure 5.1. Cell viability (%) **(A)** and TMRE mitochondrial inclusion (%) **(B)** after 24 h of exposure (37°C, 5% CO<sub>2</sub>) to digested BSY autolysate at different protein concentrations. NEGc (cells treated with medium only); POSc (cells treated with medium and 1% Triton X-100). Columns represent the mean and vertical bars the standard deviation, calculated relatively to NEGc. \* denotes a significant difference when compared with NEGc ( $p < 0.05$ ,  $n=3$ ).

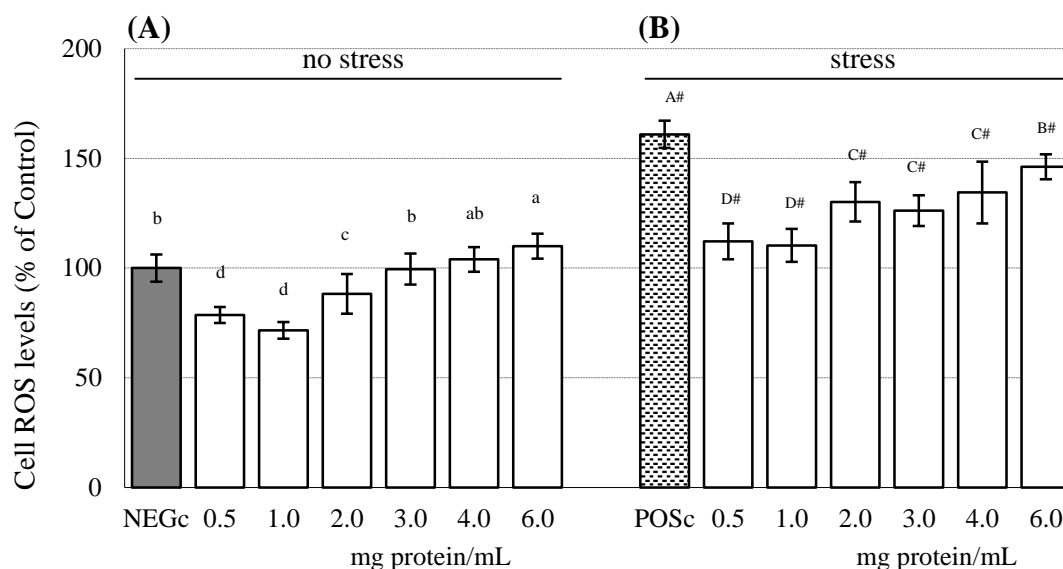


Figure 5.2. Protective effect of the digested BSY autolysate on ROS levels after 24 h of exposure (37°C, 5% CO<sub>2</sub>) at different protein concentrations (mg/mL) under no stress treatment **(A)** and after oxidative stress induced by hydrogen peroxide (6 h exposure) **(B)**. NEGc (cells treated with medium only); POSc (cells treated with medium and 1 mM hydrogen peroxide). Columns represent the mean and vertical bars the standard deviation, calculated relative to respective control. # indicates respective differences between “no oxidative stress” and “oxidative stress” treatments ( $p < 0.05$ ,  $n=3$ ). Bars labeled with different subscript and superscript letters have mean values that are significantly different at  $p < 0.05$  (ANOVA followed by Duncan's test).

### 5.3.2. Intestinal permeability of peptides from BSY autolysate

Caco-2 and Caco-2/HT29-MTX monolayers with TEER values of 360-390  $\Omega \cdot \text{cm}^2$  and 220-250  $\Omega \cdot \text{cm}^2$  at 21 days, respectively, were used in the permeability studies. Lower TEER values observed for the co-culture model are related to the establishment of looser tight junction between Caco-2 and HT29-MTX cells (131), (179). After permeability experiments, TEER values of Caco-2 and Caco-2/HT29-MTX co-culture cell monolayers remained unchanged compared to the original values (decrease less than 10%), suggesting that the digested BSY autolysate did not affect significantly the viability and integrity of cell monolayers. Figure 5.3 shows the typical RP-HPLC profile of the digested BSY autolysate used in cell permeability assays, in which six major peptide fractions were separated and numbered from P1 to P6 according to the polarity increase. Elution was monitored at 214

nm. RP-HPLC profile of permeates from Caco-2 and Caco-2/HT29-MTX co-culture cell monolayers obtained at 180 min are also shown in Figure 5.3. Similar RP-HPLC profiles were obtained in the apical and basolateral sides of Caco-2 (Figure 5.3.A) and Caco-2/HT29-MTX monolayers (Figure 5.3.B), although qualitative differences were observed on peak areas. According to the literature small peptides presenting less than 1000 kDa are transported intact through the intestinal epithelium by PepT1, a proton-coupled membrane transporter (88). However, MALDI-MS spectra of permeates confirmed the presence of oligopeptides with molecular weight higher than 1000 kDa, not only in the digested BSY autolysate but also in permeates (Figure 5.4.A and B). The paracellular transport through the intercellular junctions can be involved in the transepithelial absorption of peptides larger than three amino acid residues; although the absorptive transcytosis have been suggested as the main transport system for long-chain oligopeptides (88), (188). Moreover, as illustrated in Figure 5.4, there are more peptide fragments in the sample taken from the basolateral side than that from the apical side, which suggests a partial degradation of apical peptides into smaller fragments by the action of cell peptidases and their absorption through the Caco-2/HT29-MTX cell monolayer (178).

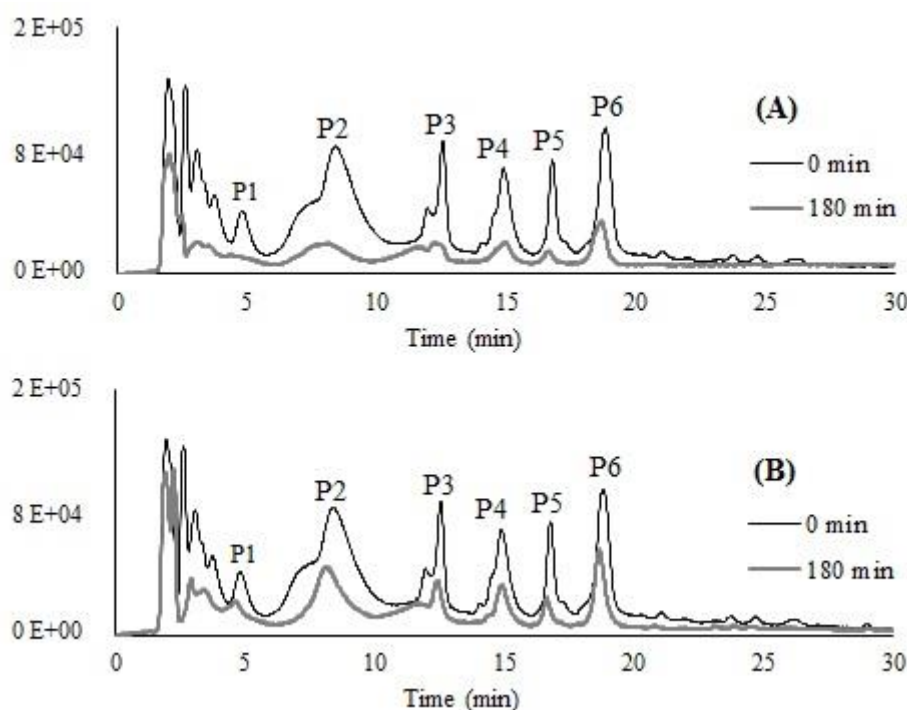


Figure 5.3. RP-HPLC chromatographic profile of digested BSY autolysate before (0 min) and after permeability (180 min) through Caco-2 cell monolayers **(A)** and Caco-2/HT29 co-culture cell monolayers **(B)**. The absorbance was monitored at 214 nm. Retention time for chromatographic peaks was: (P1) 4.2-6.2 min; (P2) 6.3-10.0 min; (P3) 10.1-13.3 min; (P4) 13.4-16.0 min; (P5) 16.1-17.5 min and (P6) 17.6-19.6 min.

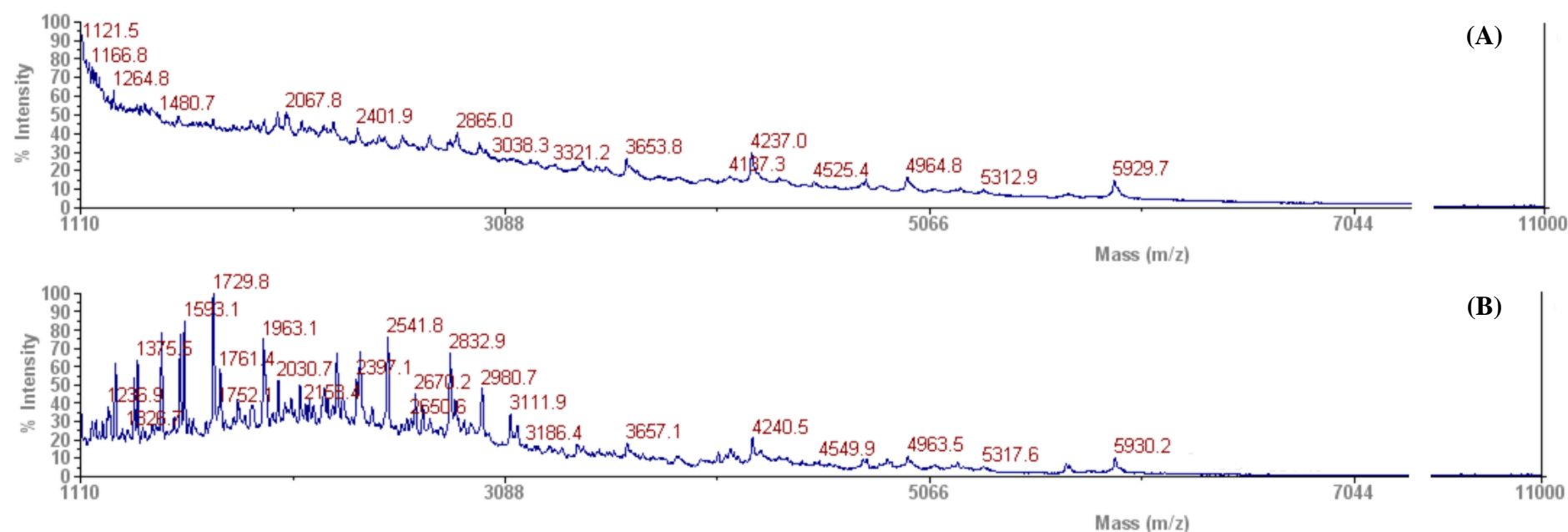


Figure 5.4. MALDI-TOF mass spectra of digested BSY autolysate added to the apical compartment at the beginning of transport experiment **(A)** and five concentrated permeate taken from the basolateral compartment after 180 min of a permeability experiment across Caco-2/HT29-MTX co-culture cell monolayer **(B)**.

The permeability profile of peptide fractions (P1 to P6) for both cell models is depicted in Figure 5.5 as the cumulative transport up to 180 min. Intense permeation of peptide fractions was observed during the first 30-60 min. In Caco-2 cell monolayers, the accumulated permeability at 180 min was significantly higher for P5 and P6 peptide fractions, which reached, respectively,  $44.9 \pm 2.6\%$  and  $55.4 \pm 1.3\%$  (Figure 5.5.A). In the case of the Caco-2/HT29-MTX co-culture cell model, the accumulated permeability was significantly higher at 180 min of transport for P2, P5 and P6 peptide fractions, reaching, respectively,  $63.5 \pm 2.6\%$ ,  $52.7 \pm 1.6\%$  and  $69.6 \pm 0.6\%$  of transport rate (Figure 5.5.B). The presence of HT29-MTX cells led to a significant transport increase of peptides when compared with the Caco-2 cell monolayer. As aforementioned, this result can be explained by the lower TEER values observed for Caco-2/HT29-MTX co-culture cell monolayer. Permeability was higher for the more hydrophobic peptides (P5 and P6 fractions), which is in agreement to data reported by other authors for other type of food peptides (127).

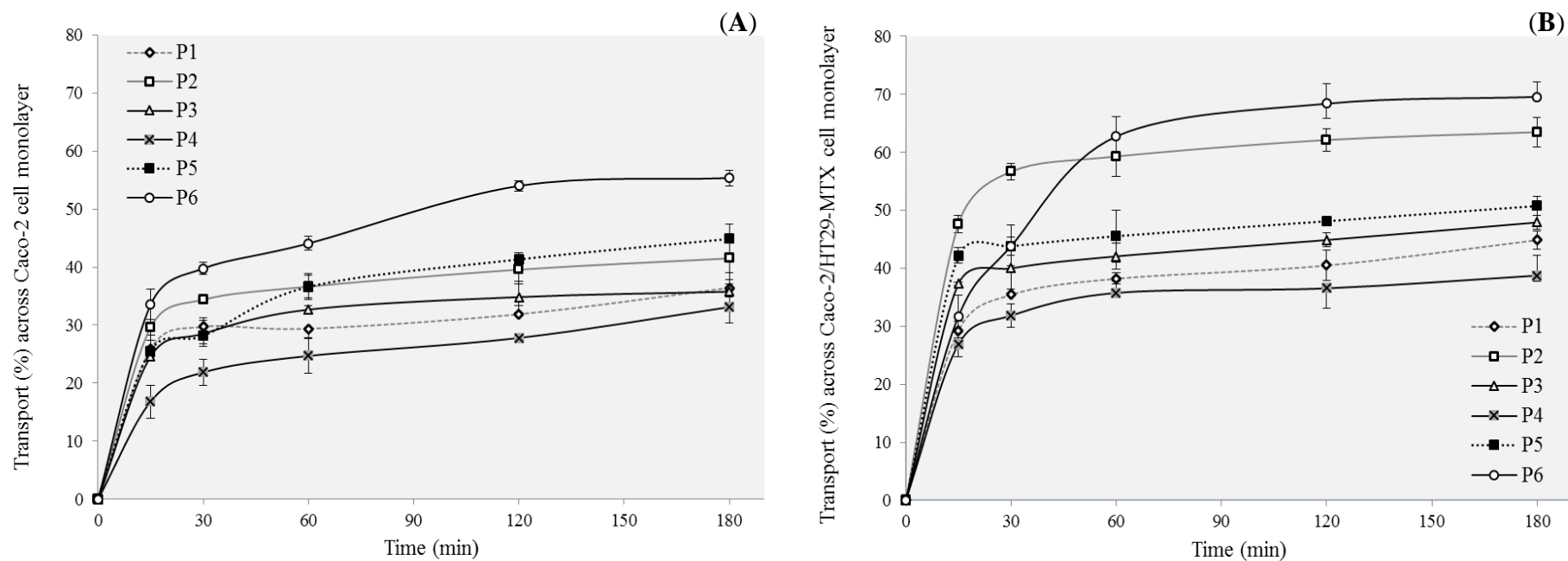


Figure 5.5. Comparative *in vitro* cumulative permeability of BSY peptides across Caco-2 cell monolayers **(A)** and Caco-2/HT29-MTX co-culture cell monolayers **(B)**. Permeation (%) was calculated from the area of each peptide fraction in the RP-HPLC chromatogram, numbered from P1 to P6 according to the increase of polarity (see Figure 5.3 for peak identification). Experiments were conducted from the apical to the basolateral compartment. Individual points and error bars represent mean  $\pm$  standard deviation (n=3).



$P_{app}$  values can be correlated with the predictable magnitude of *in vivo* absorption. In the present work, the criteria defined by Yee (189) was considered, according to which a compound with  $P_{app}$  value lower than  $10^{-6}$  cm/s indicates poor *in vivo* absorption (0-20%);  $P_{app}$  values between  $10^{-6}$ - $10^{-5}$  cm/s correspond to substances with moderate absorption (20-70%) and  $P_{app}$  values over  $10^{-5}$  cm/s suggest that compounds are well absorbed (70-100%). In this work,  $P_{app}$  values at 180 min of absorptive transport of BSY peptides across Caco-2 monolayers were in the range of  $12.4$ - $20.8 \times 10^{-6}$  cm/s (Table 5.1), suggesting extensive *in vivo* absorption. This parameter was significantly higher when the Caco-2/HT29-MTX co-culture cell monolayer was used (ranging between  $14.5$ - $26.1 \times 10^{-6}$  cm/s). This last model is presumably closer to the *in vivo* situation and, thus, more realistically simulates the intestinal epithelium (131), (132). In general, the high  $P_{app}$  values are in accordance with values reported in the literature for other food-derived peptides ( $P_{app}$  ranging  $4.1$ - $20.8 \times 10^{-6}$  cm/s) (188). The presence of mucus-producing cells makes the co-culture monolayer looser, with higher number of paracellular pores per  $\text{cm}^2$  (133), and, thus, more permeable. Similar conclusions were observed by Musatti *et al.* (179), when comparing the Caco-2 and Caco-2/HT29-MTX cell culture models to evaluate the transport and bioavailability of glutathione-enriched baker's yeast. Mucoadhesive delivery systems have been recognized as effective in enhancing the intestinal absorption of peptides and proteins (190). Other aspect which can also contribute to the high permeability observed is the fact that some compounds in complex extracts, such as, BSY autolysate, could act as permeability enhancers and cause partial opening of paracellular spaces between Caco-2 cells. These small changes in the diameter of paracellular spaces can significantly affect the permeability of small hydrophilic molecules (180), (182). For instance, Fuller *et al.* (191) investigated the effect of heat-killed yeast cell suspensions on Caco-2 cell monolayer tight junction integrity in order to examine whether yeast suspension can act as a penetration enhancer for proteins. These authors observed that heat-killed yeast cells suspensions opened tight junctions in a reversible dose- and time-dependent manner without significant cytotoxic effects being observed.

Table 5.1. Apparent permeability coefficient ( $P_{app}$ ) of BSY peptides (P1-P6) after 180 min of transport across Caco-2 cell and Caco-2/HT29-MTX co-culture cell models

Peak (retention time)	$P_{app} \times 10^{-6}$ (cm/s)	
	Caco-2 cell model	Caco-2/HT29-MTX cell model
P1 (4.2-6.2 min) *	13.6 ± 0.8 <sup>bc</sup>	16.8 ± 1.6 <sup>D</sup>
P2 (6.3-10.0 min) *	15.6 ± 3.6 <sup>bc</sup>	23.8 ± 2.6 <sup>B</sup>
P3 (10.1-13.3 min) *	13.4 ± 3.3 <sup>c</sup>	18.0 ± 1.2 <sup>CD</sup>
P4 (13.4-16.0 min)	12.4 ± 2.7 <sup>c</sup>	14.5 ± 0.9 <sup>E</sup>
P5 (16.1-17.5 min) *	18.6 ± 2.5 <sup>b</sup>	19.8 ± 1.6 <sup>C</sup>
P6 (17.6-19.6 min) *	20.8 ± 1.3 <sup>a</sup>	26.1 ± 0.6 <sup>A</sup>

Values shown are the mean ± standard deviation of three replicates and are relative to 180 min of transport assay (37°C, 5% CO<sub>2</sub>). See Figure 5.3 for peak identification. For each cell culture model, bars labeled with different subscript or superscript letters have mean values that are significantly different ( $p < 0.05$ , ANOVA followed by Duncan's test).

\* indicates significant differences between the two cell culture models ( $p < 0.05$ ).

### 5.3.3. Biological activity of BSY permeates

Antioxidant activity (evaluated by FRAP assay) and ACE-I activity (expressed as IC<sub>50</sub>) of BSY permeates recovered from Caco-2 and Caco-2/HT29-MTX transepithelial transport experiments were measured after five-fold concentration (Table 5.2). The FRAP activity of permeates from Caco-2 cell model reached the highest value of 426 µM TE/mL after 60 min, whereas for co-culture cell model, the FRAP reached the highest value of 568 µM TE/mL after 30 min. With respect to ACE-I activity the lowest IC<sub>50</sub> of permeates was observed for both models after 15 min of transepithelial transport. For the Caco-2 cell model, the IC<sub>50</sub> value of permeate was 301 µg protein/mL, whereas for Caco-2/HT29-MTX cell model, the IC<sub>50</sub> was significantly lower, 259 µg protein/mL. According to the literature, most food protein-derived peptides with ACE-I activity have low molecular mass, between two and five amino acids in their sequences, with molecular masses lower than 1000 Da (188), (192). The ACE-I activity assessed in these permeates suggests that peptides from digested BSY autolysate and from the action of cell peptidases can reach the blood stream to exert antihypertensive activity.

Table 5.2. FRAP and ACE-I activity of Caco-2 and Caco-2/HT29-MTX co-culture cell model permeates at different times of transport, five-fold concentration of permeates

Sample	FRAP ( $\mu\text{M TE/mL}$ )	IC <sub>50</sub> ( $\mu\text{g protein/mL}$ )
<i>Permeates of Caco-2 cell model</i>		
15 min	243 $\pm$ 10 c	301 $\pm$ 11 A
30 min	304 $\pm$ 17 b	367 $\pm$ 12 B
60 min	426 $\pm$ 11 a	826 $\pm$ 22 C
120 min	149 $\pm$ 8 d	1238 $\pm$ 42 D
180 min	37 $\pm$ 3 e	1981 $\pm$ 53 E
<i>Permeates of Caco-2/HT20-MTX co-culture cell model</i>		
15 min	365 $\pm$ 11 c	259 $\pm$ 18 A
30 min	568 $\pm$ 15 a	285 $\pm$ 12 B
60 min	448 $\pm$ 8 b	669 $\pm$ 21 C
120 min	213 $\pm$ 12 d	1071 $\pm$ 26 D
180 min	85 $\pm$ 6 e	1821 $\pm$ 46 E

Results are expressed as mean  $\pm$  standard deviation of triplicate experiments. For each model, mean values with different subscript (FRAP) or superscript letters (IC<sub>50</sub>) are significantly different ( $p < 0.05$ , ANOVA followed by Duncan's test).

#### 5.4. CONCLUSIONS

Data from *in vitro* GI digestion, cell cellular antioxidant assays and cell monolayer permeation studies confirmed the potential of BSY autolysate obtained from inner yeast cell content as functional food ingredient with antioxidant and ACE-I activities. GI digestion enhanced both biological activities. No cytotoxic effects were observed on Caco-2 cells after 24 h exposition to the digested BSY autolysate within a concentration range of 0.5 to 3.0 mg protein/mL. Moreover, the response to oxidative stress induced by hydrogen peroxide demonstrated the protective role of the autolysate within this concentration range, which is relevant since GI tract is a major target for oxidative stress damage due to the constant exposure to diet-derived oxidants, mutagens, and carcinogens. Additionally, high apparent permeability coefficient ( $P_{app}$ ) values for BSY peptides were observed in both models used for transepithelial transport,  $14.5\text{-}26.1 \times 10^{-6}$  cm/s for Caco-2/HT29-MTX cell monolayer and  $12.4\text{-}20.8 \times 10^{-6}$  cm/s for Caco-2 cell monolayer model. Antioxidant and ACE-I activities were also found in permeates, which suggests that bioactive compounds are well absorbed.

However, pharmacological efficacy may only be confirmed by *in vivo* studies and these results indicate that such studies are justified.

## **PART II**

### **“Sardine protein hydrolysates”**

---

#### **Chapter 6**

##### **Literature review**

*Development of sardine protein hydrolysates and their health promoting ability*

#### **Chapter 7**

*Antioxidant and antihypertensive hydrolysates obtained from by-products of cannery sardine and brewing industries*

#### **Chapter 8**

*Simulated gastrointestinal digestion and in vitro intestinal permeability of bioactive protein hydrolysates obtained from canned sardine and brewing by-products*

#### **Chapter 9**

*Anti-inflammatory activity of a hydrolysate from canned sardine and brewing by-products through inhibition of TNF- $\alpha$ -induced endothelial dysfunction in a co-culture model of Caco-2 and endothelial cells*

#### **Chapter 10**

*Characterization of hydrolysates obtained from muscle and viscera proteins of canned sardine by-products*



## **CHAPTER 6**

### **Literature review**

#### *Development of sardine protein hydrolysates and their health promoting ability*

---

This chapter presents a literature overview of the canned sardine by-product, it describes the characterization of sardine sarcoplasmic proteins, the typical process adopted for the manufacturing of SPH and the main biological activities reported.





### 6.1. Canned sardine industry

Sardine (*Sardine pilchardus*) is a small pelagic fish highly consumed among Mediterranean populations (13), (193). Great part of it is used by canned sardine industry. The canning process of sardine produces more than 60% by-products, which includes head, skin, trimmings, fins, viscera and frames (13), (102). This waste constitutes a serious environmental problem for fisheries since their discharge requires convenient management, and contains good amounts of protein rich material, which is currently processed into low market-value products, such as, animal feed, fish meal and fertilizers (102). Therefore, the recovery of added-value compounds from these materials can be of great economic importance and practical interest to promote the sustainability and competitiveness of sardine canning industry (12). Several techniques describing the recovery of essential nutrients and bioactive compounds from sardine by-products to be applied as functional food ingredients and nutraceuticals in human and animal nutrition, pharmaceuticals and cosmetics were published (1), (13), (194). Production of sardine protein hydrolysates (SPH) is one of those techniques currently employed.

### 6.2. Nutritional composition of sardine by-product

The lipid content of sardines ranges between 0.5 and 20% dw, depending on the season, stage of sexual maturity and body size. The n-3 polyunsaturated fatty acids (PUFAs), especially eicosapentaenoic acid (EPA) and docosahexaenoic acid (DHA), represent 40% of total fatty acids and are recognized to possess numerous health benefits (195). The protein content ranges between 15 and 20% dw, depending on catch location and species (195). Proteins can be divided into different groups based on their solubility: (i) 70-80% are myofibrillar proteins, being soluble in cold neutral salt solutions of fairly high ionic strength; (ii) 20-30% are sarcoplasmic proteins, being soluble in water and dilute buffers and (iii) 2-3% are structural proteins, being insoluble connective tissue proteins (194). The myofibrillar protein complexes contain myosin (50-60%) and actin (15-30%). Myosin is a large molecule containing two identical heavy chains (223 kDa) and four light chains subunits ranging from 17 to 22 kDa (195). Among sarcoplasmic proteins, myoglobin (15.3 kDa) is presumably the most important protein (196), (197). Karthikenyan *et al.* (198) and Klomklao *et al.* (199) reported that sarcoplasmic proteins from sardine muscle showed multiple bands with molecular weights between 29 and 97 kDa.

### 6.3. Potential applications of SPH

SPH are breakdown products of enzymatic hydrolysis of sardine proteins into smaller peptides (2-20 amino acids), which present various physiological functions in the organism (102). To date, SPH have been produced by enzymatic hydrolysis, autolysis (using endogenous enzymes), fermentation or combined processes (194). SPH have been reported as good nutritional supplements due to peptides composition, biological activity and easy absorption. Thus, commercial preparations of SPH are currently used in many countries as health food or nutraceuticals (194). Some examples of commercially available nutraceutical brands are the Valtryon® and the Lapis Suport®, which contain antihypertensive peptides (19).

SPH can be used as an excellent source of nitrogen for the growth of different microorganisms. For example, Ghorbel *et al.* (200) used SPH as nitrogen source for the production of extracellular lipase by the filamentous fungus *Rhizopus oryzae*. SPH have also been used in aquaculture feeds in order to enhance the growth and survival of fish. For instance, Kotzamanis *et al.* (201) reported growth performance and immunological status improvement of sea bass larvae when SPH was incorporated in diet.

SPH have also been tested successfully for their application as antioxidant agents. For instance, Khaled *et al.* (101) studied the effect of SPH on the oxidative status and blood lipid profile of rats fed with hypercholesterolemic diet. SPH reduced the malondialdehyde (MDA) concentration and increased the antioxidant enzyme (superoxide dismutase, glutathione peroxidase and catalase) activities and the high density lipoprotein (HDL) cholesterol. More recently, Athmani *et al.* (135) showed that supplementation of hypercholesterolemic diet rats with SPH efficiently decrease the lipid peroxidation in serum and target tissues, being related with the increased antioxidant enzymes activity.

Moreover, SPH have been used as techno-functional ingredients in food industry as they possess numerous important properties, such as, water holding capacity, oil absorption capacity, protein solubility, gelling activity, foaming capacity and emulsifying ability (20), (194), (202-204). SPH have been successfully tested for incorporation into different food systems, such as, cereal products, fish and meat products, desserts and crackers, as well as, protein supplements, stabilizers in beverages and flavour enhancers (194).

## 6.4. Preparation of SPH

The production of fish protein hydrolysates (as SPH) and bioactive peptides has been described in several reviews (87), (102), (194), (205), (206). The process usually consists in protein extraction, enzymatic hydrolysis, separation and purification of SPH, application of *in vitro* methods to determine the biological activities, determination of the peptide sequence and evaluation of possible structure-function relations. *In vivo* studies and synthesis of purified peptides to validate their activities require high costs and are more difficult to implement than *in vitro* studies. The main typical steps involved in producing of SPH and bioactive peptides at laboratorial and industrial scale are outlined in Figure 6.1.

### 6.4.1. Preparation of Sardine Protein concentrate (SPC)

Different techniques can be used for extracting sarcoplasmic and/or myofibrillar proteins from sardine muscle. These include the use of aqueous and organic solvents and the conventional processes of cooking, pressing, drying and hot oil extraction (194). Sardine protein concentrates (SPC) can be obtained by acidic or alkaline solubilisation followed by isoelectric protein precipitation (207), (208). This technique concentrates protein fraction, which represents 18-23% of fish muscle, and removes water and oil from the sardine muscle (13). The recovery yield ranges between 42 and 90% (13). At the end of SPC preparation, a lipid phase, an aqueous soluble phase that contains proteins, and an insoluble sediment are separated, as observed in Figure 6.2. For removal of lipid phase, multiple steps of filtration or centrifugation must be performed (194).

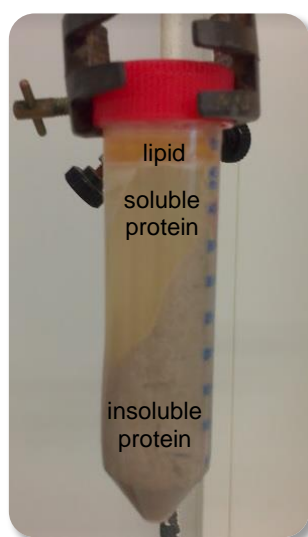


Figure 6.2. Different fractions obtained in the SPC preparation.

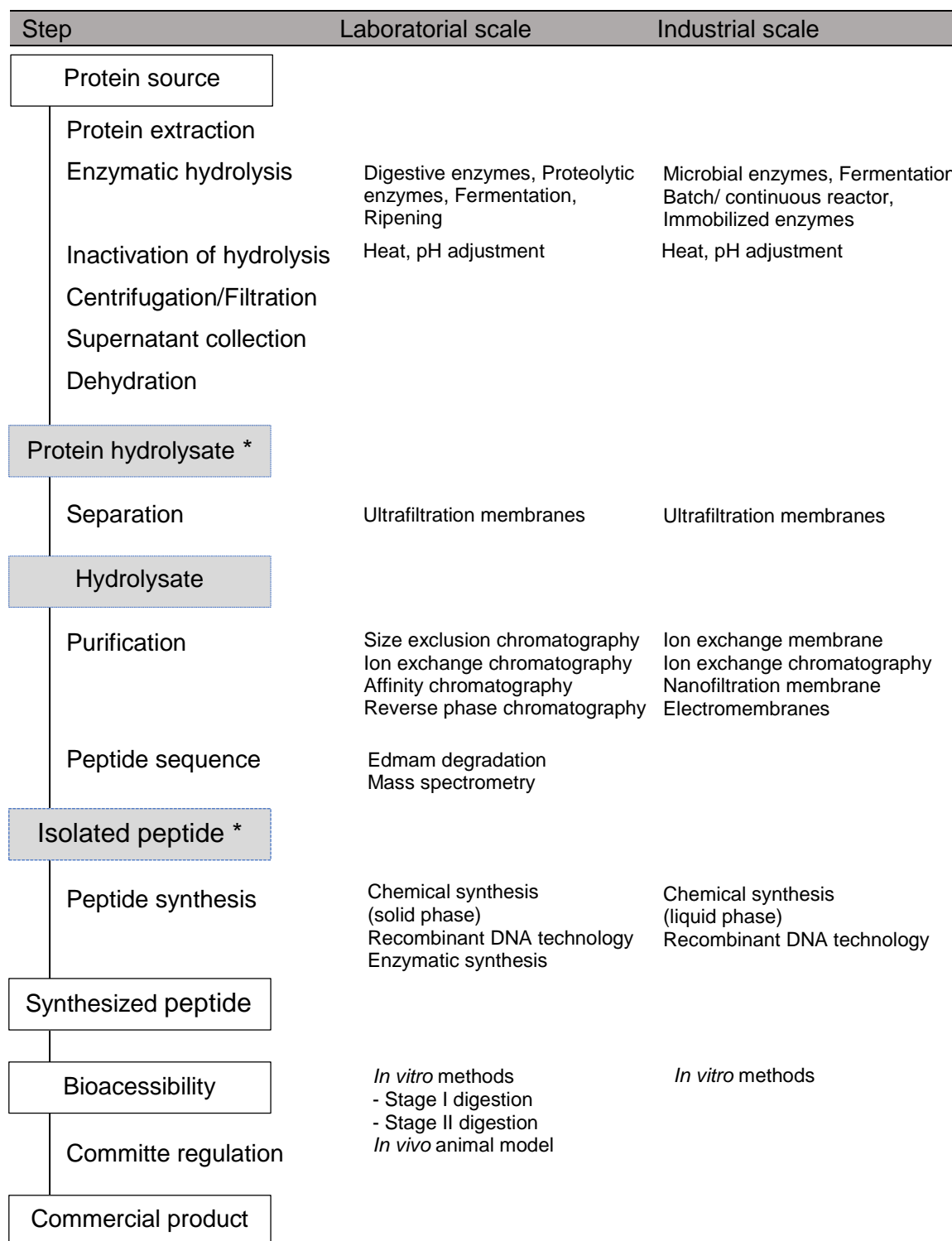


Figure 6.1. Flow diagram for the preparation of fish protein hydrolysates (as SPH) and bioactive peptides, at laboratorial and industrial scales. Adapted from (205) and (206).

\* Biological activities and bioavailability can be performed in protein hydrolysate, hydrolysate fractions and isolate peptides.

### 6.4.2. Protein hydrolysis

Hydrolysis of SPC can be performed by endogenous proteolytic enzymes already present in muscle or viscera of sardine (4), (15), (16), (101), (209) and/or by adding exogenous enzymes from other sources, which must present food grade requirements (194). Several industrial food-grade proteases, such as, Alcalase® (12), (15), (16), (20), (112), (134), (200), (202), (209-213); Neutrase® (202); Flavourzyme® (211); Protamex® (211), (214) and Subtilisin® (215) have been widely used. Enzymes from animal sources, such as, Pepsin® (17); Trypsin® (199), (213), (215), and Chymotrypsin® (15) have also been used, although to a lesser extent. Moreover, crude enzyme preparations from other microorganisms, namely, *Bacillus licheniformis* NH1 (15), (16); *Aspergillus clavatus* ES1 (15), (16); *Bacillus pumilus* A1 (101) and *Bacillus mojavensis* A21 (101) have also been used. In general, the use of exogenous enzymes is preferred to the autolysis process due to the reduction in time required to achieve similar degree of hydrolysis, as well as, better control of the hydrolysis to obtain more consistent molecular weight profiles and peptide composition (194). Besides biochemical hydrolysis, chemical hydrolysis (with either acid or base to cleave the peptide bonds) can also be performed to produce SPH. However, this method presents many limitations; the final SPH present reduced nutritional value, large amount of salt; poor functionality and restrictions to be use as flavour enhancers. Another disadvantage of acid hydrolysis is the destruction of the essential amino acid tryptophan (194).

To obtain SPC by enzymatic treatment, the material should be first suspended in water/ buffer, and then adjusted to the optimum pH and temperature of the enzyme. In some cases, the raw material is first heated to inactivate endogenous proteases before adding the exogenous enzyme. Hydrolysis reactions can occur with or without pH adjustment; hydrolysis carried out without any pH adjustment are economically desirable from an industrial point of view (216). The added acid and/ or base increase salt to the hydrolysate, which may give undesirable effects and may be difficult and costly to remove further in a process (217). The hydrolysis reaction is stopped either by using a heat treatment or by adjusting the pH. More than one centrifugation step is often required to separate the soluble proteins from the lipids and insoluble solids. The lipid content of SPH must be low to prevent alteration of the lipid fraction during storage. After solids removal, the supernatant is often adjusted to neutral pH and then dehydrated to obtain the powdered SPH (13).

Suitable enzyme and hydrolysis conditions, such as, enzyme to substrate (E/S) ratio, time and temperature, are crucial to obtain SPH with desirable biological and techno-

functional properties. Response Surface Methodology (RSM) experimental design can be used to optimize hydrolysis conditions, as well as, to predict SPH properties (102), (212). Several RSM experimental designs have been employed, including the Central Composite Design (CCD), Complete Randomized Factorial Design (CRFD), Box-Behnken Design, 2-fold Rotation Plan Centered Design and Orthogonal Design (218).

The extent of enzymatic hydrolysis can be measured by several methods. The degree of Hydrolysis (DH %) is the most commonly used, including the pH-stat technique, which is more useful for industrial application, and the trichloroacetic acid (TCA) and trinitrobenzenesulfonic acid (TNBS) methods, very useful when working at laboratorial scale (194). The basic principle of the TNBS method is that free amino groups released by proteolysis can be measured by the formation of a yellow coloured derivative measurable by spectrophotometry. This method is more sensitive when several small peptides are available (219). Other methods to measure the extent of protein degradation are RP-HPLC and SDS-PAGE. In RP-HPLC analysis, peptides are separated by polarity; small hydrophilic peptides elute first, whereas hydrophobic and/ or higher peptides are retained in the column and take longer to elute (220). The SDS-PAGE is preferable to show larger fragments resulting from proteolysis (219).

#### **6.4.3. SPH concentration and purification**

SPH contains a complex mixture of active and inactive peptides having various sizes and different amino acid composition. Therefore, several enrichment methods need to be applied to produce fractions with high concentration of bioactive peptides. SPH may be concentrated through UF membranes to obtain a more uniform product with the desired range of molecular mass (218). After enzyme inactivation, SPH is filtered through a membrane with a specific MWCO value; common MWCO membranes used are 1, 3, 5 and 10 kDa. The UF process can contain more than one UF membrane, yielding several molecular weight fractions depending on the product desired. This method is more effective for highly purified and defatted SPH. Other possible separation methods are the suction filtration of the sludge and filtering the slurry by passing it through a 2-mm mesh screen (194) and the Fast Performance Liquid Chromatography (FPLC), which is usually used to obtain peptides with molecular weights <3 kDa (218). Chromatographic techniques have been used for fractionation of protein and peptide mixtures depending on their affinity to either the mobile or stationary phases. Gel filtration chromatography (GFC) separates proteins and peptides according to their size as they pass through a gel medium in a packed

column. This technique has been used to fractionate and concentrate peptides in SPH (16) and is often combined with other separation techniques (103).

#### **6.4.4. Identification of bioactive peptides from SPH**

Amino acid analysis is important to assess the nutritional value of SPH and to identify the presence of specific amino acids with influence on the biological and techno-functional properties of SPH (102). In order to identify the peptide sequences, Liquid chromatography with tandem mass spectrometry detection (LC-MS/MS) followed by a database search, is usually used. Also, the MALDI-TOF analysis is very useful to obtain the peptide profile of protein hydrolysates or semi-purified fractions. A major limitation of this method is that the peptides with molecular masses below 0.5 kDa are difficult to identify (221).

#### **6.5. Nutritional composition of SPH**

Chemical composition of SPH is crucial from a nutritional perspective (102). Table 6.1 summarizes the Degree of hydrolysis and proximate composition obtained for various SPH reported in the literature.

The high protein content reported for SPH, which ranged between 66.4% and 87.0% (dw), is due the solubilization of proteins during hydrolysis and removal of insoluble solid matter by centrifugation. This content highlights the potential use of SPH for protein supplements intended for human nutrition (102). The low fat content of SPH is because the removal in the centrifugation step. As established by the Protein Advisory Groups of FAO, the lipid content of a SPH suitable for human consumption should not exceed 0.5% dw (194). The relatively high ash content of SPH may be due the added acid or base used for pH adjustment during hydrolysis (102). SPH contains free amino acids and short chain peptides. Its amino acid composition explains the nutritional value and the biological activities exhibited by SPH and may depend on several factors, namely, raw material, enzyme source and hydrolysis conditions.

Table 6.1. Degree of hydrolysis (DH %) and proximate composition (% dw) obtained for various SPH

Reference	(20)	(15)	(222)	(222)	(222)	(215)	(223)	(213)	(213)	(224)
Material	Head and viscera	Head and viscera	Muscle	Muscle	Muscle	Whole fish	Muscle	Muscle	Muscle	Muscle
Enzyme	Alcalase	Viscera proteases <sup>a</sup>	<i>Bacillus Pumilus</i> A1 <sup>b</sup>	<i>Bacillus mojavensis</i> A21 <sup>b</sup>	Viscera proteases <sup>a</sup>	Subtilisin + Trypsin	<i>Bacillus subtilis</i> A26 <sup>b</sup>	Alcalase	Trypsin	Subtilisin
DH (%)	10.2	8.0	14.0	7.5	8.5	13.7	<i>nr</i>	5	5	3-6
Protein (% dw)	73.1	73.0	79.1	78.2	74.4	66.4	74.3	85.8	86.6	83.9-87.0
Fat (% dw)	10.2	7.3	1.4	0.9	1.0	19.7	0.6	0.3	0.5	1.3-2.0
Moisture (% dw)	4.6	<i>nr</i>	11.6	10.5	14.6	<i>nr</i>	14.7	3.0	5.3	2.5-3.7
Ash (% dw)	12.1	12.6	11.7	10.0	10.8	<i>nr</i>	10.2	12.7	10.9	13.6-16.5

<sup>a</sup> crude enzyme preparation from sardine viscera

<sup>b</sup> crude enzyme preparation

*nr*, not reported



## 6.6. Bioactivities of SPH and derived peptides

SPH and derived bioactive peptides have been receiving special attention due to their beneficial effects in the treatment of hypertension, particularly, due to its ACE-I and antioxidant activities. Tables 6.2. and 6.3. summarize the recent research related with these biological properties; some of these studies further fractionated the SPH in order to isolate and identify individual active peptides. Other biological activities reported for SPH include immunomodulating, anti-inflammatory, hypocholesterolemic and anticancer (101), (135), (225-228).

## 6.7. Techno-functional properties of SPH

Techno-functional properties are the physicochemical properties of proteins in food applications during processing, storage and consumption (20), (218). Enzymatic hydrolysis of sardine proteins modifies the techno-functional characteristics of the native proteins, generating a mixture of free amino acids, di-, tri- and oligopeptides with lower molecular mass and increased exposure of hydrophobic groups and number of ionic groups (20), (194). The control of the enzymatic reaction is very important as prolonged hydrolysis of sardine proteins may result in the formation of highly soluble peptides, with complete absence of the techno-functional properties of the native proteins. Extensive hydrolysis may also promote the formation of undesirable bitter peptides (194). SPH had been reported to possess good solubility over a wide range of pH levels, usually tolerate strong heat without precipitating and contribute to water holding, texture and emulsifying properties when added to food product (218). Table 6.4. summarizes the main techno-functional properties exhibited by SPH, including solubility, emulsifying, foaming, water binding capacity and oil binding capacity.

### 6.7.1. Solubility

Solubility is a good indicator of the SPH functionality and affects many of the other techno-functional properties, such as, emulsifying and foaming capacities. The enhanced solubility of the SPH over a wide pH range is due to their smaller molecular size compared with the intact protein and to the new exposed ionizable amino and carboxyl groups of the amino acids (194). Although high DH may lead to high solubility, extensive hydrolysis can promote negative effects on the other techno-functional properties. Usually, to maintain or improve functionality, low DH are required (194).

Solubility is generally measured by employing the nitrogen solubility index (NSI), which is determined by suspending the sample in water, stirring and centrifuge the mixture. The supernatant is then analyzed for nitrogen content and the NSI is calculated as the percentage of the soluble nitrogen to the total nitrogen in the sample (194).

#### **6.7.2. Emulsifying properties**

The emulsifying properties of SPH are directly associated to surface properties; that is the efficiency of the SPH to reduce the interfacial tension between the hydrophobic and hydrophilic components in food products (194), (218). SPH are able to promote oil-in-water emulsions because they possess hydrophilic and hydrophobic functional groups and are water soluble. Emulsifying properties are affected by solubility, molecular size and amino acid sequence of peptides, DH%, acetylation of the peptide and type(/s) of enzyme(/s) used (218), (223). Emulsifying properties decreases with extensive hydrolysis (higher DH%, lower molecular size proteins) due to the weak interfacial films around emulsion droplets and increased with the high content of larger molecular weight peptides (or more hydrophobic peptides). Generally, peptides presenting a minimum of ~20 residues are required to promote good emulsifying properties (194), (218).

The ability of protein hydrolysates to form and stabilize emulsions are generally measured by two methods: Emulsifying activity index (EAI) and Emulsifying stability index (ESI). EAI is defined as the volume of oil that can be emulsified by the protein, while ESI refers to the ability of an emulsion to resist changes in its properties over time. Measurement involves blending the protein with oil and water, centrifuging, and measuring the total volume of emulsion (194).

#### **6.7.3. Foaming properties**

The foaming properties of a protein hydrolysate are affected by transportation, penetration and rearrangement of molecules at the air-water interface (218). The foaming properties of SPH are also affected by DH%; several studies reported the decrease of foaming properties with the increase of DH% (20), (218).

Several methods are used to measure the foaming properties of a protein hydrolysate; results are usually expressed as Foam Expansion (FE) and Foam Stability (FS). FE is the percentage of excess volume produced by whipping the protein solution compared with the

initial volume of the liquid; FS is usually measured by whipping the protein solution and measuring the time required to decrease half of the volume (194).

#### **6.7.4. *Water binding capacity***

Water binding capacity (WBC) refers to the ability of the protein to imbibe water and retain it against gravitational force within a protein matrix. This property is very important for the food industry because improves texture to a food system (194). During SPH production, enzymatic hydrolysis increase the polar groups, such as, COOH and NH<sub>2</sub>, which affects the amount of adsorbed water (233). Therefore, extensive enzymatic hydrolysis (higher DH%, low molecular weight peptides) appear to affect greater WBC because smaller peptide fragments are more hydrophilic (218).

#### **6.7.5. *Oil binding capacity***

Extensive enzymatic hydrolysis (higher DH%, low molecular weight peptides) decrease the Oil binding capacity (OBC) of SPH (218). The ability of peptides to bind fat influences food product taste, which is especially important in both meat and confectionery industries (233). For OBC measurements, protein solutions are mixed with a specified amount of fat for a particular time and then centrifuged at a low centrifugal force (194).

Table 6.2. Summary of ACE-I activity reported for various SPH and derived bioactive peptides

Fish species	Part used to prepare SPH	Enzyme used	Assay	Peptide sequence or hydrolysate	Bioactivities showed		Tested in SHR	Reference
<i>Sardinella aurita</i>	Muscle	Alcalase	IC <sub>50</sub> (HHL)	MF	44.7	μM	<i>np</i>	(112)
<i>Sardinella aurita</i>	Muscle	Alcalase	IC <sub>50</sub> (HHL)	RY	51	μM	<i>np</i>	(112)
<i>Sardinella aurita</i>	Muscle	Alcalase	IC <sub>50</sub> (HHL)	MY	193	μM	<i>np</i>	(112)
<i>Sardinella aurita</i>	Muscle	Alcalase	IC <sub>50</sub> (HHL)	LY	38.5	μM	<i>np</i>	(112)
<i>Sardinella aurita</i>	Muscle	Alcalase	IC <sub>50</sub> (HHL)	YL	82	μM	<i>np</i>	(112)
<i>Sardinella aurita</i>	Muscle	Alcalase	IC <sub>50</sub> (HHL)	IY	10.5	μM	<i>np</i>	(112)
<i>Sardinella aurita</i>	Muscle	Alcalase	IC <sub>50</sub> (HHL)	VF	43.7	μM	<i>np</i>	(112)
<i>Sardinella aurita</i>	Muscle	Alcalase	IC <sub>50</sub> (HHL)	GRP	20	μM	<i>np</i>	(112)
<i>Sardinella aurita</i>	Muscle	Alcalase	IC <sub>50</sub> (HHL)	RFP	330	μM	<i>np</i>	(112)
<i>Sardinella aurita</i>	Muscle	Alcalase	IC <sub>50</sub> (HHL)	AKK	3.13	μM	<i>np</i>	(112)
<i>Sardinella aurita</i>	Muscle	Alcalase	IC <sub>50</sub> (HHL)	RVY	250.6	μM	<i>np</i>	(112)
<i>Sardinella aurita</i>	Muscle	Alcalase	IC <sub>50</sub> (HHL)	GWAP	3.86	μM	<i>np</i>	(112)
<i>Sardinella aurita</i>	Muscle	Alcalase	IC <sub>50</sub> (HHL)	KW	1.63	μM	<i>np</i>	(112)
<i>Sardinella aurita</i>	Muscle	Alcalase	IC <sub>50</sub> (HHL)	VY	10	μM	<i>np</i>	(112)
<i>Sardinella aurita</i>	Muscle	Alcalase	IC <sub>50</sub> (FAPGG)	VY	10	μM	Δ 7.0 mmHg	(134)
<i>Sardinella aurita</i>	Muscle	Alcalase	IC <sub>50</sub> (HHL)	KW	7.8	μM	<i>np</i>	(113)
<i>Sardinella aurita</i>	Muscle	Alcalase	IC <sub>50</sub> (HHL)	hydrolysate	0.180	mg/mL	<i>np</i>	(229)
<i>Sardinella aurita</i>	Muscle	Alcalase	IC <sub>50</sub> (HHL)	hydrolysate	0.620	mg/mL	<i>np</i>	(230)
<i>Sardinella aurita</i>	Muscle	Alcalase	IC <sub>50</sub> (HHL)	hydrolysate	0.260	mg/mL	<i>np</i>	(231)
<i>Sardinella aurita</i>	Muscle	Alcalase	IC <sub>50</sub> (HHL)	fraction <sup>a</sup>	0.015	mg/mL	<i>np</i>	(231)
<i>Sardinella aurita</i>	Muscle	Alcalase	IC <sub>50</sub> (HHL)	hydrolysate	0.082	mg/mL	<i>np</i>	(112)
<i>Sardinella aurita</i>	Heads and viscera	Proteases NH1	IC <sub>50</sub> (HHL)	hydrolysate	2.1	mg/mL	<i>np</i>	(15)
<i>Sardinella aurita</i>	Heads and viscera	Alcalase	IC <sub>50</sub> (HHL)	hydrolysate	2.3	mg/mL	<i>np</i>	(15)
<i>Sardinella aurita</i>	Heads and viscera	Sardine proteases	IC <sub>50</sub> (HHL)	hydrolysate	1.2	mg/mL	<i>np</i>	(15)
<i>Sardinella aurita</i>	Heads and viscera	Chymotrypsin	IC <sub>50</sub> (HHL)	hydrolysate	1.8	mg/mL	<i>np</i>	(15)
<i>Sardinella aurita</i>	Heads and viscera	Proteases ES1	IC <sub>50</sub> (HHL)	hydrolysate	7.4	mg/mL	<i>np</i>	(15)
<i>Sardinella pilchardus</i>	Whole fish <sup>b</sup>	Subtilisin + Trypsin	IC <sub>50</sub> (FAPGG)	hydrolysate	0.439	mg/mL	<i>np</i>	(215)
<i>Sardinella pilchardus</i>	Whole fish <sup>b</sup>	Trypsin + Subtilisin	IC <sub>50</sub> (FAPGG)	hydrolysate	0.442	mg/mL	<i>np</i>	(215)

<sup>a</sup> Fractionation of the hydrolysate obtained by Matsui *et al.* (231) with IC<sub>50</sub> (0.260 mg/mL) on an ODS column with ethanol. <sup>b</sup> whole fish, including skin, bones and internal organs. IC<sub>50</sub>, peptide concentration inducing 50% inhibition values of ACE. SHR, spontaneously hypertensive rats. *np*, not performed.

Table 6.3. Summary of antioxidant activity reported for various SPH and derived bioactive peptides

Fish species	Part used to prepare SPH	Enzyme used	Peptide sequence or hydrolysate	Bioactivities showed		Reference
<i>Sardinella aurita</i>	Heads and viscera	Alcalase	hydrolysate	DPPH ( <i>nr</i> )	41%	(20)
<i>Sardinella aurita</i>	Heads and viscera	Alcalase	hydrolysate	DPPH (0.3 mg/mL) RP (0.6 mg/mL) $\beta$ -carotene	55% 0.87 39%	(209)
<i>Sardinella aurita</i>	Heads and viscera	Sardine proteases	hydrolysate	DPPH (0.3 mg/mL) RP (0.6 mg/mL) $\beta$ -carotene	41% 0.54 38%	(209)
<i>Sardinella pilchardus</i>	Whole fish <sup>a</sup>	Subtilisin+Trypsin	hydrolysate	DPPH (EC <sub>50</sub> , mg/mL) RP (5 mg/mL) ICA (EC <sub>50</sub> , mg/mL)	1.75 0.22 0.32	(215)
<i>Sardinella aurita</i>	Heads and viscera	Proteases NH1	hydrolysate	DPPH (2 mg/mL) RP (2 mg/mL) LPIC (2 mg/mL)	26% 1.98 28%	(16)
<i>Sardinella aurita</i>	Heads and viscera	Alcalase	hydrolysate	DPPH (2 mg/mL) RP (2 mg/mL) LPIC (2 mg/mL)	54% 2.24 34%	(16)
<i>Sardinella aurita</i>	Heads and viscera	Sardine proteases	hydrolysate	DPPH (2 mg/mL) RP (2 mg/mL) LPIC (2 mg/mL)	27% 1.40 54%	(16)
<i>Sardinella aurita</i>	Heads and viscera	Proteases ES1	hydrolysate	DPPH (2 mg/mL) RP (2 mg/mL) LPIC (2 mg/mL)	11% 1.75 15%	(16)
<i>Sardinella aurita</i>	Muscle	Pepsin	LQPGQGQQ	O <sub>2</sub> <sup>-</sup> , ·OH, ESR	<i>nr</i>	(232)

<sup>a</sup> whole fish, including skin, bones and internal organs.

(DPPH) 2,2-diphenyl-1-picrylhydrazyl; (RP) Reducing power; (LPIC) Lipid peroxidation inhibition capacity; ( $\beta$ -carotene)  $\beta$ -carotene bleaching method; (ICA) Iron (Fe<sup>2+</sup>) chelating activity; Electron Spin Resonance (ESR).

*nr*, not reported.

Table 6.3. Summary of antioxidant activity reported for various SPH and derived bioactive peptides (continued)

Fish species	Part used to prepare SPH	Enzyme used	Peptide sequence or hydrolysate	Bioactivities showed	Reference	
<i>Sardinella aurita</i>	Heads and viscera	Sardine proteases	LARL	DPPH	51%	(16)
<i>Sardinella aurita</i>	Heads and viscera	Sardine proteases	GGQ	DPPH	38%	(16)
<i>Sardinella aurita</i>	Heads and viscera	Sardine proteases	LHY	DPPH	63%	(16)
<i>Sardinella aurita</i>	Heads and viscera	Sardine proteases	GAH	DPPH	<i>nr</i>	(16)
<i>Sardinella aurita</i>	Heads and viscera	Sardine proteases	GAWA	DPPH	52%	(16)
<i>Sardinella aurita</i>	Heads and viscera	Sardine proteases	PHYL	DPPH	<i>nr</i>	(16)
<i>Sardinella aurita</i>	Heads and viscera	Sardine proteases	GALAAH	DPPH	54%	(16)

(DPPH) 2,2-diphenyl-1-picrylhydrazyl  
*nr*, not reported.

Table 6.4. Summary of techno-functional properties reported for various SPH

Fish species	Part used	Enzyme used	DH (%)	Techno-functional properties	Reference
<i>Sardinella aurita</i>	Heads and viscera	Alcalase	FPH1 (6.6%) FPH2 (9.3%) FPH3 (10.2%)	- Solubility (pH range 3-10): 55% - 100%, higher for FPH2 at pH 6 - Foaming (0.01%): higher for FPH1 and lower for FPH3 - Emulsifying: higher for FPH1 and lower for FPH3 - OBC (0.05%): higher for FPH2 and lower for FPH1	(20)
<i>Sardinella aurita</i>	Muscle	<i>Bacillus subtilis</i> A26 <sup>a</sup>	nr	- Solubility (pH range 1-10): higher than 70% - EAI, m <sup>2</sup> /g (0.5%, 1% and 2% w/v): 47.6, 23.4, 8.2 - ESI, min (0.5%, 1% and 2% w/v, after 10 min): 47.8, 37.0, 6.3 - FE, % (0.5%, 1% and 2% w/v): 36.4, 50.4, 76.6 - FS, % (0.5%, 1% and 2% w/v, after 30 min): 23.5, 26.6, 47.0 - WBC, g/g (0.1% w/v): 7.5 - OBC, g/g (0.1% w/v): 6.0	(223)
		<i>Bacillus pumilus</i> A1 <sup>a</sup>	14%	- Solubility (pH range 2-12): 65%-95% - EAI, m <sup>2</sup> /g (0.1%, 0.5%, 1% and 2% w/v): 76.1, 20.1, 7.3, 5.1 - ESI, min (0.1%, 0.5%, 1% and 2% w/v, after 10 min): 30.0, 28.0, 17.0, 8.2 - FE, % (0.1% w/v): 80.1 - FS, % (0.1% w/v, after 15, 30 and 45 min): 78.2, 68.9, 55.2	
<i>Sardinella aurita</i>	Muscle	<i>Bacillus mojavensis</i> A21 <sup>a</sup>	7.5%	- Solubility (pH range 2-12): 65%-85% - EAI, m <sup>2</sup> /g (0.1%, 0.5%, 1% and 2% w/v): 81.6, 11.8, 9.9, 9.2 - ESI, min (0.1%, 0.5%, 1% and 2% w/v, after 10 min): 44.4, 40.2, 24.0, 11.4 - FE, % (0.1% w/v): 85.1 - FS, % (0.1% w/v, after 15, 30 and 45 min): 80.2, 62.1, 40.3	(222)
		Viscera proteases <sup>b</sup>	8.5%	- Solubility (pH range 2-12): 65%-85% - EAI, m <sup>2</sup> /g (0.1%, 0.5%, 1% and 2% w/v): 86.6, 7.9, 11.1, 17.8 - ESI, min (0.1%, 0.5%, 1% and 2% w/v, after 10 min): 37.7, 24.0, 16.0, 15.1 - FE, % (0.1% w/v): 71.1 - FS, % (0.1% w/v, after 15, 30 and 45 min): 68.1, 59.0, 51.2	

(EAI) Emulsifying activity index; (ESI) Emulsifying stability index; (FE) Foam expansion; (FS) Foam stability; (OBC) Oil binding capacity; (WBC) Water binding capacity.

<sup>a</sup> crude enzyme preparation.<sup>b</sup> crude enzyme preparation from sardine viscera.





## CHAPTER 7

### *Antioxidant and antihypertensive hydrolysates obtained from by-products of brewing and cannery sardine industry*

---

This chapter presents the hydrolysis optimization of the sardine sarcoplasmic proteins by BSY proteases to produce a SPH with antioxidant and ACE-I activities.



## ABSTRACT

Hydrolysates with antioxidant and ACE-I activities were obtained from sarcoplasmic proteins of canned sardine by-product and proteases extracted from Brewer's spent yeast. Using Response surface methodology (RSM), hydrolysis time and temperature were selected to achieve the maximum bioactivity. Hydrolysates produced using the E/S ratio 0.27:1 (U/mg), 7 h and 50°C have shown potential use for food industry, presenting an ACE-I activity of 164 µg protein/mL and an antioxidant activity of 291 µM TE/mL. Experimental results agreed with predicted values within a 95% confidence interval. Within this work the simultaneous valorisation of two agro-industrial by-products was successfully achieved.

## 7.1. INTRODUCTION

Sardine (*Sardina pilchardus*) is the main species caught off the Portuguese coast. The vast majority of it is used in the canned sardine industry. Its by-products include head, tail, viscera and muscle around the head. Although this waste is an excellent source of proteins, it is usually processed into low market-value products, namely, fish meal and fertilizers. Therefore, improving the value of this underutilized by-product is of major interest (13). One potential application is the production of Sardine protein hydrolysates (SPH) with improved physicochemical, techno-functional and sensorial properties when compared with the intact proteins (20), (196). Additionally, similar to found for peptides derived from other marine sources (234), (235), SPH may contain bioactive peptides with a broad spectrum of pharmaceutical, cosmetic and food industry applications (87). The biological properties of SPH bioactive peptides, and their use as antioxidant, antihypertensive, antithrombotic, immunomodulatory, antimicrobial agents are now a major field of study, as reviewed recently by several authors (13), (87). To date, SPH have been produced by (i) *in vitro* enzymatic hydrolysis (Alcalase (20), (209), Protamex (211), Flavourzyme (211)); (ii) autolytic process using endogenous enzymes (crude enzyme extract from sardine viscera) (15), (16), (209); (iii) microbial fermentation (crude enzyme preparation from *Bacillus licheniformis* NH1 (15), (16), *Aspergillus clavatus* ES1 (16), *Bacillus pumilus* A1 (222), *Bacillus mojavensis* A21) (222) and (iv) simulated gastric digestion (pepsin (17), trypsin (213), chymotrypsin (15), trypsin from skipjack tuna (*Katsuwonus pelamis*) spleen (199), hepatopancreas of cuttlefish (*Sepia officinalis*)) (209). Enzymatic hydrolysis is the most widely used method, although the high cost of enzymes can make this an expensive process. Additionally, optimization of variables, namely the type of protease, pH, temperature, time and E/S ratio are required to influence the extent of hydrolysis and, the

functionalities of the final SPH (236). RSM has been successfully used to investigate the effect of these independent variables, alone and in combination, on enzymatic processes (236).

BSY (*Saccharomyces pastorianus*) is the second major by-product from brewing process and is usually used as a feed supplement after heat inactivation (5). However, before thermal inactivation it can be an excellent source of proteases, which can be used to obtain protein hydrolysates with optimum activity at pH 6 (11).

In this work, sarcoplasmic sardine proteins extracted from canned sardine by-product were used as substrate to obtain SPH. These proteins are soluble in water, present an isoelectric point around 5.0-5.5 and have low molecular weight (40-70 kDa) (207, 237). Protein hydrolysis was performed using proteases extracted from BSY. The optimum time and temperature conditions required to produce SPH with both antioxidant and ACE-I activities were studied. Hydrolysis was monitored by chromatography and electrophoresis. No previous studies were found describing the use of proteases extracted from BSY for SPH production. Furthermore, as far as the authors are aware, this is the first work where RSM methodology is used to optimize the best hydrolysis conditions to obtain in tandem two biological properties in SPH, antioxidant and ACE-I activities. This work contributes to obtain added-value for two industrial by-products.

## 7.2. MATERIAL AND METHODS

### 7.2.1. Standards and reagents

Acetonitrile HPLC grade, trifluoroacetic acid (TFA); Folin-Ciocalteu phenol reagent; 2,4,6-trinitrobenzenesulfonic acid (TNBS); L-leucine; iron (III) chloride hexahydrate; potassium ferricyanide; 2,4,6-tripyridyl-s-triazine (TPTZ); commercial angiotensin-I-converting enzyme (ACE) (EC 3.4.15.1, 5.1 U/mg); molecular weight standards from 14 to 97 kDa for SDS-PAGE separations; bovine serum albumin (BSA) and 6-hydroxy-2,5,7,8-tetramethylchroman-2-carboxylic acid (Trolox) were obtained from Sigma-Aldrich (St. Louis, MO, USA). The *o*-aminobenzoylglycyl-*p*-nitro-phenylalanylproline (*o*-ABz-Gly-Phe(NO<sub>2</sub>)-Pro) was purchased from Bachem Feinchemikalien (Bubendorf, Switzerland) and the Millipore UF membranes with MWCO of 10 kDa were purchased from Sigma-Aldrich (St. Louis, MO, USA).

### **7.2.2. Equipment**

The RP-HPLC analyses were carried out using an analytical HPLC system (Jasco, Tokyo, Japan), equipped with a quaternary low pressure gradient HPLC pump (Jasco PU-1580), a degasification unit (Jasco DG-1580-53 3-line degasser), an autosampler (Jasco AS-2057-PLUS), a MD-910 multiwavelength detector (Jasco) and a 7125 Rheodyne injector valve (California, USA). Data acquisition was accomplished using Borwin Controller software, version 1.50 (JMBS Developments, Le Fontanil, France). The SDS-PAGE separations were achieved in a Multiple Gel Casters Hoefer® (Holliston, MA), Rect., Mightly Small For 8 x 9 cm Gels Hoefer® apparatus, coupled with a UniEquip Unipack 2000 electric source (UniEquip, Munich, Germany). Spectrophotometric analyses were carried out using a BMG LABTECH's SPECTROstar Nano-microplate, cuvette UV/Vis absorbance reader (Offenburg, Germany). Fluorimetric analyses were carried out using a fluorescence microplate reader (FLUOstar Optima, BMG Labtech GmbH). Samples were freeze-dried with a Telstar freeze dryer, Cryodos-80 model (Terrassa, Spain).

### **7.2.3. By-products**

Flesh sardine by-product including head, scale, skin, blood, bone, viscera and muscle tissue was provided by the portuguese company Conservas Ramirez & Cia (Filhos), SA (Matosinhos, Portugal). Approximately 1 kg of this by-product was placed on ice during the transportation to the laboratory and prepared in the same day under refrigerated conditions. BSY (*Saccharomyces pastorianus*) was supplied as slurry by Unicer brewing (Leça do balio, Portugal). This by-product was collected in transparent glass bottles, transported to the laboratory under refrigerated conditions and stored at 4°C until preparation procedure (1 day maximum).

### **7.2.4. Preparation of the Sardine Sarcoplasmic Protein extracts (SPE)**

The whole muscle (ordinary and dark) removed manually from sardine by-product was used for extraction of sarcoplasmic proteins, according to the method of Ren *et al.* (237), with slight modifications. The sardine muscle tissue was washed twice with deionized water and mixed with 0.2 M phosphate buffer pH 6.0, ratio of 1:3 (w/v). The mixture was homogenized using an Ultra-Turrex grinder for about 2 min. Then, the homogenate was heated at 85°C for 20 min to inactivate endogenous enzymes and subsequently centrifuged at 16,000 x g for 20 min, at 4°C. The upper lipid phase was removed manually and discarded; the supernatant was collected and filtered through a Whatman No. 4 filter paper. The final clear supernatant was coded as sardine sarcoplasmic protein extract (SPE). The pH of this extract (pH 6.3) was adjusted to pH 6.0 by adding 0.2 M HCl with constant agitation. The

protein concentration of SPE, determined by Lowry method (163), was 2.40 mg/mL. This extract was kept at -20°C until used; the storage time was not more than 1 month.

#### **7.2.5. Extraction of Brewer's spent yeast (BSY) proteases**

*Saccharomyces* cell wall was destroyed under refrigerated conditions to minimize enzyme denaturation and obtain a protease rich extract. Firstly, biomass was washed three times with 0.2 M phosphate buffer pH 6.0 at a ratio 1:3 (w/v) and centrifuged at 5,000 x g, 5 min, 4°C, between each wash. Afterwards, cell wall was destroyed with glass beads at a ratio 1:1:1 (biomass: phosphate buffer pH 6.0: glass beads) (w/v/w) by vortexing 10 times (1 min each) with 1 min cooling intervals on ice. Glass beads were removed and the homogenate was centrifuged at 12,000 x g, 40 min, 4°C. The resulting clear supernatant was freeze-dried, resuspended in the same buffer (25% of the initial volume) and concentrated using a UF membrane with a MWCO of 10 kDa. The protease activity of BSY extract, performed according to Cupp-Enyard (164) protocol, was 0.725 U/mL. The BSY proteases extract was kept at -20°C until used.

#### **7.2.6. Enzymatic hydrolysis**

SPE (containing 2.40 mg protein/mL) was hydrolysed by BSY proteases (0.725 U/mL) using an E/S ratio of 0.27:1 (U/mg) and pH 6.0. For example, considering a reaction volume of 1 mL, for each 500 µL of SPE (substrate), 450 µL of BSY proteases were added; the remaining volume of 50 µL was 0.2 M sodium phosphate buffer, pH 6.0. Triplicate hydrolysis were performed, using 2 mL *eppendorf* tubes, in a shaking incubator with constant agitation (200 rpm) at different temperatures and times, according to the experimental model described in sub-section 7.2.15. Control [S+E] was the mixture of SPE and BSY proteases before hydrolysis. Inactivation of proteases to stop reaction was performed by heating at 95°C for 15 min (216). The hydrolysates were cooled on ice and centrifuged at 3,000 x g at 4°C for 10 min. The clear supernatants, containing soluble peptides and coded as H1 to H13 were collected and stored at -20°C for further analysis.

#### **7.2.7. Hydrolysis Rate (HR%)**

RP-HPLC, using the chromatographic conditions described by Ferreira *et al.* (185) was used to follow protein degradation during hydrolysis. The column was a Chrompack P 300 RP (polystyrenedivinylbenzene copolymer, 8 µm, 300Å, 150 x 4.6 mm i.d.) (Middleburg, The Netherlands). Hydrolysis rate (HR%) was based on the measurement of protein fraction that remains intact, for this purpose the peak area of the protein fraction that eluted between 24 and 33 min was measured. The peak area of [S+E] protein fraction before hydrolysis was the maximum intact protein.

The following equation was applied:

$$\text{HR (\%)} = 100 - \left[ \left( \frac{\text{peak area of protein fraction after hydrolysis}}{\text{peak area of protein fraction before hydrolysis}} \right) \times 100 \right] \quad (1)$$

### 7.2.8. Protein Recovery (PR%) and % of peptides formed

Protein recovery (PR %) was calculated as the amount of protein, determined by Bradford method (171), in the hydrolysate in comparison with the initial amount of protein, using the following equation:

$$\text{PR (\%)} = 100 - \left[ \left( \frac{\text{protein content after hydrolysis}}{\text{protein content before hydrolysis}} \right) \times 100 \right] \quad (2)$$

Additionally, the % of peptides formed in the hydrolysates was measured by subtracting the protein content evaluated by Bradford method to the total protein including peptides evaluated by Lowry method (163), using the following equation:

$$\% \text{ Peptides} = \left[ \frac{(\text{Lowry} - \text{Bradford})}{\text{Lowry}} \right] \times 100 \quad (3)$$

For both assays, a calibration curve was performed with 2 mg/mL BSA and samples were analysed in triplicate.

### 7.2.9. Degree of Hydrolysis (DH%)

Degree of Hydrolysis (DH%) was determined by measuring the increase in free amino groups using a picrylsulfonic acid solution (TNBS), according to Hsu *et al.* (238);  $\alpha$ -amino acid group was expressed in terms of L-leucine and the DH% was determined as follows:

$$\text{DH (\%)} = [(L_t - L_0)/(L_{\max} - L_0)] \times 100 \quad (4)$$

where ( $L_t$ ) was the amount of amino acid released at time ( $t$ ); ( $L_0$ ) was the amount of amino acid in original SPE, and ( $L_{\max}$ ) was the maximum amount of amino acid in SPE obtained after acid hydrolysis. For ( $L_{\max}$ ) determination, SPE (500  $\mu$ L) was mixed with 4.5 mL of 6 M HCl and the hydrolysis was run at 100°C for 24 h. Then, final acid-hydrolysed sample was filtered through Whatman paper no. 1 to remove the non-hydrolysed fragments and the supernatant was neutralized with 6 M NaOH before amino acid determination.

### 7.2.10. Ferric reducing ability (FRAP)

The measurement of FRAP was performed based on Jansen and Ruskovska (154) procedure, slightly modified. Briefly, 25  $\mu$ L of sample/ standard/ control (pure water) and 200  $\mu$ L of working FRAP reagent were pipetted in the microplate in six replicates. After that, the reaction mixture was incubated for 90 min at 37 °C, under constant agitation (200 rpm). The absorbance was measured at 600 nm. Trolox was used as a standard at 50-500  $\mu$ M to generate a calibration curve (average  $R^2 = 0.9929$ ). Results were expressed as mean values  $\pm$  standard deviations, as  $\mu$ M TE (Trolox Equivalent)/mL SPH.

#### 7.2.11. Reducing Power method (RP)

RP was measured according to the assay reported by Almeida *et al.* (156), slightly modified. Briefly, 250 µL of samples/ control (pure water) were mixed with 250 µL of sodium phosphate buffer (200 mM, pH 6.6) and 250 µL of potassium ferricyanide 1% (w/v). The mixture was incubated at 50°C for 20 min, and 250 µL of cold TCA 10% (w/v) was added to stop the reaction. *Eppendorfs* were centrifuged at 650 rpm, 10 min. Then, 500 µL of supernatant was incubated with 500 µL of deionized water and 100 µL of ferric chloride 0.1% (w/v). After 10 min reaction, the absorbance was measured at 700 nm. RP values were expressed as µg/mL.

#### 7.2.12. ACE-I activity

ACE-I activity was measured using the fluorimetric assay of Sentandreu and Toldrá (121) with the modifications reported by Quiros *et al.* (122). ACE-I percentage (I %) was calculated using the equation:

$$I \% = \{(B - A) / (B - C)\} \times 100 \quad (5)$$

where B is the fluorescence of the ACE solution without the inhibitor (SPH); A is the fluorescence of the tested sample of SPH; and C is the fluorescence of experimental blank, *o*-ABz-Gly-Phe(NO<sub>2</sub>)-Pro dissolved in 150 mM Tris-base buffer (pH 8.3), containing 1.125 M NaCl. The percent inhibition curves (using a minimum of five determinations for each sample peptide concentration) were plotted *versus* peptide concentration to estimate the mean IC<sub>50</sub> value, which is defined as the concentration required to decrease the ACE activity by 50% (122).

#### 7.2.13. SDS-Polyacrylamide gel electrophoresis (SDS-PAGE)

Proteolytic degradation of SPE was monitored by SDS-PAGE analysis. Separation gels consisted of a 4% polyacrylamide stacking gel and a 15% polyacrylamide resolving gel and were performed according to Laemmli (162) protocol. The molecular weight protein standards used were: phosphorylase β (97 kDa), bovine serum albumin (66 kDa), ovalbumin (45 kDa), carbonic anhydrase (30 kDa), trypsin inhibitor (20 kDa) and lysozyme (14 kDa). Coomassie brilliant blue R-250 was used. The protein pattern separated on SDS-PAGE was estimated for its molecular weight by plotting the logarithm of molecular weight of the protein standards against relative mobility (*Mr*).

#### 7.2.14. SPH amino acid composition

SPH presenting highest FRAP and ACE-I activities was lyophilized and amino acid analysis was performed after hydrolysis with 6 M HCl at 110°C for 24 h. Derivatization and GC/MS



were carried out according to Pérez-Palacios *et al.* (148). Amino acid composition was expressed as g/ 100 g of protein.

#### **7.2.15. Experimental design, modelling and optimization of hydrolysis conditions**

A central composite design (CCD) was built for optimization of the best hydrolysis conditions to obtain simultaneously in tandem two biological properties in SPH, antioxidant and ACE-I activities. The CCD variables under analysis were time (X1) and temperature (X2) at ranged levels of time intervals (0.40; 1.50; 4.25; 7.00 and 8.00 h) and five temperatures (20; 25; 38; 50 and 55°C), in a total of 13 runs with five centre points. CCD consisted of a complete  $2^2$ -factorial design as cubic points, with four axial points at a distance of  $\alpha = 1.414$  from the design centre and five centre points. The responses used in the experimental designs were the HR % (Y1), antioxidant activity evaluated by FRAP assay (Y2) and ACE-I activity as  $IC_{50}$  (Y3). The optimal values of response Y were obtained by solving the regression equation and by analysing the response surface and contour plots using the predictive equations of RSM. Then, the accuracy of the models was tested by conducting a set of experiments using the critical values optimized; the *t* test was conducted to compare the responses prepared under optimized conditions with those predicted by models. The statistical analyses were performed by using the software Design Expert trial version 7 (Stat-Ease Inc., Minneapolis, MN, USA).

#### **7.2.16. Statistical analysis**

The data obtained for others assays were done by using SPSS statistical software, version 22.0 (SPSS Inc., Chicago, IL). One-way analysis of variance and Duncans' test was performed to determine the significant differences at the 5% probability level. A Pearson's correlation was also used to search for correlations between the parameters under study; 1% level was considered to be significant. The *t* test was conducted to compare the responses prepared under optimized conditions with those predicted by models.

### **7.3. RESULTS AND DISCUSSION**

Preliminary experiments were conducted by univariate method to study the pH variation during hydrolysis, as well as, the influence of E/S ratio (0.10:1; 0.15:1; 0.20:1; 0.25:1 and 0.30:1 U/mg) on hydrolysis of SPE. Reactions were performed at constant temperature (37°C), while stirring at 200 rpm for 4 h. When the initial pH was 6.0 it remained in the range of 5.8 to 6.5 during the entire hydrolysis period. For this reason it was decided not adjust pH during SPE hydrolysis. From an industrial point of view, hydrolysis carried out

without any pH adjustment is economically desirable (216). Regarding to E/S ratio, 0.10:1 U/mg and 0.15:1 U/mg gave a significantly lower HR%, whereas no significant differences were found ( $p > 0.05$ ) on the HR% obtained from hydrolysis using 0.25:1 U/mg and 0.30:1 U/mg. As a result, the ratio 0.27:1 U/mg was chosen, as it is the same reported by Bougatef *et al.* (16).

The RP-HPLC profiles of SPE plus BSY proteases [S+E] without hydrolysis, and two different SPH, one presenting HR = 9.3% (25°C, 1.50 h) and another presenting HR = 83% (50°C, 7.00 h), are shown in Figure 7.1. The RP-HPLC chromatograms were divided into three fractions: “Less hydrophobic peptides” (eluted between 4 and 12 min); “Hydrophobic Polypeptides” (eluted between 12.1 and 23.9 min) and “Proteins” (eluted between 24 and 33 min). HR% determination was based on the measurement of “Proteins” fraction before and after hydrolysis.

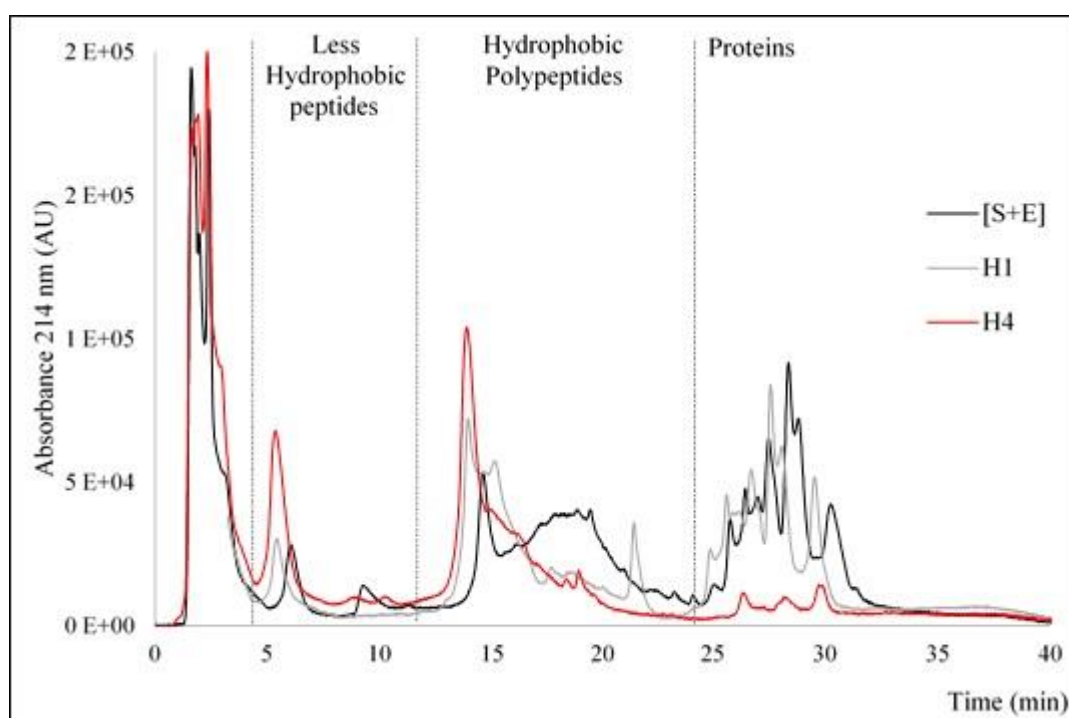


Figure 7.1. The RP-HPLC profiles of (i) SPE plus BSY proteases [S+E] without hydrolysis; (ii) SPH presenting HR = 9.3% (25°C, 1.50 h); and (iii) SPH presenting HR = 83% (50°C, 7.00 h). RP-HPLC chromatograms are divided into three fractions: “Less hydrophobic peptides” (eluted between 4 and 12 min); “Hydrophobic Polypeptides” (eluted between 12.1 and 23.9 min) and “Proteins” (eluted between 24 and 33 min). Hydrolysis rate (HR%) determination was based on the measurement of “Proteins” fraction before and after hydrolysis.

### 7.3.1. Optimization of hydrolysis conditions

Optimization of the variables affecting the antioxidant and ACE-I activities of SPH was carried out using a statistical design, by CCD. The experiments were performed in a random manner at different combinations of temperature (X1) and time (X2). The HR% (Y1), FRAP (Y2) and ACE-I activity (Y3) of SPH obtained by BSY proteases were used as responses factors for CCD (Table 7.1). Regression analyses were performed to fit the response functions. The parameters of the equations (6, 7 and 8) were explained by a quadratic model for each response and are presented as follows:

$$Y1 = -20.31 + 0.29.X1 + 4.70.X2 + 0.02.X1^2 \quad (6)$$

$$Y2 = 279.35 - 2.50.X1 - 10.21.X2 + 0.41.X1.X2 + 0.03.X1^2 - 0.42.X2^2 \quad (7)$$

$$Y3 = -78.38 + 12.51.X1 - 0.30.X1.X2 - 0.16.X1^2 - 4.48.X2^2 \quad (8)$$

where Y is the predicted response; X1 the uncoded value of variable temperature (°C) and X2 the uncoded value of variable time (h). Adequacy and significance of the quadratic model was evaluated by analysis of the variance (ANOVA) by means of Fisher's F-test. The quadratic models were validated by two diagnostic residuals, the squared correlation coefficient ( $R^2$ ) and the predictive squared correlation coefficient ( $Q^2$ ). Values of  $R^2 > 0.75$  and  $Q^2 > 0.60$  indicate adequacy of models (172). The  $R^2$  for checking the fitness of model was very good (relatively close to 1), indicating that models explained 98.6%, 98.4% and 95.3% of the variation on the HR, FRAP and ACE-I activity of sardine sarcoplasmic proteins, respectively. The  $Q^2$  values were respectively 0.9738; 0.9516 and 0.9804 for the three responses, indicating the goodness of the model. The "Adeq Precision" was higher than 4 (as desirable) for the three responses, indicating an adequate signal-to-noise ratio. The statistical analysis also showed that the "lack of fit" was not significant ( $p > 0.05$ ), which confirmed the adequacy of model to describe the experimental data and for the prediction of the three studied parameters. The independent variable X1 had a significant effect on Y1, Y2 and Y3 ( $p < 0.05$ ); X2 had significant effect on Y1 and Y2 ( $p < 0.05$ ), but not on Y3. The interactions between X1.X2 influenced Y2 and Y3 ( $p < 0.05$ ). Therefore, this model proved to be powerful for navigating the design space and describes the dependence of HR%, FRAP and ACE-I activity on temperature and time.

Table 7.1. Results from experimental design by CCD for evaluation the effects of hydrolysis temperature and time conditions on HR, FRAP and ACE-I activity

Point		T (°C)	t (h)	Hydrolysis Rate (Y1, HR %)		Antioxidant activity (Y2; FRAP $\mu$ M TE/ mL)		ACE-I activity (Y3; IC <sub>50</sub> $\mu$ g/ mL)	
code	run	X1	X2	Experimental <sup>a</sup>	Predicted <sup>b</sup>	Experimental <sup>a</sup>	Predicted <sup>b</sup>	Experimental <sup>a</sup>	Predicted <sup>b</sup>
H6	1	55	4.25	81	83	290	290	170	171
H1	2	25	1.50	9.3	7.4	235	237	177	185
H7	3	38	0.40	17	19.1	238	235	181	173
H4	4	50	7.00	83	83	290	289	164	160
H11	5	38	4.25	41	42	246	247	234	242
H12	6	38	4.25	38	42	249	247	245	242
H13	7	38	4.25	45	42	250	247	247	242
H3	8	25	7.00	29	29	219	217	210	207
H8	9	38	8.00	56	56	244	246	170	176
H10	10	38	4.25	45	42	246	247	237	242
H5	11	20	4.25	12	13	226	226	213	210
H9	12	38	4.25	41	42	245	247	246	242
H2	13	50	1.50	54	52	251	254	172	178

<sup>a</sup> Average of triplicate determinations from different experiments; <sup>b</sup> Based on CCD evaluation.

### 7.3.2. Analysis of response surfaces

Contour plots were employed to study the influence of temperature (°C) and time (h) on HR%, FRAP and ACE-I activity. HR% increased with the increasing of time and temperature (Contour plot A, Figure 7.2). The minimum predicted value of HR% (7.4%) was observed at 25°C and 1.50 h, while the maximum predicted value of HR% (83%) was observed at 50°C and 7.00 h. Extensive time of hydrolysis and high temperatures also enhanced the FRAP value of SPH (counter plot B of Figure 7.2). The minimum predicted FRAP value was 217  $\mu\text{M TE/mL}$ , observed at 25°C and 7.00 h; whereas the maximum predicted FRAP value was 289  $\mu\text{M TE/mL}$  found at 50°C and 7.00 h. Similar behaviour was observed for HR% and FRAP, suggesting that the extension of proteolysis may be favourable to enhance the antioxidant properties of SPH. Concerning to ACE-I activity, the  $\text{IC}_{50}$  increased near to the centre point design and decreased for higher temperature and extensive time of hydrolysis (counter plot C, Figure 7.2). Lower  $\text{IC}_{50}$  value (160  $\mu\text{g protein/mL}$ ), which means higher ACE-I activity, was observed when hydrolysis was performed at 50°C and 7.00 h.

### 7.3.3. Validation of the RSM model

The optimal hydrolysis conditions to maximize the antioxidant and ACE-I activities of SPH was predicted by using RSM. For that purpose, the optimization tool of the statistical program was used, which explores the response surface and gave a point prediction as a result of defined goals. The goals for each response were set to maximize the Y2 and Y3 responses to construct desirability indices. The optimal hydrolysis conditions to produce a SPH with the highest antioxidant and ACE-I (minimum  $\text{IC}_{50}$ ) activities were temperature of 50°C and hydrolysis time of 7.00 h. On these conditions, the predicted antioxidant activity was 289  $\mu\text{M TE/mL}$  and the  $\text{IC}_{50}$  was 160  $\mu\text{g protein/mL}$ . The desirability analysis in identifying the optimal conditions by the RSM was 99.2%. Results showed that there is no statistically significant difference between the experimental and estimated values within a 95% confidence interval. Thereby, the adequacy of the models in predicting the optimum hydrolysis conditions for SPH production using BSY proteases was confirmed.

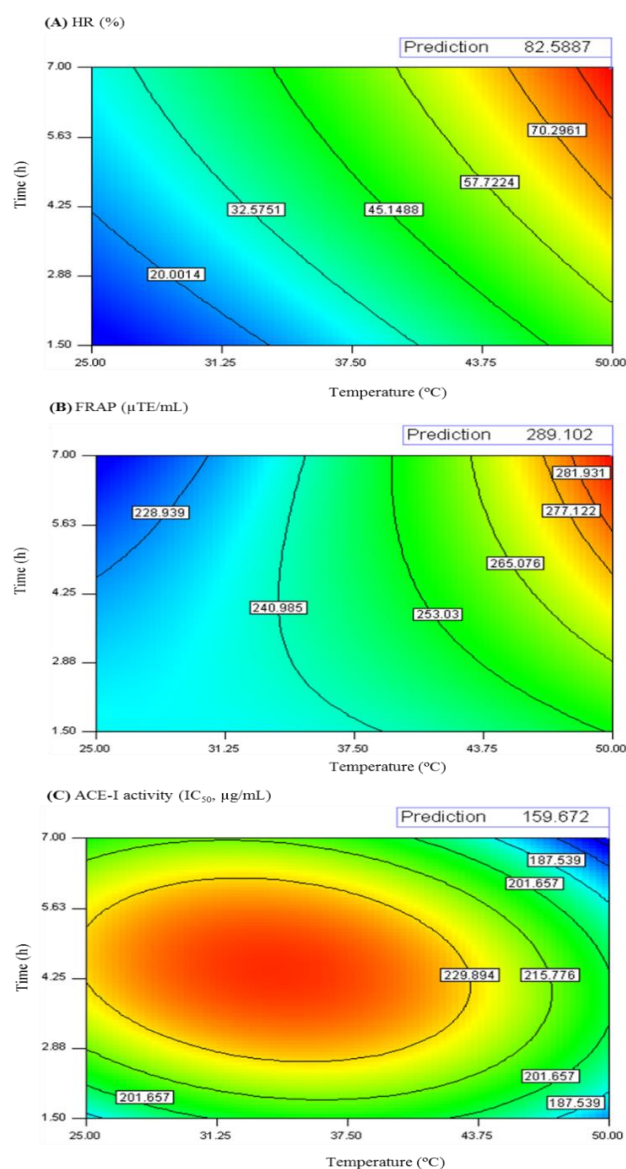


Figure 7.2. Counter plots for interaction effects of temperature (°C) and time (h) on Hydrolysis Rate (%) **(A)**; Antioxidant activity determined by FRAP assay **(B)** and ACE-I activity **(C)** of SPH. Each optimum point was identified on the response surface.

#### 7.3.4. Characterization of SPH obtained under optimum conditions

Comparison of antioxidant activity of [S+E] mixture before hydrolysis and of SPH obtained under optimum conditions was performed by FRAP and by RP, since both methods have been widely used to screen antioxidant activity of protein hydrolysates. The FRAP value of [S+E] mixture before hydrolysis was 146 μM TE/mL, whereas for SPH it increased to 291 μM TE/mL. This value is comparable to that exhibited by protein hydrolysates derived from threadfin bream surimi by-products (221 μM TE/mL) (239). With respect to RP results, [S+E] mixture before hydrolysis presented 1210 μg/mL, whereas SPH presented 1312 μg/mL. These results were comparable to those obtained for bigeye tuna

protein hydrolysates, which ranged between 948 and 12500 µg/mL (240). The ACE-I activity of [S+E] mixture before hydrolysis was  $IC_{50}$  604 µg protein/mL, whereas SPH presented an  $IC_{50}$  of 164 µg protein/mL, which is comparable to the  $IC_{50}$  described in literature for other fish protein hydrolysates. Matsui *et al.* (231) described an  $IC_{50}$  of 260 µg protein/mL for SPH prepared using 0.3% Alcalase® at pH 9, 50°C for 17 h and Cinq-Mars and Li-Cha (236) reported a Pacific hake fillet hydrolysate with an  $IC_{50}$  of 165 µg protein/mL, by incubation with 3.0% Protamex® at pH 6.5, 40°C for 125 min. Electrophoresis was performed to characterize the larger fragments resulting from proteolysis. SDS-PAGE of control sample [S+E] showed bands in the range of 12 to 51 kDa (Figure 7.3).

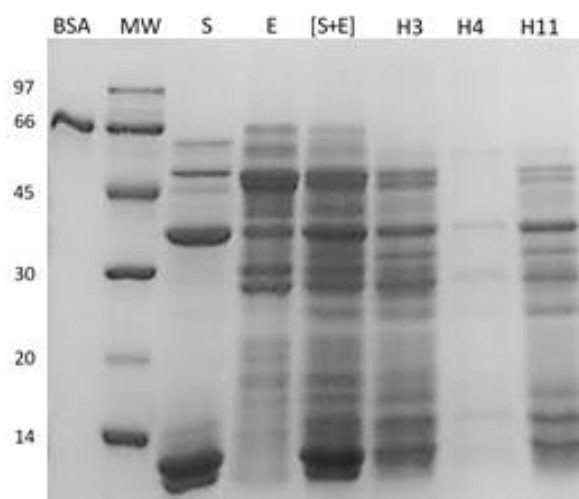


Figure 7.3. SDS-PAGE profiles of sarcoplasmic proteins plus BSY proteases [S+E] without hydrolysis and SPH. A total of 8 µL of sample was applied to each well.

Legend: Lane BSA shows bovine soro albumin (66 kDa); lane MW shows molecular weight of standard markers (14-97 kDa); lane S (*substract*) shows SPE in the absence of the BSY proteases; lane E (*enzyme*) shows BSY proteases in the absence of SPE; lane [S+E] shows SPE and BSY proteases without hydrolysis (control). Lane H3 shows SPH with HR = 29% (25°C, 7.00 h); lane H4 shows SPH with HR = 83% (50°C, 7.00 h); lane H11 shows SPH with HR = 41 % (38°C, 4.25 h).

These fractions are in agreement with the SDS-PAGE patterns of sardine sarcoplasmic proteins described by other authors (241), (242). The most abundant bands were 51 kDa, 47 KDa, 45 kDa (probably actin), 41-39 kDa a doublet band (probably from creatine kinase and aldolase) and 39-41 kDa band probably from glyceraldehyde-3-phosphate dehydrogenase. Additional bands were found at 17 and 15 kDa (242). The last

one could be from myoglobin, as observed by Chaijan *et al.* (196). Finally, two protein bands, at 13 and 12 kDa could be parvalbumins (242). Some myofibrillar proteins (90 kDa band) were also extracted during the SPE extract preparation. SDS-PAGE analysis indicates that under prolonged time and increased temperature of hydrolysis, 50°C, 7.00 h (H4, Figure 7.3), sardine sarcoplasmic proteins were extensively hydrolysed. These results are in good agreement with the results from assays that evaluate the extension of hydrolysis or the peptides formation, since this SPH presented HR% of 83, DH% of 14, PR% of 86 and 63% of peptides formed.

Low-molecular-weight peptides are widely recognized as presenting higher antioxidant and ACE-I activities, but the amino acid composition of peptides is also a crucial aspect. ACE-I peptides usually contain a proline residue at the carboxyl terminal end, whereas amino acids, such as, tyrosine, tryptophan, histidine, methionine and lysine have been known to exhibit antioxidant activity (234). Amino acid analysis of SPH prepared under the hydrolysis conditions optimized, revealed that it is rich in glutamic acid, glutamine, aspartic acid and alanine, which accounted for 18.0%, 12.4%, 10.5% and 9.0% of the total amino acids, respectively. It also presents relatively high content of hydrophobic amino acids, such as, proline (3.1%), leucine (5.6%), glycine (4.2%), isoleucine (2.2%), phenylalanine (3.2%) and valine (4.2%) and contained amino acids that exhibit antioxidant activity, namely, tyrosine (2.0%), histidine (5.8%), methionine (2.2%) and lysine (2.6%); tryptophan was not determined due to the acidic hydrolysis conditions.

## 7.4. CONCLUSIONS

Sardine sarcoplasmic proteins were hydrolysed by the proteases extracted from brewer's spent yeast to obtain hydrolysates with antioxidant and ACE-I activities. Hydrolysates produced using the E/S ratio 0.27:1 U/mg, 7.00 h and 50°C presented an antioxidant activity of 291  $\mu\text{M}$  TE/mL and an ACE-I activity ( $\text{IC}_{50}$ ) of 164  $\mu\text{g}$  protein/mL. These experimental FRAP and  $\text{IC}_{50}$  values agreed with the predicted values (289  $\mu\text{M}$  TE/mL and 160  $\mu\text{g}$  protein/mL, respectively) within a 95% confidence interval, suggesting a good fit between the models and the experimental data. Thus, RSM was an efficient statistical tool in the optimization of hydrolysis conditions. SPH presents relatively high content of hydrophobic amino acids, such as, proline, leucine, glycine, isoleucine, phenylalanine and valine, and amino acids that exhibit antioxidant activity, namely, tyrosine, histidine, methionine and lysine. Further work should be done to test antioxidant activity of this hydrolysate *in vivo*, as well as, isolate and identify the specific peptides that are responsible for these bioactive properties.



## CHAPTER 8

*Simulated gastrointestinal digestion and in vitro  
intestinal permeability of bioactive protein hydrolysates  
obtained from brewing and canned sardine industry by-  
products*

---

This chapter describes the simulated GI digestion and the *in vitro* intestinal cell permeability of the SPH with antioxidant and ACE-I activities.



## ABSTRACT

A sardine protein hydrolysate (SPH) was produced using sarcoplasmic proteins from canned sardine by-product and proteases from brewer's spent yeast (BSY), at an E/S ratio of 0.27:1 U/mg, pH 6.0, 50°C for 7 h. The SPH presented *in vitro* ACE-I activity, IC<sub>50</sub> 169 µg protein/mL and FRAP value of 288 µM TE/mL. Both activities were enhanced by UF through a 10 kDa MWCO membrane. Simulated gastrointestinal (GI) digestion increased the FRAP value, whereas the IC<sub>50</sub> remained similar. The apparent permeability coefficient (180 min, 37°C) of <10 kDa fraction across Caco-2 and Caco-2/HT29-MTX cell monolayers were 5.89×10<sup>-6</sup> cm s<sup>-1</sup> and 10.93×10<sup>-6</sup> cm s<sup>-1</sup>, respectively. Permeates presented antioxidant activity but no ACE-I activity was detected. Mass spectrometry revealed that molecules with m/z between 1000 and 5000 were transported across Caco-2/HT29-MTX cell monolayer. SPH prepared by BSY proteases is promising for the formulation of functional foods.

## 8.1. INTRODUCTION

Many food protein hydrolysates show *in vitro* antioxidant and/ or ACE-I activities. However, the bioavailability of the bioactive peptides found in these protein hydrolysates depends on several factors, such as, enzymatic degradation in GI tract, permeability through intestinal epithelium and interaction with intracellular sources of oxidative stress (181), (243-246). Simulated GI digestion and *in vitro* cell-based models allow for rapid and inexpensive screening of potential bioactive compounds (181). Due to their similarity with intestinal epithelium cells, the human colorectal adenocarcinoma Caco-2 cell line and resulting cell monolayers have been widely accepted as *in vitro* models to predict the cytotoxicity and intestinal absorption of drugs and bioactive compounds (127), (181), (246-248). Different transport routes, namely paracellular, fluid phase and adsorptive transcytosis may participate in peptide transport across Caco-2 cell monolayers (245). However, this cell model has some limitations when compared with human small intestine, including the absence of mucus-producing cells and the resulting mucus layer; higher tightness to molecular diffusion; as well as, low expression of uptake transporters and overexpression of P-glycoprotein (129), (249). To overcome some of these limitations, combinations of Caco-2 cells with mucus-producing goblet cell, such as HT29-MTX cells, have been proposed as co-culture models for permeation studies (130), (131). Co-culture of Caco-2/HT29-MTX cells leads to the establishment of monolayers with intermediate properties regarding transepithelial electrical resistance (TEER), peptide hydrolysis and absorption. The proportion of 90:10, expressed as initial cell seeding for Caco-2/HT29-MTX cells, is the

most prevalent in the literature and accepted to better mimic the natural epithelial barrier (129), (132), (133). The expression of goblet cells in HT29-MTX cell line increases absorption of lipophilic compounds compared to Caco-2 monolayer (131), (133). Indeed, some absorption enhancers have been recognized to be effective in increasing the intestinal absorption of peptides and proteins (190), (250).

We have recently reported, for the first time, a SPH prepared by the action of BSY proteases (251). Under optimum hydrolysis conditions (50°C, pH 6.0, 7 h, E/S ratio of 0.27:1 U/mg), the SPH revealed a FRAP value of 291 µM TE/mL and an ACE-I activity (IC<sub>50</sub>) of 164 µg protein/mL. These properties suggest that SPH may be an interesting ingredient for the formulation of functional foods, but further investigation, regarding its digestion and intestinal permeability is required. To best of our knowledge, no studies on *in vitro* permeability of SPH peptides produced by BSY proteases have been published. Therefore, the present work aims to investigate: (i) the effects of UF membranes on the SPH biological activities, (ii) the stability of SPH peptides to GI proteases in order to assess its adequacy for oral administration, and (iii) the resistance of SPH peptides to brush-border peptidases and its susceptibility to intestinal transport. For this last purpose, two cellular monolayer models, comprising either a monoculture of Caco-2 cells or the co-culture (90/10) of Caco-2/HT29-MTX cells, were compared. Both cells express different intestinal enzymes and provide distinct functionality to the monolayers: Caco-2 cells (absorptive-type) partially reproduce the characteristics of intestinal enterocytes, whereas HT29-MTX cells (goblet type) are able to secrete mucin and thus replicate mucus-secreting goblet cells (130), (131).

## 8.2. MATERIAL AND METHODS

### 8.2.1. Materials and cells

Pepsin, pancreatin, commercial angiotensin-I-converting enzyme (ACE) (EC 3.4.15.1, 5.1 U/mg), captopril, 6-hydroxy-2,5,7,8-tetramethylchroman-2-carboxylic acid (Trolox), trifluoroacetic acid (TFA), 3-(4,5-dimethylthiazol-2-yl)-2,5-diphenyltetrazolium bromide (MTT) and dimethyl sulfoxide (DMSO) were purchased from Sigma-Aldrich (St. Louis, MO, USA). The *o*-aminobenzoylglycyl-*p*-nitro-phenylalanylproline (*o*-ABz-Gly-Phe(NO<sub>2</sub>)-Pro) was purchased from Bachem Feinchemikalien (Bubendorf, Switzerland). The Millipore UF membranes with MWCO of 3 kDa and 10 kDa were purchased from Sigma-Aldrich (St. Louis, MO, USA). GIBCO Dulbecco's Modified Eagle Medium (DMEM), heat-inactivated fetal bovine serum (FBS), non-essential amino acids, penicillin/streptomycin, trypsin-EDTA and Hank's Balanced Salt Solution (HBSS, pH 7.0-7.4) were purchased from Invitrogen (Carlsbad, California, USA). Falcon® translucent polyethylene terephthalate (PET) cell

culture inserts (3.0 µm pore size, 24 mm diameter inserts, 4.2 cm<sup>2</sup> effective growth area) were acquired from BD Biosciences (Franklin Lakes, NJ, USA), and 6-well and 96-well microplates were purchased from Corning® Costar® (Sigma-Aldrich, St. Louis, MO, USA). Human colon carcinoma (Caco-2) cell line was obtained from the American Type Culture Collection (ATCC) and mucus producing HT29-MTX cell line was kindly provided by Dr. T. Lesuffleur (INSERM U178, Villejuif, France).

### 8.2.2. By-products

Flesh sardines (*Sardina pilchardus*) by-product including head, scale, skin, blood, bone, viscera and muscle tissue was provided by the portuguese company Conservas Ramirez & Cia (Filhos), SA (Matosinhos, Portugal). The whole muscle (ordinary and dark) was removed manually from sardine and used for preparation of sarcoplasmic protein extract, as described by Vieira and Ferreira (251). Protein concentration of sarcoplasmic protein extract, determined by the Lowry method, was 2.4 mg/mL; this extract was kept at -20°C until use. BSY (*Saccharomyces pastorianus*) was supplied by the Unicer brewing (Leça do Balio, Portugal). Cell wall was destroyed under refrigerated temperatures with glass beads at a ratio of 1:1:1 (biomass: phosphate buffer pH 6.0: glass beads); (w/v/w) by vortexing 10 times (1 min each) with 1 min cooling intervals on ice. After removing the glass beads, the homogenate was centrifuged at 12,000 x g, 40 min at 4°C. The resulting clear supernatant was freeze-dried, resuspended in the same buffer (to 25% of the initial volume) and concentrated using a 10 kDa MWCO membrane. The protease activity of the retentate, evaluated according to Cupp-Enyard (164) protocol, was 0.725 U/mL. This extract was kept at -20°C until use.

### 8.2.3. Preparation and fractionation of SPH

Sarcoplasmic protein extract was hydrolysed by BSY proteases using an E/S ratio of 0.27:1 (U/mg), pH 6.0, 50°C for 7 h. SPH was filtrated successively through 10 and 3 kDa MWCO membranes. Fractions were collected and coded as SPH<10 kDa or SPH<3 kDa for peptides permeating through the 10 kDa or 3 kDa membranes, respectively. The protein recovery (PR%) upon UF was calculated as described by Picot *et al.* (244):

$$PR (\%) = [\text{protein of filtrate} / \text{total protein of SPH}] \times 100 \quad (1)$$

Protein content was determined by the Lowry method (163).

### 8.2.4. *In vitro* Simulated GI Digestion

*In vitro* pepsin-pancreatin digestion of SPH<10 kDa was performed according to the method described by Samaranayaka *et al.* (181). For this assay, SPH<10 kDa (50 mL) was used at a final concentration of 5.0 mg protein/mL (based on Lowry method). In brief, the pH of

SPH<10 kDa solution was adjusted to 2 with 5 M HCl, then a solution of 1% (w/w) pepsin was added in a E/S ratio of 1:35 (v/v) and the mixture was incubated in a shaking incubator for 1 h, 300 rpm at 37°C. Pepsin digestion was stopped by submerging in boiling water for 10 min. The pH was then adjusted to 5.3 with a saturated NaHCO<sub>3</sub> solution and further to pH 8 with 5 M NaOH. A solution of 1% (w/w) pancreatin was added to the mixture at an E/S ratio of 1:25 (v/v), which was incubated again with shaking for 2 h, 300 rpm at 37°C. To stop the digestion by pancreatin, the solution was submerged in boiling water for 10 min. Control treatment was prepared by inactivation (boiling for 10 min) of pepsin/pancreatin before reaction with SPH<10 kDa. An aliquot of the digested samples (referred to as SPH.GI<10 kDa) was used directly for RP-HPLC analysis (performed as described in sub-section 8.2.9) and for determining antioxidant and ACE-I activities (assessed as described in sub-sections 8.2.5 and 8.2.6, respectively). The remaining SPH.GI<10 kDa samples were freeze-dried and stored at -25°C for further cell assays (described in sub-sections 8.2.7 and 8.2.8).

#### 8.2.5. Ferric Reducing Antioxidant Potential (FRAP) assay

The antioxidant activity of SPH; <10 kDa and <3 kDa fractions; SPH.GI<10 kDa and cell permeates (at 180 min of cell transport) were measured by FRAP, according to the method described by Jansen and Ruskovska (154). The absorbance was measured at 600 nm, using a BMG LABTECH's SPECTROstar Nano-microplate (Offenburg, Germany). Trolox was used as a standard at 50-500 µM to generate a calibration curve (average  $R^2 = 0.9971$ ) and results were expressed as mean values  $\pm$  standard deviations (n=3) as µM of Trolox equivalent per mL of sample (µM TE/mL).

#### 8.2.6. ACE-I activity assay

ACE-I activity of SPH; <10 kDa and <3 kDa fractions; SPH.GI<10 kDa and cell permeates (at 180 min of cell transport) was assessed in triplicate using the fluorimetric assay described by Sentandreu and Toldrá (121), with the modifications reported by Quiros *et al.* (122). ACE-I percentage (I) was calculated using the equation:

$$I \% = \{(B - A) / (B - C)\} \times 100 \quad (2)$$

where B is the fluorescence of the ACE solution without the inhibitor (SPH); A is the fluorescence of the tested sample of SPH; and C is the fluorescence of experimental blank. The percent inhibition curves were plotted *versus* peptide concentration to estimate the mean IC<sub>50</sub> value, which is defined as the concentration required to decrease the ACE activity by 50% (122). Fluorimetric analysis was carried out using a fluorescence microplate reader (FLUOstar Optima, BMG Labtech GmbH, Offenburg, Germany).

### 8.2.7. Cell viability study

The 3-(4,5-dimethylthiazol-2-yl)-2,5-diphenyltetrazolium bromide (MTT) assay was used to determine the cytotoxicity of SPH.GI<10 kDa in the viability of Caco-2 cell line. In this assay, the MTT is reduced by mitochondrial dehydrogenases to a water-insoluble formazan derivative, which can be measured at 570 nm (181). Briefly, cells ( $8 \times 10^4$  cells/mL) were seeded onto the central 60 wells of 96-well microplates in order to obtain confluent monolayers within 2 days. After that, the medium was gently aspirated and the cells were incubated for 24 h (37°C, 5% CO<sub>2</sub>) with SPH.GI<10 kDa at five different concentrations: 0.25; 0.50; 1.00; 2.00 and 4.00 mg protein/mL. Each individual plate included six replicates of negative control (medium only) and six replicates of positive control (media with 1% Triton X-100); peripheral wells on the plate were filled with sterile water to avoid evaporation of the treatment solutions. After cell treatment with test samples, the culture medium was aspirated and the attached cells were rinsed with 200 µL HBSS, followed by the addition of fresh culture medium containing 0.25 mg/L MTT. After 30 min of incubation (37°C, 5% CO<sub>2</sub>), the intracellular crystals of formazan were dissolved in 100 µL of DMSO and the absorbance was measured at 570 nm. Each sample was tested in six replicates and three independent experiments were performed. Cell viability was calculated as follows:

$$\text{Cell viability (\%)} = \left( \frac{\text{Abs sample}}{\text{Abs control}} \right) \times 100 \quad (3)$$

where Abs control was the absorbance of formazan in negative control cells and Abs sample was the absorbance of formazan in cells exposed to the test samples.

### 8.2.8. Permeability experiments

Caco-2 and HT29-MTX cell line cells were used at passages 28 and 44, respectively. The two cell lines were maintained in culture separately, in DMEM supplemented with 10% FBS, 1% non-essential amino acids, 100 U/mL penicillin and 100 µg/mL streptomycin, at 37°C under a 5% CO<sub>2</sub> water saturated atmosphere. Cells were harvested at 90% confluence with trypsin-EDTA and seeded onto PET inserts mounted in 6-well plates, at a total density of  $10^5$  cells/mL. In the case of the Caco-2 cell model, cells were seeded at  $2.8 \times 10^5$  cells/mL, while in the case of Caco-2/HT29-MTX cell co-culture model, cells of each type were mixed prior to seeding to yield a concentration of  $2.52 \times 10^5$  cells/mL and  $0.28 \times 10^5$  cells/mL for Caco-2 and HT29-MTX, respectively, as described by Antunes *et al.* (131). The culture medium was replaced every other day and the monolayers allowed differentiating for 21 days. Caco-2 and Caco-2/HT29-MTX monolayers with an integrity equivalent to a TEER higher than 200 Ω.cm<sup>2</sup> were used for permeability experiments. Lyophilized SPH.GI<10 kDa sample was dissolved in HBSS and recovered to a final concentration of 2.0 mg protein/mL (based on Lowry assay). Caco-2 monolayer and Caco-2/HT29-MTX co-culture monolayer

were gently washed twice with HBSS solution and allowed to equilibrate for 30 min at 37°C in HBSS before permeability experiments. Then, the basolateral sides of the insert were filled with 1.7 mL of HBSS solution, while 1.7 mL of SPH.GI<10 kDa (2.0 mg protein/mL in HBSS) were placed on top (apical side) of the Caco-2 and Caco-2/HT29-MTX cells monolayers. Permeability experiments were conducted at 37°C, 5% CO<sub>2</sub> water saturated atmosphere, under static conditions (i.e. without stirring). Samples (0.7 mL) were collected from the basolateral side after 15, 30, 60, 120 and 180 min of incubation and replaced with the same volume of fresh HBSS. Collected samples were used directly for chromatographic analysis (performed as described in sub-section 8.2.9) to evaluate the percentage permeability, whereas an aliquot from each permeate was concentrated by freeze-drying and then reconstituting in HBSS (20% the initial volume) in order to determine the antioxidant and ACE-I activities (as previously described in sub-sections 8.2.5 and 8.2.6). The efficiency of peptide transport, expressed as percentage of permeability for each peak (P %), was calculated according to Cinq-Mars *et al.* (127) as follows:

$$P \% = \frac{A_b}{A_a \cdot V} \times 100 \quad (4)$$

where  $A_b$  and  $A_a$  correspond, respectively, to the RP-HPLC peak areas of the peptide fraction detected in the basolateral and in the apical side and  $V$  (mL) is the volume of sample loaded in the apical side.

The apparent permeability coefficient ( $P_{app}$ , cm s<sup>-1</sup>) was calculated according to Ferraro *et al.* (184), as follows:

$$P_{app} = \frac{Q}{A \cdot C \cdot t} \quad (5)$$

where  $Q$  is the total amount of permeated compounds during the 180 min of the experiment in the basolateral side (mg),  $t$  (s) is the time of experiment,  $A$  is the monolayer area (4.52 cm<sup>2</sup>), and  $C$  (mg/mL) is the apical side concentration at time zero.

### 8.2.9. Reversed-phase high performance liquid chromatography

The RP-HPLC analysis of SPH.GI<10 kDa and respective permeates from Caco-2 cell and Caco-2/HT29-MTX cell co-culture permeability assays were performed according to the method described by Ferreira *et al.* (185). Solvent A was 0.1% TFA in water and solvent B was acetonitrile-water-TFA (95:5:0.1, v/v/v). Peptides and proteins were eluted with the following gradient: 0-5 min, 0% B; 5-9 min, 0-5% B; 9-15 min, 5-15% B; 15-25 min, 15-33% B; 25-31 min, 33-40% B; 31-37 min, 40% B; 37-45 min, 40-50% B; 45-50 min (50-0% B), in a total run time of 50 min. The flow-rate was 1.0 mL/min and the injection volume was 100 µL. UV detector absorbance was set at 214 nm. The equipment consisted of a Jasco HPLC system (Tokyo, Japan) equipped with a quaternary low pressure gradient HPLC pump



(Jasco PU-1580), a degassing unit (Jasco DG-1580-53 3-line degasser), an autosampler (Jasco AS-2057-PLUS), a MD-910 multiwavelength detector (Jasco) and a 7125 Rheodyne injector valve (California, USA). The column was a Chrompack P 300 RP (polystyrenedivinylbenzene copolymer, 8  $\mu\text{m}$ , 300 Å, 150 x 4.6 mm i.d.) (Chrompack, Middleburg, The Netherlands). Data acquisition was accomplished using the Borwin Controller software, version 1.50 (JMBS Developments, Le Fontanil, France).

#### 8.2.10. Mass spectrometry

The molecular weight profiles of permeates after transport across Caco-2/HT29-MTX were analysed by MALDI-TOF MS. Data were acquired using a 4800 MALDI-TOF/TOF (Applied Biosystems, Darmstadt, Germany) mass spectrometer in the mass-to-charge ratio ( $m/z$ ) range from 1000 to 12000. Samples were cleaned with ZipTip C18 (Millipore) using the manufacturer's instructions. Then, the eluted samples were premixed with matrix [3 mg/mL alpha-cyano-4-hydroxycinnamic acid (CHCA) in 50% (v/v) aqueous acetonitrile, 0.1% trifluoroacetic acid (TFA)], spotted onto a target plate and dried at room temperature. The 4800 MALDI-TOF/TOF was calibrated using horse myoglobine [ $m/z$  16952.56 (+1);  $m/z$  8476.78 (+2);  $m/z$  5651.85 (+3)] and cytochrome c [( $m/z$  12349.72 (+1);  $m/z$  6177.94 (+2))]. The MS data was processed using the Data Explorer 4.8 software (ABSCIEX).

#### 8.2.11. Statistical analysis

The statistical analysis was performed using the SPSS 22.0 software (SPSS, Chicago, IL, USA). The student *t*-test was performed to compare the absorptive transport between the two cell monolayer models; one-way analysis of variance (ANOVA) was carried out to allow multi-comparison test, with Duncan's post hoc test. The significance levels were set at an overall  $\alpha$  error of 5% ( $p < 0.05$ ).

### 8.3. RESULTS AND DISCUSSION

#### 8.3.1. Effect of UF on biological activities of SPH

The antioxidant activity (FRAP assay) and ACE-I activity of SPH, <10 kDa and <3 kDa fractions were assayed. Results are presented in Table 8.1. SPH showed a FRAP value of 287.7  $\mu\text{M TE/mL}$  and an ACE-I activity ( $\text{IC}_{50}$ ) of 168.5  $\mu\text{g protein/mL}$ .  $\text{IC}_{50}$  values of 260  $\mu\text{g protein/mL}$  have been previously reported for sardine muscle hydrolysates obtained by Alcalase® (231). More recently, Bougateg *et al.* (15) reported  $\text{IC}_{50}$  values ranging from 1200 to 7400  $\mu\text{g protein/mL}$  for sardine viscera hydrolysates obtained by treatment with different microbial and visceral fish serine proteases. However, the direct comparison with the  $\text{IC}_{50}$

values obtained in the present study is not reliable due to differences in the hydrolysis conditions and the methodology employed for ACE-I activity determination. UF of SPH using a 3 kDa MWCO membrane concentrated the antioxidant compounds, the FRAP value increased to 328.6  $\mu\text{M TE/mL}$  ( $p < 0.05$ ), while the fraction  $<10$  kDa exhibited the highest ACE-I activity,  $\text{IC}_{50}$  of 105.7  $\mu\text{g protein/mL}$  ( $p < 0.05$ ). These results are in agreement with Jeon *et al.* (252), who reported an improvement in  $\text{IC}_{50}$  after UF of cod frame hydrolysate with a 10 kDa MWCO membrane and an increase of antioxidant activity using a 3 kDa MWCO membrane. Also, Cinq-Mars and Li-Chan (236) observed that UF using a 10 kDa MWCO membrane significantly improved ( $\sim 70\%$ ) the  $\text{IC}_{50}$  of Pacific Hake fillet hydrolysate ( $p < 0.05$ ). Results suggest that the smaller molecular weight peptides are likely responsible for the antioxidant activity observed. However, the same conclusion was not observed for ACE-I activity. Similar conclusion was also observed for other protein hydrolysates (253), (254). Since the  $<10$  kDa fraction presented enhanced antioxidant and ACE-I activity compared with SPH, this fraction was selected to study the stability of the antioxidant and ACE-I activities after simulated GI digestion.

Table 8.1. Antioxidant and ACE-I activities of SPH, its fractions  $<10$  kDa and  $<3$  kDa and the *in vitro* GI digest of SPH $<10$  kDa

Sample	Protein Recovery (%)	FRAP ( $\mu\text{M TE/mL}$ )	$\text{IC}_{50}^*$ ( $\mu\text{g/mL}$ )
SPH	---	287.7 $\pm$ 2.6 <sup>d</sup>	168.5 $\pm$ 1.8 <sup>b</sup>
SPH $<10$ kDa	56.3 $\pm$ 1.8 <sup>a</sup>	305.8 $\pm$ 3.6 <sup>c</sup>	105.7 $\pm$ 2.2 <sup>c</sup>
SPH $<3$ kDa	27.5 $\pm$ 2.1 <sup>b</sup>	328.6 $\pm$ 2.1 <sup>b</sup>	210.6 $\pm$ 4.6 <sup>a</sup>
SPH.GI $<10$ kDa	---	343.6 $\pm$ 4.6 <sup>a</sup>	116.5 $\pm$ 3.6 <sup>c</sup>

Results are expressed as mean  $\pm$  standard deviation from two replicate experiments analyzed in triplicate. In each column the different superscript letters indicate significant differences at  $p < 0.05$ , Duncan's post hoc test.

\*  $\text{IC}_{50}$  is the concentration ( $\mu\text{g protein/mL}$ ) of sample required to inhibit 50% of the ACE activity.

### 8.3.2. Effect of simulated GI Digestion on the biological activities of SPH $<10$ kDa

Similar RP-HPLC profiles of SPH $<10$  kDa ( $p < 0.05$ ) were observed before and after GI digestion (results not shown), which suggests that SPH $<10$  kDa fraction is stable against GI proteases. Additionally, the simulated GI digestion had no effect ( $p < 0.05$ ) in the ACE-I activity ( $\text{IC}_{50}$  of 116.5  $\mu\text{g protein/mL}$ ), as observed in Table 8.1. Similarly, Cinq-Mars *et al.*

(127) reported that UF<10 kDa fraction of Pacific Hake fillet hydrolysate had similar ACE-I activity ( $IC_{50}$  of 90  $\mu$ g protein/mL) before and after simulated GI digestion. Bougateg *et al.* (15) concluded that a SPH with  $IC_{50}$  of 810  $\mu$ g protein/mL was resistant to GI proteases action, while Matsufuji *et al.* (112) reported that the  $IC_{50}$  of a sardine muscle hydrolysate (82  $\mu$ g protein/mL) did not changed after GI digestion. According to the criteria of Iroyukifujita *et al.* (109), hydrolysates and individual ACE-I peptides can be classified as “pro-drug type”, “true-drug type” or “substrate type” based, respectively, on an increased, unchanged or decreased ACE-I activity after simulated GI digestion. Therefore, based on our results, ACE-I peptides present in SPH<10 kDa can be classified as “true-drug type”. Concerning antioxidant activity, a significant ( $p < 0.05$ ) increase of the FRAP value was observed, 343.6  $\mu$ M TE/mL, indicating that GI digestion produced peptides with higher antioxidant activity. Wu and Ding (255) reported a similar effect of GI digestion in UF-10 kDa fraction of soy protein hydrolysate.

### 8.3.3. Cellular viability of SPH.GI<10 kDa

Caco-2 cells were used to evaluate the cellular viability of SPH.GI<10 kDa. Results of the MTT assay, which measures the mitochondrial succinate dehydrogenase activity, are reported in Figure 8.1. SPH.GI<10 kDa did not present toxic effects in relation to mitochondrial enzyme activity of Caco-2 cells at concentrations between 0.25 and 2.00 mg protein/mL, whereas a significant ( $p < 0.05$ ) decrease on cell viability was observed for 4.00 mg protein/mL. Moreover, the SPH.GI<10 kDa at the concentrations of 1.0 and 2.0 mg protein/mL significantly ( $p < 0.05$ ) prompted an increased cellular reactivity, reflecting higher metabolic competence. Thus, the concentration of 2.00 mg protein/mL was selected for permeability assays in order to not affect viability of cell monolayers during permeability studies.

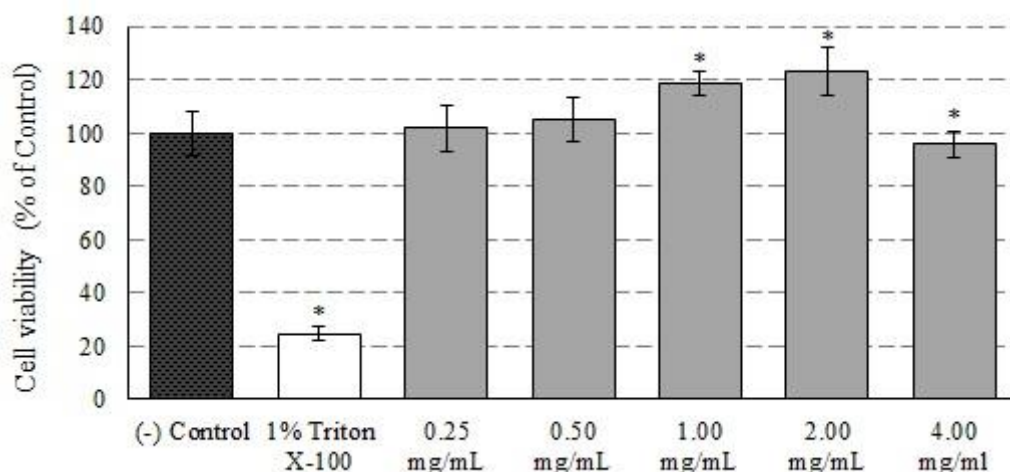


Figure 8.1. Effect of SPH.GI<10 kDa at different protein concentrations on Caco-2 cell viability, after 24 h of incubation at 37°C, 5% CO<sub>2</sub> (MTT assay). Each bar represents the mean  $\pm$  standard deviation of 3 individual experiments (6 replicates per experiment).

\* significant differences ( $p < 0.05$ ) when compared with negative control (cells incubated with medium only).

#### 8.3.4. Intestinal permeability of SPH.GI<10 kDa

In order to simulate the intestinal epithelial barrier, absorptive Caco-2 cells and mixed culture of Caco-2/HT29-MTX (90:10) cells were grown on permeable supports for 21 days. In both models, cell monolayer formation was monitored by measuring TEER values. The Caco-2 cell monolayer model presented higher TEER values (360-390  $\Omega \cdot \text{cm}^2$  at 21 days) when compared with the co-culture model (220-250  $\Omega \cdot \text{cm}^2$  at 21 days) due to the establishment of looser tight junctions between Caco-2 and HT29-MTX; these values were in agreement with previous reports (131), (132). A typical RP-HPLC chromatogram of the SPH.GI<10 kDa used in cell permeability assays is shown in Figure 8.2.A. Analyses of peptide permeability were performed using the area of peaks 1 to 11. RP-HPLC chromatograms indicate that these peptide fractions could permeate the Caco-2/HT29-MTX co-culture and the Caco-2 cell monolayers (Figure 8.2.B and C). Table 8.2 presents, for both cell models, the cumulative percentage permeability of each peptide fraction after 180 min of cell transport (37°C, 5% CO<sub>2</sub>). Transepithelial transport from apical-to-basolateral side of Caco-2/HT29-MTX cell co-culture model, after 180 min (37°C, 5% CO<sub>2</sub>) indicate high permeability, especially for peptides of peaks 5, 6, 7 and 11, which reached, respectively, 70.6%, 78.9%, 52.6% and 62.5% (Table 8.2). Lower permeability was observed for transepithelial transport from apical-to-basolateral side of Caco-2 cell culture model. After 180 min of cell transport at 37°C, higher permeability was observed for peaks 6, 9 and 11, which reached 49.6%, 41.1% and 45.2%, respectively (Table 8.2).

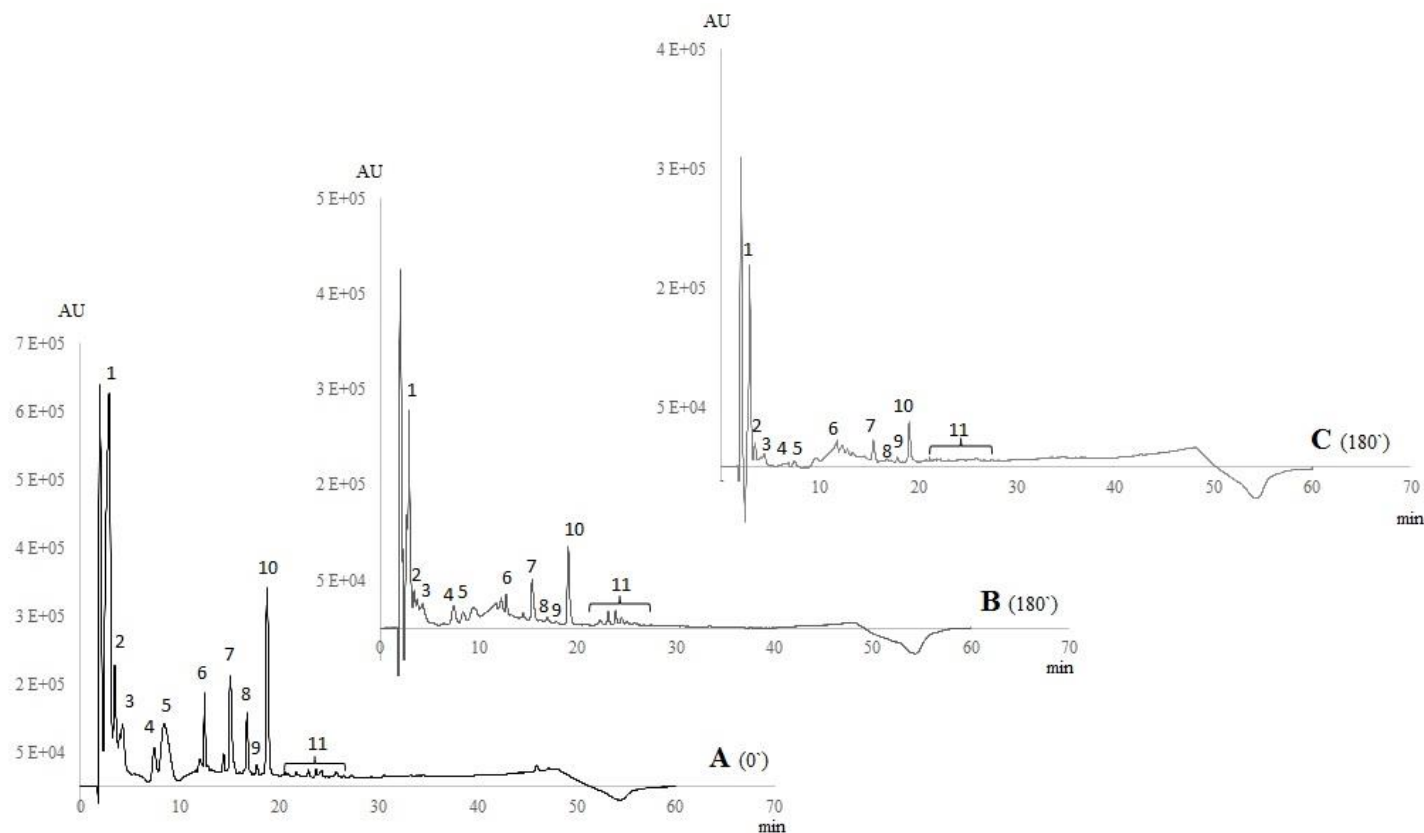


Figure 8.2. RP-HPLC chromatographic profiles of SPH.GI<10 kDa added to the apical side at the beginning of permeability experiment **(A)** and collected from the basolateral side after 180 min of transport across Caco-2/HT29-MTX co-culture cell monolayer **(B)**, and after 180 min of transport across Caco-2 cell monolayer **(C)**. The absorbance was monitored at 214 nm. Retention time for HPLC peaks are: (1) 2.9 min; (2) 3.5 min; (3) 4.3 min; (4) 7.4 min; (5) 7.5-8.5 min; (6) 10.1-12.8 min; (7) 14.4-15.1 min; (8) 16.8 min; (9) 17.8 min; (10) 18.8 min and (11) 20.5-26.8 min.

Table 8.2. Cumulative percentage permeability (P %) of SPH.GI<10 kDa peptides through the Caco-2/HT29-MTX co-culture cell monolayer and through Caco-2 cell monolayer for 180 min (37°C, 5% CO<sub>2</sub>)

Peak (min)	Cumulative percentage permeability (P %)										
	1 (2.9)	2 (3.5)	3 (4.3)	4 (7.4)	5 (7.5-8.5)	6 (10.1-12.8)	7 (14.4-15.1)	8 (16.8)	9 (17.8)	10 (18.8)	11 (20.5-26.8)
Caco-2/HT29-MTX co-culture cell monolayer											
15`	7.5 <sup>e</sup>	6.2 <sup>e</sup>	15.4 <sup>e</sup>	15.3 <sup>e</sup>	14.6 <sup>e</sup>	59.2 <sup>d</sup>	18.6 <sup>d</sup>	14.9 <sup>e</sup>	20.9 <sup>e</sup>	12.5 <sup>e</sup>	42.0 <sup>e</sup>
30`	16.3 <sup>d</sup>	12.2 <sup>d</sup>	27.1 <sup>d</sup>	25.0 <sup>d</sup>	21.6 <sup>d</sup>	73.8 <sup>c</sup>	26.1 <sup>d</sup>	15.4 <sup>d</sup>	28.4 <sup>c</sup>	19.6 <sup>d</sup>	48.4 <sup>d</sup>
60`	20.3 <sup>c</sup>	14.9 <sup>c</sup>	32.0 <sup>c</sup>	32.8 <sup>c</sup>	24.1 <sup>c</sup>	75.2 <sup>b</sup>	32.5 <sup>b</sup>	17.0 <sup>b</sup>	30.0 <sup>b</sup>	23.5 <sup>c</sup>	49.9 <sup>c</sup>
120`	22.5 <sup>b</sup>	16.5 <sup>b</sup>	34.1 <sup>b</sup>	33.7 <sup>b</sup>	49.4 <sup>b</sup>	66.8 <sup>e</sup>	32.2 <sup>c</sup>	16.3 <sup>c</sup>	25.7 <sup>d</sup>	24.7 <sup>b</sup>	52.4 <sup>b</sup>
180`	44.7 <sup>a</sup>	36.8 <sup>a</sup>	44.8 <sup>a</sup>	34.5 <sup>a</sup>	70.6 <sup>a</sup>	78.9 <sup>a</sup>	52.6 <sup>a</sup>	31.2 <sup>a</sup>	45.5 <sup>a</sup>	51.7 <sup>a</sup>	62.5 <sup>a</sup>
Caco-2 cell monolayer											
15`	0.3 <sup>d</sup>	0.0 <sup>e</sup>	0.0 <sup>e</sup>	0.0 <sup>c</sup>	0.0 <sup>c</sup>	0.0 <sup>e</sup>	0.0 <sup>e</sup>	0.0 <sup>e</sup>	0.0 <sup>e</sup>	0.0 <sup>e</sup>	0.0 <sup>d</sup>
30`	0.7 <sup>d</sup>	0.9 <sup>d</sup>	1.7 <sup>d</sup>	0.0 <sup>c</sup>	0.0 <sup>c</sup>	53.5 <sup>c</sup>	6.0 <sup>c</sup>	12.4 <sup>b</sup>	37.7 <sup>b</sup>	7.9 <sup>a</sup>	0.0 <sup>d</sup>
60`	1.4 <sup>c</sup>	1.5 <sup>c</sup>	2.2 <sup>c</sup>	0.0 <sup>c</sup>	0.0 <sup>c</sup>	51.5 <sup>d</sup>	4.3 <sup>d</sup>	9.7 <sup>d</sup>	25.0 <sup>d</sup>	4.6 <sup>c</sup>	37.5 <sup>b</sup>
120`	5.5 <sup>b</sup>	5.2 <sup>b</sup>	6.3 <sup>b</sup>	5.8 <sup>a</sup>	3.1 <sup>b</sup>	55.4 <sup>b</sup>	7.1 <sup>b</sup>	10.6 <sup>c</sup>	34.2 <sup>c</sup>	7.4 <sup>b</sup>	44.1 <sup>a</sup>
180`	15.3 <sup>a</sup>	8.1 <sup>a</sup>	12.5 <sup>a</sup>	10.6 <sup>b</sup>	4.2 <sup>a</sup>	49.6 <sup>a</sup>	15.2 <sup>a</sup>	12.9 <sup>a</sup>	41.1 <sup>a</sup>	7.4 <sup>b</sup>	45.2 <sup>a</sup>

Results are expressed as mean ± standard deviation from three chromatographic analysis and were calculated as 100 × [peak area of peptide fraction detected in basolateral side] / [peak area of peptide fraction detected in apical side]. For peak identification, see Figure 8.2. For each model, in each column the different superscript letters indicate significant differences at  $p < 0.05$ , Duncan's post hoc test.

The values of  $P_{app}$ , which reflects the rate of passage through the intestinal epithelial barrier, suggest that the peptide fractions 1 to 11 in SPH.GI<10 kDa are very likely to be absorbed in humans (Figure 8.3).  $P_{app}$  values obtained *in vitro* using cell models can be correlated with *in vivo* absorption profiles. For example, according to the criteria defined by Yee (189),  $P_{app}$  values lower than  $10^{-6}$  cm s<sup>-1</sup> indicate poor *in vivo* absorption (<30%);  $P_{app}$  values between  $10^{-6}$  and  $10^{-5}$  cm s<sup>-1</sup> correspond to substances with moderate absorption (30-70%); and  $P_{app}$  values higher than  $10^{-5}$  cm s<sup>-1</sup> suggest that substances are well absorbed (>70%). The  $P_{app}$  values (at 180 min, 37°C) for absorptive transport of SPH.GI<10 kDa peptides across Caco-2/HT29-MTX co-culture and Caco-2 cell monolayers were  $11.0 \times 10^{-6}$  cm s<sup>-1</sup> and  $5.9 \times 10^{-6}$  cm s<sup>-1</sup>, respectively. These values are in accordance with other studies, in which  $P_{app}$  of food-derived peptides varied in the range of  $0.50$ - $9.21 \times 10^{-6}$  cm s<sup>-1</sup> (129), (133), (184) and support that SPH.GI<10 kDa may undergo moderate *in vivo* absorption. The higher values of permeability and  $P_{app}$  of the co-culture model when compared with the monoculture model (Table 8.2 and Figure 8.3) can be explained by the tighter cell junctions among Caco-2 cells than between Caco-2/HT29-MTX, as previously described (130), (131). As suggested by Calatayud *et al.* (133), the co-culture monolayer presents higher number of paracellular pores per cm<sup>2</sup> and is less resistant to compound permeation. Furthermore, the mucus produced by HT29-MTX did not seem to delay the permeation of SPH.GI<10 kDa peptides, suggesting a low level of interaction with mucins and unimpaired diffusion. The modified HT29 cells are recognized for secreting gel-forming mucins, mostly MUC5AC but also MUC2 (predominant in intestinal mucus) and MUC5B (130), (256- 258). The Caco-2/HT29-MTX cell culture model, comprising mucus layer and goblet-type cells, might represent a more physiological and realistic approach compared with *in vivo* conditions and may give more accurate bioavailability predictions of the SPH.GI<10 kDa peptides.

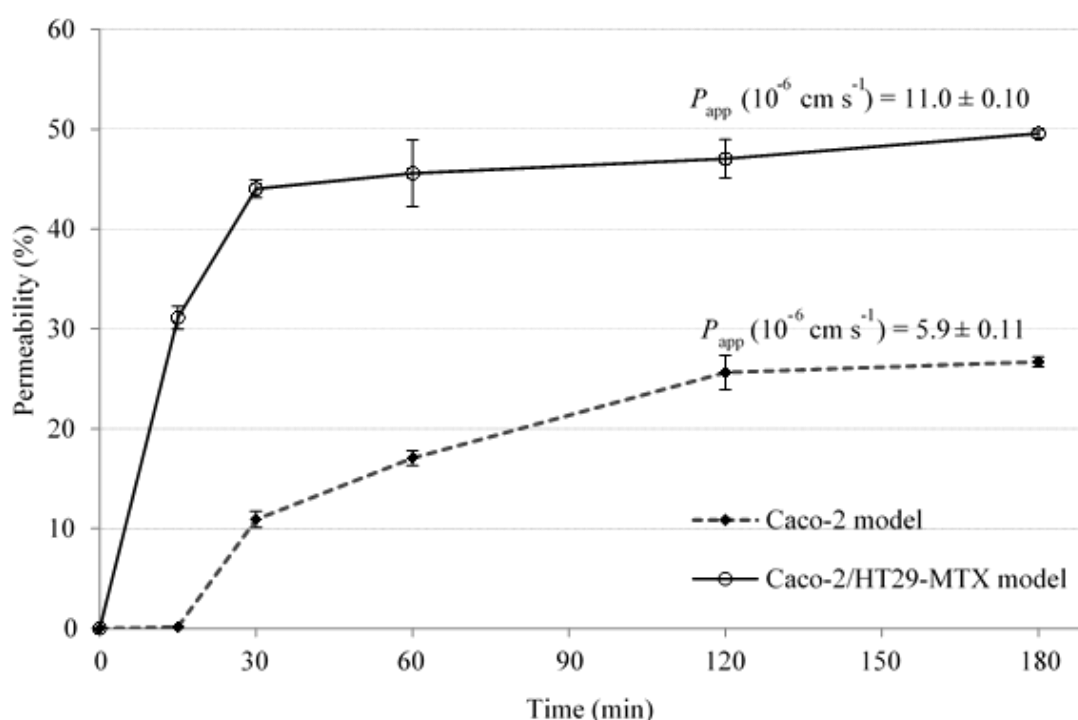


Figure 8.3. Comparative permeability (P %) as mean values  $\pm$  standard deviation bars) for sum of peptides fractions 1-11 (as present in Figure 8.2) from SPH.GI<10 kDa after 180 min (37°C) of transport across Caco-2 cell monolayer and Caco-2/HT29 co-culture cell monolayer. For both models,  $P_{app}$  values ( $10^{-6} \text{ cm s}^{-1}$ ) are reported for peptide transport from apical to basolateral chamber at 180 min ( $n=3$ ) and were significantly different at  $p < 0.05$ .

The analysis of mass spectra of SPH.GI<10 kDa permeates obtained after transport from apical-to-basolateral side of Caco-2/HT29-MTX cell monolayer also confirmed that compounds with  $m/z$  between 1000 and 5000 were transported (Figure 8.4). Although the bioavailability of large peptides with biological activity is of great interest, few studies have studied the absorption of large peptides. The  $\beta$ -CN (193–209) peptide, a hydrophobic peptide composed of 17 amino acid residues (molecular mass 1881 Da) was resistant to the action of Caco-2 brush border peptidases and the main route involved in the transepithelial transport was the transcytosis via internalized vesicles, although the paracellular transport via tight-junctions was not excluded (259). Also, the tropomyosin (Pen j 1), the major shrimp allergen with a molecular mass less than 20 kDa after GI digestion, was rapidly degraded to small peptides (molecular mass <3.5 kDa) by Caco-2 brush border peptidases and absorbed via a paracellular route (260).



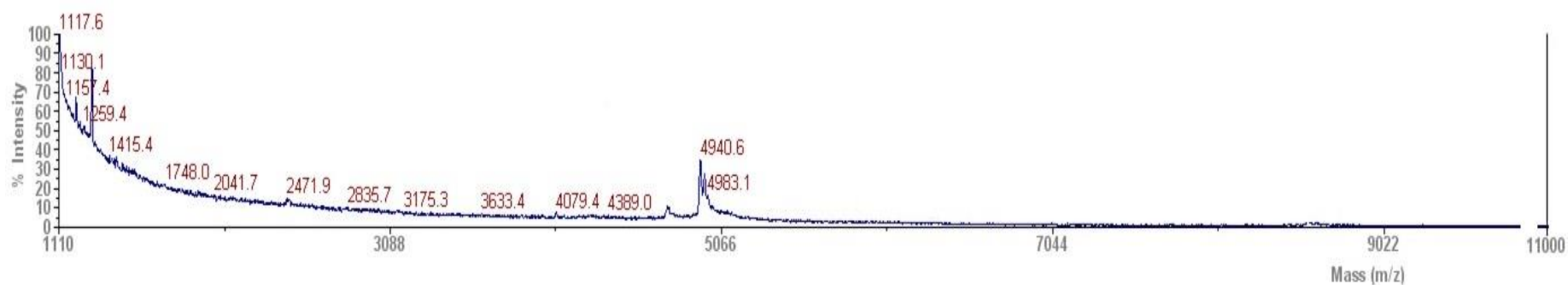


Figure 8.4. MALDI-TOF mass spectra of SPH.GI<10 kDa taken from the basolateral side after 180 min of a permeability experiment across Caco-2/HT29-MTX co-culture cell monolayer.

### 8.3.5. Effect of intestinal transport on the biological activities of SPH.GI<10 kDa

Permeates of SPH.GI<10 kDa recovered after crossing Caco-2/HT29-MTX co-culture monolayer presented a FRAP activity of 109.5  $\mu$ M TE/mL, corresponding to a 70% decrease of the previous antioxidant activity. However, no ACE-I activity was detected, even after 5 fold concentration of permeate by freeze-drying and further dissolution. Accordingly, Samaranyaka *et al.* (181) did not observe ACE-I activity for GI-digested Pacific Hake hydrolysate after 7 fold concentration. Vermeirssen *et al.* (261) also reported no ACE-I activity for GI-digested pea proteins following transepithelial procedures using Caco-2 cell monolayers. However, these authors referred that pea hydrolysate exerted a significant blood pressure lowering effect after oral administration to SHR. Presumably, the permeate concentration of ACE-I peptides was too low to be detected by the *in vitro* assay. Vermeirssen *et al.* (261) detected the ACE-I of a pea hydrolysate using 50 mg protein/mL; however this high concentration compromised the cell monolayer integrity. The initial concentration of SPH.GI<10 kDa used in the present assays was significantly lower, 2 mg protein/mL. Alternatively, the peptides that presented ACE-I activity were not those that passed through Caco-2/HT29-MTX cell monolayers or were degraded by brush border peptidases.

## 8.4. CONCLUSIONS

SPH produced by action of BSY proteases was tested after UF membrane separation to assess the effect of *in vitro* simulated GI digestion and intestinal permeability across Caco-2 culture and Caco-2/HT29-MTX cell co-culture monolayer models. UF using a 10 kDa MWCO resulted in a peptide mixture with enhanced ACE-I and antioxidant activities. The ACE-I potential of SPH<10 kDa remained unchanged upon simulated GI digestion, but no ACE-I activity was detected after cell transport, which indicates that probably the peptides responsible for ACE inhibition suffered proteolysis by cellular peptidases. Concerning antioxidant activity, the permeability assays showed that some peptide from SPH.GI<10 kDa permeated across Caco-2 cell and Caco-2/HT29-MTX cell co-culture monolayers, thereby providing further evidence of intestinal absorption and, at least, partial resistance to brush border peptidases. The apical to basolateral transport of SPH.GI<10 kDa peptides was significantly higher in the physiologically relevant Caco-2/HT29-MTX cell co-culture model. Further work is necessary to determine the sequences of peptides with antioxidant capacity and to evaluate the mechanism of their biological activities. Furthermore, studies using *in vivo* animal model systems are necessary to ascertain the evidence for both antioxidant and ACE-I potential of bioactive peptides derived from *Sardine pilchardus* by-product hydrolysate, before application as nutraceutical or functional food product ingredient.

## CHAPTER 9

*Anti-inflammatory activity of a hydrolysate from canned sardine and brewing by-products through inhibition of TNF- $\alpha$ -induced endothelial dysfunction in a co-culture model of Caco-2 and endothelial cells*

---

This chapter explores the potential anti-inflammatory properties of the SPH prepared by action of the BSY proteases.



## ABSTRACT

Sardine protein hydrolysate (SPH), prepared by hydrolysis with proteases from brewing yeast surplus, have been regarded as a bioactive hydrolysate with high antioxidant and ACE-I activities. In this study, SPH was digested, fractionated with a 10 kDa-UF membrane and desalted. The bioactivity of SPH<10 kDa was investigated on human endothelial cell line during the inflammatory process (induced by TNF- $\alpha$ ) in a co-culture model, which combines intestinal absorption with changes in endothelial metabolism. Effects of SPH<10 kDa on NO production, ROS inhibition and secretion of monocyte chemoattractant protein 1 (MCP-1), vascular endothelial growth factor (VEGF), chemokine IL-8 (IL-8) and intercellular adhesion molecule-1 (ICAM-1) were evaluated in TNF- $\alpha$  treated and untreated cells.

Upon inflammation, levels of NO, MCP-1, VEGF, IL-8, ICAM-1 and endothelial ROS were significantly increased in the co-culture and standard models. However, treatment with SPH<10 kDa at a concentration of 2.0 mg protein/mL significantly decreased all the inflammation markers when compared to TNF- $\alpha$ -treated control. This effect was more pronounced in the co-culture model, suggesting that SPH<10 kDa Caco-2 cells metabolites produced in the course of intestinal absorption may provide a more relevant protective effect against endothelial dysfunction. Additionally, indirect cross-talk between two cell types was established, suggesting that SPH<10 kDa may also bind to receptors on the Caco-2 cells, thereby triggering a pathway to secrete the pro-inflammatory compounds. Overall, co-culture model was indicated as a more physiological and realistic approach compared with *in vivo* conditions to assess the anti-inflammatory activity of SPH<10 kDa.

## 9.1. INTRODUCTION

Inflammation is a normal immune response to infection and injury, which leads to the up-regulation of a series of enzymes and signaling proteins in the affected tissues (99), (262). However, a continuous condition of (low-grade) inflammation and oxidative stress can contribute to the pathogenesis of several chronic diseases, such as, atherosclerosis, hypertension, cancer, asthma and aging-related diseases (99), (263). The endothelial barrier acts in the efficient regulation of the vascular tone, cell adhesion and vessel wall inflammation (264), (265). Endothelial dysfunction is characterized by the expression of pro-inflammatory compounds that attract white blood cells, which are converted to foam cells in the atherosclerotic plaque. At the molecular level, Nitric oxide (NO) is released through endothelial nitric oxide synthase (eNOS) and pro-inflammatory cytokines, including TNF- $\alpha$ ,

interferon- $\gamma$  (IFN- $\gamma$ ), interleukin-1 (IL-1), interleukin-8 (IL-8), monocyte chemoattractant protein-1 (MCP-1), vascular endothelial growth factor (VEGF), among others cytokines, enhance the expression levels of intercellular and vascular adhesion molecule 1 (ICAM-1 and VCAM-1) on the membrane of endothelial cells (265-268). Hence, the development of anti-inflammatory compounds, has been proposed as the key therapeutic target for preventing and treatment of chronic inflammation diseases (263), (269), (270).

Given the concerns about the side effects from prolonged usage of synthetic compounds for the prevention and treatment of chronic diseases, there is a growing interest in using natural compounds (271). Bioactive peptides of food origin may have an impact on cardiovascular health through their anti-hypertensive, anti-oxidant, anti-thrombotic anticholesterolemic effects (93). Likewise, several anti-inflammatory peptides with high molecular weight have been isolated from different protein sources. For instance, lunasin peptide (5 kDa molecular weight) (272) and lunasin-like peptide (with 8 and 14 kDa molecular weight) (273) were isolated from defatted soybean flour. Also, the SALF55-76 cyclic peptide composed of 24 amino acid residues from black tiger shrimp, exhibited the anti-inflammatory effect in LPS-stimulated RAW264.7 macrophage (274) and the >5 kDa peptide fraction from *Mytilus edulis* protein hydrolysate inhibited the NO production by 92% (275). Also, potent anti-inflammatory shellfish and fish peptides (276-278), as well as, peptide-rich protein hydrolysates (269), (270), (275), (279-281) have been produced by proteolysis of lower-quality food and underutilized materials. However, besides the efforts to elucidate mechanisms of protective effects of these compounds, most *in vitro* studies focus on their bioactivity towards endothelium (269), (270), (272-281), without taking into account the intestinal barrier that selectively absorbs and converts the food compounds (282). Recently, co-culture models of intestinal and endothelial cell cultures were established and used for testing the beneficial effects of resveratrol and grape extracts on endothelial dysfunction (268), (282). It was shown that these models were able to also establish cell-cell communication, which led towards a more relevant response to bioactive compounds at the endothelial level. Until present, only polyphenols were tested with this model (268), (282).

In a previous work, a SPH prepared by hydrolysis of sarcoplasmic proteins by BSY proteases, showed antioxidant and ACE-I activities, with promising application as a functional food material (251). However, to the best of our knowledge no information is reported about the anti-inflammatory properties of this SPH and its metabolites. In this work, we will apply this SPH on the enterocyte-like Caco-2 and the endothelial-like EA.hy926 cell culture, as well as, the Caco-2/EA.hy926 co-culture model to evaluate its beneficial effects at the endothelial level under normal and inflammatory conditions, by measurement of cell

viability, oxidative stress and the secretion of key endothelial markers (NO, MCP-1, VEGF, IL-8 and ICAM-1).

## 9.2. MATERIAL AND METHODS

### 9.2.1. Reagents and standards and cells

Tumor necrosis factor- $\alpha$  (TNF- $\alpha$ ); dimethyl sulfoxide (DMSO); 3-(4,5-dimethylthiazol-2-yl)-2,5-diphenyltetrazoliumbromide (MTT); fluorescent reagent Lucifer yellow; fluorescent probe 2',7'-dichlorofluorescein diacetate (DCFH-DA); Triton X-100; Bradford Reagent; Griess reagent, chicken egg albumin; Greiner 96-Well Multiwell Elisa plates and the Millipore 10 kDa-UF membranes were purchased from Sigma-Aldrich (St. Louis, MO, USA). The 12-well Transwell plates (0.4  $\mu$ m pore diameter, 12 mm diameter, 1.12 cm<sup>2</sup> insert membrane growth area) were from Corning (Elscolab, Kruibeke, Belgium). Phosphate Buffered Saline (PBS); Dulbecco's modified Eagle's growth medium (DMEM); glutamax<sup>TM</sup>; sodium pyruvate; fetal bovine serum; penicillin and streptomycin were from Gibco (Life Technologies, Merelbeke, Belgium). ELISA Kits (ICAM-1, MCP-1, IL-8, VEGF) were purchased from Peprotech (London, United Kingdom). All other chemicals and reagents used in this study were of analytical grade.

### 9.2.2. By-products

Sardine (*Sardina pilchardus*) by-product including head, scale, skin, blood, bone, viscera and muscle tissue was provided by the Portuguese company Conservas Ramirez (Matosinhos, Portugal). Brewing spent yeast (BSY), *Saccharomyces pastorianus*, was supplied by the brewing industry Unicer (Leça do Balio, Portugal).

### 9.2.3. Preparation of SPH

The preparation of sarcoplasmic protein extract from sardine by-product and the BSY proteases extract were prepared as described by Vieira and Ferreira (251). Protein concentration of sarcoplasmic protein extract, determined by the Bradford method (171) was 2.4 mg/mL and the protease activity of the BSY proteases extract (>10 kDa fraction), evaluated according to Cupp-Enyard protocol (164), was 0.725 U/mL. Sarcoplasmic protein extract was hydrolyzed by BSY proteases using an E/S ratio of 0.27:1 (U/mg), pH 6.0, 50°C for 7 h, as previously described by Vieira and Ferreira (251). Then, the SPH was submitted to simulated GI digestion according to Samaranayaka *et al.* (181) and fractionated using a 10 kDa-UF membrane. The resulting fractions, SPH<10 kDa and SPH>10 kDa, were

lyophilized (Telstar freeze dryer, Cryodos-80 model, Terrassa, Spain) and stored at -20 °C prior to further analysis.

#### **9.2.4. Desalting of SPH**

SPH<10 kDa and SPH>10 kDa fractions were prepared in pure water at the concentration of 10 mg/mL and desalted by solid phase extraction using an Oasis® HLB cartridge (35 cc, Waters, Waters, Milford, MA). Cartridge was first activated with methanol (0.1% formic acid) and equilibrated with 50% acetonitrile in water according to the manufacturer's protocol. Then, sample was applied, washed 4 times with water and the peptides were eluted with acetonitrile. The acetonitrile was subsequently evaporated in a rotary evaporator under vacuum and the final residues were used for the following experiments.

#### **9.2.5. Protein content**

The protein content was measured by the microprotein Bradford assay (171), using chicken egg albumin to construct the standard curve. Samples or standard (25 µL) were mixed with Bradford reagent (250 µL) and the absorbance at 595 nm was measured after 5-10 min against a reagent blank. The protein concentration in each sample was calculated based on a standard curve. The analyses were performed in triplicate.

#### **9.2.6. Cell culture routine**

The continuous human colon adenocarcinoma cell line Caco-2 ATCC®HTB37™, that differentiates into enterocyte-like cells upon confluence and the permanent human endothelial cell line EA.hy926 CRL2922™ were obtained from ATCC (American Type Culture Collection, Manassas, VA, USA). The Caco-2 cells (passage 8-20) and endothelial cells (passage 5-10) were grown separately as adherent cultures in 25 cm<sup>2</sup> tissue culture flasks (Sarstedt, Essen, Belgium) and cultivated in DMEM, high glucose, supplemented with glutamax™, sodium pyruvate, 10% (v/v) fetal bovine serum, penicillin (100 U/mL), and streptomycin (100 mg/mL). Cells were subcultured once a week with 0.25% (v/v) trypsin-EDTA and grown until 90% confluence. The culture medium was replaced every other day. Cells were incubated at 37°C and 10% CO<sub>2</sub> in a water saturated atmosphere (Mettler, VWR, Leuven, Belgium).

#### **9.2.7. Cell viability experiments**

In a first set of experiments, the effect of ultrafiltered and desalted SPH samples on Caco-2 and EA.hy926 cell monolayers viability was evaluated through the MTT assay. Caco-2 and EA.hy926 cells were separately cultivated in growth medium until 90% confluency, and subsequently seeded in 96-well plates at a concentration of 2x10<sup>4</sup> cells per well. Upon 100%



confluency, Caco-2 and EA.hy926 cells monolayers were treated with phenol red-free exposure medium (DMEM, high glucose 4.5 g/L, 1% non-essential amino acids solution) spiked with the samples (SPH<10 kDa and SPH>10 kDa, desalted or not desalted) at the concentration of 1.0 mg protein/mL, as determined by the Bradford method. The MTT assay was performed after 3-days treatment for differentiated Caco-2 cell monolayer and 2-days treatment for endothelial cell monolayer. In order to select the range of concentrations which will not affect viability of Caco-2 cell monolayers in the co-culture model establishment, the Caco-2 cell monolayer viability was also evaluated after treatment with the sample chosen at five different concentrations (0.1, 0.5, 1.0, 2.0 and 5.0 mg protein/mL).

### 9.2.8. *In vitro* cell culture models

In the monoculture model, EA.hy926 cells were seeded on a 12-well plate at concentration of  $2.5 \times 10^5$  cells per well. Upon 90-95% confluency, EA.hy926 cells were treated with desalted SPH<10 kDa sample in phenol red-free exposure medium at concentrations of 0.5 mg protein/mL and 2.0 mg protein/mL. The endothelial cells were incubated at 37°C, 10% CO<sub>2</sub> and culture medium were collected after 4 h of treatment and immediately stored at -80°C until further analyses.

For the co-culture model with Caco-2/EA.hy926 cells, as described by Toaldo *et al.* (283), Caco-2 cells were seeded on a 12-well Transwell plates at concentration of  $2.5 \times 10^5$  cells per well. Upon confluency and after 15-days differentiation, EA.hy926 cells were seeded on the basolateral compartment of the Transwell plate, at cell density of  $3 \times 10^5$  cells per well. The EA.hy926 cells were allowed to grow in the co-culture model until they reached confluency on the third day. On the fourth day of co-culture, Caco-2 cells were treated apically with SPH<10 kDa in phenol red-free exposure medium at the concentrations of 0.5 mg protein/mL and 2.0 mg protein/mL, and phenol red-free exposure medium was applied in the basolateral compartment. The cells were incubated at 37°C, 10% CO<sub>2</sub>, and culture medium were collected after 4 h of treatment and immediately stored at -80°C for further analyses.

The apparent permeability coefficient ( $P_{app}$ ) of Caco-2 cell monolayers was monitored before and after the experiments using the fluorescent reagent Lucifer yellow as an indicative marker of passive paracellular diffusion. In addition, the integrity of polarized epithelial cell monolayers was monitored before and after the experiments through TEER measurements using an automated tissue resistance measurement system (REMS, World Precision Instruments, Hertfordshire, UK). Only intact Caco-2 monolayers with TEER values above 900  $\Omega \cdot \text{cm}^2$  were used for the co-culture experiments. The Caco-2 cell monolayer integrity and its suitability for the transport experiments was also confirmed through the correlation between TEER and paracellular permeability.

### **9.2.9. Exposure to TNF- $\alpha$ to induce endothelial inflammation**

In order to investigate the cellular responses to desalted SPH<10 kDa samples under stress-induced conditions in endothelial tissue, EA.hy926 cells from co-culture and standard models were treated with TNF- $\alpha$ . In both monoculture and co-culture cell models, EA.hy926 cells were incubated for 1 h with 10 ng/mL TNF- $\alpha$  in phenol red-free exposure medium to induce high-grade inflammation in endothelium.. Next, the culture medium was aspirated and the EA.hy926 cells were rinsed twice with phenol red-free exposure medium, followed by treatment with desalted SPH<10 kDa samples for 4 h (37°C, 10% CO<sub>2</sub>). After treatment in the monoculture and co-culture models, viability of EA.hy926 cell monolayers was evaluated by the MTT assay, intracellular ROS was measured immediately and the culture medium was collected, centrifuged at 15,000 x g for 10 min and kept at -80°C until analysis, which included the measurement of NO and secreted pro-inflammatory cytokines.

#### **9.2.9.1. Cell viability study**

In the 3-(4,5-dimethylthiazol-2-yl)-2,5-diphenyltetrazolium bromide (MTT) assay, the MTT is reduced by mitochondrial dehydrogenases to a water-insoluble formazan derivative, which can be measured at 570 nm. Briefly, after cell treatment with test samples in the monoculture and co-culture models, the culture medium was aspirated and the attached cells were rinsed with 200  $\mu$ L PBS, followed by the addition of the MTT solution (1 mg/mL in phenol red-free exposure medium). After 30 min of incubation (37°C, 10% CO<sub>2</sub>), the MTT-formazan product was solubilized in 100  $\mu$ L of DMSO and the absorbance was measured at 570 nm on a Bio-Rad multiplate reader (Bio-Rad Laboratories, Hercules, CA, USA). Each sample was tested in six replicates and three independent experiments were performed.

#### **9.2.9.2. Determination of intracellular reactive oxygen species (ROS)**

The formation of reactive oxygen species (ROS) was evaluated using the oxidation sensitive dye 2',7'-dichlorofluorescein-diacetate (H2-DCFDA). Briefly, after cell treatment with test samples in the co-culture and standard models, EA.hy926 cells were loaded with 20  $\mu$ M H2-DCFDA in phenol red-free exposure medium and incubated for 30 min (37°C, 10% CO<sub>2</sub>). The cells were then washed with PBS, lysed with 0.1% Triton X-100 and centrifuged at 14,000 rpm for 10 min. The fluorescence of supernatants was immediately read in black 96-well plates at an excitation wavelength of 485 nm and an emission wavelength of 535 nm, using a Spectramax Fluorescent Plate Reader.

#### **9.2.9.3. Inhibition of NO production**

A spectrophotometric assay based on the Griess reaction was used to indirectly measure the NO production in EA.hy926 cells. Briefly, test samples were mixed with equal volume

of the Griess reagent. After 15 min at room temperature (18°C), absorbance was read at 540 nm on a Bio-Rad multiplate reader (Bio-Rad Laboratories, Hercules, CA, USA). The nitrite concentration was determined by reference to a standard curve of sodium nitrite (NaNO<sub>2</sub>) in a range of 0-20  $\mu$ M.

#### 9.2.9.4. Inhibition of pro-inflammatory cytokines production

The inhibitory effects of test samples on the expression of MCP-1, VEGF, IL-8 and ICAM-1 in the cell culture medium of co-culture and standard models was performed by enzyme immunoassay, using commercially available ELISA kits according to the manufacturer's instructions. The endothelial markers were tested in both TNF- $\alpha$ -treated and untreated EA.hy926 cells in order to determine the test samples effects on endothelium responses under inflammatory and non-inflammatory conditions. The intra-assay and inter-assay coefficients of variation for these ELISA assays were <6% and <10%, respectively. All measurements were taken twice.

#### 9.2.10. Statistical analysis

Results were expressed as mean  $\pm$  standard deviation. Statistical analysis was performed with SPSS 22.0 (SPSS Inc., Chicago, IL, USA), using One-way analysis of variance (ANOVA) followed by Student's *t*-test to assess statistical differences from control values (no treated cells) and between inflammatory and non-inflammatory conditions. Differences were accepted as statistically significant at  $p < 0.05$  or  $p < 0.01$ .

### 9.3. RESULTS

#### 9.3.1. Effect of UF, desalting and optimization of working concentrations

SPH was prepared according to the previous procedure reported (251) and submitted to simulated GI digestion. According to the literature, anti-inflammatory peptides possess a wide range of molecular weights (281). For this reason, in a first set of experiments, the effect of 10 kDa-UF membrane of SPH digest on Caco-2 and EA.hy926 cells viability was assessed. Caco-2 and EAhy926 cells were treated with the fractions SPH>10 kDa and SPH<10 kDa at the same peptide concentration of 1.0 mg/mL for 24 h, (37°C, 10% CO<sub>2</sub>) and cell viability was evaluated by the MTT assay. Results present in Figure 9.1 showed that SPH>10 kDa significantly ( $p < 0.05$ ) decreased Caco-2 and EAhy.926 cells viability when compared to SPH<10 kDa fraction. Regarding the effect of desalting process, results showed that the desalted SPH<10 kDa fraction had a positive impact on both cell lines viability in relation to the desalted SPH>10 kDa fraction significantly ( $p < 0.05$ ). As the MTT protocol performed in the present study uses cells at confluency, the attained data is not

compatible with cell proliferation. These results suggest that desalting step not only removed the excess of salt associated with hydrolysis, but also increased the relative abundance of <10 kDa compounds within the SPH, thereby improving good cell viability (284).

In a second set of experiments, the MTT assay was performed to evaluate the cytotoxicity of the desalted SPH<10 kDa fraction at five peptide concentrations. As shown in Figure 9.2, the highest Caco-2 cells and EAhy926 cell viability was observed in cells treated with desalted SPH<10 kDa at the range of 0.1 to 2.0 mg protein/mL, with a slightly decreased cell viability at the concentration of 5.0 mg protein/mL. Considering these results, two different working concentrations, 0.5 mg protein/mL and 2.0 mg protein/mL, of desalted SPH<10 kDa fraction were selected to further investigate its anti-inflammatory action in TNF- $\alpha$  stimulated endothelial cells in the monoculture and co-culture systems.

### 9.3.2. Establishment of the co-culture model

Caco-2 cells have been extensively used to study the effects of bioactive ingredients in both normal and inflammatory conditions (267), (268). In this work, the validated co-culture model by Toaldo *et al.* (283), combining absorption by differentiated Caco-2 cells and sequential effects on endothelial cells metabolism, was applied to evaluate the response of SPH<10 kDa in both TNF- $\alpha$ -activated and non-activated EA.hy926 cells. The permeability and integrity parameters of Caco-2 cell monolayer were examined before transport experiments.  $P_{app}$  values of apical-to-basolateral direction were in the range of  $5.01 \pm 0.41 \times 10^{-5}$  cm/s and the TEER values were in the range of  $1008.87 \pm 52.41 \Omega \cdot \text{cm}^2$ , indicating an intact epithelial monolayer, suitable to be used for the transport experiments.

### 9.3.3. Effects on viability of endothelial cells

The SPH<10 kDa cytotoxicity in EA.hy926 cells, under inflammatory and non-inflammatory conditions, was assessed through the MTT assay in the monoculture and co-culture models. Results present in Figure 9.3 showed that TNF- $\alpha$  treatment significantly decreased mitochondrial activity in both models. Upon TNF- $\alpha$  induced inflammation in the co-culture model, and when compared to TNF- $\alpha$ -treated control, a significant ( $p < 0.05$ ) decrease of EA.hy926 cell mitochondrial activity was observed upon 4 h treatment with the transported 0.5 mg protein/mL SPH<10 kDa fraction, while treatment with SPH<10 kDa at the highest concentration (2.0 mg protein/mL) resulted in a slight but significant ( $p < 0.05$ ) increase in mitochondrial activity. On the other hand, treatment with 2.0 mg protein/mL SPH<10 kDa significantly ( $p < 0.01$ ) increased the EA.hy926 mitochondrial activity in both models treated with TNF- $\alpha$ . These results show that under normal conditions, the extract

has a limited effect on mitochondrial respiration, whereas under inflammatory conditions, the SPH<10 kDa is able to restore the negative impact of the TNF- $\alpha$  treatment.

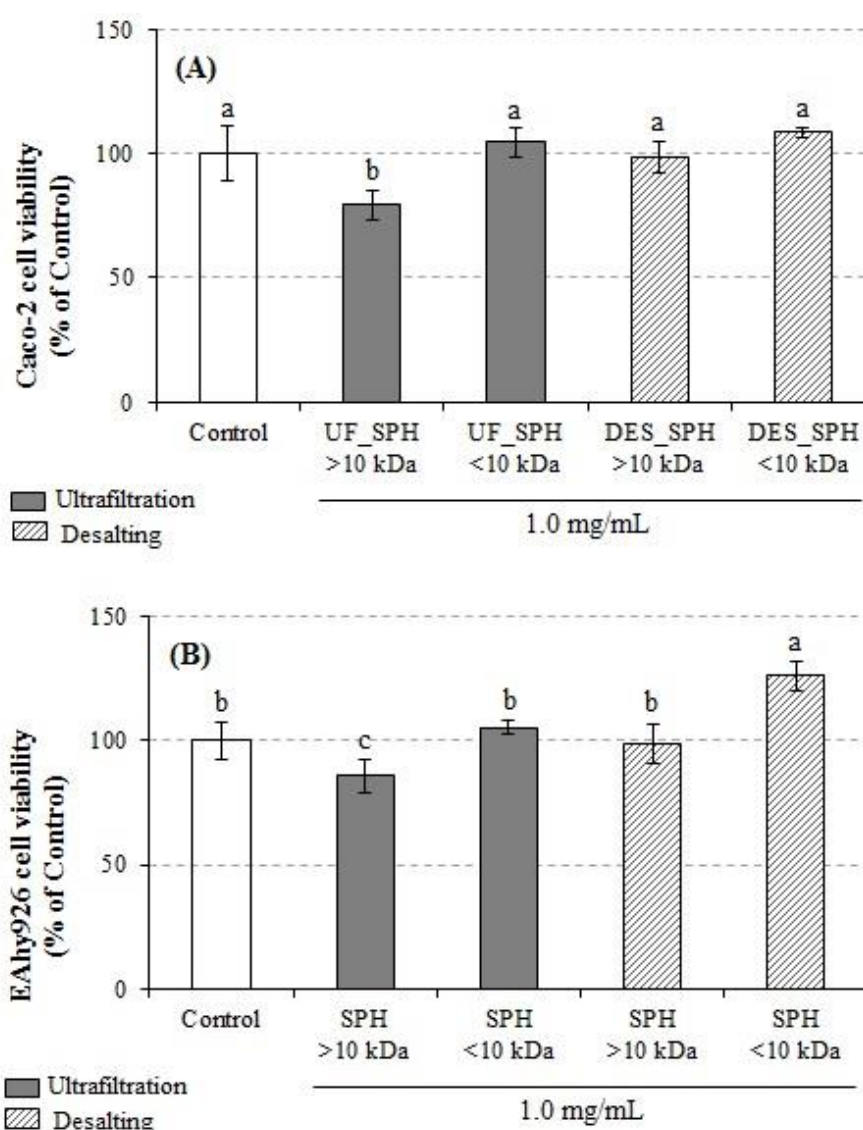


Figure 9.1. Effect of Ultrafiltration and Desalting processes of SPH, at the same protein concentration of 1.0 mg/mL (based on Bradford assay), on differentiated Caco-2 **(A)** and EAhy926 **(B)** cells viability (%) (MTT assay), after 24 h of incubation (37°C, 10% CO<sub>2</sub>). Data represent the mean  $\pm$  standard deviation, calculated relative to Control (cells treated with medium only) and are representative of three independent experiments, in six replicates. Bars labeled with different subscript letters have mean values that are significantly different at  $p < 0.05$  (ANOVA followed by Duncan's test).

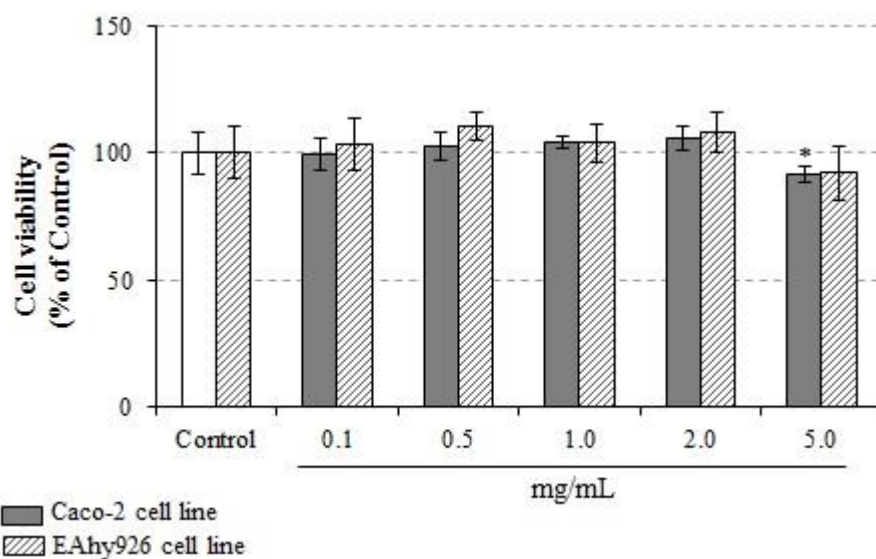


Figure 9.2. Effect of desalted SPH<10 kDa at different protein concentrations (0.1, 0.5, 1.0, 2.0 and 5.0 mg protein/mL) on differentiated Caco-2 and EAhy926 cells viability (%) (MTT assay), after 24 h of incubation (37°C, 10% CO<sub>2</sub>). Data represent the mean ± standard deviation, calculated relative to Control (cells treated with medium only) and are representative of three independent experiments, in six replicates.

\* denotes a significant difference when compared with Control ( $p < 0.05$ ).

#### 9.3.4. Effects on NO production in endothelial cells

The effect of SPH<10 kDa (and its metabolic fraction) on cellular NO production in EA.hy926 cells, under inflammatory and non-inflammatory conditions, is presented in Figure 9.4. In the co-culture model, the production of NO by endothelial cells may be the result of two mechanisms: (i) the impact of transported SPH<10 kDa fraction after 4 h metabolism by Caco-2 cells and (ii) the indirect impact of other cytokines secreted by Caco-2 cells, resulted from the crosstalk between both cell lines. By contrast, in the standard model, the NO production is the result of the direct effect of SPH<10 kDa on endothelial cell metabolism. A first observation is that NO is increased 3- to 4-fold after treatment with TNF- $\alpha$ ; this result was similar to observed by Toaldo *et al.* (283). Secondly, a concentration of 2 mg protein/mL of the extract was able to significantly decrease NO in both normal and inflammatory conditions. The effect of the SPH<10 kDa was highest in the TNF- $\alpha$  treated cultures, where NO production was reduced ( $p < 0.01$ ) in a dose-dependent manner. As verified with co-culture model, untreated EAhy926 cells did not produce detectable amounts of NO after 4 h of treatment, whereas the treatment with 2.0 mg protein/mL SPH<10 kDa

significantly ( $p < 0.05$ ) reduced the NO production. Under TNF- $\alpha$ -induced inflammation of endothelial cells, treatment with 2.0 mg protein/mL SPH<10 kDa significantly ( $p < 0.01$ ) reduced the NO production by 22%, when compared to TNF- $\alpha$ -treated control. This result suggest that SPH<10 kDa Caco-2 cell metabolites may prevent inflammatory process via regulation of the NO level.

### 9.3.5. Effects on ROS levels in endothelial cells

For intracellular ROS levels of the endothelial cells, similar observations as for NO were observed (Figure 9.5). Upon TNF- $\alpha$ -induced endothelial inflammation for both cell models, the levels of ROS were 2-fold increased ( $p < 0.01$ ) compared to untreated cells, and this effect was higher for the co-culture model. In the co-culture model, compared to TNF- $\alpha$ -treated control, a significant ( $p < 0.01$ ) decrease in ROS levels (46%) was observed in response to 4 h treatment with 2.0 mg protein/mL SPH<10 kDa. For the monoculture model, in response to TNF- $\alpha$ -induced endothelial inflammation, the protective effect was also significantly ( $p < 0.01$ ) higher for SPH<10 kDa at the concentration of 2.0 mg protein/mL (16%, when compared to compared to TNF- $\alpha$ -treated control). These results indicate a dose-dependent protective effect of the SPH<10 kDa towards TNF- $\alpha$  induced oxidative stress.

### 9.3.6. Effects on inflammation markers expression

The influence of SPH<10 kDa (and metabolites) on the secretion of the markers MCP-1, VEGF, IL-8 and ICAM-1 was evaluated in the monoculture and co-culture models. The results are presented in Figure 9.6. In TNF- $\alpha$ -treated cells, the secretion of pro-inflammatory markers was significantly ( $p < 0.01$ ) higher in comparison with basal values of the non-inflammatory conditions. Under non-inflammatory conditions, the SPH<10 kDa at the concentration of 2.0 mg protein/mL resulted in a significant ( $p < 0.05$ ) decrease on the secretion of the endothelial marker VEGF in the co-culture model and a significant decrease on the secretion of VEGF ( $p < 0.01$ ) and IL-8 ( $p < 0.05$ ) in the monoculture model. As observed in Figure 9.6, for the monoculture model, treatment of EA.hy926 cells with 2.0 mg protein/mL SPH<10 kDa significantly ( $p < 0.01$ ) decreased TNF- $\alpha$ -induced MCP-1, VEGF, IL-8 and ICAM-1 expression by 24%, 16%, 21% and 26%, respectively, when compared to TNF- $\alpha$ -treated control. For the co-culture model, this reduction ( $p < 0.01$ ) was, respectively, 46%, 35%, 47% and 44%, when compared to TNF- $\alpha$ -treated control.

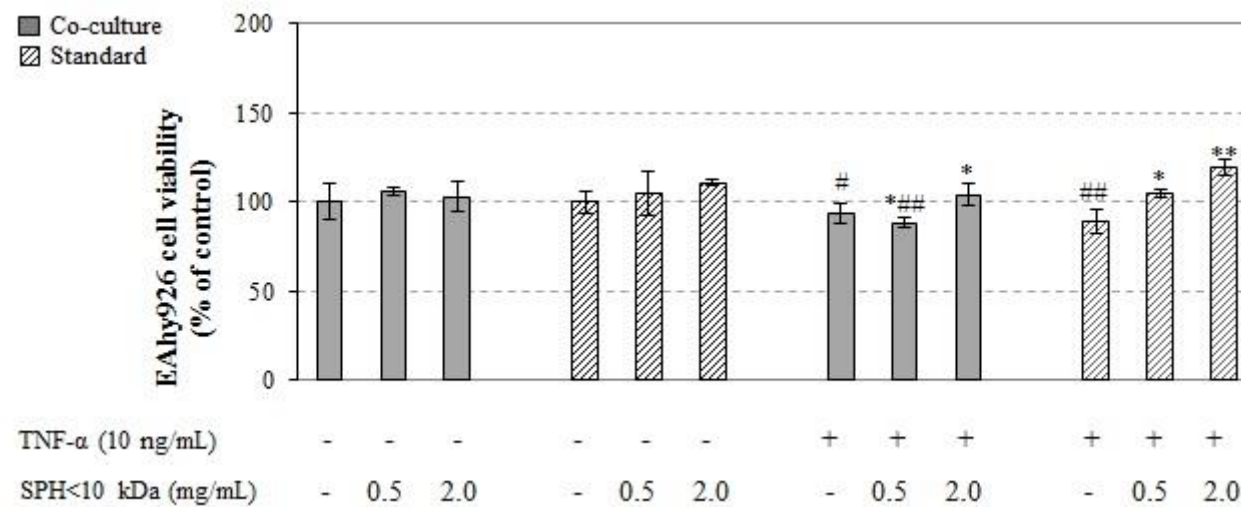


Figure 9.3. Effect of SPH<10 kDa (and metabolites) at the protein concentrations of 0.5 and 2.0 mg protein/mL on EAhy926 cells viability (%), after 4 h of incubation (37°C, 10% CO<sub>2</sub>) in the co-culture and standard models, under TNF-α-induced inflammatory (1 h of TNF-α 10 ng/mL stimulation) and non-inflammatory conditions. Data represent the mean ± standard deviation of three measurements in triplicates, in two independent experiments. Results are expressed as percentage of respective control (cells treated with medium only or with medium with TNF 10 ng/mL). Controls of non-inflammatory condition are normalized at 100% and values in the inflammatory condition are represented in comparison to the respective non-inflammatory condition. Significance was determined at \**p* < 0.05, \*\**p* < 0.01 *versus* respective control and #*p* < 0.05, ##*p* < 0.01 *versus* respective non-inflammatory condition.



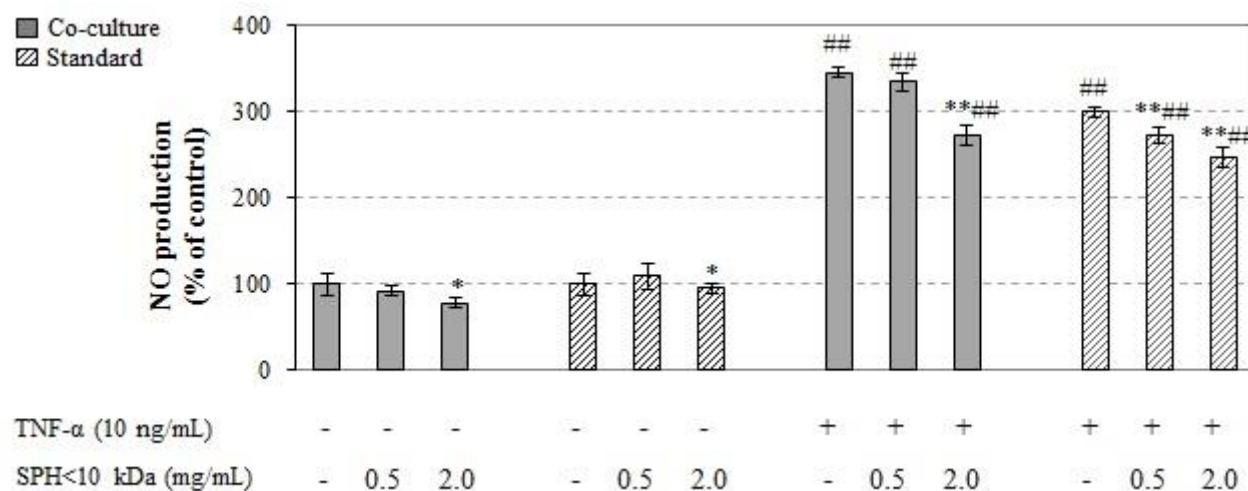


Figure 9.4. Effect of SPH<10 kDa (and metabolites) at the protein concentrations of 0.5 and 2.0 mg/mL on NO production of EAhy926 cells after 4 h of incubation (37°C, 10% CO<sub>2</sub>) in the co-culture and standard models, under TNF- $\alpha$ -induced inflammatory (1 h of TNF- $\alpha$  10 ng/mL stimulation) and non-inflammatory conditions. Data represent the mean  $\pm$  standard deviation of three measurements in triplicates, in two independent experiments. Results are expressed as percentage of respective control (cells treated with medium only or with medium with TNF 10 ng/mL). Controls of non-inflammatory condition are normalized at 100% and values in the inflammatory condition are represented in comparison to the respective non-inflammatory condition. Significance was determined at \* $p$  < 0.05, \*\* $p$  < 0.01 *versus* respective control and # $p$  < 0.05, ## $p$  < 0.01 *versus* respective non-inflammatory condition.

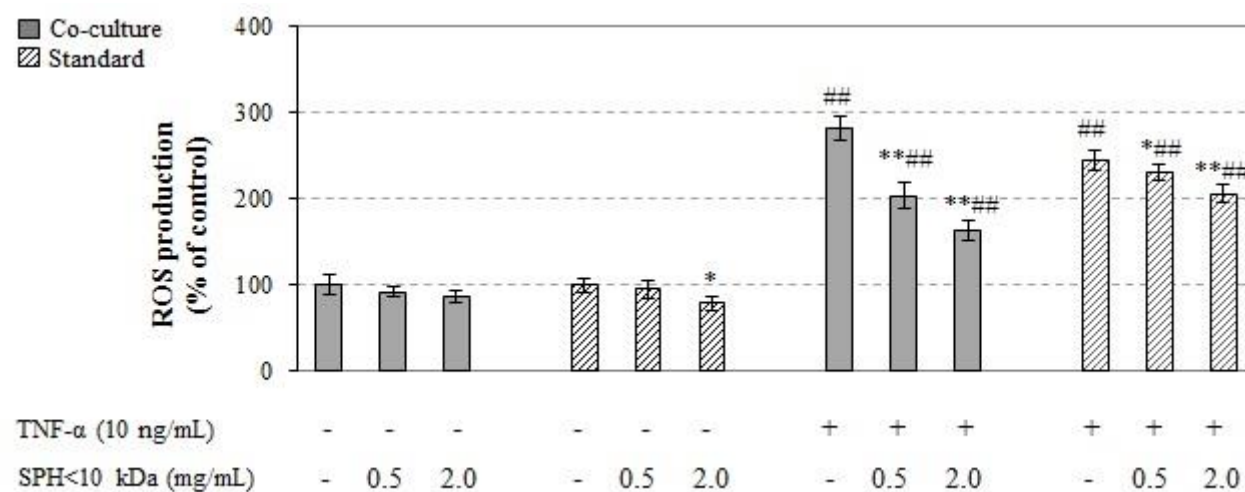


Figure 9.5. Effect of SPH<10 kDa (and metabolites) at the protein concentrations of 0.5 and 2.0 mg/mL on intracellular ROS levels of EAhy926 cells, after 4 h of incubation (37°C, 10% CO<sub>2</sub>) in the co-culture and standard models, under TNF-α-induced inflammatory (1 h of TNF-α 10 ng/mL stimulation) and non-inflammatory conditions. Data represent the mean ± standard deviation of three measurements in triplicates, in two independent experiments. Results are expressed as percentage of respective control (cells treated with medium only or with medium with TNF 10 ng/mL). Controls of non-inflammatory condition are normalized at 100% and values in the inflammatory condition are represented in comparison to the respective non-inflammatory condition. Significance was determined at \* $p < 0.05$ , \*\* $p < 0.01$  versus respective control and # $p < 0.05$ , ## $p < 0.01$  versus respective non-inflammatory condition.

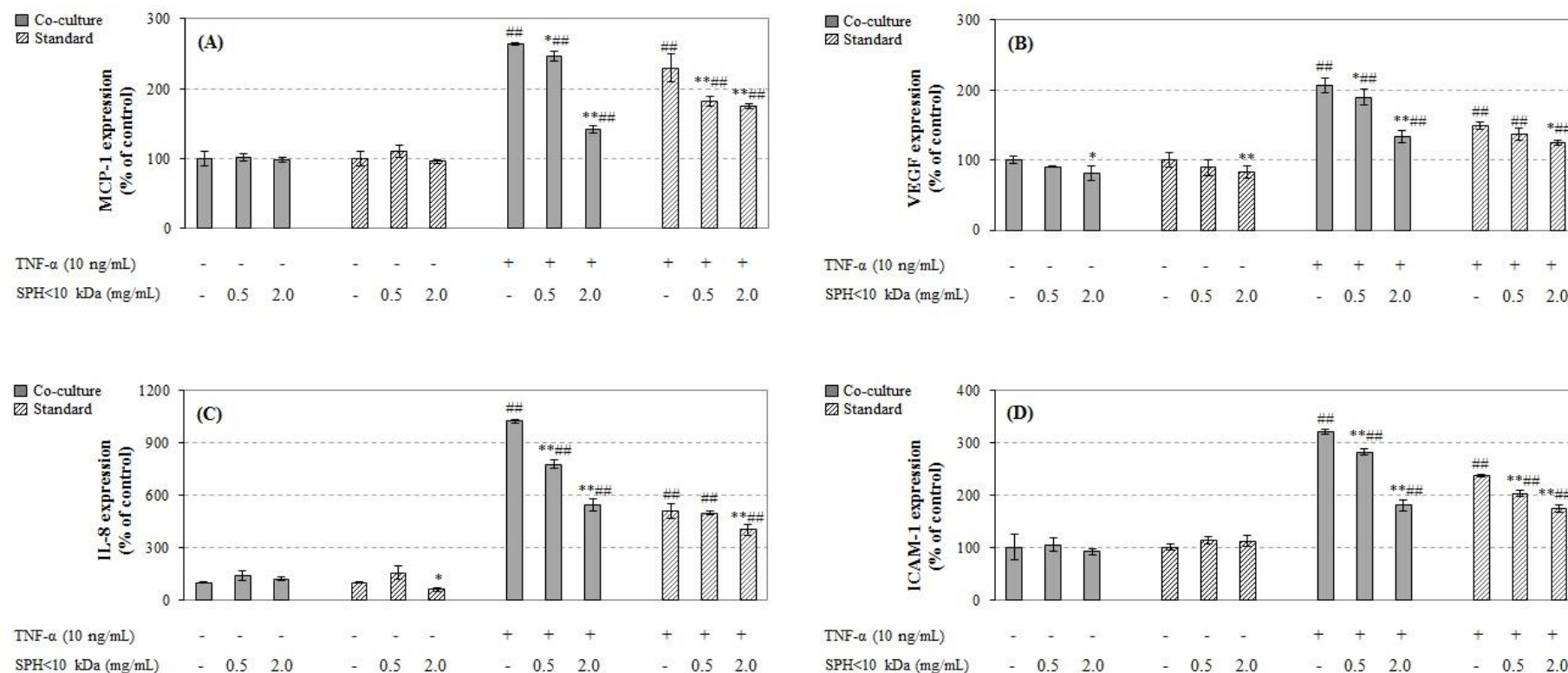


Figure 9.6. Effect of SPH<10 kDa (and metabolites) at protein concentrations of 0.5 and 2.0 mg/mL on the secretion of MCP-1 **(A)**; VEGF **(B)**; IL-8 **(C)** and ICAM-1 **(D)** in EAhy926 cells, after 4 h of incubation (37°C, 10% CO<sub>2</sub>) in the co-culture and standard models, under TNF- $\alpha$ -induced inflammatory (1 h of TNF- $\alpha$  10 ng/mL stimulation) and non-inflammatory conditions. Data represent the mean  $\pm$  standard deviation of three measurements in triplicates, in two independent experiments. Results are expressed as percentage of respective control (cells treated with medium only or with medium with TNF 10 ng/mL). Controls of non-inflammatory condition are normalized at 100% and values in the inflammatory condition are represented in comparison to the respective non-inflammatory condition. Significance was determined at \* $p$  < 0.05, \*\* $p$  < 0.01 versus respective control and # $p$  < 0.05, ### $p$  < 0.01 versus respective non-inflammatory condition.

## 9.4. DISCUSSION

In this research, we demonstrated the antioxidant and anti-inflammatory effects of SPH<10 kDa bioactive compounds on a monoculture and co-culture of an endothelial cell line with an intestinal cell line. SPH<10 kDa bioactive compounds were prepared by hydrolysis of sarcoplasmic proteins from sardine by-product with BSY proteases (251), followed by simulated GI digestion. The UF and desalting steps of SPH digest were necessary to remove background effects of the salts to the cells and to increase the peptide content. In this work, the desalted SPH<10 kDa fraction was used to investigate its potential anti-inflammatory activity through TNF- $\alpha$  stimulated cells. To date, the antioxidant and ACE-I activities of SPH has been extensively studied (218), however, to our best knowledge, the modulatory effects of these kind of hydrolysates against inflammatory reactions have not yet been reported.

Endothelial dysfunction is an inflammatory process characterized by increased oxidative stress and it is an important manifestation of cardiovascular diseases (285). In this study, a validated *in vitro* co-culture model with epithelial and endothelial cells, representing the intestinal epithelial layer and the adjacent endothelium (283), was used to investigate the anti-inflammatory effects of SPH<10 kDa and compared with its impact on a monoculture of endothelial cells. During the inflammatory process, NO was secreted by eNOS over EA.hy926 cells in the co-culture and standard models. Excessive production of NO by eNOS, which is up-regulated by inflammatory stimuli such as TNF- $\alpha$ , is considered toxic and related to various inflammatory diseases (281), (286). Thus, inhibition of NO secretion can attenuate inflammation and reduce cancer risk (286). The results obtained in this work indicated enhanced bioactivity of SPH<10 kDa Caco-2 metabolites rather than the compounds present in SPH<10 kDa. As suggested by other authors (282), in the course of intestinal absorption, SPH<10 kDa may undergo metabolization by Caco-2 cells, resulting in SPH<10 kDa metabolites at biological relevant concentrations and/ or with potential higher anti-inflammatory activity. Moreover, changes in ROS and NO levels in the co-culture model are the result of two important mechanisms: (i) direct impact by SPH<10 kDa compounds that are transported (and metabolized) through Caco-2 cells and (ii) indirect impact by cross-talk communication between intestinal and endothelial cell monolayers (287).

The inflammatory processes is also regulated by the secretion of pro-inflammatory mediators (263). NO may reduce endothelial expression of several inflammatory mediators and adhesion molecules, whose up-regulation is linked to the pathogenesis of many infectious and inflammatory diseases and cancer (285). In this work, ELISA was performed to measure the concentrations of the pro-inflammatory cytokines MCP-1, VEGF, IL-8 and

ICAM-1. The inhibitory effects of SPH<10 kDa (and metabolites) on the expression of the selected cytokines was evaluated in the co-culture and standard models, to further validate the anti-inflammatory effects previously observed. Similar to observed by Toaldo *et al.* (283), secretion of these pro-inflammatory molecules in the EAhy926 cells were largely increased by induction of inflammation with TNF- $\alpha$ . For both cell culture models, treatment with SPH<10 kDa inhibited the pro-inflammatory cytokines expression in a dose-dependent manner. Treatment with 2.0 mg protein/mL SPH<10 kDa prompted a significant ( $p < 0.01$ ) decrease in the expression of these inflammation markers. However, despite the significant effect of 2.0 mg protein/mL SPH<10 kDa (and its metabolites) on the reducing secretion of pro-inflammatory molecules in the co-culture and standard models, decreases on MCP-1, VEGF, IL-8 and ICAM-1 concentrations in relation to TNF- $\alpha$ -treated control were markedly higher in TNF- $\alpha$  treated cells controls. These findings suggest that SPH<10 kDa (and its metabolites) operate through an inhibitory regulation of the inflammatory cascade in endothelial cells. Direct incubation of endothelial cells with SPH<10 kDa (standard model) reduced the expression of these pro-inflammatory molecules, but in a lesser extent. Thus, it can be speculated that unknown intermediate metabolites with higher anti-inflammatory potential were generated when SPH<10 kDa cross the Caco-2 cell monolayer.

## 9.5. CONCLUSIONS

Our findings demonstrated that besides the antioxidant and ACE-I activity previously reported, the peptide fraction <10 kDa from sardine protein hydrolysate prepared by action of brewer's spent yeast proteases exhibited anti-inflammatory activity in TNF- $\alpha$  simulated EAhy926 cells. This bioactivity was expressed through the inhibition of NO, ROS and pro-inflammatory cytokines production (MCP-1, VEGF, IL-8 and ICAM-1). Results suggested that the protective health effects of SPH<10 kDa may not only be due to bioactive compounds composition, but also to their metabolites produced by the action of Caco-2 cell peptidases in the course of intestinal absorption. Therefore, the co-culture model, which combines the absorption by differentiated Caco-2 cells and sequential effects on endothelial cells metabolism, may represent a more physiological and realistic approach compared with *in vivo* conditions, allowing more accurate knowledge about the anti-inflammatory activity of the SPH<10 kDa studied. To the best of our knowledge, this is the first report of the anti-inflammatory activity exhibited by a SPH prepared by action of proteases extracted from brewer's spent yeast. This bioactive hydrolysate fraction could be used as an alternative therapy for the prevention of inflammatory-related diseases. However, further exploration

of the SPH<10 kDa is required to fully explore its molecular composition, its mechanisms of action and overall anti-inflammatory effects *in vivo*.

## CHAPTER 10

### *Characterization of hydrolysates obtained from muscle and viscera proteins of canned sardine by-products*

---

This chapter compares the biological activities and technological properties of different SPH prepared by BSY proteases and by two commercial enzymes: Alcalase® and Neutrase®.





## ABSTRACT

Muscle and viscera proteins from canned sardine by-products were used as substrate to obtain functional hydrolysates. Three enzymatic approaches, brewer's spent yeast (BSY) proteases, Alcalase® and Neutrase®, were applied to perform the hydrolysis at the same proteolytic activity (1 U/mL), using an E/S ratio of 0.20:1 U/mg, at 50°C and for 7 h. Hydrolysis degree (DH), antioxidant and ACE-I activities, techno-functional properties and colour were investigated. All hydrolysates presented a high protein content (52.7-83.2% dw) and low fat content (0.9-3.9% dw). Alcalase® treatment of muscle and viscera proteins resulted in higher DH (7.5 and 8.6%, respectively) and higher biological activities ( $p < 0.05$ ). Although all hydrolysates had excellent solubility at pH 4-10 range (>52.7%) and possessed techno-functional properties, treatment with BSY proteases was the approach that promoted higher emulsion (80.1 m<sup>2</sup>/g), foaming (79.2%) and oil binding capacity (5.8 g/g) of viscera sardine proteins. The hydrolysates produced in this study using the three enzymatic treatments could potentially be used in food systems due to their improved biological and techno-functional properties.

## 10.1. INTRODUCTION

Canned sardine by-products are commonly recognized as low-value resources, which represent around 50% of the product catch (13), (213). Hence, sustainable exploitation of these by-products is of major relevance. Production of SPH represents a good alternative to obtain added value ingredients. Several efforts have been made in finding SPH with antioxidant (16), (20), (209), (213), (215), (222), (223) and ACE-I activities (15), (288). Additionally, SPH have also demonstrated excellent physicochemical and techno-functional properties (20), (202), (213), (222), (223), (289). The nature of the protein substrate, the specificity of the enzyme used and the conditions used during hydrolysis (time, temperature, pH and E/S ratio), considerably influenced the molecular weight and amino acid composition of bioactive peptides and thus, their biological and techno-functional properties (103), (218).

Different SPH have been produced in recent years, the preferred commercial enzymes for most researchers are industrial food-grade proteases, namely Alcalase® (5), (6), (15), (20), (209), (211-213), (225); Flavourzyme® (211), Neutrase® (289) and Protamex® (211), (214). Also, protease preparations of bacterial origin like *Bacillus licheniformis* NH1 (15), (16), *Aspergillus clavatus* ES1 (15), (16), *Bacillus pumilus* A1 (222) and *Bacillus mojavensis* A22 (222), as well as, crude enzyme extract from viscera of sardine

(209) have yielded good results. More recently, a SPH was also efficiently produced through action of BSY proteases over sarcoplasmic proteins extracted from sardine by-products (251). However, more studies are required concerning the hydrolysis of sardine muscle and viscera proteins, because those proteins are more abundant in sardine by-products and more resistant to hydrolysis. Comparison between biological and techno-functional properties of SPH obtained by BSY proteases and from commercial proteases is also required, since enzyme specificity has impact not only on molecular size of peptides and DH, but also in the biological activities and techno-functional properties, such as solubility, emulsifying, foaming and water binding capacity (218). Protein hydrolysates promote an oil-in-water emulsion due their hydrophilic and hydrophobic groups and their charge (194). However, extensive hydrolysis may result in poor techno-functional properties of hydrolysates (218). Additionally, the colour of food hydrolysates is influenced by enzymatic browning reactions and can influence the acceptability by consumers (194).

The objective of this work was to compare hydrolysates from muscle and viscera sardine proteins obtained by BSY proteases and commercial Alcalase® and Neutrase® with respect: (i) DH using the same proteolytic activity and hydrolysis conditions; (ii) antioxidant and ACE-I activities; (iii) techno-functional properties, namely, solubility, emulsifying, foaming, water-and oil-binding capacity and colour.

## 10.2. MATERIAL AND METHODS

### 10.2.1. Reagents and standards

Acetonitrile HPLC grade; trifluoroacetic acid (TFA); sodium dodecyl sulfate (SDS); bovine serum albumin (BSA); 2,4,6-trinitrobenzenesulfonic acid (TNBS); L-leucine; 6-hydroxy-2,5,7,8-tetramethylchroman-2-carboxylic acid (Trolox); iron (III) chloride hexahydrate; 2,4,6-tripyridyl-s-triazine (TPTZ); 1,1-diphenyl-2-picrylhydrazyl (DPPH); commercial ACE (EC 3.4.15.1, 5.1 U/mg); Neutrase® (EC.3.4.24.28,  $\geq 0.8$  U/g); Alcalase® (EC 3.4.21.62,  $\geq 2.4$  U/g); soybean oil; low range of molecular weight standard (6.5-66 kDa) and the Millipore UF membranes of 10 kDa were all obtained from Sigma-Aldrich (St. Louis, MO, USA). The *o*-aminobenzoylglycyl-*p*-nitro-phenylalanylproline (*o*-ABz-Gly-Phe(NO<sub>2</sub>)-Pro) was purchased from Bachem Feinchemikalien (Bubendorf, Switzerland). Ultrapure water was obtained from a Seralpur Pro 90 CN water purification. All solutions were daily freshly prepared.

### 10.2.2. Equipments

SE-HPLC analysis were performed using a Gilson HPLC system (Gilson Medical Electronics, France) equipped with a type 302 pump, a Gilson 118 variable wavelength ultraviolet detector and a 7125 Rheodyne injector. The equipment was controlled by a Gilson 712 software. Spectrophotometric analyses were carried out using a BMG LABTECH's SPECTROstar Nano-microplate, cuvette UV/Vis absorbance reader (Offenburg, Germany). Fluorimetric analyses were carried out using a fluorescence microplate reader (FLUOstar Optima, BMG Labtech GmbH). Samples were freeze-dried with a Telstar® freeze dryer, Cryodos-80 model (Terrassa, Spain).

### 10.2.3. Sardine by-products and proteolytic enzymes

Sardines (*Sardina pilchardus*) by-products were provided by the canned industry Ramirez. SA (Matosinhos, Portugal). By-products were immediately placed in ice and transported to the laboratory, where flesh and viscera by-products were collected and separately washed twice with cold pure water and stored in sealed plastic bags at -20°C.

Proteases from BSY (*Saccharomyces pastorianus*), supplied by Unicer Bebidas S.A., brewing (Leça do Balio, Portugal), were extracted as described by Vieira *et al.* (251). Proteolytic activity, determined by Sigma's non-specific protease assay method described by Cupp-Enyard (164), was 1 U/mL. Commercially available enzymes were used at the same activity levels of BSY proteases, 1 U/mL, to compare hydrolysis efficiencies. For this purpose, Alcalase® and Neutrase® were diluted in the respective buffer, 100 mM Tris-HCl pH 8.0 and sodium phosphate buffer pH 7.0, respectively.

### 10.2.4. Hydrolyses of muscle and viscera proteins

Muscle and viscera fractions were prepared separately. The muscle/ viscera (500 g) in 1000 mL pure water were first minced with an Ultraturax® for about 5 min and then cooked at 90°C for 20 min to inactivate the endogenous enzymes. This step was important to obtain a partially defatted raw material and ensure the exclusively action of the added enzymes and thus, the reproducibility of the process (225). After cold at room temperature and centrifugation at 6,000 x g for 20 min; the upper lipid phase was removed manually and discarded, and the suspensions were collected and filtered through a Whatman No. 4 filter paper. The final clear supernatants were extracts of muscle proteins and viscera proteins. For comparative effects, 50 mL of each muscle/ viscera protein extract was used for enzymatic treatment, at the same protein concentration, 20 mg of protein/mL, based on Bradford assay (171). The pH was adjusted to the pH optimum of each enzyme preparation: BSY proteases (pH 6), Alcalase® (pH 8) and Neutrase® (pH 7). Hydrolysis was performed using the E/S ratio of 0.20:1 U/mg (1 U/mL), at 50°C for 7 h, under occasional stirring. No

pH control was chosen to avoid adding more salt to the hydrolysates (217). Control experiments were also performed without enzyme addition and were referred as MUSC.control and VISC.control. Hydrolyses were stopped at 80°C for 15 min, 1 mL of each hydrolysate was taken for determination of the DH. After cooling to room temperature, the hydrolysates were centrifuged at 10,000 x *g* for 30 min to remove sludge and the oily fraction and to collect the digested material. The clear supernatants were used for colour measurements and further freeze-dried and stored at -20°C for the other analysis. Triplicate analyses were always performed. Muscle SPH were referred as MUSC.Bsy; MUSC.Alc and MUSC.Ntr, according to the enzymatic preparation used (BSY protease extract, Alcalase® and Neutrase®), respectively, whereas viscera SPH were referred as VISC.Bsy; VISC.Alc and VISC.Ntr, respectively.

#### **10.2.5. Determination of DH and molecular weight profile of hydrolysates**

The degree of hydrolysis (DH), expressed as the percentage of peptides bonds hydrolysed, was determined by the TNBS method described by Hsu *et al.* (238). Peptides molecular weight distribution in muscle and viscera protein hydrolysates was analysed by SE-HPLC. The column used was a PSS Proteoma Analytical 100 Å column (Amersham Biosciences, UK), equilibrated with 50 mM sodium phosphate buffer, 0.15 M NaCl, pH 6.6 at a flow rate of 0.3 mL/min and calibrated using a standard mixture of 8 molecular weight markers, which covered the range between 6.5 and 66 kDa. Aliquots of hydrolysates (0.1% w/v protein) were dissolved in the mobile phase and an injection volume of 20 µL was used. Detection was monitored at 214 nm and analyses were performed, at least, in triplicate.

#### **10.2.6. Proximate Composition**

The protein and fat composition of protein extracts (MUSC.control and VISC.control) and lyophilized SPH was determined according to AOAC official methods (144). The total nitrogen content was determined by Kjeldahl method and crude protein was estimated by using the 6.25 factor. Fat content was determined by Soxhlet extraction with n-hexane for 12 h. All assays were performed in triplicate and the contents were expressed on a dry weight basis (% dw).

#### **10.2.7. Determination of antioxidant and ACE-I activities**

Antioxidant and ACE-I activities of muscle and viscera SPH were evaluated using the same protein concentration, 1.0 mg/mL. The DPPH radical-scavenging assay was performed as described by Herald *et al.* (155) with slight modifications. Trolox was used as standard at 10-500 µM to generate a calibration curve. Results were expressed as micromole Trolox equivalents per mL of hydrolysate (µM TE/mL). FRAP was performed according to the

procedure of Jansen and Ruskovska (154). Trolox was also used as standard and results were expressed as micromole Trolox equivalents per mL of hydrolysate ( $\mu\text{M TE/mL}$ ). The ACE-I activity was measured using the fluorimetric assay of Sentandreu and Toldrá (121) with the modifications reported by Quiros *et al.* (122).  $\text{IC}_{50}$  was measured as the concentration required to decrease the ACE activity by 50% (122).

#### 10.2.8. Determination of techno-functional properties

The solubility of muscle and viscera SPH was evaluated over a wide range of pH value (from pH 4 to 10) according to the procedure described by Tsumura *et al.* (290). The emulsifying activity index (EAI) and the emulsion stability index (ESI) of the muscle and viscera SPH were determined according to the method of Pearce and Kinsella (1978) (291), with the modification of Khaled *et al.* (222). Soybean oil was used for emulsification and the absorbance of the diluted solutions was measured at 500 nm. The absorbance of the diluted samples measured immediately ( $A_0$ ) and 10 min after emulsion formation ( $A_{10}$ ) were used to calculate the EAI and ESI, respectively, according to Pearce and Kinsella (291) and as reported by Jemil *et al.* (223). The foam expansion (FE) and foam stability (FS) of the muscle and viscera SPH were determined according to the method of Shahidi *et al.* (292), with the modification of Khaled *et al.* (222). Water binding capacity (WBC) of the muscle and viscera SPH was measured according to MacConnel *et al.* (293), as described by Jemil *et al.* (223). Oil binding capacity (OBC) of the muscle and viscera SPH was measured according to Lin *et al.* (294), as described by Jemil *et al.* (223).

#### 10.2.9. Colour measurement

The colour parameters  $L^*$ ,  $a^*$  and  $b^*$  of muscle and viscera SPH were determined with a tristimulus colorimeter (CR-400Chroma Meter, Konica Minolta, Japan), where  $L^*$  defines the lightness ( $0 < L^* < 100$ ) variation and parameters  $a^*$  define the red (+) to green (-) and  $b^*$  the blue (-) to yellow (+) chromaticity. The equipment was set up for illuminant D65 with  $10^\circ$  observer angle and calibrated using a standard white plate. Sample was filled in a 64 mm glass sample cup with three readings in the same place and triplicate determinations were taken per sample.

#### 10.2.10. Statistical analysis

Data were presented as mean  $\pm$  standard deviation values from three independent experiments. Statistical comparisons were performed by one-way analysis of variance (ANOVA) followed by the Duncan's multiple comparison test. Difference was considered significant at  $p < 0.05$ . All statistical calculations were performed using SPSS 22.0 (SPSS software, Chicago, U.S.A.).

## 10.3. RESULTS AND DISCUSSION

### 10.3.1. DH and molecular weight distribution profile of SPH

Alcalase® was the most efficient enzyme to hydrolyse muscle and viscera proteins. The DH of MUSC.Alc and VISC.Alc were 7.5% and 8.6, respectively; whereas MUSC.Ntr and VISC.Ntr presented DH of 6.5% and 7.8%, respectively. Lower DH was obtained when hydrolyses were performed by BSY proteases, since DH were 5.0% and 5.8% for muscle and viscera SPH, respectively. Concerning the Alcalase® treatments, the DH values obtained in this work were in the same range of reported in the literature (15), (16), (20), (213). Similarly to that observed by Quaglia *et al.* (289), Alcalase® exhibited higher hydrolytic activities than Neutrase® although, the DH values reported in this study were different because different procedures were used to prepare the protein substrates from sardine by-products, and different hydrolysis conditions were applied.

Muscle and viscera proteins presented relatively large molecular mass proteins, ranging from 29 and 97 kDa (results not shown), which was in agreement with Klomkiao *et al.* (199) and Chaijan *et al.* (196), that describe myosin (~96 kDa), myoglobin (~47 kDa) and actin (~45 kDa) as the major proteins found in these extracts. As depicted in Figure 10.1, different molecular weight distribution profiles were obtained depending on the protein substrate and enzyme used. Alcalase® treatment produced MUSC.Alc and VISC.Alc SPH with higher content of peptides with molecular weight below 14 kDa. Souissi *et al.* (20) also reported the presence of peptides with a molecular mass below 14.2 kDa in SPH prepared by Alcalase®. Neutrase® produced muscle and viscera SPH containing higher amount of protein fragments with molecular weight between 24 and 36 kDa.

### 10.3.2. Protein and lipid content of SPH

All hydrolysates presented high protein content, although muscle SPH contained higher protein content (MUSC.Bsy - 69.5%; MUSC.Alc - 83.2% and MUSC.Ntr - 79.8%) than viscera SPH (VISC.Bsy - 58.2%; VISC.Alc - 63.4% and VISC.Ntr - 52.7%). All hydrolysates presented low lipid content (ranging between 0.9-3.9%). A reduced lipid content was also reported for other SPH (20), (211), (222), (223). In general, the high protein content and low fat content of all SPH may provide an incentive for use in commercial preparations.

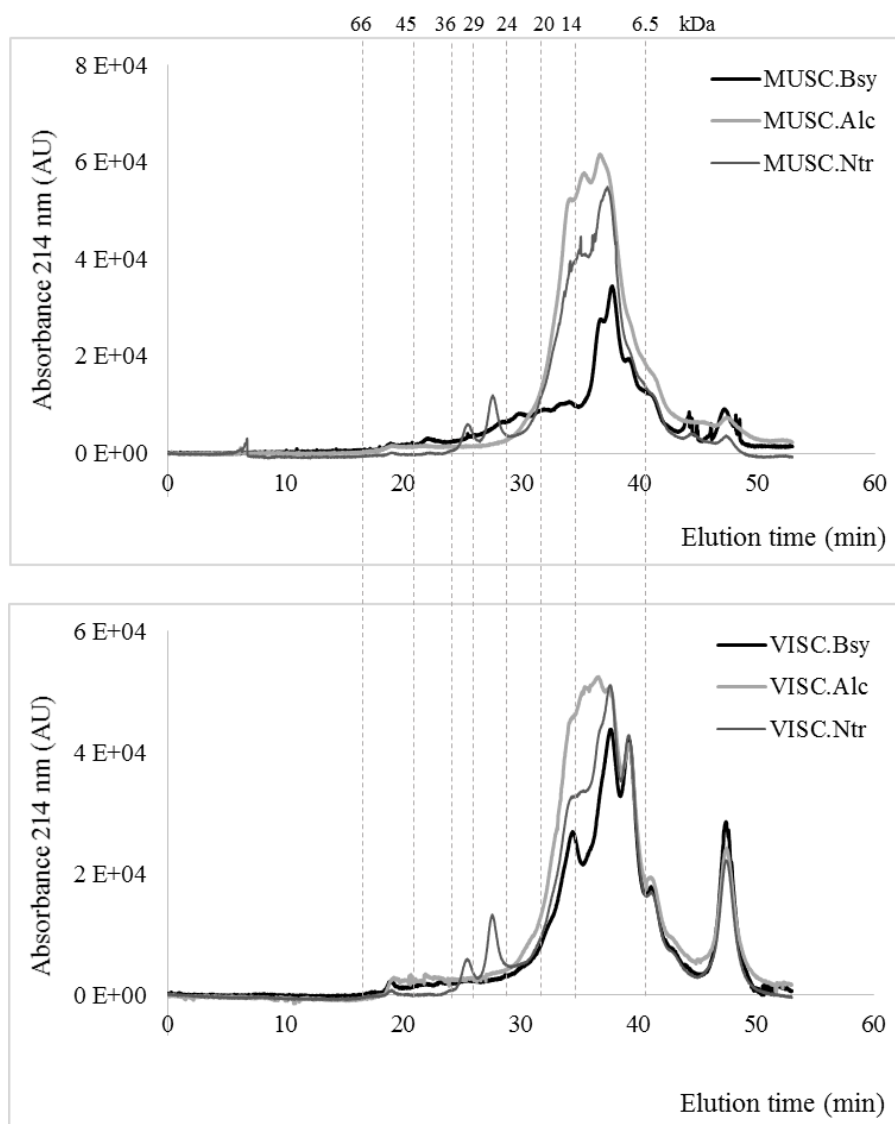


Figure 10.1. SE-HPLC profiles of muscle (MUSC) and viscera (VISC) SPH produced by Brewer's spent yeast proteases (Bsy), Alcalase® (Alc) and Neutrase® (Ntr) action. Hydrolyses were performed at 50°C for 7 h, using an E/S ratio of 0.20:1 U/mg (1 U/mL). SPH were analyzed at same protein concentration (0.1% w/v protein), using 20  $\mu$ L of this solution to the column. Absorbance (214 nm) is expressed in arbitrary units (AU). Molecular weight markers: Albumin (66 kDa), Ovalbumin (45 kDa), Glyceraldehyde-3-phosphate dehydrogenase (36 kDa), Carbonic anhydrase (29 kDa), Trypsinogen (24 kDa), Trypsin inhibitor (20 kDa),  $\alpha$ -Lactalbumin (14.2 kDa) and Aprotinin (6.5 kDa).

### 10.3.3. Determination of antioxidant and ACE-I activities

According to Table 10.1, among the muscle SPH, MUSC.Alc exhibited the highest ( $p < 0.05$ ) DPPH value (870  $\mu\text{M TE/mL}$ ), followed by MUSC.Ntr (780  $\mu\text{M TE/mL}$ ) and MUSC.Bsy (360  $\mu\text{M TE/mL}$ ). Among the viscera SPH, VISC.Alc also exhibited the highest ( $p < 0.05$ ) DPPH value (840  $\mu\text{M TE/mL}$ ), but VISC.BSY (780  $\mu\text{M TE/mL}$ ) presented highest antioxidant activity than VISC.Ntr (660  $\mu\text{M TE/mL}$ ).

Regarding to FRAP results, Alcalase® and Neutrase® were more efficient to hydrolyse the muscle sardine proteins, whereas Alcalase® was more efficient to hydrolyse the viscera sardine proteins ( $p < 0.05$ ), leading to the different products with varying antioxidant activity (Table 10.1). The results obtained suggest that all SPH contained some peptides that were electron donors and could react with free radicals to convert them to more stable products (213), (295). Similar to suggested by Medina *et al.* (213), the differences in antioxidant activities between SPH from sardine by-products might be associated with the differences in size of proteins or peptides, previously discussed based on Figure 10.1, as well, with the high hydrophobic amino acid composition.

The ACE-I activity of muscle and viscera SPH was also analysed; the amount of hydrolysate required to inhibit 50% of the ACE activity ( $\text{IC}_{50}$ ) is shown in Table 10.1. Compared to respective unhydrolysed proteins (MUSC.control and VISC. control), all the SPH presented enhanced ACE-I activity, although it was markedly different depending on the enzyme used. Muscle SPH prepared by Alcalase® exhibited the highest ( $p < 0.05$ ) ACE-I activity,  $\text{IC}_{50}$  of 619  $\mu\text{g/mL}$ , followed by the Neutrase® hydrolysates (735  $\mu\text{g/mL}$ ) and the BSY proteases hydrolysate (984  $\mu\text{g/mL}$ ). VISC.Ntr presented the highest ( $p < 0.05$ ) ACE-I activity, 550  $\mu\text{g/mL}$ , among the viscera SPH. Although values of  $\text{IC}_{50}$  for ACE-I activity of muscle and viscera SPH had been previously reported by other authors, comparisons with  $\text{IC}_{50}$  values in the present study were not fully possible due to the different methodology employed for measuring this biological activity. However, Bougatef *et al.* (15) reported  $\text{IC}_{50}$  values in the concentration range of 1200-7400  $\mu\text{g/mL}$  for SPH prepared with different proteases, whereas the  $\text{IC}_{50}$  found for Alcalase® treatment was 2300  $\mu\text{g/mL}$ . More recently, Moreno *et al.* (288) reported  $\text{IC}_{50}$  values in the range of 439-442  $\mu\text{g/mL}$  for SPH prepared with combined enzymatic treatments of Subtilisin® and Trypsin®.



Table 10.1. Antioxidant and ACE-I activities of muscle (MUSC) and visceral (VISC) SPH produced by Brewer's spent yeast proteases (Bsy), Alcalase® (Alc) and Neutrase® (Ntr) action

Sample	DPPH ( $\mu$ M TE/mL)	FRAP ( $\mu$ M TE/mL)	IC <sub>50</sub> <sup>#</sup> ( $\mu$ g protein/mL)
<i>Muscle sardine by-product</i>			
MUSC.control	220 $\pm$ 10 <sup>e</sup>	70 $\pm$ 8 <sup>de</sup>	1134 $\pm$ 17.06 <sup>a</sup>
MUSC.Bsy	360 $\pm$ 40 <sup>d</sup>	80 $\pm$ 11 <sup>d</sup>	984 $\pm$ 9.85 <sup>b</sup>
MUSC.Alc	870 $\pm$ 32 <sup>a</sup>	160 $\pm$ 13 <sup>a</sup>	619 $\pm$ 1.35 <sup>f</sup>
MUSC.Ntr	780 $\pm$ 30 <sup>b</sup>	162 $\pm$ 21 <sup>a</sup>	735 $\pm$ 2.74 <sup>f</sup>
<i>Viscera sardine by-product</i>			
VISC.control	160 $\pm$ 20 <sup>f</sup>	60 $\pm$ 14 <sup>e</sup>	987 $\pm$ 12.64 <sup>b</sup>
VISC.Bsy	780 $\pm$ 21 <sup>b</sup>	140 $\pm$ 23 <sup>b</sup>	828 $\pm$ 22.86 <sup>c</sup>
VISC.Alc	840 $\pm$ 12 <sup>a</sup>	190 $\pm$ 11 <sup>a</sup>	651 $\pm$ 6.86 <sup>e</sup>
VISC.Ntr	660 $\pm$ 23 <sup>c</sup>	110 $\pm$ 14 <sup>c</sup>	550 $\pm$ 10.68 <sup>d</sup>

Results are expressed as mean  $\pm$  standard deviation from three replicate experiments analyzed in triplicate; a hydrolysate solution of 1.0 mg/mL was used. For each assay, values within column bearing different letters are statistically different ( $p < 0.05$ ), Duncan Post Hoc test.

<sup>#</sup> IC<sub>50</sub>: concentration ( $\mu$ g protein/mL) of SPH required to inhibit 50% of ACE activity.

TE: Trolox equivalents.

### 10.3.4. Techno-functional properties of SPH

#### 10.3.4.1. Solubility

The solubility of muscle and viscera SPH, at pH ranging from 4 to 10 is shown in Figure 10.2. The minimum solubility of 10.1% and 8.7% of the MUSC.control and VISC.control, respectively, was detected at pH 5.0, i.e. the isoelectric point of sardine protein (result not shown). Muscle and viscera protein solubility was significantly ( $p < 0.05$ ) increased after enzymatic treatment. Indeed, for all SPH, the protein solubility was minimum at pH 5.0 (52.7-68.0) and increased gradually below and above pH 5, reaching approximately 77.7-95.3% at pH 10. MUSC.Alc and VISC.Alc hydrolysates, showing the highest DH (7.5% and 8.6%, respectively), as previously reported, presented higher solubility in a pH values ranging from 4 to 10 than the other SPH ( $p < 0.05$ ). The difference in solubility observed among SPH can be due to peptide length and the ratio of hydrophilic/

hydrophobic peptides (20). In general, the high solubility of SPH indicates potential applications in formulated food systems (20), (218).

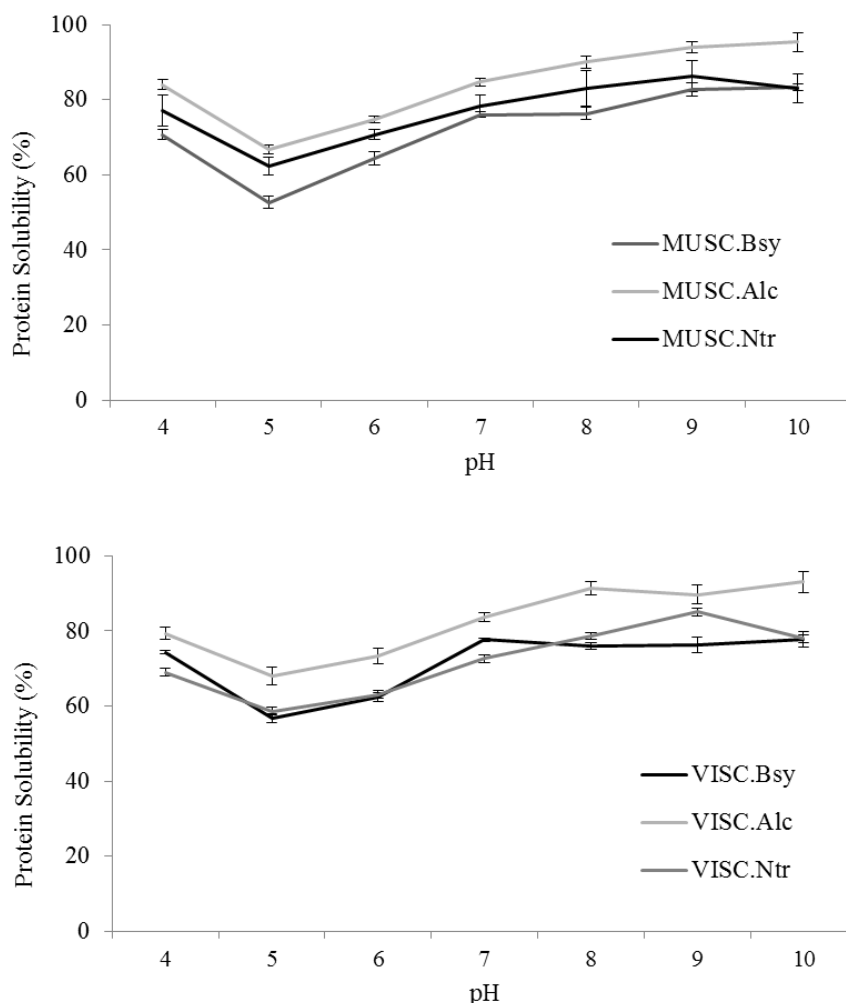


Figure 10.2. Solubility profiles of muscle (MUSC) and visceral (VISC) SPH as a function of pH (4-10 range) obtained by treatment with Brewer's spent yeast proteases (Bsy), Alcalase® (Alc) and Neutrase® (Ntr) action. Results are expressed as means  $\pm$  standard deviation from triplicate determinations; a solution of 10 mg/mL was used.

#### 10.3.4.2. Emulsifying properties

The EAI and ESI of MUSC.control and VISC.control and respective SPH at the concentrations of 0.1% (m/v) are shown in Table 10.2. This concentration was chosen because is referred to the minimum concentration needed to obtain reproducible results for the emulsifying properties (291). All SPH present enhanced emulsion properties compared to the respective undigested sardine proteins, MUSC.control (EAI=13.5 m<sup>2</sup>/g) and VISC.control (EAI=15.2 m<sup>2</sup>/g). However, a different trend was observed when the hydrolysis

was promoted for both protein sources, which indicate that emulsifying properties is influenced by the enzyme used and the protein substrate, which affects the nature of peptides produced during hydrolysis. Concerning to muscle SPH, MUSC.Alc and MUSC.Ntr presented significantly ( $p < 0.05$ ) higher EAI ( $81.6 \text{ m}^2/\text{g}$  and  $78.8 \text{ m}^2/\text{g}$ , respectively) than MUSC.Bsy ( $54.5 \text{ m}^2/\text{g}$ ), suggesting that commercial enzymes are more efficient in the reducing of the hydrophobicity and changes in peptide size during hydrolysis to promote higher oil-in-water emulsions of both substrates. It is reported that peptides should have a minimum of 20 residues to exhibit good emulsifying and interfacial properties (218). Thus, the higher emulsifying properties observed for MUSC.Alc and MUSC.Ntr are in agreement with the higher levels of peptides with MW below 14 kDa (Figure 10.1), as previously discussed. Regarding, viscera SPH, results suggest the emulsifying capacity decreased with the increase in DH. VISC.Alc with the highest DH (8.6%) presented the lowest EAI ( $78.8 \text{ m}^2/\text{g}$ ), whereas VISC.Bsy with a DH of 5.8%, presented the highest EAI,  $80.1 \text{ m}^2/\text{g}$ . Quaglia and Orban (202) reported a 1.5- to 2-fold reduction in the emulsifying capacity of the Alcalase® SPH by increasing DH from 5% to 20%. The turbidimetric method was also used to evaluate the emulsion stability, expressed as ESI, results are present in Table 10.2. The most stable emulsion of muscle and viscera SPH was obtained after hydrolysis with Alcalase®, with a stability of 66.8% and 38.5%, respectively.

#### **10.3.4.3. Foaming properties**

The FE and FS of muscle and viscera SPH at the concentration of 0.1% (m/v) are shown in Table 10.2. Results showed that all muscle and viscera SPH presented an improved foaming activity when compared to respective unhydrolysed proteins (MUSC.control and VISC.control). The foaming capacity of MUSC.bsy; MUSC.Alc and MUSC.Ntr were 57.9%, 87.4% and 77.1%, respectively, whereas it was only 25.8% for MUSC.control. The foaming capacity of VISC.Bsy; VISC.Alc and VISC.Ntr were 79.2%, 77.5% and 59.7%, respectively, significantly ( $p < 0.05$ ) higher than VISC.control, 27.5%. Native muscle and viscera sardine proteins have limited foaming due to its quaternary and tertiary structure, whereas resulting hydrolysates may lost the tertiary structure, leading to improved foam activity. Lower foaming properties of MUSC.Bsy and VISC.Ntr can be explained by the small size of peptides and also by the apparition of hydrophilic peptides during hydrolysis. This is in line with previous findings reporting decreasing foaming properties with reduced peptide size (20), (218). Further experiment on foam expansion after whipping was monitored for 30 min to study the foam stability of muscle and viscera SPH. As shown in Table 10.2, the FS was markedly decreased for all SPH. At a concentration of 0.1%, the foaming capabilities after 30 min of MUSC.bsy; MUSC.Alc and MUSC.Ntr were 39.7%, 66.8% and 59.7%, respectively. The foam properties of VISC.Bsy; VISC.Alc and VISC.Ntr were 41.5%,

38.5% and 34.5%, respectively. The trend of increased foaming activity coupled with decreased foaming stability has been reported in previous studies for other kind of SPH (20), (222), (223).

#### **10.3.4.4. Water Binding Capacity (WBC)**

The WBC of muscle and viscera SPH is shown in Table 10.2. The WBC of all SPH was significantly ( $p < 0.05$ ) higher compared to the unhydrolyzed substrates. For muscle SPH, the WBC decreased from an initial value of 1.4 g/g (MUSC.control) for 4.3, 6.9 and 5.6 g/g after hydrolysis with BSY proteases, Alcalase® and Neutrase®, respectively. For viscera SPH, VISC.Alc showed a significantly ( $p < 0.05$ ) higher WBC, 7.3 g/g, compared with the other two enzymatic treatments. From these results, the higher DH, observed for treatment with Alcalase®, appear to affect greater WBC. Other authors also showed increased WBC of SPH as peptide molecular weights decreased (223), (218). In general, the high WBC of muscle and viscera SPH prepared by action of BSY protease and commercial enzymes, Alcalase® and Neutrase®, suggest that all SPH could be used as techno-functional ingredients in food formulations to modify texture and viscosity, to reduce dehydration during storage, and to reduce energetic value.

#### **10.3.4.5. Oil Binding Capacity (OBC)**

As shown in Table 10.2, muscle and viscera SPH exhibited OBC, greater than undigested muscle and viscera proteins (MUSC.control and VISC.control). The higher OBC values for SPH might be attributed to the exposure of hydrophobic groups after enzymatic hydrolysis, allowing the physical entrapment of oil (296). MUSC.Bsy and VISC.Bsy presented the highest ( $p < 0.05$ ) OBC, 5.4 and 5.8 g/g, respectively; while muscle and viscera SPH prepared by the commercial enzymes Alcalase® and Neutrase®, showing the highest DH, presented the lowest OBC. Some authors reported that OBC of protein hydrolysates decreased with increasing DH (194) while others authors suggested no correlation between the OBC and DH of protein hydrolysates (20). The ability of peptides to bind fat influences food product taste, which is especially important in both meat and confectionery industries (218).

Table 10.2. Techno-functional properties and colour of muscle (MUSC) and visceral (VISC) SPH obtained by treatment with Brewer's spent yeast proteases (Bsy), Alcalase® (Alc) and Neutrase® (Ntr)

Parameter	MUSC.control	MUSC.Bsy	MUSC.Alc	MUSC.Ntr	VISC.control	VISC.Bsy	VISC.Alc	VISC.Ntr
EAI (m <sup>2</sup> /g) #	13.5 ± 0.30 <sup>g</sup>	54.5 ± 0.89 <sup>e</sup>	81.6 ± 0.75 <sup>a</sup>	77.0 ± 1.51 <sup>c</sup>	15.2 ± 0.30 <sup>f</sup>	80.1 ± 1.56 <sup>ab</sup>	78.8 ± 1.51 <sup>bc</sup>	66.3 ± 0.89 <sup>d</sup>
ES (min) #	0.7 ± 0.08 <sup>g</sup>	27.3 ± 1.34 <sup>e</sup>	68.4 ± 0.94 <sup>a</sup>	57.9 ± 1.16 <sup>b</sup>	1.5 ± 0.12 <sup>f</sup>	45.6 ± 4.25 <sup>d</sup>	50.4 ± 1.15 <sup>c</sup>	44.4 ± 0.30 <sup>d</sup>
FE (%) #	25.8 ± 0.35 <sup>f</sup>	57.9 ± 1.76 <sup>e</sup>	87.4 ± 0.60 <sup>a</sup>	77.1 ± 2.04 <sup>c</sup>	27.5 ± 0.35 <sup>f</sup>	79.2 ± 0.60 <sup>ab</sup>	77.5 ± 0.92 <sup>bc</sup>	59.7 ± 1.76 <sup>d</sup>
FS (%) #	4.5 ± 1.15 <sup>f</sup>	39.7 ± 0.88 <sup>e</sup>	66.8 ± 0.75 <sup>a</sup>	59.7 ± 1.36 <sup>b</sup>	5.8 ± 0.15 <sup>f</sup>	41.5 ± 0.89 <sup>d</sup>	38.5 ± 0.89 <sup>c</sup>	34.5 ± 4.30 <sup>d</sup>
WBC (g/g)	1.4 ± 0.07 <sup>h</sup>	4.3 ± 0.27 <sup>f</sup>	6.9 ± 0.12 <sup>b</sup>	5.6 ± 0.04 <sup>d</sup>	1.9 ± 0.15 <sup>g</sup>	4.8 ± 0.33 <sup>e</sup>	7.3 ± 0.08 <sup>a</sup>	6.1 ± 0.08 <sup>c</sup>
OBC (g/g)	0.8 ± 0.02 <sup>e</sup>	5.4 ± 0.19 <sup>b</sup>	4.8 ± 0.19 <sup>c</sup>	4.6 ± 0.05 <sup>c</sup>	1.4 ± 0.03 <sup>d</sup>	5.8 ± 0.23 <sup>a</sup>	5.5 ± 0.19 <sup>b</sup>	5.4 ± 0.20 <sup>b</sup>
<i>L</i> *	53.4 ± 0.02 <sup>b</sup>	49.5 ± 0.01 <sup>f</sup>	49.9 ± 0.10 <sup>ef</sup>	50.1 ± 0.01 <sup>de</sup>	55.1 ± 0.59 <sup>a</sup>	51.2 ± 0.08 <sup>c</sup>	50.1 ± 0.03 <sup>de</sup>	50.3 ± 0.05 <sup>d</sup>
<i>a</i> *	0.31 ± 0.01 <sup>b</sup>	0.32 ± 0.01 <sup>b</sup>	0.16 ± 0.02 <sup>d</sup>	0.37 ± 0.02 <sup>a</sup>	0.07 ± 0.00 <sup>e</sup>	0.09 ± 0.03 <sup>e</sup>	0.08 ± 0.02 <sup>e</sup>	0.26 ± 0.02 <sup>c</sup>
<i>b</i> *	3.23 ± 0.02 <sup>g</sup>	3.45 ± 0.02 <sup>f</sup>	4.31 ± 0.02 <sup>d</sup>	5.52 ± 0.01 <sup>b</sup>	3.46 ± 0.01 <sup>f</sup>	4.24 ± 0.01 <sup>e</sup>	5.35 ± 0.02 <sup>c</sup>	7.37 ± 0.01 <sup>a</sup>

Values are given as mean ± standard deviation from three replicate experiments analyzed in triplicate. For each parameter, values with different letters in the same line are statistically different ( $p < 0.05$ ), Duncan Post Hoc test. Emulsifying activity index (EAI; m<sup>2</sup>/g); Emulsifying stability (ES; min); Foaming Expansion (FE; %); Foaming Stability (FS, %), Water Binding Capacity (WBC; g/g); Oil binding capacity (OBC; g/g); MUSC.control, undigested muscle protein from sardine by-product; VISC.control, undigested viscera protein from sardine by-product. Muscle (MUSC) and visceral (VISC) SPH were obtained by treatment with brewer's spent yeast extract proteases (Bsy), Alcalase® (Alc) and Neutrase® (Ntr) at 50°C for 7 h, using an E/S ratio of 0.20:1 U/mg (1 U/mL). # a solution at 0.1% (m/v) was used.

### 10.3.5. Colour of SPH

As presented in Table 10.2, all hydrolysis resulted in increased enzymatic browning reactions which are assumed to have contributed to the reduction in the luminosity, giving a darker colour in muscle and viscera SPH. These results indicate that colour of SPH is influenced by the enzyme used, as well, the protein substrate. Among muscle SPH, MUSC.Bsy was the darkest ( $L^* = 49.5$ ) and least yellowish ( $b^* = 3.45$ ), whereas among the viscera SPH, VISC.Bsy was the lighter ( $L^* = 51.2$ ) and least yellowish ( $b^* = 4.240$ ). Neutrase® with a dark colour contributed to the brownish colour of the resulting SPH: MUSC.Ntr ( $b^* = 5.52$ ) and VISC.Ntr ( $b^* = 7.37$ ).

## 10.4. CONCLUSIONS

The results of this study indicate that muscle and viscera SPH obtained by different proteases exhibited biological and techno-functional properties that make them useful ingredients for food industry. Under similar hydrolysis conditions, Alcalase® was the most appropriate protease to produce muscle and viscera SPH, presenting higher antioxidant and ACE-I activities. By contrast, lower biological activity was found using BSY proteases. Further work should be done to concentrate and identify the bioactive peptides from muscle and viscera SPH and determine their biological activities *in vivo*. On the other hand, viscera SPH obtained using BSY proteases presented higher emulsion, foaming and oil binding properties, as well as, lighter colour, indicating that the use of two industry by-products, BSY and viscera protein from sardine by-products, can be applied to obtain an ingredient with specific techno-functional characteristics. However, the sensory evaluation of these SPH is obligatory for the consumer acceptance and to find compatible food matrices to add this functional ingredient.

## **PART III**

### **“Brewer’s spent grain protein hydrolysates”**

---

#### **Chapter 11**

##### **Literature review**

*Development of brewer’s spent grain protein hydrolysates and their health promoting ability*

#### **Chapter 12**

*Valorisation of Brewers’ spent grain and spent yeast through protein hydrolysates with antioxidant properties*

#### **Chapter 13**

*Antioxidant and ACE inhibitory activities of hydrolysates of brewers' spent grain proteins by proteases from spent yeast or by commercial enzymes: protective capacity in Caco-2 and HepG2 cells*





## CHAPTER 11

### Literature review

*Development of brewer's spent grain protein hydrolysates and their health promoting ability*

---

This chapter presents a literature overview of the BSG nutritional characteristics and applications, it also describes the typical enzymatic process adopted for the manufacturing of BSG protein hydrolysates and the main biological activities reported



### 11.1. Brewer's spent grain by-product: characteristics and potential applications

Barley malt is one of the main ingredients in the manufacturing of beer. The grain is rich in starch and proteins and consists of three main parts: the embryo, the endosperm (comprising the aleurone and starch) and the grain coverings (comprising the seed coat layers, pericarp and husk), as presented in Figure 11.1.A. During brewing, the nutrients from the malt necessary to produce the wort are solubilized, remaining the water insoluble proteins and the cell wall residues of the husk, pericarp and seed coat, which are referred as brewer's spent grain (BSG). Thus, BSG is defined as the "husk-pericarp-seed coat layers that covered the original barley grain", essentially composed by cellulose and non-cellulosic polysaccharides, lignin, proteins and some lipids (Figure 11.1.B). BSG also contains much of the phenolic components of the barley grain, including ferulic acid, *p*-coumaric acid, sinapic acid and caffeic acid (297), (298), (299).

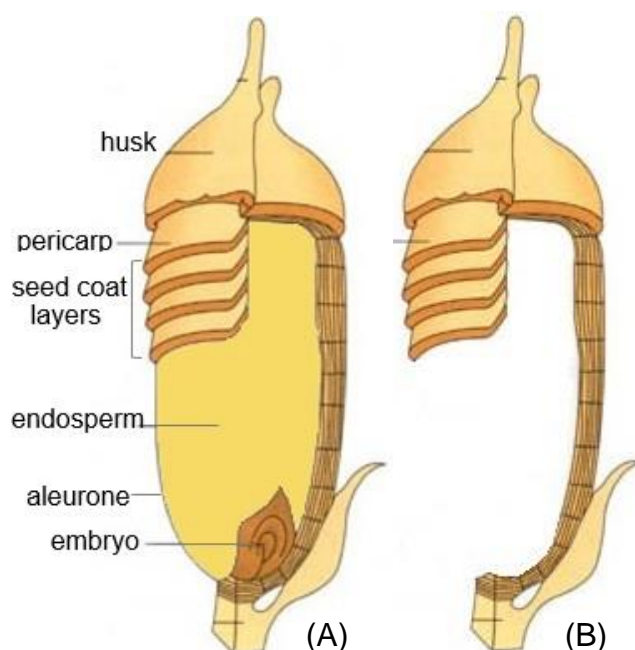


Figure 11.1. Schematic structure of a barley grain **(A)** and the BSG **(B)**.

Chemical composition of BSG is widely described in literature (2), (4), (297), (300-302). It is influenced by several parameters, namely the barley variety, the harvest time, the malting and mashing conditions, as well as, the quality and type of adjuncts added in the brewing process (297). BSG is mainly composed by ~15 to 26% of proteins (rich in glutamine and with high biological value) and ~70% of fibers (~15-25% of cellulose; ~28-35% of hemicelluloses, mostly arabinoxylans, and ~28% of lignin). Lipids (3.9-10%), ash (2.5-4.5%), vitamins, minerals (mainly calcium, phosphorus and selenium), amino acids and

phenolic compounds (mainly hydroxycinnamic acids as ferulic and *p*-coumaric) are present in lower quantities (22), (303), (304).

The use of BSG is still limited, being almost used as land fill or for animal feed (providing all the essential amino acids and fiber). However, given its production in large quantities throughout the year at relative low cost, and its nutritional and functional characteristics, BSG is a by-product of great interest for the sectors of biotechnology, food and pharmaceutical industries (4), (6), (302). Indeed, several efforts have been made in using BSG for microorganism's cultivation and extraction of added-value compounds, namely sugars, proteins, amino acids and antioxidants. BSG was also found to be applicable in enzymes production, as adsorbent for removing organic materials from effluents and immobilization of various substances (2), (305). Moreover, BSG protein isolates and hydrolysates can be used as food texture enhancers due to their emulsifying properties (7), (8) and may present antimicrobial (306), antioxidant (307), (308), anti-inflammatory (307) and ACE-I activities (253), (309). BSG is also considered a major biomass resource for the production of second generation biofuels, it can be used for ethanol production using a bioconversion process (305). Table 11.1 summarizes the proximate composition of BSG and its potential applications.

Table 11.1. Proximate composition (% dw) and potential applications of BSG

Compound	% dw <sup>a</sup>	Potential application	Function	Reference
Proteins	~15-26	- Animal feed	- addition of RUP <sup>c</sup> to lactating cows diet to increase milk yield	(305), (310)
- hordeins A,B,C	(~50)	- Human nutrition (dietary fibre-rich and protein-rich flours)	- promotion of nutritional value of bakery products	(301), (310), (311)
- albumins	(~2)		- cholesterol decrease	
- glutenins			- intestinal digestion benefit	
			- growth and sporulation enhancement	(312)
		- Production of BSG protein concentrates/isolates	- phenolic source	(308), (309)
			- antioxidant activity	(7), (8)
			- ACE-I activity	(4), (299)
			- techno-functional properties	
		- Production of BSG protein hydrolysates with functional and bioactive properties	- antioxidant activity	(307), (313)
			- anti-inflammatory activity	(306), (253)
			- immunomodulatory activity	
			- ACE-I activity	
Fiber	~70	- Extraction of arabinoxilans	- immunomodulatory activity	(314), (315)
- cellulose	(~15-25)		- prebiotic activities	(316)
- hemicellulose	(~28-35) <sup>b</sup>			
- lignin	(~28)			

<sup>a</sup> Chemical composition (% dw) as reported by (4) and (308).

<sup>b</sup> Mostly represented by arabinoxilans.

<sup>c</sup> Rumen undegradable protein.

Table 11.1. Proximate composition (% dw) and potential applications of BSG (continued)

Compound	% dw <sup>a</sup>	Potential application	Function	Reference
Polysaccharides - $\beta$ glucan - starch	12	- Production of $\beta$ glucan extracts	- cholesterol decrease - insulin response	(317), (318)
Phenolics - ferulic acid - <i>p</i> -coumaric acid - caffeic acid - sinapic acid	~1.7%	- Production o phenolic extracts	- antioxidant activity - anti-carcinogenic activity - anti-atherogenic activity - anti-inflammatory activity	(298), (303) (299), (302) (319), (320) (321)
Lipids	3.9-10	- Oil extraction		(22)
Minerals	2.5-4.5	- Calcium, phosphorus, selenium supplements		(22)
<b>Other applications</b>				
- Production of charcoal; production of lactic acid; production of xylitol and pullulan; substrate for enzyme production				(297), (305)
- Additive or carrier in brewing; production of energy and biogas; production of constructing bricks; paper manufacture; adsorbent				(100)

<sup>a</sup> Chemical composition (% dw) as reported by (4) and (308).

## 11.2. Preparation of BSG protein hydrolysates

The applications of BSG insoluble proteins can be increased by applying chemical and enzymatic hydrolysis (7). The first step is the extraction of proteins from BSG (307). BSG protein isolates are then submitted to hydrolysis to obtain the BSG protein hydrolysates. These hydrolysates have been characterized as a mixtures of polypeptides, oligopeptides and amino acids, some of them claimed to possess bioactive activities (100).

### 11.2.1. *Extraction of BSG proteins*

Recovery of BSG proteins requires the use of pretreatment or vigorous disruption procedures. The extraction conditions usually include: mechanical shearing to reduce particle size, addition of reducing agents to disrupt disulphide bonds, determination of the optimal sodium hydroxide concentrations, weight/volume ratios and extraction temperature (308). Table 11.2 summarizes examples of treatments applied to extract the BSG proteins, to produce the hydrolysates and its biological activities when it was evaluated.

An integrated process to valuate BSG proteins and arabinoxylans as food ingredients (4) was developed by our group. The intellectual property of this integrated process was assured (322). For this purpose, a sequential extraction of proteins and arabionoxilans from BSG with increasing alkali (KOH or NaOH) concentrations, 0.1 M, 0.5 M, and 4 M was optimized. This integrated extraction process allowed a yield of 82-85% of the BSG total proteins and 66-73% of total arabinoxylans, with formation of a cellulose rich residue presenting very low nitrogen content.

### 11.2.2. *Hydrolysis of BSG proteins*

Hydrolysis of BSG proteins has been used to generate compounds and peptides with potential biological activities. Enzymes are specific in their action, thus enzymatic hydrolysis is advantageous when compared with chemical hydrolysis. Identification of the proteolytic enzyme/(s) with appropriate specificity to release the bioactive compounds is an important step (309). Enzymatic hydrolysis presents two important benefits, since it does not destroy the amino acids, limiting the effects on nutritional properties, and allows controlled processing, determining which peptides are produced. Consequently, peptide characteristics, namely molecular weight, charge and exposure of hydrophobic groups and reactive amino acid side chains influence the functionalities of BSG protein hydrolysates, such as, solubility, viscosity, sensory properties and emulsifying and foaming behavior, as

well, the biological activities (7). As summarized in Table 11.2., BSG has been hydrolyzed by proteases from different sources: animal (Corolase PP, Trypsin, Pepsin); vegetal (Corolase L10, Promod 144MG); and microbial (Alcalase 2.4L, Flavourzyme 500 L, Protex6L, Protamex, Promod 24P, Promod 439, Prolyve 1000).

### 11.3. Biological properties of BSG protein hydrolysate

Due their biological activities, BSG protein isolates and BSG protein hydrolysates have numerous applications in human nutrition, including protein supplementation of geriatric and sports nutrition products, energy drinks and weight-loss diets for clinical applications (as treatment of Crohn's disease, liver disease and ulcerative colitis) (307). The composition of BSG isolates and hydrolysates in bioactive peptides, amino acids, vitamins and phenolic compounds may explain the bioactivities observed.

Ferulic acid and *p*-coumaric acid are present at relatively high concentrations in BSG; 1860-1948 mg/g dw and 565-794 mg/g dw, respectively (323). These compounds are mainly present in the bound form, requiring strong alkali or hydrolytic enzymes for their solubilisation (304) and show antioxidant, anti-inflammatory, anti-atherogenic and anti-cancer bioactivities (302). On the other hand, given the prevalence of proline and alanine residues within the amino acid sequences of BSG proteins, it is likely that peptides with high ACE and DPP-IV inhibitory activities could be released during BSG protein hydrolysis (309). The most relevant properties recognized in BSG protein isolates and hydrolysates are: antioxidant, anti-inflammatory, ACE-I,  $\alpha$ -glucosidase inhibitory and DPP-IV inhibitory activities. Table 11.2 also summarizes the main biological activities assessed in BSG protein isolates and BSG protein hydrolysates.



Table 11.2. Treatments applied to extract the BSG proteins, to produce the BSG protein hydrolysates and its biological activities when it was evaluated

BSG protein extraction		BSG protein hydrolysis					
Alkaline extraction	Protein (% dw)	Enzyme	Hydrolysis	DH (%)	Assay	Bioactivity assessed	Reference
BSG protein isolates							
Two sequential extractions using 0.1 M NaOH for 1 h at 25°C, followed by acid precipitation at pH 3.8	59%	<i>np</i>	<i>np</i>	<i>np</i>	- TPC - FRAP - DPPH	- 0.0003-0.0046 mg GAE/mg dw - 0.16-4.33 mg TE/g dw - <i>nd</i> - 5.34%	(308)
Three sequential extractions using 0.1 M, 0.5 M and 4 M KOH for 24 h at 25°C, followed by acid precipitation at pH 3.0	82-85%	<i>np</i>	<i>np</i>	<i>np</i>	<i>np</i>	<i>np</i>	(4)
Extraction with 0.1 M NaOH for 1 h at 60°C, followed by acid precipitation at pH 4.0	60%	Alcalase	E/S ratio (2.5% v/w), 60°C, pH 9, 2 h	13 <sup>a</sup>	<i>np</i>	<i>np</i>	(7)
Extraction with 0.1 M NaOH for 1 h at 60°C, followed by acid precipitation at pH 4.0	60%	Flavourzyme	E/S ratio (5.0% v/w), 40°C, pH 9, 3 h	6 <sup>b</sup>	<i>np</i>	<i>np</i>	(7)
Extraction with 0.1 M NaOH for 1 h at 60°C, followed by acid precipitation at pH 4.0	60%	Pepsin	E/S ratio (5.0% v/w), 60°C, pH 3, 3 h	8 <sup>b</sup>	<i>np</i>	<i>np</i>	(7)

<sup>a</sup> Degree of hydrolysis (DH %) calculated by the pH-stat method.

<sup>b</sup> Degree of hydrolysis (DH %) calculated by the o-phthaldialdehyde method.

TPC, Total phenolic content; FRAP, Ferric ion reducing antioxidant power; DPPH, 2,2-diphenyl-1-picrylhydrazyl.

*np*, not performed.

Table 11.2. Treatments applied to extract the BSG proteins, to produce the BSG protein hydrolysates and its biological activities when it was evaluated (continued)

BSG protein extraction		BSG protein hydrolysis			Assay	Bioactivity assessed	Reference
Alkaline extraction	Protein (% dw)	Enzyme	Hydrolysis	DH (%)			
BSG protein hydrolysates							
Two sequential extractions using 0.1 M NaOH for 1 h at 50°C, followed by acid precipitation at pH 3.8	49%	Alcalase	E/S ratio (2.5% v/w), 50°C, pH 7, 4 h	np	- TPC - SOD (U937 cell line) - IL-2 (U937 cell line) - IL-4 (U937 cell line) - IL-10 (U937 cell line) - IFN-γ (U937 cell line)	- 0.055 mg GAE/mg dw - 87.20% - 81.74% - 94.80% - 88.41% - 78.86%	(307)
Two sequential extractions using 0.1 M NaOH for 1 h at 50°C, followed by acid precipitation at pH 3.8	49%	Flavourzyme	E/S ratio (2.5% v/w), 50°C, pH 7, 4 h	np	- TPC - SOD (U937 cell line) - IL-2 (U937 cell line) - IL-4 (U937 cell line) - IL-10 (U937 cell line) - IFN-γ (U937 cell line)	- 0.046 mg GAE/mg dw - 76.71% - 93.73% - 99.86% - 97.42% - 81.89%	(307)
Two sequential extractions using 0.1 M NaOH for 1 h at 50°C, followed by acid precipitation at pH 3.8	49%	Corolase PP	E/S ratio (2.5% v/w), 50°C, pH 7, 4 h	np	- TPC - SOD (U937 cell line) - IL-2 (U937 cell line) - IL-4 (U937 cell line) - IL-10 (U937 cell line) - IFN-γ (U937 cell line)	- 0.034 mg GAE/mg dw - 66.25% - 89.74% - 89.54% - 92.40% - 73.22%	(307)
Two sequential extractions using 0.1 M NaOH for 1 h at 25°C, followed by acid precipitation at pH 3.8	50%	Trypsin 250	E/S ratio (1.0% w/w), 50°C, pH 7, 4 h	4.7 <sup>c</sup>	- α-glucosidase	- 66.81% (7.5 mg/mL)	(309)

TPC, Total phenolic content; SOD, Superoxide dismutase activity assay; IL-2, Interleukin-2; IL-4, Interleukin-4; IL-10, Interleukin-10; IFN- $\gamma$ , Interferon- $\gamma$ .  
np, not performed.

Table 11.2. Treatments applied to extract the BSG proteins, to produce the BSG protein hydrolysates and its biological activities when it was evaluated (continued)

BSG protein extraction		BSG protein hydrolysis					
Alkaline extraction	Protein (% dw)	Enzyme	Hydrolysis	DH (%)	Assay	Bioactivity assessed	Reference
BSG protein hydrolysates							
Two sequential extractions using 0.1 M NaOH for 1 h at 25°C, followed by acid precipitation at pH 3.8	50%	Corolase PP	E/S ratio (1.0% w/w), 50°C, pH 7, 4 h	13.0 <sup>c</sup>	- DPP-IV	- 70.96% (3.5 mg/mL)	(309)
Two sequential extractions using 0.1 M NaOH for 1 h at 25°C, followed by acid precipitation at pH 3.8	50%	Prolyve 1000	E/S ratio (1.0% w/w), 50°C, pH 7, 4 h	13.8 <sup>c</sup>	- ACE-I activity	- 89.25% (1.0 mg/mL)	(309)
Two sequential extractions using 0.1 M NaOH for 1 h at 25°C, followed by acid precipitation at pH 3.8	44%	Alcalase	E/S ratio (1.0% w/w), 50°C, pH 7, 4 h	12.1 <sup>c</sup>	- ACE-I activity (IC <sub>50</sub> )	- 0.32 mg/mL	(253)
Two sequential extractions using 0.1 M NaOH for 1 h at 25°C, followed by acid precipitation at pH 3.8	44%	Corolase PP	E/S ratio (1.0% w/w), 50°C, pH 7, 4 h	16.4 <sup>c</sup>	- ACE-I activity (IC <sub>50</sub> )	- 0.69 mg/mL	(253)
Two sequential extractions using 0.1 M NaOH for 1 h at 25°C, followed by acid precipitation at pH 3.8	44%	Flavourzyme	E/S ratio (1.0% w/w), 50°C, pH 7, 4 h	15.1 <sup>c</sup>	- ACE-I activity (IC <sub>50</sub> )	- 0.50 mg/mL	(253)

<sup>c</sup> Degree of hydrolysis (DH %) calculated by the TNBS method.  
IC<sub>50</sub>, Protein concentration inducing 50% inhibition values for ACE.



## CHAPTER 12

### *Valorisation of Brewers' spent grain and spent yeast through protein hydrolysates with antioxidant properties*

---

This chapter presents the hydrolysis optimization of BSG proteins by BSY proteases to produce BSG protein hydrolysates with enhanced antioxidant activity.



## ABSTRACT

Brewers' spent grain (BSG) and Brewer's spent yeast (BSY) are the main by-products of the brewing process, with currently limited valuable applications. However, BSG protein fraction can be a valuable substrate for enzymatic hydrolysis to produce hydrolysates with biological properties and BSY contains numerous vacuole proteases, which can be used to obtain these hydrolysates. Thus, the objective of this work was to explore the valorisation of these two brewing by-products, based on the production of BSG protein hydrolysates that present antioxidant properties. Response surface methodology (RSM) was employed to optimize the hydrolysis of BSG proteins using BSY proteases, based on degree of hydrolysis (DH %), total phenolic content (TPC) and antioxidant activity (FRAP assay). Reverse phase chromatography was also used to monitor the Hydrolysis Rate (HR %) and the potential presence of endogenous and other inhibitors of BSY proteases was also investigated.

BSG protein hydrolysate prepared at 50°C, pH 6.0, during 6 h and using an E/S ratio of 0.29:1 U/mg presented maximum bioactivity with DH % of 17.1%, TPC of 1.65 mg GAE/mL and FRAP value of 1.88 mg TE/mL. A good correlation was obtained between HR (%) and DH (%) ( $R^2 = 0.9281$ ). The experimental values agreed with the predicted values ( $p < 0.05$ ), suggesting a good fit between the models and the experimental data. BSY proteases involved in the hydrolysis of BSG proteins were serine peptidases and metallopeptidases.

## 12.1. INTRODUCTION

BSG, the residual solid fraction of barley malt and other used grains remaining after filtration of wort, and BSY comprises around 85% and 15% of brewing by-products, respectively (3). Currently, their main application is limited to animal feed. However, due to the fact that both by-products are available at low or no cost through the year and both present high nutritional values, they are promising raw materials to be exploited for human nutrition and biotechnological processes (7), (297). Hence, the development of economically achievable technologies for valorisation of these two by-products should be promoted.

BSG is a ligno-cellulosic material rich in proteins, approximately 15-26% (dw), as well, in phenolic compounds (namely, hydroxycinnamic acids, ferulic acid, *p*-coumaric acid, sinapic acid and caffeic acid), which exhibit antioxidant properties (299), (308), (319), (320). In order to increase the potential applications of the BSG insoluble proteins, chemical or enzymatic hydrolysis is commonly applied (308). The enzymes used determine the

composition of the peptides produced and, therefore, biological and technological functionalities of the final BSG protein hydrolysates (8), (307), (309). Different approaches have been conducted to reuse BSG proteins, using commercial enzymes, such as, Alcalase, Flavourzyme, Pepsin, Corolase, Trypsin and Protamex. BSG hydrolysates present a potential role as functional food ingredients in the management of type II diabetes, hypertension and immunomodulatory effects (307), (309). Also, BSG protein hydrolysates have been produced with good emulsifying and foaming properties (7), (8).

While several attempts have been conducted to prepare BSG protein hydrolysates using expensive commercial enzymes, to our knowledge there are no published reports related to utilization of proteases from BSY. BSY is considered a GRAS raw material, containing several vacuole proteases (serine, aspartyl and metalloproteases), which act at pH 6 (10), (11). In fact, proteases from other types of yeast have been used to obtain hydrolysates with biological activity (64), (324), (325). BSY extract, rich in proteases, can be produced cheaply by mechanic disruption using glass beads (50).

The focus of the present study was on the bioactive potential of BSG protein hydrolysates prepared using proteases extracted from BSY. The first aim was to optimize the best hydrolysis conditions through a RSM approach with the purpose of obtaining value-added hydrolysates with antioxidant properties; and secondly, search for the potential presence of endogenous inhibitors of BSY proteases on BSG protein hydrolysis. The total phenolic content (TPC) and the antioxidant activity, using the ferricyanide reducing power assay (FRAP) of the BSG protein hydrolysates was investigated. Results generated from this study are expected to may economically benefit the brewing process, due to the reuse of the two major by-products, spent grain and spent yeast surplus, as well as, to provide the consumers with a new functional ingredient.

## **12.2. MATERIAL AND METHODS**

### **12.2.1. By-products**

Brewing by-products were kindly supplied by Unicer brewing (Leça do Balio, Portugal). A composite sample of BSG (25% dw) was obtained from worts that had similar formulation and manufacturing process, briefly, the milled barley malt was mixed with hot water at 60°C during 2 h to obtain the wort, the mashing temperature raised to about 75-78°C. Lautering was performed using a mash filter, first wort run-off undiluted, and the extract that remains with the grains was washed with hot water (75-78°C). Syrup from maize grain was added directly to the kettle containing the filtered wort to obtain wort of 15.5° Plato and produce



lager beer. BSG samples were vacuum-packed and stored in polypropylene bags at -20 °C until use.

BSY (*Saccharomyces pastorianus*) biomass was collected from a tank that contained the yeast surplus, and transported in 1 L glass bottles to laboratory under refrigerated conditions and stored at 4°C until preparation procedure (1 day maximum). The BSY resulted from harvesting and repitching the yeast 3 to 6 times, which is a common practice in most breweries. Only yeast surplus from fermentations that exhibited normal fermentation characteristics was collected in the tank. The yeast slurry was thick and creamy with very little trub and no “off” flavours and “off” aromas. Yeast slurry viability was evaluated by manual counting on a standard microscope using a hemacytometer and a methylene blue solution (0.1%).

### 12.2.2. Reagents

Folin-Ciocalteu phenol reagent; trifluoroacetic acid (TFA); 2,4,6-tripyridyl-s-triazine (TPTZ); iron (III) chloride hexahydrate; bovine serum albumin (BSA); 6-hydroxy-2,5,7,8-tetramethylchroman-2-carboxylic acid (Trolox); 2,4,6-trinitrobenzenesulfonic acid (TNBS); gallic acid; L-leucine; L-tyrosine and inhibitors of peptidases (Pepstatin A, E-64, PMSF, EDTA and Bestatin) were all purchased from Sigma-Aldrich (St. Louis, MO, USA). Acetonitrile HPLC grade, sodium acetate, aluminium chloride and sodium hydroxide were purchased from Merck (Darmstadt, Germany). Ultra-pure water was obtained from a Seral-Seralpur Pro 90 CN water purifying system. The Millipore UF membranes with a MWCO of 10 kDa were purchased from Sigma-Aldrich (St. Louis, MO, USA).

### 12.2.3. Apparatus

The RP-HPLC analyses were carried out using an analytical HPLC system (Jasco, Tokyo, Japan), equipped with a quaternary low pressure gradient HPLC pump (Jasco PU-1580), a degasification unit (Jasco DG-1580-53 3-line degasser), an autosampler (Jasco AS-2057-PLUS), a MD-910 multiwavelength detector (Jasco) and a 7125 Rheodyne injector valve (California, USA). Data acquisition was accomplished using Borwin Controller software, version 1.50 (JMBS Developments, Le Fontanil, France). The column was a Chrompack P 300 RP (polystyrenedivinylbenzene copolymer, 8 µm, 300Å, 150 x 4.6 mm i.d.) (Middleburg, The Netherlands). Spectrophotometric analyses were carried out using a BMG LABTECH's SPECTROstar Nano-microplate, cuvette UV/Vis absorbance reader (Offenburg, Germany).

### 12.2.4. Preparation of BSY proteases

The BSY extract rich in proteases was prepared according to a previous work from Vieira *et al.* (50). After removing the glass beads, the homogenate was centrifuged at 12,000 x g,

40 min at 4°C. The resulting clear supernatant was freeze-dried, resuspended in the same buffer (to 25% of the initial volume) and concentrated using a 10 kDa MWCO membrane. Protease activity, assayed by Sigma's non-specific protease assay method described by Cupp-Enyard (164), was 0.725 U/mL. This extract was kept at -20°C until used.

#### **12.2.5. Preparation of BSG protein fraction**

BSG proteins were extracted according to a previous work with slightly modifications (4). Briefly, BSG without pre-treatment (100 g) was added to 200 mL of 0.5 M KOH solution (ratio 1:2, w/v) for 2 h, 40°C, with continuous shaking. After decantation and centrifugation at 15,000 x g, 4°C during 15 min, the extract was acidified to pH 3 with a solution of 2 M citric acid. Further centrifugation was proceeded to obtain a final residue of BSG protein fraction. No protease activity was found in this protein fraction when evaluated by Cupp-Enyard assay (164). The solubility of BSG protein fraction was determined by the method of Celus *et al.* (7) at different pH levels. The same amount of extract (1 g) was dispersed in 10 mL of different buffers, at 4°C.: (i) 100 mM citrate-phosphate (pH 5.0, 6.0 and 7.0), (ii) 100 mM Tris-HCl (pH 8.0 and 9.0) and (iii) 100 mM glycine-NaOH (pH 10.0). The pH was adjusted and the dispersions were shaken for 1 h at 4°C and then centrifuged at 12,000 x g, at 4°C for 30 min. Protein content of the supernatant was determined following Bradford method (171), using BSA as standard. Protein solubility was expressed as percentage of protein in the solution in comparison to that of total protein in the extract. Based on the best pH results, the freeze-dried extract was dissolved with optimum pH buffer and stored at -20°C for further use.

#### **12.2.6. Enzymatic Hydrolysis**

##### **12.2.6.1. Experimental Design**

RSM, using a Design Expert software (version 7.0, trial Stat-Ease Inc., Minneapolis, MN, USA), was used to investigate the influence of the independent variables (X): time, temperature and enzyme-substrate ratio (U/mg) on the hydrolysis of BSG protein fraction using a BSY protease extract, and to optimize them. The temperature ranged from 35°C to 50°C, time ranged from 2 h to 6 h and E/S ratio ranged from 0.11:1 U/mg to 0.29:1 U/mg. The average of degree of hydrolysis (DH %); total phenolic content (TPC in mg GAE/mL) and antioxidant activity (FRAP in mg TE/mL) were selected as the response (Y). The full CCD method was applied and the experiments were conducted according to the experimental design depicted in Table 12.1.

Totally, 20 runs containing six replicates at the centre point were carried out. All reactions were performed in triplicate, using 2 mL *ependorf* tubes, in a shaking incubator with constant agitation (200 rpm). For all assays, 50 mL of a solution containing 5 mg of BSG

proteins/mL dissolved in tris-HCl was used as substrate for BSY proteases and the pH of hydrolysis reaction was fixed at pH 6.0. Hydrolysis experiments were performed without any pH adjustment and controls were performed using the protein fractions from enzyme and substrate, without any enzymatic treatment. Reactions were finished by heating the solution to 95°C for 15 min, assuring enzyme inactivation. Aliquots (50 µL) of final hydrolysates were withdrawn for colorimetric determination of DH (%). The remaining material was centrifuged at 3,000 x g at 4°C for 10 min to separate the undigested substrate and to collect the hydrolysate material. BSG protein hydrolysates (coded as H1-H20) were kept at -20°C to further studies.

#### **12.2.6.2. Determination of Degree of Hydrolysis (DH %) and Hydrolysis Rate (HR %)**

The degree of hydrolysis (DH%), expressed as the percentage of peptide bonds hydrolysed was determined in triplicate using the TNBS method, as described by Hsu *et al.* (238). BSG protein hydrolysis was also evaluated through RP-HPLC, using the chromatographic conditions described by Ferreira *et al.* (185). HR (%) was calculated based on the measurement of protein fraction (eluted between 40 and 50 min) that remains intact after hydrolysis.

#### **12.2.6.3. Determination of total phenolic content (TPC)**

The TPC was measured using the Folin-Ciocalteu method, as previously described by Herald *et al.* (155). This assay measures the ability of a compound to reduce the yellow oxidising Folin-Ciocalteu reagent to a blue/green colour; absorbance is measured spectrophotometrically at 765 nm. Gallic acid was used as a standard at 10-500 µM to produce a calibration curve (average  $R^2 = 0.9983$ ) and results were expressed as mg of Gallic Acid equivalent per mL of sample (mg GAE/ mL).

#### **12.2.6.4. Ferric Ion Reducing Antioxidant Power (FRAP) assay**

The antioxidant activity was estimated according to the procedure of Jansen and Ruskovska method (154). This assay is based on the principle of the reduction of the ferric-tripyridyltriazine complex to the ferrous form, upon which an intense blue colour develops and the change of absorbance is measured at 595 nm. Trolox, a water-soluble analogue of tocoferol, was used as standard at 10-500 µM to generate a calibration curve (average  $R^2 = 0.9975$ ) and results were expressed as mg of Trolox equivalent per mL of sample (mg TE/mL).

#### **12.2.7. Effect of potential inhibitors on BSG protein hydrolysis by BSY proteases**

Since BSY proteases showed higher activity on BSG proteins at pH 6.0, the potential presence of natural inhibitors was evaluated, according to the protocol described by Bolumar *et al.* (326), with slight modifications. BSY protease extract was split into two aliquots: the first was kept at pH 7.0, the second was adjusted to pH 5.0; both extracts were incubated at 25°C for 20 h. Then, the activity of BSY proteases on BSG proteins was assessed at 50°C and pH 6.0. Respective control of BSY proteases, kept at pH 5 and 6 and incubated at 25°C for 20 h, without the addition of BSG protein were assayed simultaneously. The reaction was stopped by adding 10% (w/v) trichloroacetic acid (TCA) and the absorbance of the soluble TCA peptides was examined at 280 nm. The percentage activity in inhibition assays was reported considering 100% activity in the absence of inhibitor. Additionally, the effect of inhibitors of BSY proteases on BSG proteins was studied in order to identify the type of catalytic peptidases responsible for the hydrolysis of BSG proteins. The following inhibitors were used: phenylmethylsulfonyl fluoride (PMSF) for serine peptidases; EDTA for metallopeptidases; bestatin for aminopeptidases (metallopeptidases); pepstatin A for aspartic acid peptidases and E-64 for the cysteine peptidases. The procedure used was according to Garcia-Carreño (327) and is outlined in Table 12.2. Each inhibitor was added so that the final concentration was 0.01 and 0.05 mM pepstatin A, E-64 and Bestatin; 1 and 2 and 10 mM PMSF and 20 mM EDTA. The concentrations of each inhibitor was chosen according to the manufacturer's instructions. The BSY peptidases activity in the absence of inhibitors was determined by adding buffer instead of inhibitor. In order to investigate the potential inhibitory effect of the solvent on the activity of BSY peptidases, a solvent control (methanol) was prepared. Additionally, to eliminate the effect of absorption of the inhibitor and the enzyme extract, two blanks (inhibition blank and blank activity) were prepared. The reaction was stopped by adding 10% (w/v) trichloroacetic acid (TCA) and the absorbance of the soluble TCA peptides was examined at 280 nm. Residual activity was calculated as relative (%) considering control treatments as 100%.

Table 12.2. Procedure for studying the effect of inhibitors of BSY proteases on BSG proteins

Conditions	Inhibition	Inhibition Blank	Activity	Blank activity	Solvent Control
Buffer <sup>a</sup>	+	+	+	+	+
Inhibitor <sup>b</sup>	+	+	-	-	-
Enzyme	+	+	+	+	+
Solvent <sup>c</sup>	-	-	-	-	+
Incubation	25°C, 60 min, pH 6.0				
TCA 10%	-	+	-	+	-
Substrate	+	+	+	+	+
Incubation	50°C, 30 min, pH 6.0				
TCA 10%	+	-	+	-	-
Incubation	Room temperature, 30 min				
Centrifugation	10,000 x g, 10 min				
Measure	280 nm				

<sup>a</sup> 100 mM sodium phosphate, pH 6.0.<sup>b</sup> PMSF, EDTA, bestatin, pepstatin A, or E-64.<sup>c</sup> methanol.

+ means that this condition was included.

### 12.2.8. Statistical analysis

All measurements were done in triplicate and data were reported as mean  $\pm$  standard deviation. The statistical analyses were done using Design-Expert software version 7.0 (Stat-Ease, Inc., USA). Analysis of variance (ANOVA) was performed and regression coefficients of linear, quadratic, and interaction terms were determined. Adequacy of the model was evaluated using model analysis, coefficient of determination ( $R^2$ ), and lack of fit test. Significance of the equation was determined by  $F$  value at a probability ( $p > F$ ) less than 0.05. The regression coefficients were employed to create contour plots using the regression models.

## 12.3. RESULTS AND DISCUSSION

### 12.3.1. Influence of pH on solubility and hydrolysis of BSG protein fraction

The protein rich isolate from BSG contained 49.1% (dw) protein, as determined by Kjeldahl method, which is in agreement with the content outlined by other authors (4), (307). Preliminary experiments were performed using a univariate method to study the influence of pH on solubility of BSG proteins using 5 mg of protein/mL. Figure 12.1.A shows the BSG

protein solubility at different pH levels. Low solubility (10%) was found at pH 6. The isoelectric point is probably around pH 5. Solubility reached its maximum value between pH 8 and pH 9 (100). These results are in agreement with those reported by Celus *et al.* (7). The effect of pH on the hydrolysis of BSG proteins by BSY proteases was determined at a pH range of 5-10 and at a temperature of 37°C, for 4 h. The results obtained are presented in Figure 12.1.B and show that BSY proteases acted on BSG proteins on the studied pH range. At pH 6-7, BSY proteases showed higher activity, being pH 6 the optimum pH for BSG protein hydrolysis. Moreover, results showed that when hydrolysis was performed at pH 6, the pH value remained in the range of 5.8 to 6.4 during the entire hydrolysis period. The same range of pH variation was observed when hydrolysis was performed at pH 5 and 8. For this reason, in accordance with other authors, it was decided not to adjust the pH during BSG protein hydrolysis, which constitutes an economical advantage.

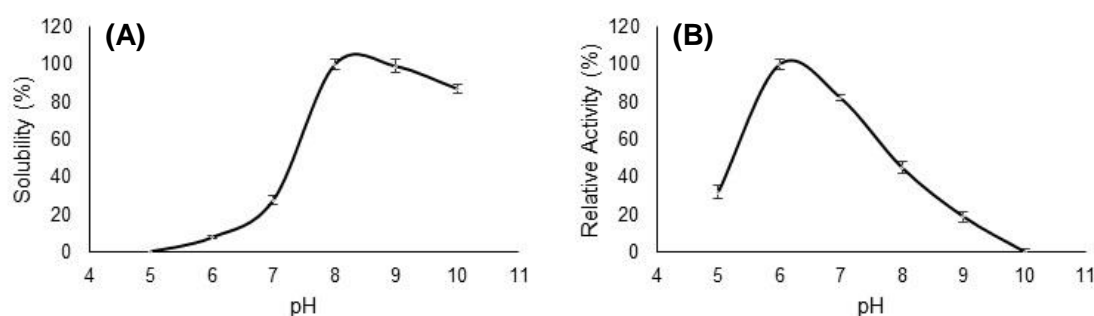


Figure 12.1. Effect of pH on solubility of BSG protein fraction, at 25°C, **(A)**. Effect of pH on hydrolysis of BSG protein fraction by BSY proteases, at 37°C, **(B)**. Relative Activity (%) was estimated considering 100% the highest activity detected in this assay.

### 12.3.2. Central composite design and response surface method

The experimental conditions and values of DH%, TPC and FRAP assays of BSG protein hydrolysates are reported in Table 12.1. Results showed that the DH (%) ranged from 8.90% (H9: 30°C, 4.0 h, E/S: 0.20:1) to 17.1% (H8: 50 °C, 6.0 h, E/S: 0.29:1); TPC ranged from 1.10 mg GAE/mL (H1: 35°C, 2.0 h, E/S: 0.11:1) to 1.65 mg GAE/mL (H8: 50°C, 6.0 h, E/S: 0.29:1) and the antioxidant activity, evaluated by FRAP assay, ranged from 0.55 mg TE/mL (H13: 43°C, 4.0 h, E/S: 0.05:1) to 1.88 mg TE/mL (H8: 50°C, 6.0 h, E/S: 0.29:1).

The model summary and the results obtained from ANOVA are detailed on Table 12.3. The adequacy of the 2FI model was evaluated by means of Fisher's *F*-test. The model *F* value for DH, TPC and FRAP responses were, respectively, 17.58, 46.25 and 123.22, indicating the significance of the model. The linear terms (*X*<sub>1</sub>, *X*<sub>2</sub>, *X*<sub>3</sub>) and the quadratic

terms ( $X1^2$ ,  $X2^2$ ,  $X3^2$ ) had a significant effect ( $p < 0.01$ ) on the three responses. The cross-product ( $X1.X2$  and  $X1.X3$ ) terms presented values of prob  $> F$  less than 0.05, that denotes that they are significant terms for the Y1 and Y3 responses; the cross-product  $X2.X3$  had a significant effect on Y2 response. The quadratic models can be used for monitoring the effects of hydrolysis conditions on the DH, TPC and FRAP of BSG proteins digested by BSY proteases. Coefficient of determination ( $R^2$ ) for checking the fitness of model were close to 1, which indicated that models explained, respectively, 88.7%, 95.5%, and 98.3% of the variation in the hydrolysis conditions on the DH, TPC and FRAP of BSG proteins. "Adeq Precision" was higher than 4 for the three responses, indicating an adequate signal-to-noise ratio. Moreover, the statistical analysis of variance also revealed that there was a non-significant ( $p > 0.05$ ) lack of fit, which further validates the model. Thus, the response surface 2FI model is adequate and significant. Equations (1), (2) and (3) shows the dependence of DH (Y1), TPC (Y2) and FRAP (Y3) on temperature ( $X1$ ), time ( $X2$ ) and E/S ratio ( $X3$ ), respectively. The parameters of the equation were obtained by multiple regression analysis of the experimental data.

$$Y1 = -307.41 + 0.60.X1 - 0.96.X2 - 1.29.X3 + 0.05.X1.X2 + 100.00.X1.X3 - 877.X1^2 - 0.11.X2^2 - 5.44.X3^2 \quad (1)$$

$$Y2 = -215.34 + 0.11.X1 + 0.11.X2 + 625.76.X3 - 99.8.X1^2 - 471.X2^2 - 706.34.X3^2 \quad (2)$$

$$Y3 = -228.15 + 0.11.X1 + 0.02.X2 - 0.20.X3 + 303.X1.X2 + 0.12.X1.X3 + 0.28.X2.X3 - 131.X1^2 - 0.01.X2^2 - 735.11.X3^2 \quad (3)$$

### 12.3.3. The effect of temperature, time and E/S ratio on the response value

Curve analysis of response surfaces for experimental design allowed prediction of response function of the effects of the temperature, time and E/S ratio. Model equations are visualized in the form of three-dimensional surface plots, which are constructed by plotting the response on the Z-axis against any two independent variables, while maintaining other variables at their optimal levels. As shown in Figure 12.2, the DH, TPC and FRAP increased at hydrolysis conditions at pH 6.0 until temperature, time and E/S ratio reached an optimum point of 50°C, 6 h and an E/S ratio of 0.29:1 U/mg. BSG protein hydrolysate prepared under these conditions (H8, Table 12.1) presented DH % of 17.10%, TPC of 1.65 mg GAE/mL and FRAP value of 1.88 mg TE/ mL. In terms of antioxidant activity, surface plots indicated that the same optimum conditions for higher DH may be favourable to enhance the

antioxidant properties of the BSG protein hydrolysate. Since some free amino acids and small peptides have been found to possess antioxidant activity, it seems that extension of hydrolysis may be favourable to enhance the antioxidant properties of the hydrolysate (328).

Table 12.1. Experimental design for evaluation of the effects of hydrolysis conditions at pH 6.0 on Hydrolysis Degree (DH %), total phenolic content (TPC) and FRAP assay of BSG protein fraction by BSY proteases

Point <sup>a</sup>		T (°C)	t (h)	E/S ratio	DH (Y1, %)		TPC (Y2, mg GAE/mL)		FRAP (Y3, mg TE/mL)	
code	run	X1	X2	X3	Exp <sup>b</sup>	Pred <sup>c</sup>	Exp <sup>b</sup>	Pred <sup>c</sup>	Exp <sup>b</sup>	Pred <sup>c</sup>
H3	1	35.0	6.0	0.11	9.50	9.86	1.27	1.24	0.75	0.69
H2	2	50.0	2.0	0.11	10.50	11.20	1.35	1.34	0.80	0.77
H6	3	50.0	2.0	0.29	14.20	14.25	1.59	1.59	1.31	1.36
H4	4	50.0	6.0	0.11	13.10	13.72	1.52	1.50	1.12	1.11
H12	5	43.0	7.4	0.20	13.90	13.51	1.60	1.60	1.35	1.36
H13	6	43.0	4.0	0.05	11.60	10.72	1.12	1.17	0.55	0.62
H7	7	35.0	6.0	0.29	11.10	10.82	1.52	1.50	1.14	1.15
H10	8	55.0	4.0	0.20	16.20	15.42	1.59	1.58	1.46	1.44
H8	9	50.0	6.0	0.29	17.10	17.38	1.65	1.67	1.88	1.90
H17	10	43.0	4.0	0.20	13.50	13.65	1.57	1.54	1.26	1.23
H20	11	43.0	4.0	0.20	13.80	13.65	1.58	1.54	1.20	1.23
H15	12	43.0	4.0	0.20	13.90	13.65	1.54	1.54	1.25	1.23
H16	13	43.0	4.0	0.20	14.50	13.65	1.53	1.54	1.20	1.23
H11	14	43.0	0.6	0.20	11.40	11.20	1.34	1.38	0.76	0.77
H9	15	30.0	4.0	0.20	8.90	9.09	1.14	1.19	0.56	0.60
H5	16	35.0	2.0	0.29	10.80	10.59	1.41	1.40	0.80	0.79
H18	17	43.0	4.0	0.20	12.40	13.65	1.52	1.54	1.25	1.23
H14	18	43.0	4.0	0.35	13.80	14.09	1.61	1.60	1.55	1.50
H1	19	35.0	2.0	0.11	10.10	10.24	1.10	1.05	0.56	0.52
H19	20	43.0	4.0	0.20	13.70	13.65	1.52	1.54	1.21	1.23

<sup>a</sup> Experiments were conducted in a random order; <sup>b</sup> Average of triplicate determinations from different experiments; <sup>c</sup> Predicted values based on CCD evaluation.



Table 12.3. Model summary and analysis of variance (ANOVA) for DH% (Y1), TPC (Y2) and FRAP (Y3)

Source	Sum of Squares			Mean Square			F value			p-value		
	Y1	Y2	Y3	Y1	Y2	Y3	Y1	Y2	Y3	Y1	Y2	Y3
Model	84.31	0.55	2.44	9.37	0.062	0.27	17.58	46.25	123.22	< 0.0001*	< 0.0001*	< 0.0001*
X1- °C	48.28	0.18	0.84	48.28	0.18	0.84	90.59	132.40	380.91	< 0.0001*	< 0.0001*	< 0.0001*
X2- h	6.48	0.063	0.42	6.48	0.063	0.42	12.15	47.42	192.03	0.0059*	< 0.0001*	< 0.0001*
X3- E/S	13.74	0.22	0.95	13.74	0.22	0.95	25.79	165.91	429.72	0.0005*	< 0.0001*	< 0.0001*
X1.X2	4.21	3.001E <sup>-004</sup>	0.016	4.21	3.001E <sup>-004</sup>	0.016	7.89	0.23	7.48	0.0185**	0.6452	0.0210**
X1.X3	3.65	4.950E <sup>-003</sup>	0.050	3.65	4.950E <sup>-003</sup>	0.050	6.84	3.72	22.52	0.0258**	0.0827	0.0008**
X2.X3	0.18	3.321E <sup>-003</sup>	0.020	0.18	3.321E <sup>-003</sup>	0.020	0.34	2.49	9.05	0.5740	0.1454	0.0132**
X1 <sup>2</sup>	3.51	0.045	0.079	3.51	0.045	0.079	6.58	34.13	35.74	0.0281**	0.0002*	0.0001*
X2 <sup>2</sup>	3.02	5.122E <sup>-003</sup>	0.047	3.02	5.122E <sup>-003</sup>	0.047	5.67	3.85	21.31	0.0385**	0.0783	0.0010*
X3 <sup>2</sup>	2.79	0.047	0.051	2.79	0.047	0.051	5.24	35.43	23.20	0.0451**	0.0001*	0.0007*
Residual	5.33	0.013	0.022	0.53	1.332E <sup>-003</sup>	2.202E <sup>-003</sup>	1.23	3.67	4.35	0.4140	< 0.0001*	0.0663
Lack of Fit	2.94	0.010	0.018	0.59	2.093E <sup>-003</sup>	3.581E <sup>-003</sup>						
Pure Error	2.39	2.852E <sup>-003</sup>	4.119E <sup>-003</sup>	0.48	5.703E <sup>-004</sup>	8.238E <sup>-004</sup>						
Total	89.64	0.57	2.46									
<hr/>												
R <sup>2</sup> pred (Y1) = 0.7125		R <sup>2</sup> adj (Y1) = 0.8870		ratio = 16.055								
R <sup>2</sup> pred (Y2) = 0.8523		R <sup>2</sup> adj (Y2) = 0.9554		ratio = 23.935								
R <sup>2</sup> pred (Y3) = 0.9417		R <sup>2</sup> adj (Y3) = 0.9830		ratio = 41.409								

Y1, Degree of hydrolyses (DH %); Y2, Total Phenolic Content (mg GAE/mL); Y3, Antioxidant activity determined by FRAP assay (mg TE/mL).

\* Significance at  $p < 0.01$ . \*\* Significance at  $p < 0.05$ .

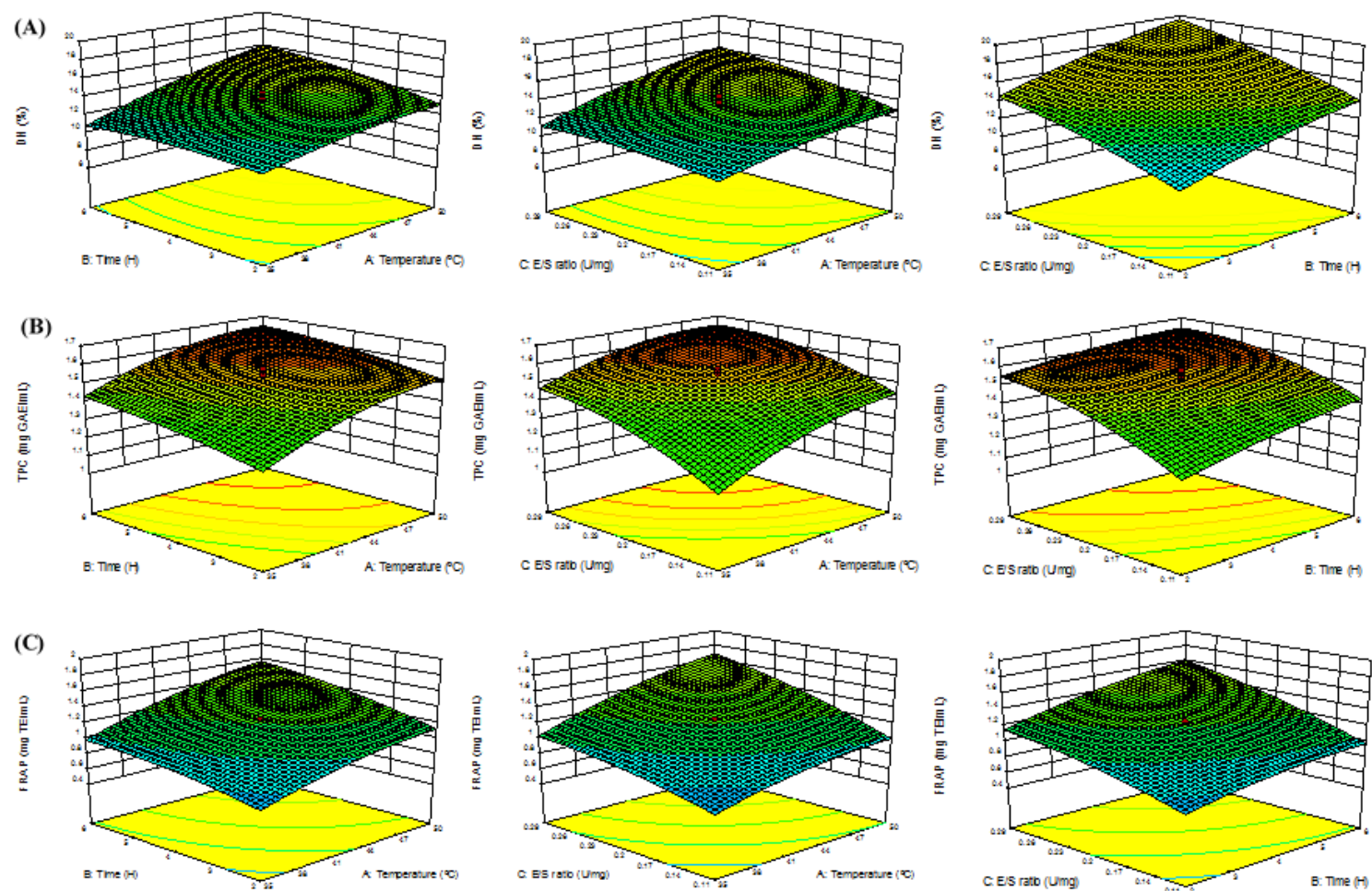


Figure 12.2. Response surface plots for the effects of variable incubation temperature (°C), incubation time (h) and E/S ratio (U/mg) on the responses: **(A)** Degree of Hydrolysis (DH %); **(B)** Total Phenolic contents (TPC) and **(C)** Antioxidant activity (FRAP assay).

#### 12.3.4. Validation of the RSM model

Desirability indices were constructed to obtain the optimum experimental conditions to maximize the bioactivities of BSG protein hydrolysate. The confirmatory experiments were conducted with the parameters suggested by experimental model, in three different runs, and the *t* test was applied to compare the DH, TPC and FRAP values of BSG protein hydrolysates prepared under optimized conditions at pH 6.0 with those predicted by models. BSG protein hydrolysate prepared at 50°C, 6.0 h and E/S ratio of 0.29:1 U/mg showed the maximum results for the three responses. Under these hydrolysis conditions, the experimental values of DH, TPC and FRAP were, respectively, 17.6%, 1.68 mg GAE/mL and 1.84 mg TE/mL; and the predicted values, were respectively, 17.4%, 1.67 mg GAE/mL and 1.90 mg TE/mL. These results showed that there is no statistically significant difference between the experimental and estimated values within a 95% confidence interval for the three responses. Thereby, the adequacy of the models in predicting the optimum hydrolysis condition was confirmed.

#### 12.3.5. Hydrolysis monitoring by RP-HPLC

Hydrolysis was also monitored by RP-HPLC. Figure 12.3 shows the RP-HPLC profiles of BSG protein hydrolysates with different DH. As elution was monitored at 214 nm, this implies that the level of smallest peptides is underestimated. Chromatographic profiles showed that peak area of "Polypeptide fraction" increased with increasing DH, being significantly higher ( $p < 0.05$ ) for H8, prepared at 50°C, 6.0 h, E/S: 0.29:1 U/mg. Furthermore, strong correlations were found between measurements from HR (%) and DH (%) ( $R^2 = 0.8861$ ).

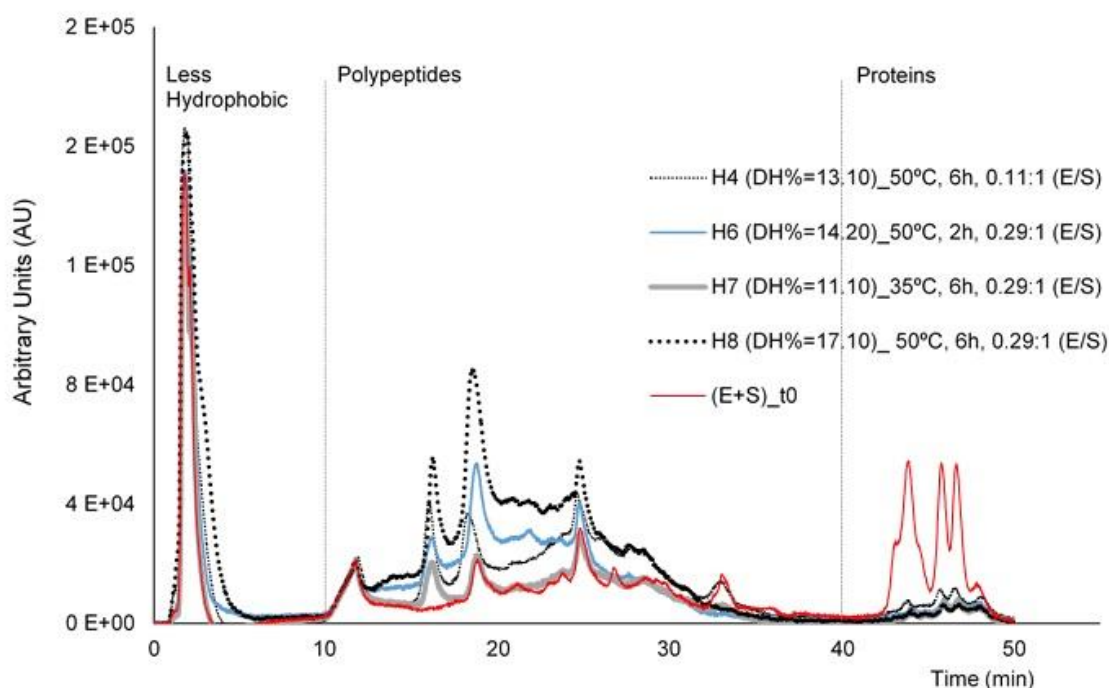


Figure 12.3. Chromatograms obtained by RP-HPLC analysis of BSG proteins hydrolysates (n=3).

#### 12.3.6. Effect of potential natural inhibitors on BSY proteases activity over BSG proteins

*Saccharomyces cerevisiae* yeast, a species related to *Saccharomyces pastorianus*, contains various peptidases, including serine peptidases (peptidase B, carboxypeptidase Y and carboxypeptidase K) and metallopeptidases (aspartyl metallopeptidase, peptidase D and carboxypeptidase S). These enzymes, as well, some potential enzyme inhibitors, are localized in the cytoplasm and usually have optimal activity at pH 6-7 (11). Following disruption of yeast cells, complexes are formed between the inhibitor and vacuole peptidases. Therefore, to inactivate the endogenous inhibitors of vacuole peptidases different strategies, such as, long incubation periods at 25°C and acid pH have been used (327), (328).

In this work, the BSY proteases activity over BSG proteins (at 50°C, pH 6.0) was evaluated after incubation of the BSY at 25°C, 20 h, at pH 5 and 7. Results indicated that after 20 h of incubation at pH 7 and 25°C, the activity of BSY proteases over BSG proteins was reduced by about 31% compared to the activity observed in the beginning of treatment (results not shown). This result suggests the presence of potential natural inhibitors of vacuole peptidases, which were not inactivated under extended periods of incubation, at pH 7 and 25°C. On the other hand, after incubation at 25°C and pH 5 for 20 h, it was found

that the activity of BSY peptidases was doubled compared to activity observed in the beginning of treatment (results not shown), suggesting no effect of natural inhibitors of vacuole peptidases in the hydrolysis of BSG proteins, presumably due to its inactivation at pH 5 and 25 °C during 20 h.

#### **12.3.7. Effect of potential inhibitors on BSY proteases activity over BSG proteins**

The effect of inhibitors on the BSY proteases activity over BSG proteins was also evaluated in order to ascertain which type of catalytic peptidases are responsible for the hydrolysis under optimal conditions of temperature and pH (50°C and pH 6.0). Results presented in Table 12.4 show that none of the inhibitors reduced more than 50% of BSY proteases activity over BSG proteins and no inhibition was observed in the presence of Pepstatin A and E-64 at concentrations of 0.01 mM and 0.05 mM. The weak inhibition caused by these two inhibitors at the higher concentration used, which suggest that the enzymes present in BSY responsible for hydrolysis of BSG proteins under the assay conditions are not cysteine peptidases and aminopeptidases (type catalytic metallopeptidases). On the other hand, EDTA, at a concentration of 20 mM, reduced 50% the activity of BSY proteases and PMSF, at a concentration of 2 mM, reduced by approximately 31% of BSY activity over BSG proteins. The main BSY proteases responsible for the hydrolysis of BSG proteins, under the optimum conditions, can belong to the class of serine peptidases and metallopeptidases. However, as BSY contain a mixture of various peptidases and compounds, this can lead to erroneous conclusions. In fact, some components of the BSY may affect the enzyme-inhibitor binding and, moreover, the active site of the peptidases may not be truly accessible to binding of the inhibitor (329). Thus, it would be necessary to purify the BSY proteases in order to confirm the catalytic type (s) of peptidase (s) that is (are) responsible (s) for its hydrolysis.

Table 12.4. Effect of inhibitors on BSG protein hydrolysis by BSY proteases

Synthetic Inhibitors	Catalytic type	Concentration (mM)	Residual enzyme activity (%) <sup>a</sup>
Pepstatin A	Aspartic acid	0.01	105 ± 1.58
		0.05	103 ± 2.04
E-64	Cystein	0.01	107 ± 3.08
		0.05	91 ± 0.98
PMSF	Serine	1	95 ± 1.18
		2	69 ± 2.12
EDTA	Metallo	10	71 ± 1.78
		20	50 ± 2.01
Bestatin	Metallo (aminopeptidases)	0.01	102 ± 1.05
		0.05	93 ± 1.04

<sup>a</sup> % Residual enzyme activity was the remaining activity after 60 min incubation of enzyme with corresponding inhibitor. Data represents the mean ± standard deviations of three replications.

## 12.4. CONCLUSIONS

The present study showed that the BSG proteins were effectively hydrolysed by BSY proteases; the final protein hydrolysates presented improved biological properties, namely, better TPC and FRAP activity. RSM was an efficient statistical methodology to optimize the hydrolysis conditions; high DH (%) led to high TPC and antioxidant activity. The highest TPC (1.65 mg GAE/mL) and FRAP value (1.88 mg TE/mL) was achieved using an E/S ratio of 0.29:1 U/mg, a reaction time of 6 h, a reaction temperature of 50°C and a reaction pH of 6.0. The experimental values agreed with the predicted value within a 95% confidence interval, suggesting a good fit between the models and the experimental data. Good agreement was observed with RP-HPLC results. Apparently, the main BSY proteases responsible for the hydrolysis of BSG proteins, under the optimum conditions, probably belong to the class of serine peptidases and metallopeptidases. The reuse of these two agro-industrial by-products is advisable from both economic and environmental standpoints.

## CHAPTER 13

*Antioxidant and ACE inhibitory activities of hydrolysates of brewers' spent grain proteins by proteases from spent yeast or by commercial enzymes: protective capacity in Caco-2 and HepG2 cells*

---

This chapter compares the biological activities of different BSG protein hydrolysates prepared by BSY proteases and two commercial enzymes: Alcalase® and Neutrase®.





## ABSTRACT

Protein fraction of Brewers' spent grain (BSG) was used as substrate to obtain bioactive hydrolysates. Three enzymatic approaches were applied to perform the hydrolysis: Brewer's spent yeast (BSY) proteases, Neutrase® and Alcalase®, at the same proteolytic activity (1 U/mL), using an E/S of 0.10:1 U/mg, at 50°C, for 4 h. BSG hydrolysates DH%, PR%, proximate composition, molecular weight distribution and hydrophobicity were compared. Moreover, hydrolysates and their <10 kDa and <3 kDa fractions were tested for antioxidant and ACE-I activities. The effect of <10 kDa fractions on Caco-2 and HepG2 cell lines viability, mitochondrial membrane potential and oxidative stress was also investigated. Hydrolysates produced by Alcalase® presented significantly ( $p < 0.05$ ) higher ACE-I activity ( $IC_{50}$  0.385 mg protein/mL) and antioxidant capacity by TPC and FRAP assays (0.083 mg GAE/mg dw; 0.101 mg TE/mg dw, respectively) than other hydrolysates. Fractions <3 kDa of hydrolysates from BSY proteases and from Neutrase® presented enhanced ACE-I activities, whereas <10 kDa fraction presented increased TPC and FRAP values ( $p < 0.05$ ). The fraction <10 kDa of BSG protein hydrolysates exerted a protective effect against free-radical induced cytotoxicity in Caco-2 and HepG2 cells. Therefore, these BSG protein hydrolysates may be useful functional ingredients.

## 13.1. INTRODUCTION

Brewers' spent grain (BSG) is the insoluble fraction of wort separated after the mashing phase of beer production. It is the major by-product from brewing process and is mainly composed by a lignocellulosic material and proteins, with high glutamine and proline contents (7). The protein content of BSG is approximately 20% (dw basis) and hordeins account for over 50% of the total proteins (4), (309). Although BSG main use is for animal feeding, other possible applications have been studied, because it presents high potential to be used for production of protein hydrolysates with biological properties (7), (307-309).

The conditions employed on enzymatic hydrolysis, mainly the type of protease and the degree of hydrolysis, affect the peptides composition, as well as, the hydrolysates bioactivity (330). Commercially available enzymes have been commonly employed to undertake the hydrolytic process; these include Alcalase, Pepsine, Trypsin, Flavourzyme, Protamex, Prolyve, Promod, Corolase PP, among others (253), (307), (309). Our group has experience on the hydrolysis of BSG protein fraction using an enzyme extract from BSY. These hydrolysates present a DH of 17.6%, TPC of 1.65 mg GAE/mL and FRAP of 1.88 mg TE/mL. However, besides conventional chemical assays for screening the antioxidant

activity of BSG protein hydrolysates, it is important to study the biological effects using *in vitro* cell models, which mimic the target site of oxidative stress *in vivo*. The human intestinal epithelial cell line (Caco-2) and the human hepatocarcinoma cell line (HepG2) have been considered reliable models widely used for biochemical and nutritional studies (331-337). Although BSG protein hydrolysates exhibit *in vitro* antioxidant activity in chemical assays, little information is available regarding their antioxidant ability on cell-based models.

BSG protein hydrolysates exhibiting antioxidant potential may also contain peptides with other biological activities, such as, ACE-I activity. ACE inhibition plays a key role in the treatment of hypertension and ACE-I peptides are generally small sized peptides, less than 3 or 5 kDa, often carrying polar amino acid residues, such as, proline (253), (330). Few studies have focused on the production of BSG hydrolysates with ACE-I effects. In fact, Connolly *et al.* (253) reported for the first time the ability of BSG protein hydrolysates to inhibit ACE; BSG proteins hydrolyzed with Alcalase, Flavourzyme and Corolase resulted in an IC<sub>50</sub> of 0.32 mg protein/mL, 0.69 mg protein/mL and 0.50 mg protein/mL, respectively. No studies have yet reported the ability of BSG protein hydrolysates produced by BSY proteases to inhibit ACE.

The aims of the present study were (i) to compare the capacity of proteases extracted from BSY to hydrolyze the BSG protein substrate with that of two commercially available proteases, Neutrase® and Alcalase®; (ii) to assess the potential bioactivity of the hydrolysates obtained by measuring the *in vitro* antioxidant and ACE-I activities and (iii) to measure the ability of these hydrolysates to protect Caco-2 and HepG2 cell lines regarding cell viability, mitochondrial integrity and oxidative stress.

## 13.2. MATERIAL AND METHODS

### 13.2.1. Reagents and cells

Unless otherwise stated, all chemicals were purchased from Sigma-Aldrich (St. Louis, MO, USA) and the cell culture reagents were purchased from Gibco® (Invitrogen Corporation, Paisley, UK). Neutrase® (EC.3.4.24.28) and Alcalase® (EC 3.4.21.62) were purchased from Sigma-Aldrich (St. Louis, MO, USA) and ABz-Gly-Phe(NO<sub>2</sub>)-Pro was purchased from Bachem Feinchemikalien (Bubendorf, Switzerland). The Millipore UF membranes with a MWCO of 3 and 10 kDa were purchased from Sigma-Aldrich (St. Louis, MO, USA). Ultrapure water was obtained from a Seralpur Pro 90 CN water purification. Caco-2 and HepG2 cell lines were obtained from the American Type Culture Collection (ATCC). Dulbecco's modified eagle's medium (DMEM) with high glucose, heat-inactivated fetal bovine serum (FBS), 0.25% trypsin/1 mM EDTA, antibiotic solution (10,000 U/mL penicillin,

10,000 µg/mL streptomycin), Hanks balanced salt solution (HBSS) were purchased from Invitrogen Corporations (Paisley, UK).

### 13.2.2. Equipments

The RP-HPLC analysis was carried out using an analytical HPLC system (Jasco, Tokyo, Japan), equipped with a quaternary low pressure gradient HPLC pump (Jasco PU-1580), a degasification unit (Jasco DG-1580-53 3-line degasser), an autosampler (Jasco AS-2057-PLUS), a MD-910 multiwavelength detector (Jasco) and a 7125 Rheodyne injector valve (California, USA). The data acquisition was accomplished using Borwin Controller software, version 1.50 (JMBS Developments, Le Fontanil, France). SE-HPLC analyses were performed using a Gilson HPLC system (Gilson Medical Electronics, France), equipped with a type 302 pump, a Gilson 118 variable wavelength ultraviolet detector and a 7125 Rheodyne injector. The equipment was controlled by a Gilson 712 software. Spectrophotometric analyses were carried out using a BMG LABTECH's SPECTROstar Nano-microplate, cuvette UV/Vis absorbance reader (Offenburg, Germany). Fluorimetric analyses were carried out using a fluorescence microplate reader (FLUOstar Optima, BMG Labtech GmbH).

### 13.2.3. BSG protein extraction

BSG was supplied by Unicer brewing (Leça do Balio, Portugal). BSG protein substrate was prepared by alkaline extraction and subsequent acid precipitation, as previously described by Vieira *et al.* (4). Briefly, BSG (100 g) was added to 200 mL of 0.5 M KOH solution (ratio 1:2, w/v) for 2 h at 40°C, with continuous shaking. After centrifugation at 15,000 x *g*, at 4°C during 15 min, the extract was acidified to pH 3 with a solution of 2 M citric acid. The final residue of BSG presented a protein content of 49.13% dw (based on the Kjeldahl method) and maximum solubility in Tris-HCl buffer, pH 8.0.

### 13.2.4. BSY proteases and commercial enzymes

BSY, supplied by Unicer brewing (Leça do Balio, Portugal), was collected from the brewery with four reuses in the fermentation process. The BSY extract rich in proteases was prepared according to a previous work (177). Proteolytic activity, determined by Sigma's non-specific protease method described by Cupp-Enyard (164), was 1 U/mL. Commercially available enzymes Neutrase® and Alcalase® were used at the same activity levels to compare hydrolysis efficiencies. For this purpose, Neutrase® and Alcalase® were diluted in the respective buffer, sodium phosphate buffer pH 7.0 and 100 mM Tris-HCl pH 8.0, to have the same proteolytic activity of 1 U/mL.

### 13.2.5. Preparation of Brewers' spent grain protein hydrolysates

A BSG protein solution of 15 mg of protein/mL (based on Lowry assay) (163) was used as substrate for the three enzymatic treatments. Hydrolysis of BSG proteins were performed with the BSY extract, with Neutrase® and with Alcalase®, according to the conditions described in Table 13.1. Triplicate assays using a final volume of 100 mL were performed for each enzyme, using a thermostatically controlled water bath with constant shaking and without pH adjustment. Control assays were performed using substrate and enzyme, without any incubation treatment. The hydrolysates (coded as BSYH, NTH and ALH) were heated at 95°C for 15 min, assuring the enzymes inactivation. A volume of 400 µL of hydrolysates was withdrawn for determination of the DH (%) and PR (%). Then, the remaining mixture was centrifuged (5,000 x g; 20 min; 4°C) to collect the hydrolysate material. Half volume of the supernatant was subjected to UF, the other half volume was lyophilized and kept at -20°C for further chemical and molecular weight characterization.

### 13.2.6. Determination of Degree of Hydrolysis (DH %) and Protein Recovery (PR %)

The degree of hydrolysis (DH %), expressed as the percentage of peptides bonds hydrolyzed was determined in triplicate using the TNBS method, as described by Hsu *et al.* (238). The α-amino acids were expressed in terms of L-leucine and the DH% was determined using the following equation:

$$DH (\%) = [(Lt - L0)/(Lmax - L0)] \times 100 \quad (1)$$

where Lt corresponded to the amount of α-amino acid released after 30 min. L0 was the amount of α-amino acid in original BSG protein substrate. Lmax was the maximum amount of α-amino acid in BSG protein substrate obtained after acid hydrolysis (6 M HCl at 105°C for 24 h).

Protein recovery (PR %) was calculated as the amount of protein present in the final hydrolysate relative to the initial amount of protein present in the reaction mixture (control), using the following equation:

$$PR (\%) = 100 - \left[ \left( \frac{\text{protein content after hydrolysis}}{\text{protein content before hydrolysis}} \right) \times 100 \right] \quad (2)$$

Protein content was determined using the Lowry's method (163).

Table 13.1. Conditions used for preparation of BSG protein hydrolysates

Enzyme	Activity (U/mL)	Optimum Conditions				Enzyme composition	Enzyme Source
		pH	T (°C)	Time (h)	E/S ratio <sup>(iii)</sup>		
BSY proteases	1 <sup>(i)</sup>	6.0	50	6	10	Serine and Metalloproteases	<i>Saccharomyces pastorianus</i>
Neutrase®	1 <sup>(ii)</sup>	7.0	50	6	10	Metalloprotease	<i>Bacillus amyloliquefaciens</i>
Alcalase®	1 <sup>(iii)</sup>	8.0	50	6	10	Alkaline serine endopeptidase	<i>Bacillus licheniformis</i>

<sup>(i)</sup> Proteolytic activity determined by the Sigma's non-specific protease assay.

<sup>(ii)</sup> Proteolytic activity obtained after dilution of the commercially available enzyme with respective buffer: 100 mM sodium phosphate buffer (pH 7); 100 mM Tris-HCl (pH 8.0).

<sup>(iii)</sup> E/S ratio of 0.10:1 U/mg (10 mL enzyme for 100 mL of BSG protein solution of 15 mg of protein/mL (based on the Lowry method).

### **13.2.7. Characterization of BSG protein hydrolysates**

#### **13.2.7.1. Proximate composition analysis**

Lyophilized BSG protein hydrolysates were analyzed in terms of protein content (total nitrogen was determined by the Kjeldahl method  $\times 6.25$ ), fat content (Soxhlet extraction with n-hexane for 12 h), ash content (incineration in a muffle furnace at 550°C until the ash had a white appearance) and dry matter (oven at 105°C until constant weight), determined according to AOAC official methods (144). All assays were performed in triplicate and the contents were expressed on a dry weight basis (% dw).

#### **13.2.7.2. Molecular weight distribution profile**

Molecular weight distributions of BSG protein hydrolysates were determined by SE-HPLC. The column used was a PSS Proteoma Analytical 100 Å column (Amersham Biosciences, UK), equilibrated with 50 mM sodium phosphate buffer, 0.15 M NaCl, pH 6.6 at a flow rate of 0.5 mL/min and calibrated using a standard mixture of eleven molecular weight markers: Myosin (205 kDa),  $\beta$ -Galactosidase (116 kDa), Phosphorilase  $\beta$  (97 kDa), Transferrin (80 kDa), BSA (66 kDa), Glutamate dehydrogenase (55 kDa), Ovalbumin (45 kDa), Carbonic anhydrase (30 kDa), Trypsin inhibitor (21 kDa), Lysozyme (14 kDa) and Aprotinin (6.6 kDa). Aliquots of samples (0.1 % w/v protein) were dissolved in the mobile phase and an injection volume of 20  $\mu$ L was used. Detection was monitored at 214 nm and analyses were performed in triplicate.

#### **13.2.7.3. Proteins and peptides profile**

RP-HPLC was carried out according to the method of Ferreira *et al.* (185). Gradient elution was carried out at a flow-rate of 1 mL/min, using a mixture of two solvents. Solvent A was 0.1% (v/v) TFA in water and solvent B was acetonitrile-water-trifluoroacetic acid 95:5:0.1 (v/v/v). Aliquots of samples (0.1% w/v protein) were dissolved in solvent A, filtered through 0.2  $\mu$ m syringe filters and injected (50  $\mu$ L) on a Chrompack P 300 RP (polystyrenedivinylbenzene copolymer, 8  $\mu$ m, 300Å, 150 x 4.6 mm i.d.) (Chrompack, Middleburg, The Netherlands) column maintained at room temperature. Detector response was monitored at 214 nm and analyses were performed in triplicate.

### **13.2.8. Ultrafiltration of BSG protein hydrolysates**

BSG protein hydrolysates were fractionated through UF membranes with MWCO of 10 and 3 kDa. Unfractionated hydrolysates and respective fractions <10 kDa and <3 kDa were lyophilized and stored at -20°C. ACE-I activity, chemical antioxidant activity, and cell-based antioxidant activity assays were further performed.

### 13.2.9. ACE-I activity

The ACE-I activity of hydrolysates and their <10 kDa and <3 kDa fractions were determined at the concentration of 1.0 mg/mL. ACE was extracted from rabbit lung acetone powder with 100 mM sodium borate buffer (pH 8.3) containing 300 mM NaCl, according to the procedure described by Minervini *et al.* (165). Prior to assay, the supernatant was diluted 10-fold with 50 mM potassium phosphate buffer, pH 8.3, so that it would have the same ACE activity as the commercial preparation (3 U/mg of protein). ACE-I activity was measured using the fluorimetric assay of Sentandreu and Toldrá (121), with the modifications reported by Quirós *et al.* (122). ACE-I percentage (I) was calculated using the equation:

$$I \% = \{(B - A) / (B - C)\} \times 100 \quad (3)$$

where B is the fluorescence of the ACE solution without the inhibitor (BSG hydrolysate); A is the fluorescence of the tested sample of BSG hydrolysate; and C is the fluorescence of experimental blank, *o*-ABz-Gly-Phe(NO<sub>2</sub>)-Pro dissolved in 150 mM Tris-base buffer (pH 8.3), containing 1.125 M NaCl. The percent inhibition curves (using a minimum of five determinations for each sample peptide concentration) were plotted *versus* protein concentration to estimate the mean IC<sub>50</sub> value, which is defined as the concentration required to decrease the ACE activity by 50% (122). Protein content was determined using the Lowry's method (163).

### 13.2.10. Chemical antioxidant activities

The chemical antioxidant activities of hydrolysates and their <10 kDa and <3 kDa fractions were determined at the concentration of 1.0 mg/mL. The TPC was measured using the Folin-Ciocalteu method as previously described by Herald *et al.* (155). Gallic acid was used as standard at 10-500 µM to produce a calibration curve (average  $R^2 = 0.9899$ ) and absorbance was measured at 765 nm. Results were expressed as mg of Gallic acid equivalent per mg of sample (mg GAE/mg dw). The FRAP was estimated according to the procedure of Jansen and Ruskovska (154). Trolox was used as standard at 10-500 µM to generate a calibration curve (average  $R^2 = 0.9968$ ) and absorbance was measured at 595 nm. Results were expressed as mg of Trolox equivalent per mg of sample (mg TE/mg dw).

### 13.2.11. Cell-based antioxidant activities

#### 13.2.11.1. Cell culture routine

Caco-2 (human colon adenocarcinoma cell line) and HepG2 (human hepatocarcinoma cell line) cells were routinely cultured in 75 cm<sup>2</sup> flasks (BD Biosciences, Oxford, UK) using DMEM with high glucose medium, supplemented with 10% FBS and 1% antibiotic solution (10,000 U/mL penicillin, 10,000 µg/mL streptomycin). The cells were incubated at 37°C under a humidified atmosphere condition that contained 5% CO<sub>2</sub>. The medium was changed

every other day. When cells reached 70-80% confluent monolayer cells, cells were detached by trypsinization (0.25% trypsin) and subcultured over a maximum of 10 passages.

#### **13.2.11.2. Samples preparation to cell culture studies**

For all BSG protein hydrolysates, <10 kDa lyophilized fractions were dissolved in HBSS to obtain two final concentrations: 0.1 mg/mL and 1.0 mg/mL.

#### **13.2.11.3. Cell viability determination**

Cell viability was determined using the MTT (3-(4,5-dimethylthiazol-2-yl)-2,5-diphenyltetrazolium bromide) assay, as previously reported by Dias da Silva *et al.* (183). Caco-2 and HepG2 cells at the same density of  $8 \times 10^4$  cells/well were seeded onto the central 60 wells of 96-well plates (BD Biosciences, Oxford, UK) to obtain confluent monolayers within 2 days. Then, the cells were incubated for 24 h at 37°C with the <10 kDa samples at the concentrations of 0.1 mg/mL and 1.0 mg/mL. Peripheral wells on the plate were filled with sterile water to avoid evaporation of the treatment solutions. A media blank (no cells) to account for the color of the samples; a negative control (NEGc, cells treated with medium only) and a positive control (POSc, cells treated with medium and 1% Triton X-100) were also included in the plate. After cell treatment with the test samples, the culture medium was aspirated and the attached cells were rinsed with 200  $\mu$ L HBSS, followed by the addition of fresh culture medium containing 0.25 mg/L MTT. After 30 min of incubation (37°C, 5% CO<sub>2</sub>), the formed intracellular crystals of formazan were dissolved in 100  $\mu$ L 100% dimethyl sulfoxide (DMSO). The quantity of formazan crystals was determined by measuring the absorbance at 570 nm. Cell viability (%) was calculated relative to the maximum viability of NEGc. Data were obtained from three independent experiments, with each plate containing six replicates of each test sample.

#### **13.2.11.4. Mitochondrial integrity determination**

Mitochondrial integrity was performed by measuring the tetramethylrhodamine ethyl ester perchlorate (TMRE) inclusion, as previously reported by Dias da Silva *et al.* (183). TMRE is a cell permeable fluorescent dye that specifically stains live mitochondria and accumulates in proportion to mitochondrial membrane potential (Dcm). Maintenance of Dcm is extremely important for normal cell function (183). For both cell lines,  $8 \times 10^4$  cells were seeded onto 96-well black plates. After 24 h, the media was gently aspirated and the cells were incubated with each <10 kDa samples at concentrations of 0.1 mg/mL and 1.0 mg/mL (at 37°C, 5% CO<sub>2</sub>). At the end of the 24 h incubation period, the cells were rinsed twice with HBSS and incubated at 37°C with 100  $\mu$ L of 2 mM TMRE for 30 min. Then, the media was gently



aspirated and replaced by 0.2% BSA in HBSS. Fluorescence was measured at 37°C set to 544 nm excitation and 590 nm emission. TMRE mitochondrial inclusion (%) was calculated relative to the maximum levels of NEGc. Data were obtained from three independent experiments, with each plate containing six replicates of each test sample.

#### 13.2.11.5. ROS production

The intracellular reactive oxygen species (ROS) production was monitored by means of the 2',7'-dichlorodihydrofluorescein diacetate (DCFH-DA) assay, as previously reported by Dias da Silva *et al.* (183). For this determination and for both cell lines,  $8 \times 10^4$  cells per well were seeded onto 96-well black plates and allowed to attach for 24 h. On the day of the experiment, the cells were rinsed with HBSS and incubated with 200  $\mu$ L per well of <10 kDa samples at concentrations of 0.1 mg/mL and 1.0 mg/mL, for 24 h (37°C, 5% CO<sub>2</sub>). A negative control (NEGc, cells treated with medium only) was also included in the plate. After a 24 h treatment period, cells were rinsed twice with HBSS and incubated with 10 mM DCFH-DA for 30 min (37°C, 5% CO<sub>2</sub>). After removal of the DCFH-DA and further washing with HBSS, the formation of 2',7'-dichlorodihydrofluorescein (DCF), due to the oxidation of DCFH-DA in the presence of intracellular ROS, was read at an excitation wavelength of 485 nm and an emission wavelength of 530 nm. Cell ROS production (%) was calculated relative to the maximum ROS levels of NEGc. Data were obtained from three independent experiments, with each plate containing six replicates of each test sample.

In parallel, the cellular protection of <10 kDa samples against a cytotoxic agent was evaluated. Oxidative stress was induced in both confluent cell cultures by addition of 1 mM H<sub>2</sub>O<sub>2</sub>. For this purpose, cells were submitted to the 24 h treatment period described above but, in this case, 1 mM H<sub>2</sub>O<sub>2</sub> was added 6 h before the ROS measurement. Cell ROS production (%) was calculated relative to the maximum ROS levels of positive control (POSc, cells treated with H<sub>2</sub>O<sub>2</sub>).

#### 13.2.12. Statistical analysis

Data were presented as mean  $\pm$  standard deviation from three independent experiments unless stated otherwise. Statistical comparisons were performed by one-way analysis of variance (ANOVA) followed by the Duncan's multiple comparison test. Difference was considered significant at  $p < 0.05$ . All statistical calculations were performed using SPSS 22.0 (SPSS software, Chicago, U.S.A.).

### 13.3. RESULTS AND DISCUSSION

#### 13.3.1. Measuring the extent of hydrolysis

BSG proteins were hydrolyzed by three different enzyme approaches: a BSY extract rich in proteases, Neutrase® and Alcalase®. Hydrolyses were carried out under the same conditions: 50°C, 4 h and using the same E/S ratio of 0.10:1 U/mg; enzymes were compared at the same proteolytic activity (1 U/mL). Few studies have been conducted comparing enzymes on the basis of their proteolytic activity, usually researchers compare enzyme activity on a weight basis of enzymes used in the reaction mixture, which constitutes a limitation (194). The DH (%) was used as an indicator of the hydrolysis progress and PR (%) as an indicator of the hydrolysis yield (219), (295). The hydrolysis yield (%) of BSG protein hydrolysates (% dw) is present in Table 13.2. Results show that the DH % for BSYH, NTH and ALH were 8.27%, 4.63% and 10.4%, respectively. Higher hydrolysis was observed for ALH. Results from PR % were 58.9%, 37.2% and 62.2% for BSYH, NTH and ALH, respectively. Similar to observed by other authors (194), (338), Alcalase® exhibited higher hydrolytic activities than Neutrase®, although these values are different from those observed by other authors, in which Alcalase® treatment was used to produce BSG protein hydrolysates (253), (309). For instance, Connolly *et al.* (309) reported a DH (%) of ~12% when BSG protein was hydrolyzed at 50°C, pH 9, using an E/S ratio of 2.5% (v/w) for 4 h. These differences can be explained by the different procedures used to prepare the BSG protein substrate, different hydrolysis conditions applied, namely, the proteolytic activity of enzyme and reaction time, as well as, the different methods employed to evaluate the DH %.

#### 13.3.2. Proximate composition of BSG protein hydrolysates

The proximate composition of BSG protein hydrolysates (% dw) obtained by the three enzymatic treatments is presented in Table 13.2. The protein content was similar in the three hydrolysates, ranging between 68.0-76.6% (dw). The nutritional composition of ALH was different from that reported by Celus *et al.* (8). This difference may be attributed to the difference in raw materials and the processes involved in preparing the Alcalase hydrolysates. BSYH presented the highest content of ash (8.12%), presumably due to the buffer required for the preparation of the BSY extract rich in proteases, but a significantly ( $p < 0.05$ ) lower content in fat (2.42%). In general, the high protein content and low fat content of all hydrolysates may provide an incentive for use in commercial preparations.

Table 13.2. Hydrolysis yield (%) and proximate composition (% dw) of BSG protein hydrolysates

Sample code	Hydrolysis Yield (%)		Proximate Composition (% dw)		
	DH <sup>(i)</sup>	PR <sup>(ii)</sup>	Protein	Ash	Fat
BSYH	8.27±0.97 <sup>a</sup>	58.9±1.71 <sup>a</sup>	76.7±4.10 <sup>a</sup>	8.12±3.30 <sup>a</sup>	2.42±0.75 <sup>b</sup>
NTH	4.63±0.62 <sup>b</sup>	37.2±1.49 <sup>b</sup>	68.0±4.97 <sup>a</sup>	6.53±0.38 <sup>b</sup>	3.84±0.50 <sup>a</sup>
ALH	10.4±1.42 <sup>a</sup>	62.2±2.15 <sup>a</sup>	71.3±3.30 <sup>a</sup>	6.87±0.14 <sup>b</sup>	4.59±0.35 <sup>a</sup>

<sup>(i)</sup> Degree of hydrolysis (DH %) determined with TNBS.

<sup>(ii)</sup> Protein recovery (PR %) determined by Lowry method.

Results are expressed as mean ± standard deviation of triplicate experiments. For each assay, means that do not share a letter are significantly different at  $p < 0.05$ . Statistical analysis were performed by ANOVA followed by Duncan's multiple comparison test.

### 13.3.3. Molecular weight distribution and peptides/proteins profile

The BSG protein substrate consisted of relatively large molecular mass proteins, containing hordeins D (~96 kDa) and mostly hordeins C (~55-80 kDa) and hordeins B (~35-50 kDa), as reported by Vieira *et al.* (4) and Celus *et al.* (339) (results not shown). In agreement with Connolly *et al.* (253), 54.6% of the large mass components of the BSG protein substrate were higher than ~15 kDa. After enzymatic treatments, proteins were broken down into smaller molecular weight peptides; the distribution profiles obtained are presented in Figure 13.1.A. Results showed that BSG protein hydrolysates were composed of a wide range of protein/peptide bands with molecular weight less than ~62 kDa for BSYH; less than ~60 kDa for NTH and less than ~50 kDa for ALH. BSYH was composed of major protein bands with molecular weight of ~45 and ~21 kDa and the highest ( $p < 0.05$ ) quantity of low molecular weight peptides (< 6.6 kDa). ALH showed a major protein band with molecular weights between ~21 and 6.6 kDa. Of the three enzymes, NTH had the lowest percentage of low molecular weight peptides (< 6.6 kDa) and an appreciable protein band with molecular weight between ~60 kDa and ~52 kDa, denoting the lowest efficiency in protein breakdown. In general, the molecular weight profiles of these hydrolysates are in agreement with the values of DH% and PR% obtained for the three treatments.

The RP-HPLC profiles of BSG protein hydrolysates with different DH% are presented in Figure 13.1.B, which demonstrated considerable variation in peptide composition. RP-HPLC profiles were divided into three fractions: fraction I consisted of the "less hydrophobic fragments" eluting between 4 and 12.5 min, fraction II contained the "hydrophobic

polypeptides” that eluted between 12.5 and 25 min and fraction III contained the “protein fractions” with elution between 25 and 55 min. Proteins eluted mainly in fraction III, similarly to what was already observed in our previous study (4). Comparing the percentage area of the three fractions relative to the total area of the RP-HPLC chromatogram, results show that with increasing DH, the level of fraction I increased, while the proportions of fractions II and III decreased. The higher percentage area of fraction I was observed for ALH, which had also higher DH%. In opposite, NTH presented the smallest area of fraction I, suggesting that this enzyme is not very efficient in the BSG protein hydrolysis.

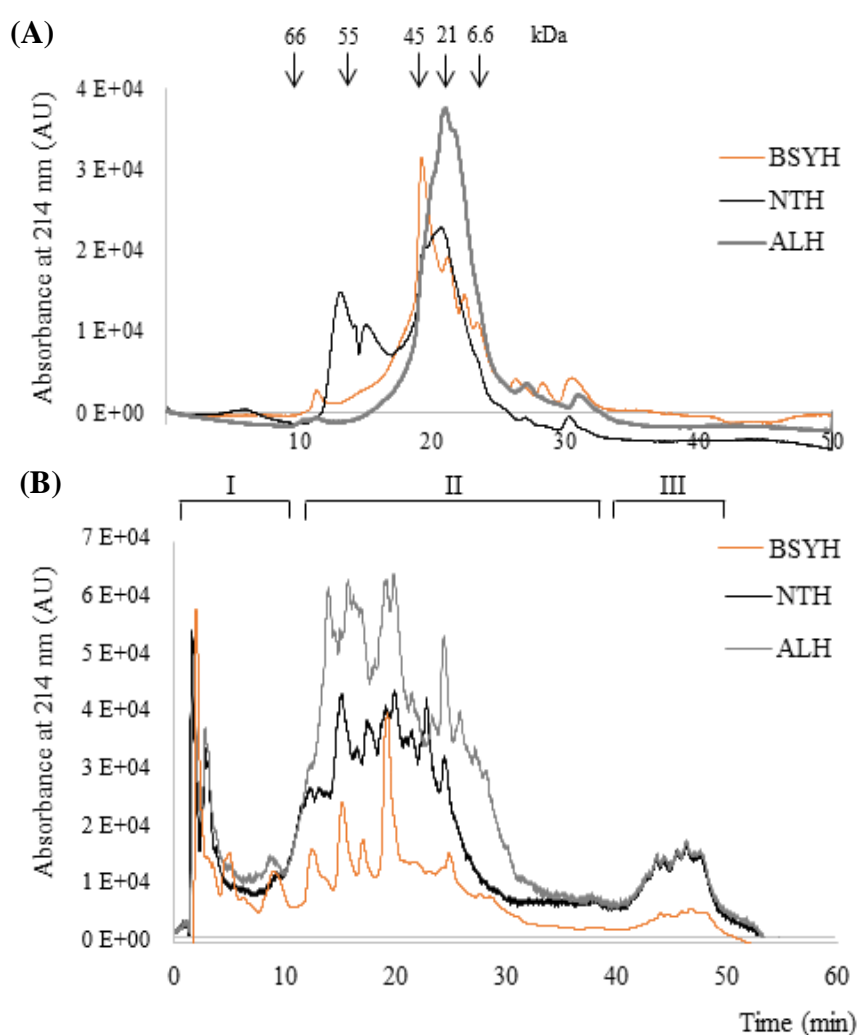


Figure 13.1. SE-HPLC **(A)** and RP-HPLC **(B)** profiles of BSG protein hydrolysates with different DH (%), obtained after enzymatic hydrolysis with BSY extract (BSYH), Neutrase® (NTH) and Alcalase® (ALH). Absorbance (214 nm) is expressed in arbitrary units (AU). In the SE-HPLC profile, elution times of molecular weight markers with molecular weight between 6.6 and 66 kDa are indicated from left to right. BSG protein hydrolysates were analyzed at same protein concentration (1 mg/mL), using 20  $\mu$ L of this solution to the column. RP-HPLC profiles are divided into three fractions: I- “Less hydrophobic”; II- “Polypeptides” and III- “Proteins”.

#### 13.3.4. Effect of UF on ACE-I activity of BSG protein hydrolysates

BSG protein hydrolysates were fractionated using two kinds of UF membranes (10 and 3-kDa MWCO membranes) and two kinds of permeates were obtained, the fractions <10 kDa and the fractions <3 kDa. It should be highlighted that the molecular weight distributions of these fractions was similar, although the relative proportions of the peaks varied according to the MWCO size of the membrane used, meaning that the UF technique enriched the fractions of their respective size rather than accurately separated the proteins and peptides according to size (340). The BSG protein substrate, the hydrolysates and <10 kDa and <3 kDa fractions were screened for their ACE-I potential at 1.0 mg/mL. The ACE-I activities obtained are presented in Figure 13.2.A. The results show that the  $IC_{50}$  of BSG protein substrate (coded as NT; no treatment) was 1.45 mg protein/mL, meaning that some peptides with ACE-I could be naturally present in BSG protein substrate, as a result of the alkaline procedure employed for extraction of protein fraction. ALH showed the strongest ACE-I activities ( $p < 0.05$ ) among the three hydrolysates tested, with an  $IC_{50}$  of 0.385 mg protein/mL. This result is correlated with the higher DH observed for this enzymatic treatment. Other authors also obtained a good correlation between the DH and the  $IC_{50}$  (253), (309), (341). Moreover, this result is in agreement with that reported recently by Connolly *et al.* (253), in which the ACE-I activity of BSG protein hydrolysates using Alcalase® was evaluated using the fluorimetric assay, and an  $IC_{50}$  of 0.340 mg protein/mL was observed. Small differences with the  $IC_{50}$  values obtained in this work may be due to the differences in temperature, E/S ratio and time conditions employed in the generation of the hydrolysates, as well as, with some differences in the method used to determine the ACE-I activity. The  $IC_{50}$  values of BSYH and NTH were 0.820 mg protein/mL and 0.615 mg protein/mL, respectively. In order to determine if the observed ACE-I activities are due to specific molecular mass fractions in the protein hydrolysate, UF was performed. ACE-I activity tends to increase with the decrease of molecular weight. In the case of BSYH and NTH, using a 3 kDa MWCO, this activity was enhanced. The  $IC_{50}$  values of the <3 kDa fractions were respectively, 0.652 and 0.512 mg protein/mL, corresponding to an increase of 20% and 17% of ACE-I activity. These results are in accordance with previously studies, which reported that ACE-I peptides are composed of a small number of amino acids, less than 3 kDa (342), (330). For BSYH, no statistical differences ( $p < 0.05$ ) were observed between the ACE-I activity obtained for <10 kDa and <3 kDa fractions. In opposite, for ALH, the <10 kDa fraction allowed an enhancement of 19% on the ACE-I activity ( $IC_{50}$  of 0.312 mg protein/mL). This result is in agreement with Connolly *et al.* (253), who reported that the  $IC_{50}$  values of the unfractionated hydrolysate were lower than the respective 5 kDa and 3 kDa fractions.

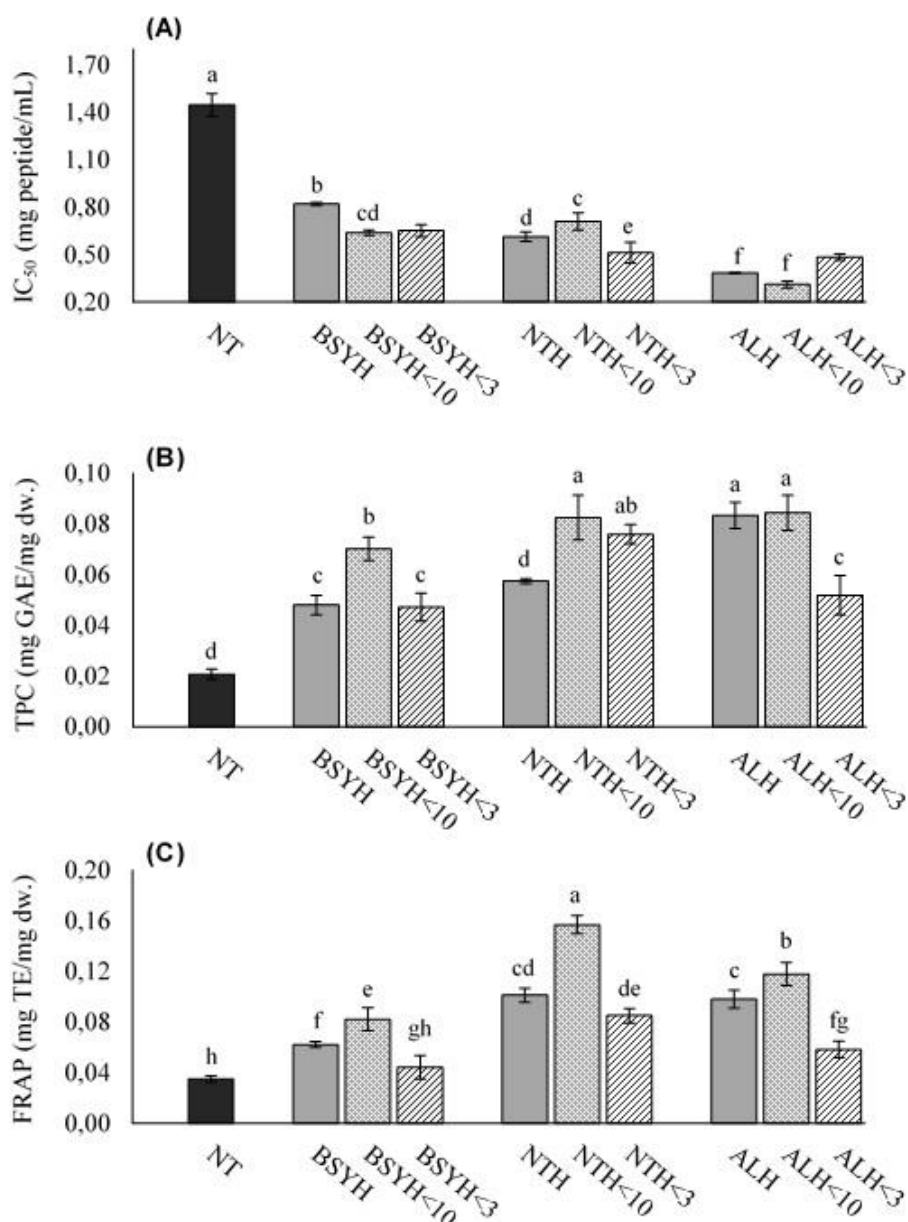


Figure 13.2. Comparison of ACE-I activity **(A)**, Total Phenolic Content **(B)** and FRAP **(C)** of BSG protein starting material (NT, no treatment), full BSG protein hydrolysates (BSYH, NTH, ALH) and respective <10 kDa and <3 kDa fractions. Each bar represents the mean ± standard deviation of triplicate experiments. For each assay, bars labeled with different letters have mean values that are significantly different at  $p < 0.05$ . Statistical analysis were performed by ANOVA followed by Duncan's multiple comparison test.

### 13.3.5. Effect of UF on antioxidant activity of BSG protein hydrolysates

Chemically based antioxidant activities of the BSG protein substrate, hydrolysates and fractions <10 kDa and <3 kDa were investigated based on the TPC and FRAP assays. Results are presented in Figure 13.2.B and 13.2.C, respectively. Results show that all

hydrolysates had significantly ( $p < 0.05$ ) higher antioxidant activities compared to BSG protein substrate (TFC of 0.021 mg GAE/mg dw and FRAP of 0.035 mg TE/mg dw). ALH showed significantly ( $p < 0.05$ ) higher TPC (0.083 mg GAE/mg dw) compared to NTH (0.057 mg GAE/mg dw) and BSYH (0.048 mg GAE/mg dw). The result obtained for Alcalase® treatment can be compared with the BSG protein hydrolysate reported by Aoife *et al.* (307), in which hydrolysis was performed with Alcalase®, using an E/S ratio of 1% (v/w), pH 9, for 4 h at 60°C. The lower TPC value reported by these authors, 0.055 mg GAE/mg dw, can be explained by the different procedure used to prepare the BSG protein substrate and by the different hydrolysis conditions applied. In general, the UF step using a 10 kDa MWCO increased values of TPC. NT<10 kDa (0.082 mg GAE/mg dw) and AL<10 kDa (0.084 mg GAE/mg dw) presented significantly higher TPC ( $p < 0.05$ ) compared to BSYH<10 kDa (0.070 mg GAE/mg dw).

The FRAP assay measures the ability of a compound to reduce  $\text{Fe}^{3+}$  (ferric ion) to  $\text{Fe}^{2+}$  (ferrous ion), thus, indicating the antioxidant potential of a compound. FRAP results presented in Figure 13.2.C show that BSG protein hydrolysates prepared with Alcalase® (DH = 10.4%) and Neutrase® (DH = 4.63%) presented similar antioxidant activity ( $p < 0.05$ ), 0.101 mg TE/mg dw and 0.098 mg TE/mg dw, respectively. In opposite, BSYH with a DH of 8.27% presented the lowest FRAP activity, 0.062 mg TE/mg dw. These results suggest that the antioxidant activity of BSG protein hydrolysates does not necessarily increase with DH%. As reported by other authors, the antioxidant activity of a protein hydrolysate is dependent not only on the molecular size of the peptides present, but markedly on the presence of specific peptide sequences and their amino acid composition (239), (343). Further UF using a 10 kDa MWCO enhanced the FRAP values of NTH, ALH and BSYH ( $p < 0.05$ ). The BSYH<10 kDa showed antioxidant activity of 0.082 mg TE/mg dw, whilst NTH<10 kDa showed antioxidant activity of 0.157 mg TE/mg dw and ALH presented 0.129 mg TE/mg dw. UF using a 3 kDa MWCO reduced the FRAP values of NTH, ALH and BSYH ( $p < 0.05$ ), thus, no benefits were observed in this fraction.

### 13.3.6. Cellular antioxidant activities

The <10 kDa fractions obtained from BSG protein hydrolysates presented higher *in vitro* antioxidant activities were selected to evaluate the cellular antioxidant activity. This determination represents an effective biological method due to similarities in the characteristics related to the uptake and metabolism of antioxidants within the living cells of the target organs (335). Therefore, these fractions were screened at two different concentrations, 0.1 mg/mL and 1.0 mg/mL, for their cytotoxic effects on cell viability, mitochondrial integrity and ROS generation. Two widely used human cell lines were evaluated to assess the GI tract and liver target organ cytotoxicity as a consequence of

exposure to these fractions. Cell viability, defined as the potential of a compound to induce cell death (336), was assessed using the MTT assay. In this study, a clear difference between the HepG2 cell line (human liver) and the Caco-2 cell line (human intestine) was observed regarding the exposure to <10 kDa fractions. Results showed a significantly ( $p < 0.05$ ) concentration-dependent decrease (maximum of 26%) in Caco-2 cell viability compared with the NEGc, after 24 h of exposure to <10 kDa fractions (Figure 13.3.A). This result indicates a relatively low cytotoxic effect for Caco-2 cell model at concentrations of 1.0 mg/mL, which is in agreement to the observed by other kind of hydrolysates (337), (181), (344). In the case of HepG2 cell line, the ALH<10 kDa fraction, at the concentration of 0.1 mg/mL, significantly ( $p < 0.05$ ) decreased the viability below 35% of the NEGc ( $p < 0.05$ ). On the other hand, the BSYH< 10 kDa fraction, at the concentration of 1.0 mg/mL, showed a significant increase ( $p < 0.05$ ) in HepG2 cells viability (Figure 13.3.B).

In order to investigate whether the <10 kDa fractions could disturb the mitochondrial function, the mitochondrial membrane potential was evaluated through the TMRE inclusion. Results present in Figure 13.3.A showed that, except for ALH<10 kDa at the concentration of 1.0 mg/mL, all fractions were not effective in generating significant mitochondrial disruption in Caco-2 cell line, with decreases less than ~6% compared to NEGc. Regarding the HepG2 cell line (Figure 13.3.B), as observed for cell viability, the TMRE inclusion was significantly ( $p < 0.05$ ) lower for ALH<10 kDa at both test concentrations, 0.1 and 1.0 mg/mL. These results support the view of differential sensitivity of BSG protein hydrolysates among HepG2 and Caco-2 cellular models, but further investigation is needed.



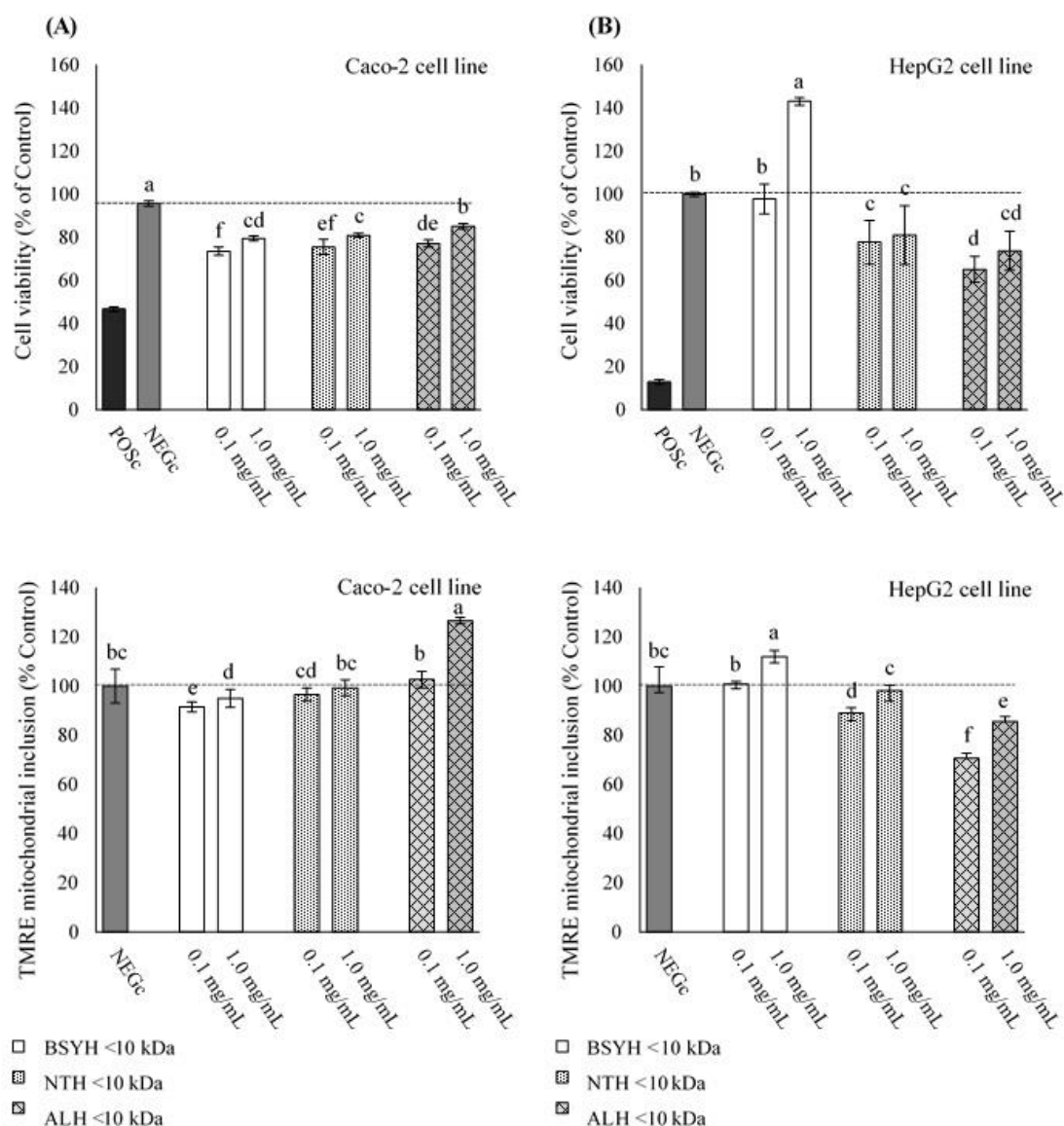


Figure 13.3. Effect of BSG protein hydrolysates (<10 kDa fractions) on cell viability (%) and TMRE mitochondrial inclusion (%) in Caco-2 cell line **(A)** and HepG2 cell line **(B)**, after 24 h of incubation at 37°C, 5% CO<sub>2</sub>. Each bar represents the mean  $\pm$  standard deviation. NEG<sub>c</sub> (cells treated with medium only) and POS<sub>c</sub> (cells treated with medium and 1% Triton X-100). For each assay (and for each cell model), bars labeled with different letters have mean values that are significantly different at  $p < 0.05$ . Statistical analysis were performed by ANOVA followed by Duncan's multiple comparison test.

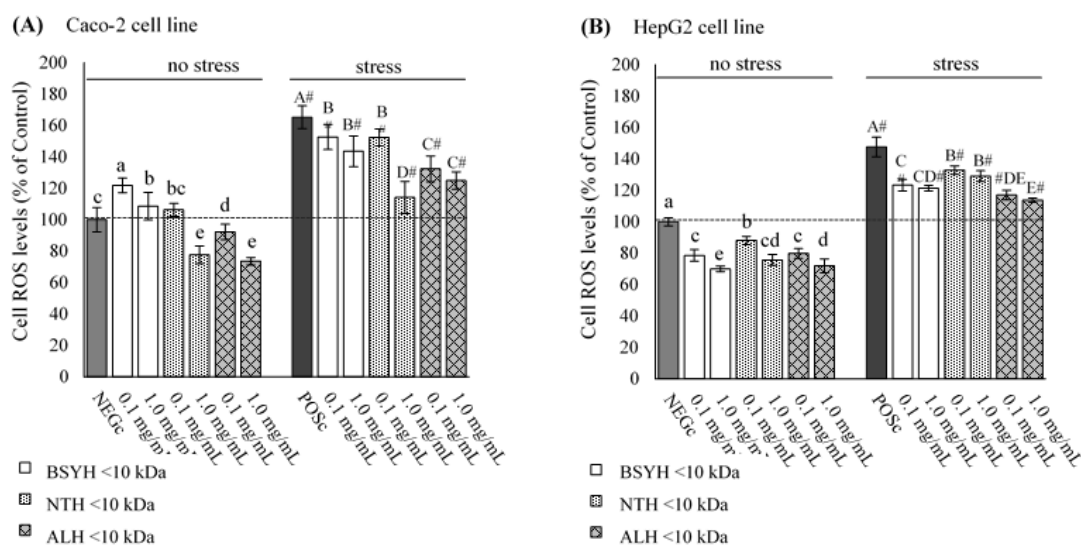


Figure 13.4. Protective effect of BSG protein hydrolysates (<10 kDa fractions at concentrations of 0.1 and 1.0 mg/mL) for 24 h against oxidative stress induced by H<sub>2</sub>O<sub>2</sub> (6 h of exposure) in Caco-2 cell line **(A)** and HepG2 cell line **(B)**. Each bar represents the mean  $\pm$  standard deviation. NEGc (cells treated with medium only); POSc (cells treated with medium and H<sub>2</sub>O<sub>2</sub>). (#) indicates respective differences between “no oxidative stress” and “oxidative stress” treatments at  $p < 0.05$ . For “no oxidative stress” treatment (and for each cell model), bars labeled with different subscript letters have mean values that are significantly different at  $p < 0.05$ . For “oxidative stress” treatment (and for each cell model), bars labeled with different superscript letters have mean values that are significantly different at  $p < 0.05$ . Statistical analysis were performed by ANOVA followed by Duncan's multiple comparison test.

### 13.4. CONCLUSIONS

In conclusion, the <3 kDa fraction of ALH displayed the highest ACE-I activity, whereas <10 kDa fractions presented increased *in vitro* antioxidant potential and inhibited the intracellular ROS generation, as well, exerted a protective ability against H<sub>2</sub>O<sub>2</sub> induced oxidative damage in Caco-2 and HepG2 cell lines. While much evidence exists with regard to BSG protein hydrolysates obtained from commercial enzymes, to our knowledge, this is the first study on the bioactivity of BSG protein hydrolysates prepared by a BSY extract rich in proteases. Therefore, the results obtained in this work suggest that these kind of hydrolysates may be useful functional ingredients to be used in food or pharmaceutical industries. Further work must be undertaken to identify the peptides that are responsible for exerting these activities.

# General conclusions and future prospects

---



## GENERAL CONCLUSIONS

The experimental work presented in this Ph.D. thesis is an effort to find a scientific basis for the valorisation of the main agro-industrial by-products from brewing and canned sardine industry. The sustainable exploitation of these by-products is of major relevance for both industries, in terms of economic and environmental perspectives. Brewer's spent yeast (BSY) autolysates, sardine protein hydrolysates (SPH) and brewer's spent grain (BSG) protein hydrolysates were prepared through RSM optimization and presented enhanced *in vitro* antioxidant and/ or ACE-I activities, when compared to the initial raw materials, suggesting its potential use as new bioactive ingredients. The major findings of the research undertaken are briefly discussed as follows.

**Part I** of this dissertation was focused on the potential reuse of BSY (*Saccharomyces pastorianus*), the second major by-product of the brewing process. A mechanic disruption method (using glass beads, under refrigerated conditions) of yeast cells and removal of the cell wall fraction was applied to produce a BSY extract, which comprises the inner content of yeast cells. Usually, autolysis is the conventional process applied to produce BSY extracts and recover the  $\beta$ -glucans and fibre fractions. Autolytic process involves incubation of cell suspensions of BSY at temperatures ranging from 45 to 60°C with a reaction time between 8 and 72 h; the final autolysate is a mixture of the cell wall and the inner yeast cell content. By contrast, the adoption of mechanic disruption before autolysis allowed the effective separation of two important cell fractions: (i) yeast cell wall rich in  $\beta$ -glucans and fibre and (ii) the intracellular content (BSY extract) composed by proteins, proteases, RNA, minerals and vitamins - both potential ingredients to be used in the formulation of functional foods and nutraceuticals.

The nutritional composition, antioxidant activity and phenolic compounds profile of BSY extract obtained by mechanic disruption was described in **Chapter 2**. Data showed that BSY extract presented high content of proteins (64%) with an amino acid profile well-balanced for human consumption (PER of 2.4), RNA (4%), vitamins (B3, B6 and B9), macrominerals and trace elements. Additionally, BSY extract presented *in vitro* antioxidant activity and phenolic compounds in both the free and bounded forms, namely, gallic acid, protocatechuic acid, ( $\pm$ )catechin, *p*-coumaric, ferulic and cinnamic acids. Besides these compounds explain the antioxidant activity of the BSY extract, others that were not evaluated, namely, glutathione, maillard reaction products, sulfur-containing amino acids,

peptides as the peptide cyclo(His-Pro), and polysaccharides may also contribute to the observed activity.

The brewer's yeast is reused in the fermentation process several times until its disposal, therefore the influence of serial repitching on the bioactivity of the BSY extract was investigated in **Chapter 3**. BSY extracts were prepared from yeast biomass with 2, 3, 4 reuses, as well as, from a mixture of yeast biomass with different number of reuses in the brewing process. The TPC, TFC, antioxidant properties, ACE-I and proteolytic activities were in the range of 255-304  $\mu\text{M}$  GAE/mL; 187-308  $\mu\text{M}$  CE/mL; 255-304  $\mu\text{M}$  TE/mL (FRAP assay), 255-304  $\mu\text{M}$  TE/mL (DPPH assay); 255-304  $\mu\text{M}$  TE/mL (RP assay), 266-468  $\mu\text{g}$  protein/mL ( $\text{IC}_{50}$ ) and 0.14-0.22 U/mL, respectively. The antioxidant activity of BSY extract was comparable to the conventional synthetic antioxidant ascorbic acid, tested at the concentration of 500  $\mu\text{M}$ , suggesting that BSY extract has potential application as a natural antioxidant ingredient in food systems. Additionally, the proteolytic activity of the BSY extracts indicated that in opposite to the conventional autolytic process, which applies high temperatures, the mechanic disruption process under refrigerated conditions employed in this work presents the advantage of recovery of native enzyme fraction. Hence, BSY extract was found to be a promising source of proteases to be used in the production of protein hydrolysates from different food matrices. Data of this experimental work also showed that the number of the yeast reuses in the brewing process does not influence significantly the antioxidant activity of BSY extracts; exhibiting, however, a negative effect in the proteolytic and ACE-I activities. Moreover, TPC, TFC, antioxidant properties and ACE-I activity presented good stability during a storage period of 6 months at  $-25^{\circ}\text{C}$ , although the proteolytic activity of BSY extracts decreased of approximately 50% after 4 months of storage at  $-25^{\circ}\text{C}$ . This last result indicated that the use of BSY extract as a source of proteases implies correct management and storage period for less than 4 months.

In **Chapter 4**, the BSY extract (rich in proteins and proteases) was submitted to autolysis, with the aim to enhance the antioxidant and ACE-I activities. RSM was the statistical methodology applied to optimize the autolysis conditions (temperature and time). Optimum autolysis conditions were  $36.0^{\circ}\text{C}$ , 6.0 h, pH of 6.0 by which, the BSY autolysate presented TPC, FRAP and ACE-I activity of 385  $\mu\text{M}$  GAE/mL, 374  $\mu\text{M}$  TE/mL and 379  $\mu\text{g}$  protein/mL, respectively. Those activities were significantly higher than the biological activities of the original BSY extract. In comparison with the conventional autolytic process, the autolysis process optimized in this work employs mild conditions (lower temperatures and reduced autolysis time), which can be economically advantageous from an industrial point of view. On the other hand, this process overcomes some limitations associated with

conventional autolytic process, such as, the low extraction yield, difficult separation of cell debris, production of several off-favour compounds and risk of deterioration due the microbial contamination.

As described in **Chapter 5**, the low-molecular-weight fraction of BSY autolysate was concentrated through 5 kDa MWCO - UF membrane and its bioactivity was investigated after simulated GI digestion; resistance to brush-border peptidases and transepithelial transport across Caco-2 and Caco-2/HT29-MTX co-culture cell monolayers. Data obtained after simulated GI digestion showed enhanced biological activity of BSY autolysate and protective effect against oxidative stress induced by hydrogen peroxide in Caco-2 cells. These results are of great relevance since GI tract is a major target for oxidative stress damage due to the constant exposure to diet-derived oxidants, mutagens, and carcinogens. Additionally, the antioxidant and ACE-I activities found in cell permeates indicate that bioactive compounds present in the BSY autolysate were well absorbed. In comparison with Caco-2 cell model, higher permeability was found in the Caco-2/HT29-MTX co-culture cell model, which is recognized as more physiological and a realistic approach of the *in vivo* intestinal conditions. Antioxidant and ACE-I activities of permeates suggest that bioactive peptides from digested BSY autolysate and from the action of brush-border peptidases were well absorbed. Mass spectrometry revealed that peptides with  $m/z$  between 1000 and 5000 were transported across Caco-2/HT29-MTX co-culture cell monolayer, presumably via transcytosis mechanisms. Permeability of those oligopeptides was suggested to be related to the presence of permeability enhancers in BSY extract.

The **Parts II and III** of this dissertation were addressed to the potential utilization of BSY proteases over two different protein substrates, proteins extracted from sardine by-products (animal origin) and BSG proteins (vegetal origin), in order to produce protein hydrolysates with enhanced antioxidant and/ or ACE-I activities. For this purpose, the BSY extract prepared by mechanic disruption under refrigerated temperatures was freeze-dried, resuspended in the same buffer (25% of the initial volume) and concentrated using a UF membrane with a UF MWCO of 10 kDa. Through this procedure, the proteolytic activity of the BSY extract increased around 4 fold. No enzyme purification was performed, hence the production of SPH and the BSG protein hydrolysates resulted from the action of a mixture of several BSY proteases.

Considering that the sarcoplasmic proteins represent 20-30% of total sardine proteins and are characterized for its higher solubility and digestion compared to the myofibrillar proteins, the first attempt to produce SPH by action of BSY proteases was performed in this

protein fraction (**Chapter 7**). RSM was used to optimize the hydrolysis conditions in order to obtain a SPH with enhanced antioxidant and ACE-I activities. SPH produced using the E/S ratio 0.27:1 U/mg (0.725 U/mL), 50°C for 7 h, at pH of 6.0 presented a FRAP value of 290  $\mu$ M TE/mL, an ACE-I activity ( $IC_{50}$ ) of 164  $\mu$ g protein/mL and relatively high content of hydrophobic amino acids, such as, proline, leucine, glycine, isoleucine, phenylalanine and valine; as well, amino acids that exhibit antioxidant activity, namely, tyrosine, histidine, methionine and lysine.

As reported in **Chapter 8**, FRAP value and ACE-I activity of SPH were enhanced by UF, using a 10 kDa MWCO - UF membrane. The ACE-I potential of SPH remained unchanged upon simulated GI digestion (117  $\mu$ g protein/mL) but no ACE-I activity was detected after cell transport, which indicates that probably the bioactive compounds responsible for the ACE inhibition suffered proteolysis by brush-border peptidases. Regarding to antioxidant activity, the permeability assays showed that some SPH bioactive compounds permeated across Caco-2 and Caco-2/HT29-MTX co-culture cell monolayers, thereby providing further evidence of intestinal absorption. Similar to that observed for transepithelial transport of BSY autolysates, the Caco-2/HT29-MTX co-culture cell model also showed significantly higher apical to basolateral transport of SPH peptides when compared with Caco-2 cell model. This result suggested a low level of interaction with mucins produced by HT29-MTX and unimpaired diffusion of the SPH bioactive compounds. Moreover, mass spectrometry revealed that peptides with  $m/z$  between 1000 and 5000 were transported across Caco-2/HT29-MTX co-culture cell monolayer, presumably via transcytosis mechanisms.

The SPH (after simulated GI digestion) was also screened for its anti-inflammatory activity (**Chapter 9**). For this purpose, a co-culture model, which combines the absorption by differentiated Caco-2 cells and sequential effects on endothelial cells metabolism, was compared with the standard method, which exclusively considers the direct exposition effect of SPH on endothelial cells metabolism. Data demonstrated that SPH exhibited anti-inflammatory activity in TNF- $\alpha$  simulated endothelial cells, through the inhibition of NO, ROS and pro-inflammatory cytokines production, MCP-1, VEGF, IL-8 and ICAM-1. Likewise, results suggested that the protective health effects of SPH might not only be due to SPH bioactive compounds, but also due to their metabolites produced by the action of Caco-2 cell peptidases in the course of intestinal absorption. In this regard, the co-culture model, which represents a more physiological and realistic approach compared with *in vivo* conditions, allowed more accurate knowledge about the anti-inflammatory activity of the SPH studied.



Due to the fact that BSY proteases efficiently hydrolysed the sarcoplasmic proteins from sardine by-products, the action of this enzymatic preparation was also evaluated on muscle and viscera proteins, recognized as proteins more resistant to hydrolysis. The bio-functional and techno-functional properties of the muscle and viscera SPH were compared with properties obtained by SPH produced using commercial enzymes, Alcalase® and Neutrase®, which are widely used in the SPH preparation (**Chapter 10**). Muscle and viscera SPH were produced at the same hydrolysis conditions, using the same protein substrate concentration, 20 mg of protein/mL, an E/S ratio of 0.20:1 U/mg (1 U/mL), 50°C and 7 h of treatment. The results obtained in this chapter indicated that the type of enzyme used influenced the bio-functional and techno-functional properties of SPH. Among all treatments Alcalase® produced SPH with higher DH% and higher antioxidant and ACE-I activities for both muscle [DPPH of 870 µM TE/mL and ACE-I (IC<sub>50</sub>) of 619 µg protein/mL] and viscera proteins [DPPH of 840 µM TE/mL and ACE-I (IC<sub>50</sub>) of 651 µg protein/mL]. BSY enzymatic approach produced muscle and viscera SPH with lower DH% and lower bio-functional activities. However, viscera SPH prepared by BSY proteases presented significantly higher emulsion (80.1 m<sup>2</sup>/g), foaming (79.2%) and oil binding capacity (5.8 g/g) compared with other viscera SPH. All SPH were considered potential ingredients to be incorporated into various food formulations to improve rheological properties.

BSG protein fraction was another substrate investigated for BSY proteases action. BSG hydrolysates with improved biological activities can be an alternative approach for valorisation of the second major brewing by-product. As described in **Chapter 12**, the hydrolysis conditions optimized by RSM were: E/S ratio of 0.29:1 U/mg (0.725 U/mL), 50°C, 6 h, pH of 6.0; which allowed the maximum DH of 17.1%, TPC of 1.65 mg GAE/mL and FRAP value of 1.88 mg TE/mL. The main BSY proteases responsible for the BSG protein hydrolysis were indicated as belonging to the class of serine peptidases and metallopeptidases.

Afterwards, the efficiency of the BSY proteases for production of BSG protein hydrolysates was compared with two commercial enzymes: Alcalase® and Neutrase® (**Chapter 13**). The same proteolytic activity (1 U/mL), protein substrate concentration (15 mg of protein/mL), E/S ratio of 0.10:1 U/mg, 50°C and 4 h treatment were applied to prepare BSG protein hydrolysates. Additionally, the effect of UF using 10 and 3 kDa MWCO membranes on antioxidant and ACE-I activities of these hydrolysates was investigated. Data showed that among the three enzymatic approaches, Alcalase® BSG protein hydrolysate presented the highest ACE-I activity (385 µg protein/mL), whereas the IC<sub>50</sub> values of BSG protein hydrolysates prepared by BSY proteases and Neutrase® action were

820 and 615 µg protein/mL, respectively. UF with 10 kDa MWCO membrane increased the ACE-I activity of Alcalase® BSG protein hydrolysate (312 µg protein/mL), as well, the *in vitro* antioxidant potential (TPC of 0.084 mg GAE/mg dw and FRAP of 0.129 mg TE/mg dw). In general, all the three <10 kDa UF fractions of BSG protein hydrolysates inhibited the intracellular ROS generation and exerted a protective ability against hydrogen peroxide induced oxidative damage in Caco-2 and HepG2 cell lines at concentrations of 1 mg protein/mL, suggesting its potential use in food systems as natural additives possessing antioxidant properties.

In this work, the biological activities (antioxidant, ACE-I and anti-inflammatory) reported were screened exclusively through *in vitro* assays. Therefore, it is important to highlight the limitations associated to the *in vitro* assays, since they are less representative of the physiological situation and no conclusions can be made in the long term. However, in a first attempt to screen the biological activities of new potential bioactive ingredients, *in vitro* models reveal several advantages over *in vivo* experiments with laboratory animals and clinical trials in humans. For instance, they pose no ethical restrictions, are more reproducible and suited for standard operation, have lower costs, allow fast screening of numerous samples and are easier to investigate underlying mechanisms.

Compared to literature, where emphasis is put on the isolation of antioxidant and ACE-I peptide(s) and their *in vitro* biological activities and *in vivo* pharmacological effects, this dissertation addressed the *in vitro* antioxidant and ACE-I activities of complex autolysates/ hydrolysates. Accordingly, the antioxidant and ACE-I activities exhibited by BSY autolysates, SPH and BSG protein hydrolysates resulted from the synergistic effect of a mixture of several compounds, such as, peptides, amino acids and phenolic compounds. As GI digestion and intestinal transport are the major barriers in the bioavailability of antioxidant and ACE-I bioactive compounds, research was focused on the effects of simulated GI proteases/peptidases in the formation and degradation of bioactive compounds and its susceptibility to intestinal transport. The ACE-I activity after simulated GI digestion was more pronounced for sarcoplasmic SPH (IC<sub>50</sub> of 117 µg protein/mL) than for BSY autolysate (IC<sub>50</sub> of 345 µg protein/mL). This result could suggest that SPH produced from action of BSY proteases on sarcoplasmic proteins from sardine by-products presented higher and potential to exert biological activity *in vivo*.

The comparison of ACE-I activities of BSY autoysates, SPH and BSG protein hydrolysates with other results reported in the literature is a difficult task due the use of different *in vitro* assays. However, the new bioactive ingredients produced in this work have

potential to be used in the prevention of hypertension or as initial treatment in mild hypertensive individuals.

In conclusion, this Ph.D. thesis revealed that BSY, the second major by-product from brewing process is a valuable source of proteins and proteases for the production of protein autolysates and hydrolysates. The promising antioxidant and ACE-I activities of BSY autolysates, SPH and BSG protein hydrolysates produced during the present study makes them potential ingredients to be explored in functional foods, cosmetic and pharmaceutical products. Hence, the results from this experimental work will contribute for the sustainability of brewing and canned sardine industry through the development of value-added products with greater commercial market.

## FUTURE PROSPECTS

As aforementioned in **Chapter 6**, several scientific, technological and regulatory issues should be comprehensively addressed if the major goal is the development of new bioactive ingredients to be incorporate in food chain or used as pharmaceutical agents in human nutrition and health. Thus, considering the conclusions obtained within this Ph.D. thesis, additional studies should be undertaken before application of BSY autolysate, SPH and BSG protein hydrolysates as nutraceutical or functional food ingredients, namely:

- (i) the purification and identification of the bioactive compounds responsible for the *in vitro* biological activities;
- (ii) the confirmation of the *in vivo* biological activities through animal model systems;
- (iii) the sensory evaluation of the potential new ingredients for the consumer acceptance.

The major barriers in the bioavailability of antioxidant compounds and ACE-I peptides are GI digestion and intestinal transport. In this work, permeability studies using the Caco-2 cell and Caco-2/HT28-MTX co-culture cell models provided evidence to support the possibility that antioxidant compounds present in the BSY autolysate and sarcoplasmic SPH were transported through the intestinal epithelium and may exert antioxidant activity *in vivo*. However, the identification of antioxidant peptides was not assessed during the present study and hence the mechanism of antioxidant action, the fate of antioxidant compounds during GI digestion and intestinal transport, as well as, the mechanisms of cell transport are need to be elucidated.

On the other hand, although the ACE-I activity of BSY autolysate was detected in the Caco-2 and Caco-2/HT28-MTX co-culture cell permeates, in case of sarcoplasmic SPH permeates no ACE-I activity was detected at the concentration tested, 2.0 mg proteins/mL. Although it was suggested that ACE-I peptides were degraded by brush border peptidases, there is also a possibility that sarcoplasmic SPH peptides present ACE-I activity if higher concentrations were used in this assay. Furthermore, as discussed in **Chapter 7**, the inhibition of ACE-I activity is not the only mechanism by which bioactive peptides can act as antihypertensive agents; bioactive peptides can also exhibit opiate and/ or vasorelaxing properties. Furthermore, since the sarcoplasmic SPH also presents high antioxidant potential, the antioxidant compounds could contribute to reduce the oxidative stress-related damage and, thereby, still reduce hypertension. Thus, it would be interesting to assess other possible antihypertensive mechanisms of sarcoplasmic SPH peptides. Moreover, the efficacy of BSY autolysate and sarcoplasmic SPH in cardiovascular diseases should be tested via *in vivo* animal model systems, firstly with spontaneously hypertensive rats (SHR) and further through clinical trials with human volunteers to validate the effective biological activity *in vivo*. Studies with sarcoplasmic SHR can involve measurement of systolic arterial blood pressure and determination of ACE activity and angiotensin II levels in plasma, after BSY autolysate or sarcoplasmic SPH oral administration (by gavage using a ball ended feeding needle). Additionally, the effect of chronic (oral) administration of BSY autolysate or sarcoplasmic SPH on structural patophysiological changes can be performed.

Once the potential biological activities of BSY autolysate and sarcoplasmic SPH peptides are established through clinical trials, further research is needed to identify appropriate functional food applications, as well as, to overcome problems during incorporating of these potential bioactive ingredients into food matrices. One possible problem is the bitterness associated with low molecular weight peptides and amino acids, probably present in BSY autolysate and sarcoplasmic SPH. In this case, the application of exo- and endo-peptidases to remove bitter amino acids without losing intended activity could be done. Other alternative is to mask the bitter taste via encapsulation of the compounds of interest, thus avoiding bitter taste perception and bioactive peptide degradation during digestion. Sensory studies will be required for this step.

Another problem to face is the possible interactions of bioactive compounds with other components in the food matrix during processing and storage period. Encapsulation of bioactive compounds is an effective strategy to overcome this limitation. Also, possible allergic reactions by incorporating bioactive compounds into functional foods may occur. Although BSY autolysate and sarcoplasmic SPH were non-toxic to Caco-2 cells when incubated for 24 h, at concentrations lower than 4.0 mg protein/mL, the present study did

not look into the possible allergenicity associated with these potential nutraceuticals. Thus, considering these potential limitations, more research work is needed in order to develop a functional food acceptable by consumers and without adverse effects.

Concerning the main findings obtained in **Chapter 9**, relative to the potential anti-inflammatory activity of sarcoplasmic SPH, further investigation of the sarcoplasmic SPH is required regarding its molecular composition, mechanisms of action and overall anti-inflammatory effects *in vivo*. With respect to the potential techno-functional properties observed for viscera SPH prepared by BSY proteases treatment (**Chapter 10**), its potential use as a multi-functional ingredient in emulsion-type food formulations should be also investigated. Finally, concerning to BSG protein hydrolysates (**Chapter 12**) further assays should be undertaken to evaluate the effects of simulated GI digestion and *in vitro* permeability transport on the biological activities. Moreover, before its exploitation as nutraceutical or a functional ingredient, its biological efficacy should be ascertained through *in vivo* assays.



## Bibliografic references

---





## BIBLIOGRAFIC REFERENCES

1. He S, Franco C, Zhang W. Functions, applications and production of protein hydrolysates from fish processing co-products (FPCP). *Food Res Int.* 2013;50(1):289-97.
2. Mussatto SI. Biotechnological potential of brewing industry by-products. In: Singh nee' Nigam P, Pandey A, editors. *Biotechnology for agro-industrial residues utilisation*: Springer; 2009. p. 313-326.
3. Unicer Bebidas de Portugal, SGPS. S.A. Management report. Portugal; 2013
4. Vieira E, Rocha MAM, Coelho E, Pinho O, Saraiva JA, Coimbra MA. Valuation of brewer's spent grain using a fully recyclable integrated process for extraction of proteins and arabinoxylans. *Ind Crops Prod.* 2014;52:136-43.
5. Ferreira IMPLVO, Pinho O, Vieira E, Tavela JG. Brewer's *Saccharomyces* yeast biomass: characteristics and potential applications. *Trends Food Sci Technol.* 2010;21(2):77-84.
6. Bekatorou A, Plessas S, Mantzourani I. Biotechnological exploitation of brewery solid wastes for recovery or production of value-added products. In: R Rai V, editor. *Advances in Food Biotechnology*: John Wiley & Sons Ltd; 2015. p. 393-414.
7. Celus I, Brijs K, Delcour JA. Enzymatic hydrolysis of brewers' spent grain proteins and technofunctional properties of the resulting hydrolysates. *J Agric Food Chem.* 2007;55(21):8703-10.
8. Celus I, Brijs K, Delcour JA. Fractionation and characterization of brewers' spent grain protein hydrolysates. *J Agric Food Chem.* 2009;57(12):5563-70.
9. Hassan HMM. Antioxidant and immunostimulating activities of yeast (*Saccharomyces cerevisiae*) autolysates. *World Appl Sci J.* 2011;15(8):1110-9.
10. Yeast Handling/Processing. Technical Evaluation Report Compiled by OMRI for the USDA National Organic Program. United States Department of Agriculture; 2014.
11. Hecht KA, O'Donnell AF, Brodsky JL. The proteolytic landscape of the yeast vacuole. *Cell Logist.* 2014;4(1):e28023.
12. Castro-Ceseña AB, del Pilar Sánchez-Saavedra M, Márquez-Rocha FJ. Characterisation and partial purification of proteolytic enzymes from sardine by-products to obtain concentrated hydrolysates. *Food Chem.* 2012;135(2):583-9.
13. Ferraro V, Carvalho AP, Piccirillo C, Santos MM, Castro PM, Pintado ME. Extraction of high added value biological compounds from sardine, sardine-type fish and mackerel canning residues - a review. *Mater Sci Eng C Mater Biol Appl.* 2013;33(6):3111-20.

14. Instituto Nacional de Estatística, IP. Estatísticas da Pesca 2010. Portugal; 2010.
15. Bougatef A, Nedjar-Arroume N, Ravallec-Plé R, Leroy Y, Guillochon D, Barkia A, Nasri M. Angiotensin I-converting enzyme (ACE) inhibitory activities of sardinelle (*Sardinella aurita*) by-products protein hydrolysates obtained by treatment with microbial and visceral fish serine proteases. Food Chem. 2008;111(2):350-6.
16. Bougatef A, Nedjar-Arroume N, Manni L, Ravallec R, Barkia A, Guillochon D, Nasri M. Purification and identification of novel antioxidant peptides from enzymatic hydrolysates of sardinelle (*Sardinella aurita*) by-products proteins. Food Chem. 2010;118(3):559-65.
17. Benhabiles MS, Abdi N, Drouiche N, Lounici H, Pauss A, Goosen MFA, Mameri N. Fish protein hydrolysate production from sardine solid waste by crude pepsin enzymatic hydrolysis in a bioreactor coupled to an ultrafiltration unit. Mater Sci Eng C. 2012;32(4):922-8.
18. EFSA Panel on Dietetic Products, Nutrition and Allergies (NDA); Scientific opinion on the safety of 'sardine peptide product' as a novel food ingredient. EFSA Journal 2010; 8(5):1684. [17 pp.].
19. Harnedy PA, FitzGerald RJ. Bioactive peptides from marine processing waste and shellfish: a review. J Funct Foods. 2012;4(1):6-24.
20. Souissi N, Bougatef A, Triki-Ellouz Y, Nasri M. Biochemical and functional properties of *Sardinella* (*Sardinella aurita*) by-product hydrolysates. Food Technol Biotechnol. 2007;45(2):187.
21. Bokulich NA, Bamforth CW. The microbiology of malting and brewing. Microbiol Mol Biol Rev. 2013;77(2):157-72.
22. dos Santos Mathias TR, de Mello PPM, Ervulo EFC. Solid wastes in brewing process: a review. J. Brew. Distilling. 2014;5(1):1-9.
23. Hellborg L, Piškur J. Yeast diversity in the brewing industry. In: Preedy VR, editor. Beer in health and disease prevention. New York: Elsevier: Academic Press; 2011. p. 1068-73.
24. Northern Arizona University. Yeast diagram [image on the Internet]. 2008 [cited 2016 Jan 10]. Available from: <http://www4.nau.edu/biology/bio205/handouts.htm>.
25. Caballero-Córdoba GM, Sgarbieri VC. Nutritional and toxicological evaluation of yeast (*Saccharomyces cerevisiae*) biomass and a yeast protein concentrate. J Sci Food Agric. 2000;80(3):341-51.
26. Saksinchai S, Suphantharika M, Verduyn C. Application of a simple yeast extract from spent brewer's yeast for growth and sporulation of *Bacillus thuringiensis* subsp. *kurstaki*: a physiological study. World J Microbiol Biotechnol. 2001;17(3):307-16.

27. Supphantharika M, Khunrae P, Thanardkit P, Verduyn C. Preparation of spent brewer's yeast beta-glucans with a potential application as an immunostimulant for black tiger shrimp, *Penaeus monodon*. *Bioresour Technol.* 2003;88(1):55-60.
28. Alvim ID, Vilela ESD, Baldini VLS, Bragagnolo N, Sgarbieri VC. Produção piloto de derivados de levedura (*Saccharomyces* sp.) para uso como ingrediente na formulação de alimentos. *Braz J Food Technol.* 1999;2(1, 2):119.
29. Chae HJ, Joo H, In MJ. Utilization of brewer's yeast cells for the production of food-grade yeast extract. Part 1: Effects of different enzymatic treatments on solid and protein recovery and flavour characteristics. *Bioresour Technol.* 2001;76(3):253-8.
30. Yamada EA, Sgarbieri VC. Yeast (*Saccharomyces cerevisiae*) protein concentrate: preparation, chemical composition, and nutritional and functional properties. *J Agric Food Chem.* 2005;53(10):3931-6.
31. Bekatorou A, Psarianos C, Koutinas AA. Production of food grade yeasts. *Food Technol. Biotechnol.* 2006;44(3):407-415.
32. Pinto L, Lopes M, Carvalho Filho C, Alves L, Benevides C. Determinação do valor nutritivo de derivados de levedura de cervejaria (*Saccharomyces* spp.). *Revista Brasileira de Produtos Agroindustriais.* 2013;15(1):7-17.
33. Herrero E, Ros J, Bellí G, Cabiscol E. Redox control and oxidative stress in yeast cells. *BBA.* 2008;1780(11):1217-35.
34. Moradas-Ferreira P, Costa V, Piper P, Mager W. The molecular defences against reactive oxygen species in yeast. *Mol Microbiol.* 1996;19(4):651-8.
35. Jamieson DJ. Oxidative stress responses of the yeast *Saccharomyces cerevisiae*. *Yeast.* 1998;14(16):1511-27.
36. Abbas CA. Production of antioxidants, aromas, colours, flavours, and vitamins by yeasts. In: Querol A, Fleet G, editors. *Yeasts in food and beverages*: Springer Berlin Heidelberg; 2006. p. 285-334.
37. Iliev A, Aleksandrov S, Kozarekova-Yovkova D. Changes of antioxidant activities of baker's and active dry yeasts during incubation. *First national conference of Biotechnology*; Sofia 2015. p. 49-62.
38. Carochi M, Ferreira IC. A review on antioxidants, prooxidants and related controversy: natural and synthetic compounds, screening and analysis methodologies and future perspectives. *Food Chem Toxicol.* 2013;51:15-25.
39. Salar RK, Certik M, Brezova V, Brlejšova M, Hanusova V, Breierová E. Stress influenced increase in phenolic content and radical scavenging capacity of *Rhodotorula glutinis* CCY 20-2-26. *3 Biotech.* 2013;3(1):53-60.

40. Moreira M. Extraction and characterization of natural antioxidants from brewing industry by-products [dissertation]. Porto: Faculty of Sciences: University of Porto; 2013.
41. Hancock RD, Galpin JR, Viola R. Biosynthesis of L-ascorbic acid (vitamin C) by *Saccharomyces cerevisiae*. FEMS Microbiol Lett. 2000;186(2):245-50.
42. Jones EW. Three proteolytic systems in the yeast *Saccharomyces cerevisiae*. J Biol Chem. 1991;266(13):7963-6.
43. Kato M, Kuzuhara Y, Maeda H, Shiraga S, Ueda M. Analysis of a processing system for proteases using yeast cell surface engineering: conversion of precursor of proteinase A to active proteinase A. Appl Microbiol Biotechnol. 2006;72(6):1229-37.
44. Roy MK, Watanabe Y, Tamai Y. Induction of apoptosis in HL-60 cells by skimmed milk digested with a proteolytic enzyme from the yeast *Saccharomyces cerevisiae*. J Biosci Bioeng. 1999;88(4):426-32.
45. Jung EY, Lee HS, Choi JW, Ra KS, Kim MR, Suh HJ. Glucose tolerance and antioxidant activity of spent brewer's yeast hydrolysate with a high content of Cyclo-His-Pro (CHP). J Food Sci. 2011;76(2):C272-8.
46. Zhang L, Jin Y, Xie Y, Wu X, Wu T. Releasing polysaccharide and protein from yeast cells by ultrasound: selectivity and effects of processing parameters. Ultrason Sonochem. 2014;21(2):576-81.
47. Lamoolphak W, Goto M, Sasaki M, Suphantharika M, Muangnapoh C, Prommuang C, Shotipruk A. Hydrothermal decomposition of yeast cells for production of proteins and amino acids. J Hazard Mater. 2006;137(3):1643-8.
48. In M-J, Kim DC, Chae HJ. Downstream process for the production of yeast extract using brewer's yeast cells. Biotechnol Bioprocess Eng. 2005;10(1):85-90.
49. Champagne CP, Gaudreau H, Conway J. Effect of the production or use of mixtures of baker's or brewer's yeast extracts on their ability to promote growth of *Lactobacilli* and *Pediococci*. Electron J Biotechnol. 2003;6(3):185-97.
50. Vieira E, Brandão T, Ferreira IMPLVO. Evaluation of brewer's spent yeast to produce flavour enhancer nucleotides: influence of serial repitching. J Agric Food Chem. 2013;61(37):8724-9.
51. Gaspar L, Camargo F, Gianeti M, Campos PM. Evaluation of dermatological effects of cosmetic formulations containing *Saccharomyces cerevisiae* extract and vitamins. Food Chem Toxicol. 2008;46(11):3493-500.
52. Hatoum R, Labrie S, Fliss I. Antimicrobial and probiotic properties of yeasts: from fundamental to novel applications. Front Microbiol. 2012;3:421.

53. Hosseinzadeh P, Djazayeri A, Mostafavi S-A, Javanbakht MH, Derakhshanian H, Rahimiforoushani A, Djalali M. Brewer's yeast improves blood pressure in type 2 diabetes mellitus. *Iran J Public Health*. 2013;42(6):602.
54. Chemical composition and biochemistry of yeast biomass. In: Halasz A, Lasztity R, editors. *Use of yeast biomass in food production*. USA: CRC Press, Inc; 1991. p. 23-41.
55. RingØ E, Olsen RE, Gifstad TØ, Dalmo RA, Amlund H, Hemre GI, Barke AM. Prebiotics in aquaculture: a review. *Aquac Nutr*. 2010;16(2):117-36.
56. Robbins E, Seeley R. Cholesterol lowering effect of dietary yeast and yeast fractions. *J Food Sci*. 1977;42(3):694-8.
57. Bell S, Goldman VM, Bistrian BR, Arnold AH, Ostroff G, Forse RA. Effect of  $\beta$ -glucan from oats and yeast on serum lipids. *Crit Rev Food Sci Nutr*. 1999;39(2):189-202.
58. Nakamura T, Hitomi Y, Yoshida M, Shirasu Y, Tsukui T, Shimasaki H. Effect of yogurt supplemented with brewer's yeast cell wall on levels of blood lipids in normal and hypercholesterolemic adults. *J Oleo Sci*. 2002;51(5):323-34.
59. Nakamura T, Agata K, Nishida S, Shirasu Y, Iino H. Effects of yogurt supplemented with brewer's yeast cell wall on intestinal environment and defecation in healthy female adults. *Biosci Microflora*. 2001;20(1):27-34.
60. Pacheco MTB, Sgarbieri VC. Hydrophilic and rheological properties of brewer's yeast protein concentrates. *J Food Sci*. 1998;63(2):238-43.
61. de Melo ANF, de Souza EL, da Silva Araujo VB, Magnani M. Stability, nutritional and sensory characteristics of French salad dressing made with mannoprotein from spent brewer's yeast. *LWT- Food Sci Technol*. 2015;62(1, Part 2):771-4.
62. Vetrivel J, Saravanamuthu R, Dhivaharan V. Biotechnological potential and industrial application of yeast. In: DK Maheshwari, Dubey RC, Saravanamurthu R, editors. *Industrial exploitation of microorganisms*. New Delhi IK International Publishing House Pvt. Ltd; 2010. p. 1-11.
63. Liu H, Lin JP, Cen PL, Pan YJ. Co-production of S-adenosyl-L-methionine and glutathione from spent brewer's yeast cells. *Process Biochem*. 2004;39(12):1993-7.
64. Roy MK, Watanabe Y, Tamai Y. Yeast protease B-digested skimmed milk inhibits angiotensin-I-converting-enzyme activity. *Biotechnol Appl Biochem*. 2000;31(Pt 2):95-100.
65. Sánchez B, Reverol L, Galindo-Castro I, Bravo A, Rangel-Aldao R, Ramírez JL. Brewer's yeast oxidoreductase with activity on Maillard reaction intermediates of beer. *Tech. Q. Master Brew. Assoc. Am*. 2003;40(3):204-21.
66. Liu D, Zeng X-A, Sun D-W, Han Z. Disruption and protein release by ultrasonication of yeast cells. *Innov Food Sci Emerg Technol*. 2013;18(0):132-7.

67. Shynkaryk M, Lebovka N, Lanoisellé J-L, Nonus M, Bedel-Clotour C, Vorobiev E. Electrically-assisted extraction of bio-products using high pressure disruption of yeast cells (*Saccharomyces cerevisiae*). J Food Eng. 2009;92(2):189-95.
68. Liu D, Lebovka N, Vorobiev E. Impact of electric pulse treatment on selective extraction of intracellular compounds from *Saccharomyces cerevisiae* yeasts. Food Bioproc Tech. 2013;6(2):576-84.
69. Geciova J, Bury D, Jelen P. Methods for disruption of microbial cells for potential use in the dairy industry - a review. Int Dairy J. 2002;12(6):541-53.
70. Klimek-Ochab M, Brzezińska-Rodak M, Żymańczyk-Duda E, Lejczak B, Kafarski P. Comparative study of fungal cell disruption - scope and limitations of the methods. Folia Microbiol. 2011;56(5):469-75.
71. Agrawal PB, Pandit AB. Isolation of  $\alpha$ -glucosidase from *Saccharomyces cerevisiae*: cell disruption and adsorption. Biochem Eng J. 2003;15(1):37-45.
72. Tanguler H, Erten H. Utilisation of spent brewer's yeast for yeast extract production by autolysis: the effect of temperature. Food Bioprod Process. 2008;86(4):317-21.
73. Hernawan T, Fleet G. Chemical and cytological changes during the autolysis of yeasts. J Ind Microbiol. 1995;14(6):440-50.
74. Kim D, Chae H, Oh N, In M. Effect of cell lytic enzyme on the production of yeast extract. J Kor Soc Agric Chem Biotechnol. 2001;44:273-5.
75. Kim. Jae-Ho; Lee D-HJ, Seoung-Chan; Chung, Kun-Sub; Lee, Jong-Soo Characterization of antihypertensive angiotensin I-converting enzyme inhibitor from *Saccharomyces cerevisiae*. J Microbiol Biotechnol. 2004;14(6):1318-23.
76. Bayarjargal EM, Ariunsaikhan T, Odonchimeg M, Uurzaikh T, Gan-Erdene T, Regdel D. Utilization of spent brewer's yeast *Saccharomyces cerevisiae* for the production of yeast enzymatic hydrolysate. Mong J Chem. 2011;12(38):88-91.
77. Bayarjargal EM, Ariunsaikhan T, Lkhagvamaa E, Ankhtsetseg B, Gan-Erdene T, Regdel D. Antioxidant properties of pancreatic hydrolysates from various protein sources. Mong J Chem. 2014;15:43-6.
78. Chung Y, Chae H, Kim D, Oh N, Park M, Lee Y, In M-J. Selection of commercial proteolytic enzymes for the production of brewer's yeast extract. Food Eng Progr. 1999;3:159-63.
79. Estevez PMM, inventor; Google Patents, assignee. Process for obtaining bioactive peptide and polysaccharide extracts from spent brewer's yeast and uses thereof. Patent WO2014102757 A1. 2014 Jul 3.
80. Dzogbefia V, Amoke E, Oldham J, Ellis W. Production and use of yeast pectolytic enzymes to aid pineapple juice extraction. Food Biotechnol. 2001;15(1):25-34.

81. Dzogbefia V, Djokoto D. Combined effects of enzyme dosage and reaction time on papaya juice extraction with the aid of pectic enzymes - a preliminary report. *J Food Biochem.* 2006;30(1):117-22.
82. Rakin M, Vukasinovic M, Siler-Marinkovic S, Maksimovic M. Contribution of lactic acid fermentation to improved nutritive quality vegetable juices enriched with brewer's yeast autolysate. *Food Chem.* 2007;100(2):599-602.
83. Dzogbefia V, Ofosu G, Oldham J. Evaluation of locally produced *Saccharomyces cerevisiae* pectinase enzyme for industrial extraction of starch from cassava in Ghana. *Sci. Res. Essays.* 2008;3(8):365-9.
84. Păucean A, Pârlog RM, Vodnar DC, Socaciu C, Mudura E. HPLC Analysis of vitamin B3 and vitamin C from a dairy product containing brewer's yeast. *J Agroaliment Proc Technol.* 2010;16(2):136-40.
85. Smith E-A, Myburgh J, Osthoff G, de Wit M. Acceleration of yoghurt fermentation time by yeast extract and partial characterisation of the active components. *J Dairy Res.* 2014;81(04):417-23.
86. Kanauchi O, Igarashi K, Ogata R, Mitsuyama K, Andoh A. A yeast extract high in bioactive peptides has a blood-pressure lowering effect in hypertensive model. *Curr Med Chem.* 2005;12(26):3085-90.
87. Bhat ZF, Kumar S, Bhat H. Bioactive peptides of animal origin: a review. *J Food Sci Technol.* 2015:1-16.
88. Samaranayaka AGP, Li-Chan ECY. Food-derived peptidic antioxidants: a review of their production, assessment, and potential applications. *J Funct Foods.* 2011;3(4):229-54.
89. Vercruysse L, Van Camp J, Smagghe G. ACE inhibitory peptides derived from enzymatic hydrolysates of animal muscle protein: a review. *J Agric Food Chem.* 2005;53(21):8106-15.
90. Huang D, Ou B, Prior RL. The chemistry behind antioxidant capacity assays. *J Agric Food Chem.* 2005;53(6):1841-56.
91. Prior RL, Wu X, Schaich K. Standardized methods for the determination of antioxidant capacity and phenolics in foods and dietary supplements. *J Agric Food Chem.* 2005;53(10):4290-302.
92. Elias RJ, Kellerby SS, Decker EA. Antioxidant activity of proteins and peptides. *Crit Rev Food Sci Nutr.* 2008;48(5):430-41.
93. Erdmann K, Cheung BW, Schröder H. The possible roles of food-derived bioactive peptides in reducing the risk of cardiovascular disease. *J Nutr Biochem.* 2008;19(10):643-54.

94. Badarinath A, Rao KM, Chetty CMS, Ramkanth S, Rajan T, Gnanaprakash K. A review on *in-vitro* antioxidant methods: comparisons, correlations and considerations. *Int J Pharmtech Res.* 2010;2(2):1276-85.
95. Kim S-K, Wijesekara I. Development and biological activities of marine-derived bioactive peptides: a review. *J Funct Foods.* 2010;2(1):1-9.
96. Pisoschi AM. Methods for total antioxidant activity determination: a review. *Biochem Anal Biochem.* 2011;1(1).
97. Gulcin I. Antioxidant activity of food constituents: an overview. *Arch Toxicol.* 2012;86(3):345-91.
98. Alam MN, Bristi NJ, Rafiquzzaman M. Review on *in vivo* and *in vitro* methods evaluation of antioxidant activity. *Saudi Pharm J.* 2013;21(2):143-52.
99. Chakrabarti S, Jahandideh F, Wu J. Food-derived bioactive peptides on inflammation and oxidative stress. *Biomed Res Int.* 2014;2014.
100. McCarthy AL, O'Callaghan YC, O'Brien NM. Protein hydrolysates from agricultural crops - bioactivity and potential for functional food development. *Agriculture.* 2013;3(1):112-30.
101. Ben Khaled H, Ghilissi Z, Chtourou Y, Hakim A, Ktari N, Fatma MA, Barkia A, Sahnoun Z, Moncef Nasri M. Effect of protein hydrolysates from sardinelle (*Sardinella aurita*) on the oxidative status and blood lipid profile of cholesterol-fed rats. *Food Res Int.* 2012;45(1):60-8.
102. Chalamaiah M, Dinesh kumar B, Hemalatha R, Jyothirmayi T. Fish protein hydrolysates: Proximate composition, amino acid composition, antioxidant activities and applications: a review. *Food Chem.* 2012;135(4):3020-38.
103. Sila A, Bougatef A. Antioxidant peptides from marine by-products: Isolation, identification and application in food systems: a review. *J Funct Foods.* 2016;21:10-26.
104. Ruiz-Gimenez P, Marcos JF, Torregrosa G, Lahoz A, Fernandez-Musoles R, Valles S, Alborch E, Manzanares P, Salom JB. Novel antihypertensive hexa- and heptapeptides with ACE-inhibiting properties: from the *in vitro* ACE assay to the spontaneously hypertensive rat. *Peptides.* 2011;32(7):1431-8.
105. Udenigwe CC, Mohan A. Mechanisms of food protein-derived antihypertensive peptides other than ACE inhibition. *J Funct Foods.* 2014;8(0):45-52.
106. Wijesekara I, Kim SK. Angiotensin-I-converting enzyme (ACE) inhibitors from marine resources: prospects in the pharmaceutical industry. *Mar Drugs.* 2010;8(4):1080-93.
107. Chen J, Wang Y, Ye R, Wu Y, Xia W. Comparison of analytical methods to assay inhibitors of angiotensin I-converting enzyme. *Food Chem.* 2013;141(4):3329-34.



108. Ben Henda Y, Labidi A, Arnaudin I, Bridiau N, Delatouche R, Maugard T, Piot JM, Sannier F, Thiéry V, Bordenave-Juchereau S. Measuring angiotensin-I converting enzyme inhibitory activity by micro plate assays: comparison using marine cryptides and tentative threshold determinations with captopril and losartan. *J Agric Food Chem.* 2013;61(45):10685-90.
109. Iroyukifujita H, Eiichiyokoyama K, Yoshikawa M. Classification and antihypertensive activity of angiotensin I-converting enzyme inhibitory peptides derived from food proteins. *J Food Sci.* 2000;65(4):564-9.
110. Wu J, Aluko RE, Nakai S. Structural requirements of angiotensin I-converting enzyme inhibitory peptides: quantitative structure-activity relationship study of di- and tripeptides. *J Agric Food Chem.* 2006;54(3):732-8.
111. Nakano D, Ogura K, Miyakoshi M, Ishii F, Kawanishi H, Kurumazuka D, Kwak CJ, Ikemura K, Takaoka M, Moriguchi S, Iino T, Kusumoto A, Asami S, Shibata H, Kiso Y, Matsumura Y. Antihypertensive effect of angiotensin I-converting enzyme inhibitory peptides from a sesame protein hydrolysate in spontaneously hypertensive rats. *Biosci Biotechnol Biochem.* 2006;70(5):1118-26.
112. Matsufuji H, Matsui T, Seki E, Osajima K, Nakashima M, Osajima Y. Angiotensin I-converting enzyme inhibitory peptides in an alkaline protease hydrolyzate derived from sardine muscle. *Biosci Biotechnol Biochem.* 1994;58(12):2244-5.
113. Terashima M, Oe M, Ogura K, Matsumura S. Inhibition strength of short peptides derived from an ACE inhibitory peptide. *J Agric Food Chem.* 2011;59(20):11234-7.
114. Cushman D, Cheung H. Spectrophotometric assay and properties of the angiotensin-converting enzyme of rabbit lung. *Biochem Pharmacol.* 1971;20(7):1637-48.
115. Wu J, Aluko RE, Muir AD. Improved method for direct high-performance liquid chromatography assay of angiotensin-converting enzyme-catalyzed reactions. *J Chromatogr A.* 2002;950(1):125-30.
116. Watanabe T, Mazumder TK, Nagai S, Tsuji K, Terabe S. Analysis method of the angiotensin-I converting enzyme inhibitory activity based on micellar electrokinetic chromatography. *Anal Sci.* 2003;19(1):159-61.
117. Cushman DW, Cheung H, Sabo E, Ondetti M. Design of potent competitive inhibitors of angiotensin-converting enzyme. Carboxyalkanoyl and mercaptoalkanoyl amino acids. *Biochem.* 1977;16(25):5484-91.
118. Vermeirssen V, Van Camp J, Verstraete W. Optimisation and validation of an angiotensin-converting enzyme inhibition assay for the screening of bioactive peptides. *J Biochem Biophys Methods.* 2002;51(1):75-87.

119. Murray BA, Walsh DJ, FitzGerald RJ. Modification of the furanacryloyl-L-phenylalanylglycylglycine assay for determination of angiotensin-I-converting enzyme inhibitory activity. *J Biochem Biophys Methods*. 2004;59(2):127-37.
120. Lahogue V, Réhel K, Taupin L, Haras D, Allaume P. A HPLC-UV method for the determination of angiotensin I-converting enzyme (ACE) inhibitory activity. *Food Chem*. 2010;118(3):870-5.
121. Sentandreu MÁ, Toldrá F. A rapid, simple and sensitive fluorescence method for the assay of angiotensin-I converting enzyme. *Food Chem*. 2006;97(3):546-54.
122. Quiros A, del Mar Contreras M, Ramos M, Amigo L, Recio I. Stability to gastrointestinal enzymes and structure-activity relationship of beta-casein-peptides with antihypertensive properties. *Peptides*. 2009;30(10):1848-53.
123. Carbonell-Capella JM, Buniowska M, Barba FJ, Esteve MJ, Frígola A. Analytical methods for determining bioavailability and bioaccessibility of bioactive compounds from fruits and vegetables: a review. *Compr Rev Food Sci Food Saf*. 2014;13(2):155-71.
124. Power O, Jakeman P, FitzGerald R. Antioxidative peptides: enzymatic production, *in vitro* and *in vivo* antioxidant activity and potential applications of milk-derived antioxidative peptides. *Amino Acids*. 2013;44(3):797-820.
125. van Breemen RB, Li Y. Caco-2 cell permeability assays to measure drug absorption. *Expert Opin Drug Metab Toxicol*. 2005;1(2):175-85.
126. Shimizu M, Tsunogai M, Arai S. Transepithelial transport of oligopeptides in the human intestinal cell, Caco-2. *Peptides*. 1997;18(5):681-7.
127. Cinq-Mars CD, Hu C, Kitts DD, Li-Chan EC. Investigations into inhibitor type and mode, simulated gastrointestinal digestion, and cell transport of the angiotensin I-converting enzyme-inhibitory peptides in Pacific hake (*Merluccius productus*) fillet hydrolysate. *J Agric Food Chem*. 2008;56(2):410-9.
128. Kleiveland, CR. Co-cultivation of Caco-2 and HT-29MTX. In: Verhoeckx K, Cotter P, López-Expósito I, Kleiveland C, Lea T, Mackie A, Requena T, Swiatecka D, Wichers H, editors. *The impact of food bioactives on health, in vitro and ex vivo models*: Springer International Publishing; 2015. p. 135-140.
129. del Mar Contreras M, Sancho A, Recio I, Mills C. Absorption of casein antihypertensive peptides through an *in vitro* model of intestinal epithelium. *Food Dig*. 2012;3(1-3):16-24.
130. Hilgendorf C, Spahn-Langguth H, Regardh CG, Lipka E, Amidon GL, Langguth P. Caco-2 versus Caco-2/HT29-MTX co-cultured cell lines: permeabilities via diffusion, inside- and outside-directed carrier-mediated transport. *J Pharm Sci*. 2000;89(1):63-75.

131. Antunes F, Andrade F, Araujo F, Ferreira D, Sarmento B. Establishment of a triple co-culture *in vitro* cell models to study intestinal absorption of peptide drugs. *Eur J Pharm Biopharm.* 2013;83(3):427-35.
132. Araujo F, Sarmento B. Towards the characterization of an *in vitro* triple co-culture intestine cell model for permeability studies. *Int J Pharm.* 2013;458(1):128-34.
133. Calatayud M, Vazquez M, Devesa V, Velez D. *In vitro* study of intestinal transport of inorganic and methylated arsenic species by Caco-2/HT29-MTX cocultures. *Chem Res Toxicol.* 2012;25(12):2654-62.
134. Kawasaki T, Seki E, Osajima K, Yoshida M, Asada K, Matsui T, Osajima Y. Antihypertensive effect of valyl-tyrosine, a short chain peptide derived from sardine muscle hydrolyzate, on mild hypertensive subjects. *J Hum Hypertens.* 2000;14(8):519-23.
135. Athmani N, Dehiba F, Allaoui A, Barkia A, Bougatef A, Lamri-Senhadj MY, Nasri M, Boualga A. *Sardina pilchardus* and *Sardinella aurita* protein hydrolysates reduce cholesterolemia and oxidative stress in rat fed high cholesterol diet. *J Exp Integr Med, Jan-Mar.* 2015;5(1):47.
136. Liu X-Y, Wang Q, Cui SW, Liu H-Z. A new isolation method of  $\beta$ -D-glucans from spent yeast *Saccharomyces cerevisiae*. *Food Hydrocoll.* 2008;22(2):239-47.
137. Aïmanianda V, Clavaud C, Simenel C, Fontaine T, Delepierre M, Latgé J-P. Cell wall  $\beta$ -(1, 6)-glucan of *Saccharomyces cerevisiae* structural characterization and *in situ* synthesis. *J Biol Chem.* 2009;284(20):13401-12.
138. Petravić-Tominac V, Zechner-Krpan V, Berković K, Galović P, Herceg Z, Srećec S, Srećec S, Špoljarić I. Rheological properties, water-holding, and oil-binding capacities of particulate beta-glucans, isolated from spent brewer's yeast by three different procedures. *Food Technol Biotechnol.* 2011;49(1):56-64.
139. Martins ZE, Erben M, Gallardo AE, Silva R, Barbosa I, Pinho O, Ferreira IMPLVO. Effect of spent yeast fortification on physical parameters, volatiles and sensorial characteristics of home-made bread. *Int J Food Sci Technol.* 2015;50(8):1855-63.
140. Vieira E, Moura C, Almeida T, Meireles S, Brandão T, Pinho O, Ferreira IMPLVO. Influence of serial repitching on beer polypeptide profiles. *J Am Soc Brew Chem.* 2012;70(4):275-9.
141. Rizzo M, Ventrice D, Varone MA, Sidari R, Caridi A. HPLC determination of phenolics adsorbed on yeasts. *J Pharm Biomed Anal.* 2006;42(1):46-55.
142. Edens NK, Reaves LA, Bergana MS, Reyzer IL, O'Mara P, Baxter JH, Snowden MK. Yeast extract stimulates glucose metabolism and inhibits lipolysis in rat adipocytes *in vitro*. *J Nutr.* 2002;132(6):1141-8.

143. EFSA Panel on Dietetic Products, Nutrition and Allergies. Scientific Opinion on the safety of 'yeast beta-glucans' as a Novel Food ingredient. *EFSA Journal*. 2011;9(5):2137-59.
144. Gaithersburg MD. Official methods of analysis of AOAC International. 17<sup>th</sup> ed. USA: Association of Analytical Communities; 2000.
145. Schmitt MR, Budde AD. Wort free amino nitrogen analysis adapted to a microplate format. *J Am Soc Brew Chem*. 2012;70(2):95.
146. Liwarska-Bizukojc E, Ledakowicz S. RNA assay as a method of viable biomass determination in the organic fraction of municipal solid waste suspension. *Biotechnol Lett*. 2001;23(13):1057-60.
147. Herbert D, Phipps P, Strange R. Chemical analysis of microbial cells. *Methods Microbiol*. 1971;5(Part B):209-344.
148. Pérez-Palacios T, Melo A, Cunha S, Ferreira IMPLVO. Determination of free amino acids in coated foods by GC-MS: optimization of the extraction procedure by using statistical design. *Food Anal Methods*. 2014;7(1):172-80.
149. Energy and protein requirements. Report of a joint FAO/WHO/UNU Expert Consultation technical report FAO/WHO and United Nations University, Geneva. 1990;724:116-29.
150. Lee YB, Elliott JG, Rickansrud DA, Hagberg EYC. Predicting protein efficiency ratio by the chemical determination of connective tissue content in meat. *J Food Sci* 1978;43(5):1359-62.
151. Parlog RM, Nicula A, Nicula T, Socaciu C. The optimization of extraction and HPLC analysis of vitamins B from yeast products. *Bulletin UASVM Agriculture*. 2008;65(2).
152. Grotzkyj Giorgi M, Howland K, Martin C, Bonner AB. A novel HPLC method for the concurrent analysis and quantitation of seven water-soluble vitamins in biological fluids (plasma and urine): a validation study and application. *Sci World J*. 2012;2012:359721.
153. Ciulu M, Solinas S, Floris I, Panzanelli A, Pilo MI, Piu PC, Spano N, Sanna G. RP-HPLC determination of water-soluble vitamins in honey. *Talanta*. 2011;83(3):924-9.
154. Jansen E, Ruskovska T. Comparative analysis of serum (anti)oxidative status parameters in healthy persons. *Int J Mol Sci*. 2013;14(3):6106-15.
155. Herald TJ, Gadgil P, Tilley M. High-throughput micro plate assays for screening flavonoid content and DPPH-scavenging activity in sorghum bran and flour. *J Sci Food Agric*. 2012;92(11):2326-31.
156. Almeida IMC, Barreira JCM, Oliveira MBPP, Ferreira ICFR. Dietary antioxidant supplements: benefits of their combined use. *Food Chem Toxicol*. 2011;49(12):3232-7.

157. Khanam UKS, Oba S, Yanase E, Murakami Y. Phenolic acids, flavonoids and total antioxidant capacity of selected leafy vegetables. *J Funct Foods*. 2012;4(4):979-87.
158. Institute of Medicine (US) Committee to Review Dietary Reference Intakes for Vitamin D and Calcium. In: Ross AC, Taylor CL, Yaktine AL, Del Valle, editors. *Dietary Reference Intakes for Calcium and Vitamin D*. Washington (DC): National Academies Press (US); 2011. Summary Tables. Available from: <http://www.ncbi.nlm.nih.gov/books/NBK56068/>
159. Hjortmo S, Patring J, Jastrebova J, Andlid T. Inherent biodiversity of folate content and composition in yeasts. *Trends Food Sci Technol*. 2005;16(6):311-6.
160. Jang J-H, Lee J-S. Antihypertensive angiotensin I-converting enzyme inhibitory activity and antioxidant activity of *Vitis hybrid-Vitis coignetiae* red wine made with *Saccharomyces cerevisiae*. *Mycobiology*. 2011;39(2):137-9.
161. Lee BH. Yeast-based processes and products. *Fundamentals of food biotechnology*: John Wiley & Sons, Ltd; 2015. p. 205-39.
162. Laemmli UK. Cleavage of structural proteins during the assembly of the head of bacteriophage T4. *Nature*. 1970;227(5259):680-5.
163. It's Fast IsE, Blue IT. Determination of total protein by the Lowry method using the BioTek Instruments' ELx808 Microplate Reader. 2006.
164. Cupp-Enyard C. Sigma's non-specific protease activity assay - casein as a substrate. *JoVE*. 2008;19(899).
165. Minervini F, Algaron F, Rizzello C, Fox P, Monnet V, Gobbetti M. Angiotensin I-converting-enzyme-inhibitory and antibacterial peptides from *Lactobacillus helveticus* PR4 proteinase-hydrolyzed caseins of milk from six species. *Appl Environ Microbiol*. 2003;69(9):5297-305.
166. Yamada EA, Alvim ID, Santucci MCC, Sgarbieri VC. Composição centesimal e valor protéico de levedura residual da fermentação etanólica e de seus derivados. *Rev nutr*. 2003;16(4):423-32.
167. Slaughter JC, Nomura T. Activity of the vacuolar proteases of yeast and the significance of the cytosolic protease inhibitors during the post-fermentation decline phase. *J Inst Brew*. 1992;98(4):335-8.
168. Rodarte MP, Dias DR, Vilela DM, Schwan RF. Proteolytic activities of bacteria, yeasts and filamentous fungi isolated from coffee fruit (*Coffea arabica* L.). *Acta Sci Agron*. 2011;33(3):457-64.
169. Mirzaei M, Mirdamadi S, Ehsani MR, Aminlari M, Hosseini E. Purification and identification of antioxidant and ACE-inhibitory peptide from *Saccharomyces cerevisiae* protein hydrolysate. *J Funct Foods*. 2015;19, Part A:259-68.

170. Jang J-H, Jeong S-C, Lee J-K, Lee J-S. Digestion pattern of antihypertensive Angiotensin I-converting enzyme inhibitory peptides from *Saccharomyces cerevisiae* in a successive simulated gastrointestinal bioreactor. *Mycobiology*. 2011;39(1):67-9.
171. Bradford Protein Assay. Bio-protocol Bio101: e45 <http://www.bio-protocol.org/e45> 2011.
172. Mandenius CF, Brundin A. Bioprocess optimization using design-of-experiments methodology. *Biotechnol Prog*. 2008;24(6):1191-203.
173. Goudarzi M, Madadlou A, Mousavi M, Emam-Djomeh Z. Optimized preparation of ACE-inhibitory and antioxidative whey protein hydrolysate using response surface method. *Dairy Sci Technol*. 2012;92(6):641-53.
174. Guo Y, Pan D, Tanokura M. Optimisation of hydrolysis conditions for the production of the angiotensin-I converting enzyme (ACE) inhibitory peptides from whey protein using response surface methodology. *Food Chem*. 2009;114(1):328-33.
175. Thammakiti S, Supphantharika M, Phaesuwan T, Verduyn C. Preparation of spent brewer's yeast  $\beta$ -glucans for potential applications in the food industry. *Int J Food Sci Technol*. 2004;39(1):21-9.
176. Boonyeun P, Shotipruk A, Prommuak C, Supphantharika M, Muangnapoh C. Enhancement of amino acid production by two-step autolysis of spent brewer's yeast. *Chem Eng Commun*. 2011;198(12):1594-602.
177. Vieira EF, Teixeira J, Ferreira IMPLVO. Valorisation of brewer's spent grain and spent yeast through protein hydrolysates with antioxidant properties. *Eur Food Res Technol*. 2016. DOI: 10.1007/s00217-016-2696-y.
178. Gallego M, Grootaert C, Mora L, Aristoy MC, Van Camp J, Toldrá F. Transepithelial transport of dry-cured ham peptides with ACE inhibitory activity through a Caco-2 cell monolayer. *J Funct Foods*. 2016;21:388-95.
179. Musatti A, Devesa V, Calatayud M, Vélez D, Manzoni M, Rollini M. Glutathione-enriched baker's yeast: production, bioaccessibility and intestinal transport assays. *J Appl Microbiol*. 2014;116(2):304-13.
180. Kosińska A, Andlauer W. Modulation of tight junction integrity by food components. *Food Res Int*. 2013;54(1):951-60.
181. Samaranayaka AG, Kitts DD, Li-Chan EC. Antioxidative and angiotensin-I-converting enzyme inhibitory potential of a Pacific Hake (*Merluccius productus*) fish protein hydrolysate subjected to simulated gastrointestinal digestion and Caco-2 cell permeation. *J Agric Food Chem*. 2010;58(3):1535-42.

182. Laitinen LA, Galkin A, Vuorela HJ, Marvola ML, Vuorela PM. Effects of extracts of commonly consumed food supplements and food fractions on the permeability of drugs across Caco-2 cell monolayers. *Pharmaceu Res.* 2004;21(10):1904-16.
183. da Silva DD, Silva E, Carmo H. Combination effects of amphetamines under hyperthermia - the role played by oxidative stress. *J Appl Toxicol.* 2014;34(6):637-50.
184. Ferraro V, Ferreira Jorge R, Cruz IB, Antunes F, Sarmento B, Castro PML, Pintado ME. *In vitro* intestinal absorption of amino acid mixtures extracted from codfish (*Gadus morhua* L.) salting wastewater. *Int J Food Sci Technol.* 2014;49(1):27-33.
185. Ferreira IMPLVO, Eça R, Pinho O, Tavares P, Pereira A, Cecília Roque A. Development and validation of an HPLC/UV method for quantification of bioactive peptides in fermented milks. *J Liq Chromatogr Relat Technol.* 2007;30(14):2139-47.
186. Putnam KP, Bombick DW, Doolittle DJ. Evaluation of eight *in vitro* assays for assessing the cytotoxicity of cigarette smoke condensate. *Toxicol In Vitro.* 2002;16(5):599-607.
187. Ward MW, Huber HJ, Weisova P, Dussmann H, Nicholls DG, Prehn JH. Mitochondrial and plasma membrane potential of cultured cerebellar neurons during glutamate-induced necrosis, apoptosis, and tolerance. *J Neurosci.* 2007;27(31):8238-49.
188. Ding L, Wang L, Zhang Y, Liu J. Transport of antihypertensive peptide RVPSL, ovotransferrin 328–332, in human intestinal Caco-2 cell monolayers. *J Agric Food Chem.* 2015;63(37):8143-50.
189. Yee S. *In vitro* permeability across Caco-2 cells (colonic) can predict *in vivo* (small intestinal) absorption in man - fact or myth. *Pharm Res.* 1997;14(6):763-6.
190. Jin Y, Song Y, Zhu X, Zhou D, Chen C, Zhang Z, Huang Y. Goblet cell-targeting nanoparticles for oral insulin delivery and the influence of mucus on insulin transport. *Biomaterials.* 2012;33(5):1573-82.
191. Fuller E, Duckham C, Wood E. Disruption of epithelial tight junctions by yeast enhances the paracellular delivery of a model protein. *Pharmaceu Res.* 2007;24(1):37-47.
192. Escudero E, Mora L, Toldrá F. Stability of ACE inhibitory ham peptides against heat treatment and *in vitro* digestion. *Food Chem.* 2014;161:305-11.
193. Silva A, Carrera P, Massé J, Uriarte A, Santos MB, Oliveira PB, Soares E, Porteiro C. Geographic variability of sardine growth across the northeastern Atlantic and the Mediterranean Sea. *Fish Res.* 2008;90(1–3):56-69.
194. Kristinsson HG, Rasco BA. Fish protein hydrolysates: production, biochemical, and functional properties. *Crit Rev Food Sci Nutr.* 2000;40(1):43-81.

195. Park JD, Yongsawatdigul J, Choi YJ, Park JW. Biochemical and conformational changes of myosin purified from Pacific sardine at various pHs. J Food Sci. 2008;73(3):C191-7.
196. Chaijan M, Benjakul S, Visessanguan W, Faustman C. Characterisation of myoglobin from sardine (*Sardinella gibbosa*) dark muscle. Food Chem. 2007;100(1):156-64.
197. Park JD. Characterization of myosin, myoglobin, and phospholipids isolated from Pacific Sardine (*Sardinops Sagax*). [dissertation]. Oregon: Food Science and Technology: Oregon State University; 2008.
198. Karthikeyan M, Mathew S, Shamasundar BA, Rakash VP. Fractionation and properties of sarcoplasmic proteins from oil sardine (*Sardinella longiceps*): influence on the thermal gelation behavior of washed meat. J Food Sci. 2004;69(3):79-84.
199. Klomklao S, Benjakul S, Visessanguan W, Kishimura H, Simpson BK. Proteolytic degradation of sardine (*Sardinella gibbosa*) proteins by trypsin from skipjack tuna (*Katsuwonus pelamis*) spleen. Food Chem. 2006;98(1):14-22.
200. Ghorbel S, Souissi N, Triki-Ellouz Y, Dufossé L, Guérard F, Nasri M. Preparation and testing of *Sardinella* protein hydrolysates as nitrogen source for extracellular lipase production by *Rhizopus oryzae*. World J Microbiol Biotechnol. 2005;21(1):33-8.
201. Kotzamanis Y, Gisbert E, Gatesoupe F, Infante JZ, Cahu C. Effects of different dietary levels of fish protein hydrolysates on growth, digestive enzymes, gut microbiota, and resistance to *Vibrio anguillarum* in European sea bass (*Dicentrarchus labrax*) larvae. Comp Biochem Physiol A Mol Integr Physiol. 2007;147(1):205-14.
202. Quaglia G, Orban E. Influence of enzymatic hydrolysis on structure and emulsifying properties of sardine (*Sardina pilchardus*) protein hydrolysates. J Food Sci. 1990;55(6):1571-3.
203. Shahidi F. Seafood processing by-products. In: Shahidi F, Botta JR, editors. Seafoods: chemistry, processing technology and quality: Springer US; 1994. p. 320-34.
204. Chaijan M, Benjakul S, Visessanguan W, Faustman C. Physicochemical properties, gel-forming ability and myoglobin content of sardine (*Sardinella gibbosa*) and mackerel (*Rastrelliger kanagurta*) surimi produced by conventional method and alkaline solubilisation process. Eur Food Res Technol. 2006;222(1-2):58-63.
205. Ryan JT, Ross RP, Bolton D, Fitzgerald GF, Stanton C. Bioactive peptides from muscle sources: meat and fish. Nutrients. 2011;3(9):765-91.



206. Carrasco-Castilla J, Hernández-Álvarez AJ, Jiménez-Martínez C, Gutiérrez-López GF, Dávila-Ortiz G. Use of proteomics and peptidomics methods in food bioactive peptide science and engineering. *Food Eng Reviews*. 2012;4(4):224-43.
207. Batista I, Pires C, Nelhas R. Extraction of sardine proteins by acidic and alkaline solubilisation. *Food Sci Technol Int*. 2007;13(3):189-94.
208. Cortes-Ruiz JA, Pacheco-Aguilar R, Garciasanchez G, Lugo-Sanchez ME. Functional characterization of a protein concentrate from bristly sardine made under acidic conditions. *J Aquat Food Prod*. 2001;10(4):5-23.
209. Barkia A, Bougatef ALI, Khaled HB, Nasri M. Antioxidant activities of sardinelle heads and/or viscera protein hydrolysates prepared by enzymatic treatment. *J Food Biochem*. 2010;34:303-20.
210. Matsui T, Matsufuji H, Seki E, Osajima K, Nakashima M, Osajima Y. Inhibition of angiotensin I-converting enzyme by *Bacillus licheniformis* alkaline protease hydrolyzates derived from sardine muscle. *Biosci Biotechnol Biochem*. 1993;57(6):922-5.
211. Kechaou ES, Dumay J, Donnay-Moreno C, Jaouen P, Gouygou J-P, Bergé J-P, Amar RB. Enzymatic hydrolysis of cuttlefish (*Sepia officinalis*) and sardine (*Sardina pilchardus*) viscera using commercial proteases: effects on lipid distribution and amino acid composition. *J Biosci Bioeng*. 2009;107(2):158-64.
212. Taheri A, Abedian Kenari A, Motamedzadegan A, Habibi Rezaie M. Optimization of goldstripe sardine (*Sardinella gibbosa*) protein hydrolysate using Alcalase® 2.4L by response surface methodology. *CyTA - J Food*. 2011;9(2):114-20.
213. Morales-Medina R, Tamm F, Guadix AM, Guadix EM, Drusch S. Functional and antioxidant properties of hydrolysates of sardine (*S. pilchardus*) and horse mackerel (*T. mediterraneus*) for the microencapsulation of fish oil by spray-drying. *Food Chem*. 2016;194:1208-16.
214. Dumay J, Allery M, Donnay-Moreno C, Barnathan G, Jaouen P, Carbonneau ME, Pascal J, Bergé JP. Optimization of hydrolysis of sardine (*Sardina pilchardus*) heads with Protamex: enhancement of lipid and phospholipid extraction. *J Sci Food Agric*. 2009;89(9):1599-606.
215. García-Moreno PJ, Batista I, Pires C, Bandarra NM, Espejo-Carpio FJ, Guadix A, Guadix EM. Antioxidant activity of protein hydrolysates obtained from discarded Mediterranean fish species. *Food Res Int*. 2014;65, Part C(0):469-76.
216. Aristotelis T, Himonides AKDT, Anne J. Morris. A study of the enzymatic hydrolysis of fish frames using model systems. *Food Nutr Sci*. 2011;2(6):575-85.
217. Aspino SI, Horn SJ, H. Eijssink VG. Enzymatic hydrolysis of Atlantic cod (*Gadus morhua* L.) viscera. *Process Biochem*. 2005;40(5):1957-66.

218. Halim NRA, Yusof HM, Sarbon NM. Functional and bioactive properties of fish protein hydolysates and peptides: a comprehensive review. *Trends Food Sci Technol.* 2016;51:24-33.
219. Chove LM, Grandison AS, Lewis MJ. Comparison of methods for analysis of proteolysis by plasmin in milk. *J Dairy Res.* 2011;78(2):184-90.
220. Toldrá F, Sentandreu MA, Aristoy M-C. Determination of Proteolysis. In: Nollet LML, Toldra F, editors. *Handbook of processed meats and poultry analysis.* USA: CRC Press; 2008. p. 163-171.
221. Léonil J, Gagnaire V, Mollé D, Pezennec S, Bouhallab Sd. Application of chromatography and mass spectrometry to the characterization of food proteins and derived peptides. *J Chromatogr A.* 2000;881(1):1-21.
222. Khaled HB, Ktari N, Ghorbel-Bellaaj O, Jridi M, Lassoued I, Nasri M. Composition, functional properties and *in vitro* antioxidant activity of protein hydrolysates prepared from sardinelle (*Sardinella aurita*) muscle. *J Food Sci Technol.* 2014;51(4):622-33.
223. Jemil I, Jridi M, Nasri R, Ktari N, Ben Slama-Ben Salem R, Mehiri M, Hajji M, Nasria M. Functional, antioxidant and antibacterial properties of protein hydrolysates prepared from fish meat fermented by *Bacillus subtilis* A26. *Process Biochem.* 2014;49(6):963-72.
224. García-Moreno PJ, Guadix A, Guadix EM, Jacobsen C. Physical and oxidative stability of fish oil-in-water emulsions stabilized with fish protein hydrolysates. *Food Chem.* 2016;203:124-35.
225. Ravallec-Plé R, Charlot C, Pires C, Braga V, Batista I, Van Wormhoudt A, Le Gal Y, Fouchereau-Péron M. The presence of bioactive peptides in hydrolysates prepared from processing waste of sardine (*Sardina pilchardus*). *J Sci Food Agric.* 2001;81(11):1120-5.
226. Fitzgerald A, Rai P, Marchbank T, Taylor G, Ghosh S, Ritz B, Playford RJ. Reparative properties of a commercial fish protein hydrolysate preparation. *Gut.* 2005;54(6):775-81.
227. Erdmann K, Grosser N, Schipporeit K, Schröder H. The ACE inhibitory dipeptide Met-Tyr diminishes free radical formation in human endothelial cells via induction of heme oxygenase-1 and ferritin. *J Nutr.* 2006;136(8):2148-52.
228. Louala S, Hamza-Reguig S, Benyahia-Mostefaoui A, Boualga A, Lamri-Senhadj MY. Effects of highly purified sardine proteins on lipid peroxidation and reverse cholesterol transport in rats fed a cholesterol-rich diet. *J Funct Foods.* 2011;3(4):321-8.

229. Sugiyama K, Egawa M, Onzuka H, Oba K. Characteristics of sardine muscle hydrolysates prepared by various enzymic treatments. *Bull Jpn Soc Sci Fish.* 1991;75:475-9.
230. Ukeda H, Matsuda H, Kuroda H, Osajima K, Matsufuji H, Osajima Y. Preparation and separation of angiotensin I converting enzyme inhibitory peptides. *J Agric Chem Soc of Japan.* 1991; 65:1223-1228.
231. Matsui T, Matsufuji H, Seki E, Osajima K, Nakashima M, Osajima Y. Inhibition of angiotensin I-converting enzyme by *Bacillus licheniformis* alkaline protease hydrolyzates derived from sardine muscle. *Biosci Biotechnol Biochem.* 1993;57(6):922-5.
232. Suetsuna K, Ukeda H. Isolation of an octapeptide which possesses active oxygen scavenging activity from peptic digest of sardine muscle. *Nippon Suisan Gakkaishi.* 1999;65(6):1096-9.
233. Taheri A, Anvar S, Ahari H, Fogliano V. Comparison the functional properties of protein hydrolysates from poultry byproducts and rainbow trout (*Onchorhynchus mykiss*) viscera. *Iran J Fish Sci.* 2013;12(1):154-69.
234. Nazeer R, Deeptha R. Antioxidant activity and amino acid profiling of protein hydrolysates from the skin of *Sphyraena barracuda* and *Lepturacanthus savala*. *Int J Food Prop.* 2013;16(3):500-11.
235. Zhang L, Liu Y, Lu D, Han J, Lu X, Tian Z, Wang Z. Angiotensin converting enzyme Inhibitory, antioxidant activities, and antihyperlipidaemic activities of protein hydrolysates from Scallop Mantle (*Chlamys Farreri*). *Int J Food Prop.* 2015;18(1):33-42.
236. Cinq-Mars CD, Li-Chan EC. Optimizing angiotensin I-converting enzyme inhibitory activity of Pacific hake (*Merluccius productus*) fillet hydrolysate using response surface methodology and ultrafiltration. *J Agric Food Chem.* 2007;55(23):9380-8.
237. Ren J, Zhao M, Shi J, Wang J, Jiang Y, Cui C, Kakuda Y, Xue SJ. Optimization of antioxidant peptide production from grass carp sarcoplasmic protein using response surface methodology. *Food Sci Technol.* 2008;41(9):1624-32.
238. Hsu K-C. Purification of antioxidative peptides prepared from enzymatic hydrolysates of tuna dark muscle by-product. *Food Chem.* 2010;122(1):42-8.
239. Wiriayaphan C, Chitsomboon B, Yongsawadigul J. Antioxidant activity of protein hydrolysates derived from threadfin bream surimi byproducts. *Food Chem.* 2012;132(1):104-11.
240. Yang P, Ke H, Hong P, Zeng S, Cao W. Antioxidant activity of bigeye tuna (*Thunnus obesus*) head protein hydrolysate prepared with Alcalase. *Int J Food Sci Technol.* 2011;46(12):2460-6.

241. Yongsawatdigul J, Hemung B-O. Structural changes and functional properties of Threadfin Bream sarcoplasmic proteins subjected to pH-shifting treatments and lyophilization. *J Food Sci.* 2010;75(3):C251-C7.
242. Ladrat C, Verrez-Bagnis V, Noël J, Fleurence J. *In vitro* proteolysis of myofibrillar and sarcoplasmic proteins of white muscle of sea bass (*Dicentrarchus labrax L.*): effects of cathepsins B, D and L. *Food Chem.* 2003;81(4):517-25.
243. Miguel M, Davalos A, Manso MA, de la Pena G, Lasuncion MA, Lopez-Fandino R. Transepithelial transport across Caco-2 cell monolayers of antihypertensive egg-derived peptides. PepT1-mediated flux of Tyr-Pro-Ile. *Mol Nutr Food Res.* 2008;52(12):1507-13.
244. Picot L, Ravallec R, Fouchereau-Peron M, Vandanjon L, Jaouen P, Chaplain-Derouiniot M, Guérard F, Chabeaud A, Legal Y, Alvarez OM, Bergé JP, Piot JM, Batista I, Pires C, Thorkelsson G, Delannoy C, Jakobsen G, Johansson I, Bourseau P. Impact of ultrafiltration and nanofiltration of an industrial fish protein hydrolysate on its bioactive properties. *J Sci Food Agric.* 2010;90(11):1819-26.
245. Ding L, Zhang Y, Jiang Y, Wang L, Liu B, Liu J. Transport of egg white ACE-inhibitory peptide, Gln-Ile-Gly-Leu-Phe, in human intestinal Caco-2 cell monolayers with cytoprotective effect. *J Agric Food Chem.* 2014;62(14):3177-82.
246. Wiriyaphan C, Xiao H, Decker EA, Yongsawatdigul J. Chemical and cellular antioxidative properties of threadfin bream (*Nemipterus spp.*) surimi byproduct hydrolysates fractionated by ultrafiltration. *Food Chem.* 2015;167:7-15.
247. Pérez-Vega JA, Olivera-Castillo L, Gómez-Ruiz JÁ, Hernández-Ledesma B. Release of multifunctional peptides by gastrointestinal digestion of sea cucumber (*Isostichopus badionotus*). *J Funct Foods.* 2013;5(2):869-77.
248. Sarmento B, Andrade F, Silva SBd, Rodrigues F, das Neves J, Ferreira D. Cell-based *in vitro* models for predicting drug permeability. *Expert Opin Drug Metab Toxicol.* 2012;8(5):607-21.
249. Sambuy Y, De Angelis I, Ranaldi G, Scarino M, Stammati A, Zucco F. The Caco-2 cell line as a model of the intestinal barrier: influence of cell and culture-related factors on Caco-2 cell functional characteristics. *Cell Biol Toxicol.* 2005;21(1):1-26.
250. Renukuntla J, Vadlapudi AD, Patel A, Boddu SHS, Mitra AK. Approaches for enhancing oral bioavailability of peptides and proteins. *Int J Pharm.* 2013;447(0):75-93.
251. Vieira EF, Ferreira IMPLVO. Antioxidant and antihypertensive hydrolysates obtained from by-products of cannery sardine and brewing industries. *Int J Food Prop.* 2016. DOI:10.1080/10942912.2016.1176036.

252. Jeon Y-J, Byun H-G, Kim S-K. Improvement of functional properties of cod frame protein hydrolysates using ultrafiltration membranes. *Process Biochem.* 1999;35(5):471-8.
253. Connolly A, O'Keeffe MB, Piggott CO, Nongonierma AB, FitzGerald RJ. Generation and identification of angiotensin converting enzyme (ACE) inhibitory peptides from a brewers' spent grain protein isolate. *Food Chem.* 2015;176:64-71.
254. Lee S-H, Qian Z-J, Kim S-K. A novel angiotensin I converting enzyme inhibitory peptide from tuna frame protein hydrolysate and its antihypertensive effect in spontaneously hypertensive rats. *Food Chem.* 2010;118(1):96-102.
255. Wu J, Ding X. Characterization of inhibition and stability of soy-protein-derived angiotensin I-converting enzyme inhibitory peptides. *Food Res Int.* 2002;35(4):367-75.
256. Gouyer V, Wiede A, Buisine MP, Dekeyser S, Moreau O, Lesuffleur T, Hoffmann W, Huet G. Specific secretion of gel-forming mucins and TFF peptides in HT-29 cells of mucin-secreting phenotype. *Biochim Biophys Acta.* 2001;1539(1-2):71-84.
257. Behrens I, Stenberg P, Artursson P, Kissel T. Transport of lipophilic drug molecules in a new mucus-secreting cell culture model based on HT29-MTX cells. *Pharm Res.* 2001;18(8):1138-45.
258. Pontier C, Pachot J, Botham R, Lenfant B, Arnaud P. HT29-MTX and Caco-2/TC7 monolayers as predictive models for human intestinal absorption: role of the mucus layer. *J Pharm Sci.* 2001;90(10):1608-19.
259. Regazzo D, Mollé D, Gabai G, Tomé D, Dupont D, Leonil J, Boutrou R. The (193–209) 17-residues peptide of bovine  $\beta$ -casein is transported through Caco-2 monolayer. *Mol Nutr Food Res.* 2010;54(10):1428-35.
260. Kunimoto A, Yokoro M, Murota K, Yamanishi R, Suzuki-Yamamoto T, Suzuki M, Yutani C, Doi S, Hiemori M, Yamashita H, Takahashi Y, Tsuji H, Kimoto M. Gastrointestinal digestion and absorption of Pen j 1, a major allergen from Kuruma prawn, *Penaeus japonicus*. *Biosci Biotechnol Biochem.* 2011;75(7):1249-58.
261. Vermeirssen V, Van Camp J, Verstraete W. Fractionation of angiotensin I converting enzyme inhibitory activity from pea and whey protein *in vitro* gastrointestinal digests. *J Sci Food Agric.* 2005;85(3):399-405.
262. Millán-Linares MdC, Bermúdez B, Yust MdM, Millán F, Pedroche J. Anti-inflammatory activity of lupine (*Lupinus angustifolius* L.) protein hydrolysates in THP-1-derived macrophages. *J Funct Foods.* 2014;8:224-33.
263. Kim YS, Ahn CB, Je JY. Anti-inflammatory action of high molecular weight *Mytilus edulis* hydrolysates fraction in LPS-induced RAW264.7 macrophage via NF-kappaB and MAPK pathways. *Food Chem.* 2016;202:9-14.

264. Hsu W-H, Lee B-H, Lu I-J, Pan T-M. Ankaflavin and monascin regulate endothelial adhesion molecules and endothelial NO synthase (eNOS) expression induced by tumor necrosis factor- $\alpha$  (TNF- $\alpha$ ) in human umbilical vein endothelial cells (HUVECs). *J Agric Food Chem*. 2012;60(7):1666-72.
265. Zhang W-c, Wang Y-g, Zhu Z-f, Wu F-q, Peng Y-d, Chen Z-y, Yang J-h, Wu J-j, Lian Y-t, He M-a, Wu T-c, Cheng L-x. Regulatory T cells protect fine particulate matter-induced inflammatory responses in human umbilical vein endothelial cells. *Mediators Inflamm*. 2014;2014.
266. Chao PY, Huang YP, Hsieh WB. Inhibitive effect of purple sweet potato leaf extract and its components on cell adhesion and inflammatory response in human aortic endothelial cells. *Cell Adh Migr*. 2013;7(2):237-45.
267. Mukhopadhyaya A, Noronha N, Bahar B, Ryan MT, Murray BA, Kelly PM, O'Loughlin IB, O'Doherty JV, Sweeney T. The anti-inflammatory potential of a moderately hydrolysed casein and its 5 kDa fraction in *in vitro* and *ex vivo* models of the gastrointestinal tract. *Food Funct*. 2015;6(2):612-21.
268. Grootaert C, Kamiloglu S, Capanoglu E, Van Camp J. Cell systems to investigate the impact of polyphenols on cardiovascular health. *Nutrients*. 2015;7(11):9229-55.
269. Cheng M-L, Wang H-C, Hsu K-C, Hwang J-S. Anti-inflammatory peptides from enzymatic hydrolysates of tuna cooking juice. *Food Agric Immunol*. 2015, 26(6): 770-781.
270. Ko S-C, Jeon Y-J. Anti-inflammatory effect of enzymatic hydrolysates from *Styela clava* flesh tissue in lipopolysaccharide-stimulated RAW 264.7 macrophages and *in vivo* zebrafish model. *Nutr Res Pract*. 2014;9(3):219-26.
271. Chakrabarti S, Wu J. Bioactive peptides on endothelial function. *Food Science and Human Wellness*. 2016;5(1):1-7.
272. de Mejia EG, Dia VP. Lunasin and lunasin-like peptides inhibit inflammation through suppression of NF- $\kappa$ B pathway in the macrophage. *Peptides*. 2009;30(12):2388-98.
273. Dia VP, Wang W, Oh V, De Lumen B, De Mejia EG. Isolation, purification and characterisation of lunasin from defatted soybean flour and *in vitro* evaluation of its anti-inflammatory activity. *Food Chem*. 2009;114(1):108-15.
274. Lin MC, Lin SB, Lee SC, Lin CC, Hui CF, Chen JY. Antimicrobial peptide of an anti-lipopolysaccharide factor modulates of the inflammatory response in RAW264.7 cells. *Peptides*. 2010;31(7):1262-72.
275. Park SY, Ahn CB, Je JY. Antioxidant and anti-inflammatory activities of protein hydrolysates from *Mytilus edulis* and ultrafiltration membrane fractions. *J Food Biochem* 2014;38(5):460-8.

276. Hwang JW, Lee SJ, Kim YS, Kim EK, Ahn CB, Jeon YJ, Moon SH, Jeon BT, Park PJ. Purification and characterization of a novel peptide with inhibitory effects on colitis induced mice by dextran sulfate sodium from enzymatic hydrolysates of *Crassostrea gigas*. *Fish Shellfish Immunol.* 2012;33(4):993-9.
277. Lee S-J, Kim E-K, Kim Y-S, Hwang J-W, Lee KH, Choi D-K, Choi DK, Kang H, Moon SH, Jeon BT, Park PJ. Purification and characterization of a nitric oxide inhibitory peptide from *Ruditapes philippinarum*. *Food Chem Toxicol.* 2012;50(5):1660-6.
278. Kim E-K, Kim Y-S, Hwang J-W, Kang SH, Choi D-K, Lee K-H, Lee JS, Moon SH, Jeon BT, Park PJ. Purification of a novel nitric oxide inhibitory peptide derived from enzymatic hydrolysates of *Mytilus coruscus*. *Fish & Shellfish Immunol.* 2013;34(6):1416-20.
279. Kangsanant S, Thongraung C, Jansakul C, Murkovic M, Seechamnaturakit V. Purification and characterisation of antioxidant and nitric oxide inhibitory peptides from Tilapia (*Oreochromis niloticus*) protein hydrolysate. *Int J Food Sci Technol.* 2015;50(3):660-5.
280. Rho H-S, Kim H, Kim J, Karadeniz F, Ahn B-N, Nam K-H, Seo Y, Kong C-S. Anti-inflammatory effect of by-products from *Haliothis discus hannai* in RAW 264.7 cells. *J Chem.* 2015;2015.
281. Ahn CB, Cho YS, Je JY. Purification and anti-inflammatory action of tripeptide from salmon pectoral fin byproduct protein hydrolysate. *Food Chem.* 2015;168:151-6.
282. Kuntz S, Asseburg H, Dold S, Römpf A, Fröhling B, Kunz C, Rudloff S. Inhibition of low-grade inflammation by anthocyanins from grape extract in an *in vitro* epithelial-endothelial co-culture model. *Food Funct.* 2015;6(4):1136-49.
283. Toaldo IM, Grootaert C, Gonzales GH, Kamiloglu S, Bordignon-Luiz MT, Van Camp J. Resveratrol and its metabolites synergistically improve TNF-  $\alpha$ -induced endothelial dysfunction in a co-culture model of Caco-2 and endothelial cells – A targeted metabolomics study. 2016. (*under review*).
284. Sun X, Chakrabarti S, Fang J, Yin Y, Wu J. Low molecular-weight fractions of Alcalase hydrolyzed egg ovomucin extract exert anti-inflammatory activity in Human dermal fibroblasts through the inhibition of TNF mediated NF- $\kappa$ B pathway. *Nutr Res.* 2016. (*in press*).
285. Hadi HA, Carr CS, Suwaidi J. Endothelial dysfunction: cardiovascular risk factors, therapy, and outcome. *Vasc Health Risk Manag.* 2005;1(3):183.
286. Ndiaye F, Vuong T, Duarte J, Aluko RE, Matar C. Anti-oxidant, anti-inflammatory and immunomodulating properties of an enzymatic protein hydrolysate from yellow field pea seeds. *Eur J Nutr.* 2012;51(1):29-37.

287. Maaser C, Schoeppner S, Kucharzik T, Kraft M, Schoenherr E, Domschke W, Luegering N. Colonic epithelial cells induce endothelial cell expression of ICAM-1 and VCAM-1 by a NF-kappaB-dependent mechanism. Clin Exp Immunol. 2001;124(2):208-13.
288. García-Moreno PJ, Espejo-Carpio FJ, Guadix A, Guadix EM. Production and identification of angiotensin I-converting enzyme (ACE) inhibitory peptides from Mediterranean fish discards. J Funct Foods. 2015;18:95-105.
289. Quaglia GB, Orban E. Enzymic solubilisation of proteins of sardine (*sardina pilchardus*) by commercial proteases. J Sci Food Agric. 1987;38(3):263-9.
290. Tsumura K, Saito T, Tsuge K, Ashida H, Kugimiya W, Inouye K. Functional properties of soy protein hydrolysates obtained by selective proteolysis. LWT-Food Sci Technol. 2005;38(3):255-61.
291. Pearce KN, Kinsella JE. Emulsifying properties of proteins: evaluation of a turbidimetric technique. J Agric Food Chem. 1978;26(3):716-23.
292. Shahidi F, Han X-Q, Synowiecki J. Production and characteristics of protein hydrolysates from capelin (*Mallotus villosus*). Food chem. 1995;53(3):285-93.
293. McConnell A, Eastwood M, Mitchell W. Physical characteristics of vegetable foodstuffs that could influence bowel function. J Sci Food Agric. 1974;25(12):1457-64.
294. Lin MJ-Y, Humbert E, Sosulski F. Certain functional properties of sunflower meal products. J Food Sci. 1974;39(2):368-70.
295. Benjakul S, Morrissey MT. Protein hydrolysates from Pacific whiting solid wastes. J Agric Food Chem. 1997;45(9):3423-30.
296. Ktari N, Jridi M, Bkhairia I, Sayari N, Ben Salah R, Nasri M. Functionalities and antioxidant properties of protein hydrolysates from muscle of zebra blenny (*Salaria basilisca*) obtained with different crude protease extracts. Food Res Int. 2012;49(2):747-56.
297. Mussatto SI, Dragone G, Roberto IC. Brewers' spent grain: generation, characteristics and potential applications. J Cereal Sci. 2006;43(1):1-14.
298. Szwajgier D, Waśko A, Targoński Z, Niedźwiadek M, Bancarzewska M. The use of a novel ferulic acid esterase from *Lactobacillus acidophilus* K1 for the release of phenolic acids from brewer's spent grain. J Inst Brew. 2010;116(3):293-303.
299. McCarthy AL, O'Callaghan YC, Connolly A, Piggott CO, FitzGerald RJ, O'Brien NM. Phenolic extracts of brewers' spent grain (BSG) as functional ingredients – Assessment of their DNA protective effect against oxidant-induced DNA single strand breaks in U937 cells. Food Chem. 2012;134(2):641-6.



300. Fukuda M, Kanauchi O, Araki Y, Andoh A, Mitsuyama K, Takagi K, Toyonaga A, Sata M, Fujiyama Y, Fukuoka M, Matsumoto Y, Bamba T. Prebiotic treatment of experimental colitis with germinated barley foodstuff: a comparison with probiotic or antibiotic treatment. *Int J Mol Med*. 2002;9(1):65-70.
301. Kanauchi O, Mitsuyama K, Araki Y. Development of a functional germinated barley foodstuff from brewer's spent grain for the treatment of ulcerative colitis. *J Am Soc Brew Chem*. 2001;59(2):59-62.
302. McCarthy AL, O'Callaghan YC, Piggott CO, FitzGerald RJ, O'Brien NM. Brewers' spent grain; bioactivity of phenolic component, its role in animal nutrition and potential for incorporation in functional foods: a review. *Proc Nutr Soc*. 2013;72(1):117-25.
303. Santos M, Jiménez J, Bartolomé B, Gómez-Cordovés C, Del Nozal M. Variability of brewer's spent grain within a brewery. *Food Chem*. 2003;80(1):17-21.
304. Liyana-Pathirana C, Shahidi F. Importance of insoluble-bound phenolics to antioxidant properties of wheat. *J Agric Food Chem*. 2006;54(4):1256 - 64.
305. Aliyu S, Bala M. Brewer's spent grain: a review of its potentials and applications. *Afr J Biotechnol*. 2013;10(3):324-31.
306. Kotlar C, Ponce A, Roura S. Improvement of functional and antimicrobial properties of brewery byproduct hydrolysed enzymatically. *Food Sci Technol*. 2013;50(2):378-85.
307. McCarthy AL, O'Callaghan YC, Connolly A, Piggott CO, FitzGerald RJ, O'Brien NM. *In vitro* antioxidant and anti-inflammatory effects of brewers' spent grain protein rich isolate and its associated hydrolysates. *Food Res Int*. 2013;50(1):205-12.
308. Connolly A, Piggott CO, FitzGerald RJ. Characterisation of protein-rich isolates and antioxidative phenolic extracts from pale and black brewers' spent grain. *Int J Food Sci Technol*. 2013;48(8):1670-81.
309. Connolly A, Piggott CO, FitzGerald RJ. *In vitro*  $\alpha$ -glucosidase, angiotensin converting enzyme and dipeptidyl peptidase-IV inhibitory properties of brewers' spent grain protein hydrolysates. *Food Res Int*. 2014;56:100-7.
310. Hassona H. High fibre bread containing brewer's spent grains and its effect on lipid metabolism in rats. *Food/Nahrung*. 1993;37(6):576-82.
311. Öztürk S, Özboy Ö, Cavidoğlu İ, Köksel H. Effects of brewer's spent grain on the quality and dietary fibre content of cookies. *J Inst Brew*. 2002;108(1):23-7.
312. Szponar B, Pawlik KJ, Gamian A, Dey ES. Protein fraction of barley spent grain as a new simple medium for growth and sporulation of soil actinobacteria. *Biotechnol Lett*. 2003;25(20):1717-21.

313. McCarthy AL, O'Callaghan YC, Connolly A, Piggott CO, FitzGerald RJ, O'Brien NM. Brewers' spent grain (BSG) protein hydrolysates decrease hydrogen peroxide (H<sub>2</sub>O<sub>2</sub>)-induced oxidative stress and concanavalin-A (con-A) stimulated IFN-gamma production in cell culture. *Food Funct.* 2013;4(11):1709-16.
314. Van Craeyveld V, Swennen K, Dornez E, Van de Wiele T, Marzorati M, Verstraete W, Delaedt Y, Onagbesan O, Decuypere E, Buyse J, De Ketelaere B, Broekaert WF, Delcour JA, Courtin CM. Structurally different wheat-derived arabinoxylooligosaccharides have different prebiotic and fermentation properties in rats. *J Nutr.* 2008;138(12):2348-55.
315. Delcour J, Courtin C, Broekaert W, Swennen K, Verbeke K, Rutgeers P, inventors, Google Patents, assignee. Prebiotic preparation. CA 2569856 C. 2014 Set 16.
316. Broekaert W, Courtin C, Damen B, Delcour J, inventors, Google Patents, assignee. Nutriment containing arabinoxylan and oligosaccharides. US 8741376 B2. 2014 Jun 3.
317. Cho SS, Samuel P. Fiber ingredients: Food applications and health benefits. USA: CRC Press; 2009.
318. Roos AA, Persson T, Krawczyk H, Zacchi G, Stålbrand H. Extraction of water-soluble hemicelluloses from barley husks. *Bioresour Technol.* 2009;100(2):763-9.
319. Meneses NGT, Martins S, Teixeira JA, Mussatto SI. Influence of extraction solvents on the recovery of antioxidant phenolic compounds from brewer's spent grains. *Sep Purif Technol.* 2013;108(0):152-8.
320. Moreira MM, Morais S, Carvalho DO, Barros AA, Delerue-Matos C, Guido LF. Brewer's spent grain from different types of malt: Evaluation of the antioxidant activity and identification of the major phenolic compounds. *Food Res Int.* 2013;54(1):382-8.
321. Piggott CO, Connolly A, FitzGerald RJ. Application of ultrafiltration in the study of phenolic isolates and melanoidins from pale and black brewers' spent grain. *Int J Food Sci Technol.* 2014;49(10):2252-9.
322. Coimbra MA, Ferreira, IMPLVO, Rocha, MAM, Vieira, EMF, Saraiva, JMA, Pinho, OMC, inventors; Google Patents, assignee. Integrated process for extracting proteins and arabinoxylans from brewer's spent grain. Patent WO 2012069889 A1. 2012 Mai 31.
323. Hernanz D, Nuñez V, Sancho AI, Faulds CB, Williamson G, Bartolomé B, Gómez-Cordovés C. Hydroxycinnamic acids and ferulic acid dehydrodimers in barley and processed barley. *J Agric Food Chem.* 2001;49(10):4884-8.

324. Kuwabara Y, Nagai S, Yoshimitsu N, Nakagawa I, Watanabe Y, Tamai Y. Antihypertensive effect of the milk fermented by culturing with various lactic acid bacteria and a yeast. *J Ferment Bioeng.* 1995;80(3):294-5.
325. Chaves-Lopez C, Tofalo R, Serio A, Paparella A, Sacchetti G, Suzzi G. Yeasts from Colombian Kumis as source of peptides with Angiotensin I converting enzyme (ACE) inhibitory activity in milk. *Int J Food Microbiol.* 2012;159(1):39-46.
326. Bolumar T, Sanz Y, Aristoy MC, Toldrá F. Protease B from *Debaryomyces hansenii*: purification and biochemical properties. *Int J Food Microbiol.* 2005;98(2):167-77.
327. García-Carreño FL. Protease inhibition in theory and practice. *Biotechnol Educ.* 1992;3(4):145-50.
328. Fang Y-Z, Yang S, Wu G. Free radicals, antioxidants, and nutrition. *Nutrition.* 2002;18(10):872-9.
329. Hayashi R, Oka Y, Doi E, Hata T. Activation of intracellular proteinases of yeast: Part I. Occurrences of inactive precursors of proteinases B and C and their activation Part II. Activation and some properties of pro-proteinase C. *Agric Biol Chem.* 1968;32(3):359-66.
330. Pokora M, Eckert E, Zambrowicz A, Bobak Ł, Szołtysik M, Dąbrowska A, Chrzanowska J, Polanowski A, Trziszka T. Biological and functional properties of proteolytic enzyme-modified egg protein by-products. *Food Sci Nutr.* 2013;1(2):184-95.
331. Goya L, Martín MÁ, Ramos S, Mateos R, Bravo L. A cell culture model for the assessment of the chemopreventive potential of dietary compounds. *Curr Nutr Food Sci.* 2009;5(1):56-64.
332. Cheli F, Baldi A. Nutrition-Based Health: Cell-based bioassays for food antioxidant activity evaluation. *J Food Sci.* 2011;76(9):197-205.
333. Kannan A, Hettiarachchy NS, Marshall M, Raghavan S, Kristinsson H. Shrimp shell peptide hydrolysates inhibit human cancer cell proliferation. *J Sci Food Agric.* 2011;91(10):1920-4.
334. Serra AT, Duarte RO, Bronze MR, Duarte CMM. Identification of bioactive response in traditional cherries from Portugal. *Food Chem.* 2011;125(2):318-25.
335. Shi Y, Kovacs-Nolan J, Jiang B, Tsao R, Mine Y. Antioxidant activity of enzymatic hydrolysates from eggshell membrane proteins and its protective capacity in human intestinal epithelial Caco-2 cells. *J Funct Foods.* 2014;10:35-45.
336. Sahu SC, Zheng J, Graham L, Chen L, Ihrle J, Yourick JJ, Sprando RL. Comparative cytotoxicity of nanosilver in human liver HepG2 and colon Caco2 cells in culture. *J Appl Toxicol.* 2014;34(11):1155-66.

337. Yarnpakdee S, Benjakul S, Kristinsson HG, Bakken HE. Preventive effect of Nile tilapia hydrolysate against oxidative damage of HepG2 cells and DNA mediated by H<sub>2</sub>O<sub>2</sub> and AAPH. J Food Sci Technol. 2015;52(10):6194-205.
338. Shamloo M, Bakar J, Mat Hashim D, Khatib A. Biochemical properties of red tilapia (*Oreochromis niloticus*) protein hydrolysates. Int Food Res J. 2012;19(1):183-8.
339. Celus I, Brijs K, Delcour JA. The effects of malting and mashing on barley protein extractability. J Cereal Sci. 2006;44(2):203-11.
340. Mukhopadhyaya A, Noronha N, Bahar B, Ryan MT, Murray BA, Kelly PM, Kelly PM, O'Loughlin IB, O'Doherty JV, Sweeney T. Anti-inflammatory effects of a casein hydrolysate and its peptide-enriched fractions on TNF $\alpha$ -challenged Caco-2 cells and LPS-challenged porcine colonic explants. Food Sci Nutr. 2014;2(6):712-23.
341. Forghani B, Ebrahimpour A, Bakar J, Abdul Hamid A, Hassan Z, Saari N. Enzyme hydrolysates from *Stichopus horrens* as a new source for Angiotensin-converting enzyme inhibitory peptides. Evid Based Complement Alternat Med. 2012: 2012: 236384.
342. Di Bernardini R, Mullen AM, Bolton D, Kerry J, O'Neill E, Hayes M. Assessment of the angiotensin-I-converting enzyme (ACE-I) inhibitory and antioxidant activities of hydrolysates of bovine brisket sarcoplasmic proteins produced by papain and characterisation of associated bioactive peptidic fractions. Meat Sci. 2012;90(1):226-35.
343. Alemán A, Pérez-Santín E, Bordenave-Juchereau S, Arnaudín I, Gómez-Guillén MC, Montero P. Squid gelatin hydrolysates with antihypertensive, anticancer and antioxidant activity. Food Res Int. 2011;44(4):1044-51.
344. Zhang Q-X, Ling Y-F, Sun Z, Zhang L, Yu H-X, Kamau SM, Lu RR. Protective effect of whey protein hydrolysates against hydrogen peroxide-induced oxidative stress on PC12 cells. Biotechnol Lett. 2012;34(11):2001-6.